HERIOT-WATT UNIVERSITY

EDINBURGH

DEPARTMENT OF MECHANICAL ENGINEERING

THE PROPAGATION OF PRESSURE WAVES AND CRITICAL FLOW IN TWO-PHASE MIXTURES

by

PETER A. HALL, M.Sc.

Thesis presented for the Degree of Doctor of Philosophy

December 1971

PREFACE

In view of the range of subjects investigated, this thesis has necessarily assumed rather complicated form. This short introductory note is intended to explain why this form has been adopted and to make it easier for the reader to follow the text.

The investigation falls naturally into two portions, the velocity of pressure waves in two-phase mixtures and the related choking flow phenomena. As experimental investigations have been undertaken only in the former, it is this topic which is dealt with first in the text.

Chapters 1 - 4 are devoted specifically to the propagation of pressure waves, whereas any general discussions which are relevant to both sonic velocity and critical flow, such as slip velocity ratio and heat transfer coefficient, are contained in the second portion of the thesis (i.e. Chapters 5 - 8). The mathematical analyses have in general been confined to the appendices, except where an analysis is relatively simple and does not interupt the text unnecessarily.

The first chapter introduces the subject of the sonic velocity in two-phase media and surveys the existing theoretical treatments. The predictions of the present theories for the velocity of sinusoidal, step and impulse pressure waves in one-component bubbly mixtures (Appendices A and B) are also discussed in this chapter.

Chapters 2 and 3 deal with the experimental investigations into the velocity of pressure waves in air/water and steam/water mixtures respectively. Both chapters commence with a short survey of experimental techniques developed and results obtained by previous experimenters. The present experimental techniques are described and the results compared with the theoretical predictions obtained in chapter 1.

Little is known of the attenuation of pressure waves in two-phase media and it was for this reason that chapter 4 was included in this thesis.

Relevant information has been gathered and discussed with particular reference to the wave attenuations measured in the present experimental programme.

Chapter 5 is intended as an introduction to the subject of choking flow in two-phase mixtures and contains an extensive survey of existing theoretical models of the phenomena. It becomes apparent that the slip velocity ratio is an important parameter within these theories and hence chapter 6 is a digression on this subject. Following a brief literature survey, a mathematical model to determine the slip velocity ratio in a bubbly mixture is proposed and the predictions compared to existing measurements in air/water mixtures.

In chapter 7, the basic assumptions and restrictions on the present analysis of non-equilibrium choking flow in two-phase one-component mixtures are discussed and the slip velocity ratio model described in chapter 6, is incorporated into the equations describing the critical flow model. Particular attention is paid to the choice of empirical formulae defining the two-phase frictional pressure drop and the heat transfer coefficient at the bubble (liquid interface, (Sections 7.2.1 and 7.6). These two sections both contain a survey of expressions used by previous authors and a graphical comparison.

Having formulated the critical flow equations in chapter 7, chapter 8 is devoted to the numerical solution and the discussion of the results. Because of the large number of flow parameters which exist in a two-phase choking flow, section 8.2 contains a brief survey of experimental measuring techniques which enable the most important parameters to be correlated in Figures 39-46.

The effects of non-homogeneous bubble distributions in a two-phase critical flow are discussed in section 8.5, where a bubbly/annular flow pattern is considered. Chapter 8 concludes with a section on supersonic

critical flow in a one-component two-phase bubbly mixture.

A summary of the work covered in this thesis, together with the conclusions and suggestions for further work in this field, is contained in the final chapter.

List of Contents

1. THE VELOCITY OF SOUND AND THE PROPAGATION VELOCITY OF SMALL AMPLITUDE WAVES IN TWO-PHASE MEDIA

Introduction

The sonic velocities in two-phase one- and two-component mixtures have been the subject of considerable investigation [1, 2], this being prompted, principally, by its relevance to the choking flow phenomena in such media [3, 4].

It is expected that knowledge of sound wave velocities will lead to the development of an acoustical method for the detection of nucleation within the primary coolant system of a nuclear reactor and also provide an alternative method of determining flow voidage in two component systems [5, 6]. Departures of a one-component mixture from thermodynamic equilibrium, during the propagation of a pressure wave, are also of interest in determining the rates of vaporization occurring in flashing systems [7].

Due to the strong dependence on flow regime of the above phenomena and the improbability of obtaining a general solution for all phase distributions it has been necessary to restrict the present work to bubbly mixtures.

The two major properties which influence the velocity of pressure waves in a two-phase one-component medium are the variation of medium compressibility and mass transfer between the phases. In an attempt to separate these two effects both air/water and steam/water mixtures have been used in the present work.

Existing literature tends to concentrate on the velocity of large amplitude step or "shock" waves and

hence the "no mass transfer" sonic velocity in steam/water mixtures and the "adiabatic" sonic velocity in air/water mixtures. To investigate heat and mass transfer effects between the phases, the propagation velocities of sinusoidal pressure waves have been measured and by correlating experimental results with a theoretical analysis, based on conduction controlled rates of vaporization and condensation, an estimate made of the heat transfer coefficient of the bubble/liquid interface in such media.

A theory is also presented for the propagation velocity of step and impulse waves which is found to predict previous experimental results (5). The "bulk" velocities of such waves are found to be markedly dependent on the "steepness" of the wave front and the time since the generation of the wave.

1.1 Velocity of sound in air/water mixtures

1.1.1 Literature survey

The propagation velocity of an infinitesimal amplitude pressure wave through an elastic medium is known to be the sonic velocity, defined by the equation

$$C = (\rho K)^{-\frac{1}{2}} \qquad 1.1$$

where K, the compressibility, is the reciprocal of the bulk modulus of elasticity of the medium.

A homogeneous two-phase two-component mixture can have a density of the same order as the liquid phase and a compressibility similar to that of the gas phase. From equation 1.1 it can be seen that this will lead to *sonic velocities, within the mixture, much lower than* those found in either of the individual components.

The compressibility of a medium is defined as

$$K = -\frac{1}{V}\left(\frac{\partial V}{\partial p}\right) \qquad 1.2$$

It is the evaluation of this expression which makes it possible to obtain many non-unique values for the sonic velocity. If the compression/expansion processes which occur within the gas phase are assumed to be adiabatic, the derivative $(\partial V/\partial p)$ is evaluated at constant entropy. However, should the processes be isothermal, the evaluation is at constant temperature. In general the processes may be polytropic, in which case

$$PV^n = \text{constant} .$$

Probably the first analytical study of the velocity of sound in a homogeneous bubbly air/water mixture was made by Mallock [8]. Assuming a mean

density of the medium defined by

$$\rho = \alpha\rho_A + (1-\alpha)\rho_w \qquad 1.3$$

a mean bulk modulus of elasticity

$$E_M = \frac{E_w E_A}{\alpha E_w + (1-\alpha) E_A} \qquad 1.4$$

and using equation 1.1 the following equation for the sonic velocity was obtained

$$\frac{C_{TP}}{C_A} = \frac{\left(\frac{\alpha}{1-\alpha}+1\right)\left(\frac{E_A}{E_w}\right)^{1/2}}{\left\{\left(\frac{\alpha}{1-\alpha}+\frac{E_A}{E_w}\right)\left(\frac{E_A}{P_w}\frac{\alpha}{1-\alpha}+1\right)\right\}^{1/2}} \qquad 1.5$$

This was shown to have a minimum value at $\alpha = 50\%$.

The same result was obtained by Barclay[5] who also found equation 1.5 to agree with experimental results.

Wood[10] derived an equation, basically the same as above in terms of the compressibility.

$$C^2 = \left(\alpha\rho_A + (1-\alpha)\rho_w\right)^{-1}\left(\alpha K_A + (1-\alpha)K_w\right)^{-1} \qquad 1.6$$

This equation was used by Karplus[10] to successfully predict experimental results. It was also indicated that for isothermal charges

$$K_A = 1/P \qquad 1.7$$

and for adiabatic

$$K_A = 1/\gamma P$$

The compressibility of the liquid phase was assumed to be zero.

Re-writing equation 1,6, the sonic velocity in a two-phase mixture in terms of the individual sonic velocities of each phase can be shown to be[11]

$$C^2 = \left(\alpha\rho_A + (1-\alpha)\rho_w\right)^{-1}\left(\frac{\alpha}{\rho_A C_A^2} + \frac{1-\alpha}{\rho_w C_w^2}\right)^{-1}$$

where for isothermal changes

$$C_A^2 = RT$$

and for adiabatic 1.9

$$C_A^2 = \gamma RT$$

This expression was simplified by Henry and Fauske[12] by assuming the density ratio $\rho_A/\rho_w \ll 1.0$ and the liquid phase incompressible . The resulting equation for the velocity of propagation of small amplitude waves in a bubbly mixture was

$$\frac{C_{TP}^2}{C_A^2} = \left(\alpha^2 + \frac{\alpha(1-\alpha)\rho_w}{\rho_g}\right)^{-1} \qquad 1.10$$

In this case the difference between adiabatic and isothermal sonic velocity is defined in the evaluation of C_A (equations 1.9).

A more detailed analysis made by Gouse and Brown[1] and based on thermodynamic considerations, led to the adiabatic velocity of sound in a low quality two-phase two-component mixture being given by

$$\frac{C_{TP}^2}{C_A^2} = \frac{\left(\frac{\rho_A}{\rho_w} + \frac{x}{1-x}\right)^2}{\frac{\gamma x}{1-x}} \qquad 1.11$$

x being the mass fraction (mass of gas/mass of mixture).

The relation between the adiabatic and isothermal sonic velocities was shown to be

$$\frac{C_{TP(ADIABATIC)}}{C_{TP(ISOTHERMAL)}} = \frac{\frac{(C_v)_w}{(C_v)_A} + \frac{\gamma x}{1-x}}{\frac{(C_v)_w}{(C_v)_A} + \frac{x}{1-x}} \qquad 1.12$$

1.1.2 Velocity of small amplitude sinusoidal pressure waves

It may be expected that high frequency sinusoidal pressure waves will propagate at the adiabatic sonic velocity and the lower frequency waves at the isothermal sonic velocity. However no theory has been found which considers the variation of wave velocity over the range of frequencies at which the transition from adiabatic to isothermal behaviour of the gas phase is likely to occur. Spitzer [13] derived formulae to predict the propagation velocity of waves with frequency approaching the bubble resonance frequency. The very small range of voidages permissible in using these formulae ($0 < \alpha < 0.03$) makes this theory inapplicable to the present work. Also the wave frequencies used in the present experimental work are much lower than the expected resonance frequency of the bubbles. (Section 1.3.4)

Using equations 1.1 and 1.2 the sonic velocity in an elastic medium can be written

$$C^2 = \frac{-V^2}{(\partial V/\partial p)} \qquad 1.13$$

the evaluation of the derivative term being undefined at present. For a two-phase two-component system with no slip occurring between the phases, the average specific volume is defined by

$$V = xV_A + (1-x)V_w \qquad 1.14$$

where the quality (x) is constant for a given flow.

If the gas phase is assumed to act polytropically with index n for a given frequency wave, and the

liquid phase is considered incompressible then

$$PV_n^n = \text{Constant}$$

and

$$\partial V_w / \partial p = 0$$

hence $\frac{\partial V}{\partial p}$ can be determined and equation 1.13 reduces to

$$C^2 = \frac{n P V_w}{(1-\alpha)\alpha} \qquad 1.15$$

This result may also be obtained using equation 1.10 and assuming a low quality medium with the sonic velocity in the gas phase being given by an equation of the form of 1.9.

Gouse and Brown's [1] prediction for the adiabatic sonic velocity, given by equation 1.11, reduces to the above equation (1.15) with n = 1.0 which corresponds to the present isothermal sonic velocity prediction. However equation 1.12 indicates no significant difference between adiabatic and isothermal sonic velocities at mass fractions below 0.1 which contains the range of voidages used in the present experimental work.

The variation of the polytropic index (n) of the gas phase from unity to a value of 1.4 (for air) with increasing wave frequency, has been studied by Mawardi [14]. This will be discussed further in Chapter 2.

The rate of heat transfer between the liquid phase and the bubbles determines whether adiabatic or isothermal conditions prevail within the gas phase, hence the mechanisms which will be described in section 7.5 are probably significant. However, as the heat transfer coefficient of the interphase surface can only be estimated, it appears that at present, the relation between the

polytropic index of the gas phase and the pressure wave frequency can only be determined empirically from experimental data.

The two limiting curves of equation 1.15 (n = 1.0 and n = 1.4) are shown in Fig. 1 for comparison with experimental results (10) .

1.2 Velocity of sound in steam/water mixtures (literature survey)

The sonic velocity in a two-phase one-component medium is less well defined than in a two-component mixture. The difference between the "adiabatic" and "isothermal" velocities of sound in an air/water mixture, described in the previous section is small when compared to the range of "sonic" velocities which may occur in a steam/water mixture.

In such a mixture the sonic velocity is defined by the equations 1.13 and 1.14. However, because of the possibility of mass transfer occurring between the phases, the change in the specific volume of the mixture with pressure variations is given by

$$\frac{\partial V}{\partial p} = x\left(\frac{\partial V_g}{\partial p}\right) + (1-x)\left(\frac{\partial V_f}{\partial p}\right) + (V_g - V_f)\left(\frac{\partial x}{\partial p}\right) \qquad 1.16$$

It is the evaluation of the differential terms on the R.H.S. of this equation, which makes it impossible to define a unique sonic velocity for a given mixture, unless the thermodynamic state of the mixture is known.

If no mass transfer is assumed to occur during the passage of the wave through the medium, then $\partial x/\partial p = 0$ and the derivatives $\partial V_g/\partial p$ and $\partial V_f/\partial p$ are evaluated under isentropic conditions. This will lead to sonic

velocities of a similar order to those within a two-component mixture.

Should condensation or evaporation occur within the fluid, then $\partial x/\partial p$ is finite and determined by the thermodynamic properties of the mixture. The evaluation of the derivatives $\partial V_g/\partial p$ and $\partial V_f/\partial p$ in this case is uncertain and represents the main difference between the theoretical analyses of Karplus [15] and Davis [16].

Karplus assumed isentropic conditions and was able to re-write equation 1.16 in the form

$$\left(\frac{\partial V}{\partial p}\right)_s = x\left(\frac{\partial V_{fg}}{\partial p} - \frac{V_{fg}}{S_{fg}}\frac{\partial S_{fg}}{\partial p}\right) + \frac{\partial V_f}{\partial p} - \frac{V_{fg}}{S_{fg}}\frac{\partial S_f}{\partial p} \qquad 1.17$$

where $V_{fg} = V_g - V_f$

$S_{fg} = S_g - S_f$

the differential terms were determined by a graphical method using tabulated values from standard steam tables. The values of "equilibrium" sonic velocity obtained using the above equation were almost identical to the results given by Davis who evaluated the gradients $\partial V_f/\partial p$ and $\partial V_g/\partial p$ along the saturation line of the P-V. diagram. $(\partial x/\partial p)_s$ was calculated using the basic laws of thermodynamics, i.e.

The first law, for an isentropic change can be written

$$\delta Q = \delta E + \frac{p\delta V}{J} = 0$$

By definition $h = E + \frac{pV}{J}$

Hence combining the above two equations

$$\delta h = -\frac{V\delta p}{J}$$

For a two-phase mixture

$$h = x h_g + (1-x) h_f$$

therefore

$$\frac{dh}{dp} = \frac{dh_f}{dp} + x\frac{dh_{fg}}{dp} + h_{fg}\frac{dx}{dp}.$$

substituting for $\frac{dh}{dp}\left(\approx \frac{\delta h}{\delta p}\right)$

$$\Rightarrow \quad \left(\frac{\partial x}{\partial p}\right)_s = \frac{V}{J h_{fg}} - \frac{1}{h_{fg}}\left(\frac{\partial h_f}{\partial p}\right)_{sat} - \frac{x}{h_{fg}}\left(\frac{\partial h_{fg}}{\partial p}\right) \qquad 1.18$$

The terms on the R.H.S. were obtained using standard steam tables. The resulting values of $(\partial x/\partial p)_s$ were used in equation 1.16 and hence the "equilibrium" sonic velocity calculated using equation 1.13.

The no-mass transfer sonic velocity was calculated [16] assuming isentropic conditions to exist, the derivatives being obtained from standard tables using the expression

$$\left(\frac{\partial V}{\partial p}\right)_s = \left(\frac{\partial V}{\partial p}\right)_T - \left(\frac{\partial V}{\partial S}\right)_p \left(\frac{\partial S}{\partial p}\right)_T \qquad 1.19$$

In practice, measured propagation velocities of pressure waves have been found to approximate more closely to the no-mass transfer sonic velocity and hence this is the velocity which has been the subject of most analytical investigations.

By considering a vapour continuous two-phase system to act as an elastic medium, Deich [17] calculated the propagation velocity of longitudinal elastic oscillations and hence showed that the no-mass transfer sonic velocity in such a two-phase system to be given by

$$C^2_{NMT} = \frac{nP}{x\rho\left(1 + (1-x)\frac{\mu_f}{x\mu_g}\right)} \qquad 1.20$$

where n is the polytropic index of the vapour phase. As in this analysis, the initial fluid is assumed to be at rest, the phase velocities shown in equation 1.20 are

induced by the passing of the pressure wave. Best agreement with experiment was obtained when the velocity ratio $u_f/u_g \approx 0.0$, i.e. when the water droplets are considered sufficiently large not to be accelerated by the pressure wave. In this case equation 1.20 reduces to the sonic velocity in a single phase vapour medium.

A more general equation was derived by Dvornichenko[18] for application at all mass dryness fractions (x). Using basic thermodynamic principles and again assuming χ = constant the result obtained was:-

$$C^2_{NMT} = \frac{\gamma p}{\rho\left(1 - \frac{(1-x)p}{\rho_f}\right)} \qquad 1.21$$

For small mass qualities and voidages such that $\alpha \rho_g \ll (1-\alpha)\rho_f$, this reduces to equation 1.15 ($n \equiv \gamma$) which was derived for a two-component system.

Other Russian authors have published work in this field[19,20] but this has been restricted to vapour continuous steam/water mixtures.

Grolmes and Fauske[21] defined the "Homogeneous-frozen" or no-mass transfer sonic velocity in a two-phase one-component system as

$$C^2_{NMT} = \left(\frac{\alpha \rho}{\rho_g C_g^2} + \frac{(1-\alpha)\rho}{\rho_f C_f^2}\right)^{-1} \qquad 1.22$$

If the compressibility of the liquid phase is neglected and Cg is assumed to be given by an equation of the form 1.9, this also reduces to equation 1.15.

Hence it can be seen that for low voidage media, the no-mass transfer sonic velocity in a steam/water mixture is almost identical to the adiabatic sonic velocity in an air/water mixture. From equation 1.15 the ratio of the velocities is given by

$$\frac{C_{NMT}}{C_{ADIABATIC}} = \left(\frac{\gamma_s}{\gamma_A}\frac{V_f}{V_w}\right)^{1/2} \qquad 1.23$$

The isentropic index, γ, in a water vapour at 212°F is $\gamma_s = 1.33$ and in air $\gamma_A = 1.4$ [22]. If V_f and V_w represent the specific volumes of water at 212°F and 60°F respectively, then numerically

$$\frac{C_{NMT}}{C_{ADIABATIC}} \approx 1.0 \qquad 1.24$$

Although, as mentioned previously, experimental measurements have suggested that the majority of pressure waves travel at approximately the no-mass transfer sonic velocity [12], propagation velocities significantly lower have been measured, indicating that some mass transfer occurs during the passage of various types of pressure waves through a two-phase one-component mixture.

It is proposed that the velocity at which a sinusoidal pressure wave is transmitted through a steam/water mixture will vary according to the frequency, at very low frequencies the fluid remaining in thermodynamic equilibrium and at high frequencies the pressure variations occurring at a sufficient rate to prevent mass transfer taking place between the phases.

1.3 Propagation velocity of small amplitude sinusoidal waves in a two-phase one-component mixture

A theoretical analysis of the system, based on the two-phase flow equations derived in Chapter 7, is given in Appendix A. The perturbation technique, used to solve the equations, is well known and generally applied in the solution of stability problems.

In the analysis it is assumed that the initial

or ambient fluid is stationary with the two phases in thermodynamic equilibrium. It is also required that the medium is completely homogeneous with no slip velocity being induced between the phases by the passing of the pressure wave.

Within a medium subject to these restrictions it is shown that the propagation velocity of a small amplitude sinusoidal pressure wave is given by:-

$$U_{SINE} = \left\{ \frac{1}{2\lambda^2} \left(x \left| \frac{\partial V_g}{\partial p} \right| + \frac{mq}{m^2+n^2} \right) \left(1 + \sqrt{1 + \left(\frac{nq}{x \left| \frac{\partial V_g}{\partial p} \right| (m^2+n^2) + mq} \right)^2} \right) \right\}^{-\frac{1}{2}} \qquad 1.25$$

where $\lambda = xV_g + V_f$ $\qquad q = V_g \frac{\partial T_s}{\partial p}$

$m = \frac{h_{fg}}{C_w}$ $\qquad n = \frac{h_{fg}}{h} \frac{\omega}{A}$

and h is defined by equation 7.43 (chapter 7). However due to the uncertainty of the relation between the frequencies of sinusoidal changes of quality and pressure (appendix A), it may only be relevant to obtain a constant value of h giving best correlation to experimental data.

The two limiting velocities given by equation 1.25 can be shown to be:-

when w = o; $$U_{SINE} = \frac{xV_g + V_F}{\left[x \left| \frac{\partial V_g}{\partial p} \right| + \frac{C_w V_g}{h_{fg}} \left(\frac{\partial T_s}{\partial p} \right) \right]^{\frac{1}{2}}} = C_{EQ} \qquad 1.26$$

and w = ∞; $$U_{SINE} = \frac{xV_g + V_F}{\left(x \left| \frac{\partial V_g}{\partial p} \right| \right)^{\frac{1}{2}}} = C_{NMT} \qquad 1.27$$

These predictions of sonic velocities in a steam/water medium are compared to the numerical results presented by Davis (16) in Fig. 2. The discrepancy between the predicted no-mass transfer curves is possibly due to the evaluation

of $\partial V_g/\partial p$ as equations 1.27 and 1.13 are identical in form. In the present computations the differential terms were evaluated along the saturation line of the P-V diagram, using an empirical equation, the accuracy of which is discussed in section 7.6. Davis evaluated $\partial v/\partial p$ under isentropic conditions.

1.4 Propagation velocity of small amplitude step and triangular pressure waves in a two-phase one-component mixture

Appendix B gives a tentative analysis for the propagation velocities of step and triangular waves within such medium as discussed in the previous section. Due to the restrictions imposed on the solution in order for the Laplace Transformation to be obtained analytically, the results can only be valid for very low quality systems.

The wave shape at time t after the initiation of the wave (t = o) are given by the expressions.

$$\Delta p_{STEP} = \Delta p_o \ \text{erfc} \ \frac{\ell\sqrt{b}}{2c\sqrt{t}}$$

$$\Delta p_{TRI} = \Delta p_o \frac{\tau \ell \sqrt{b}}{2c\sqrt{\pi t^3}} \ e^{-\frac{\ell^2 b}{4c^2 t}} \qquad 1.28$$

where 2τ represents the initial "time" thickness of the triangular wave and Δp_o the initial wave maximum pressure. Fig. 3.1 shows the predicted change of shape of the waves as they propagate through a two-phase medium.

The above equations are only valid for small amplitude waves ($\Delta p/p \ll 1$) and hence do not include changes in wave shape due to compressibility effects, only wave dispersion due to the variation of sonic velocity and attenuation with wave frequency analysed in sections 1.3 and 4.2. In many experimental investigations it has been assumed that the velocity of a step wave is characterized

by the velocity of the leading point or "foot" of the wave-front [15] [21], however due to the difficulty in mathematically describing this point, the above equations can only be used to determine the velocity of selected points on the waveform.

In the case of a step wave this point was taken to be the mid-point of the wavefront where $\Delta p = \Delta p_o / 2$. The velocity of this point was assumed to be the mean propagation velocity of the wave.

Similarly the mean propagation velocity of a triangular wave was taken to be the velocity of the point on the waveform where $\partial \Delta p / \partial \ell = o$, with Δp representing a maximum value.

Applying the above conditions to equations 1.28 yielded the propagation velocities :—

$$U_{STEP} = \frac{0.94}{\sqrt{bt}} C_{NMT} \qquad 1.29$$

$$U_{TRI} = \frac{1.4}{\sqrt{bt}} C_{NMT} \qquad 1.30$$

It can be seen that the velocity of the waves is predicted to continuously decrease with time elapsed (and hence distance) since the generation of the wave.

The point t = o represents a singularity within the equations and hence the solutions cannot be valid for very small time intervals.

Despite the restrictions made on the application of equations 1.29 and 1.30, they will be shown, in section 1.4.3, to give an estimate of the velocity of small rarefaction waves in very low quality two-phase one-component systems.

1.4.1 Heat transfer coefficient within this type of wave

The constant b in equations 1.29 and 1.30 is defined by:-

$$b = \frac{V_g \frac{\partial T_s}{\partial P} hA}{\pi \left|\frac{\partial V_g}{\partial P}\right| h_{fg}}$$

where h is a heat transfer coefficient.

As no slip velocity occurs within the assumed system, the heat transfer across the bubble surface is probably given by the theories of Carslaw and Jaeger (83) and Edwards (56) (section 7.5.1). In the physical system it is likely that, due to the change of wave shape, the value of h will vary as the wave proceeds through the medium. A constant value of h was used in the theory presented here so representing a mean heat transfer coefficient.

Under such conditions it was suggested by Dickson (7) that the average heat transfer coefficient in a flashing flow was of the order 1.0 BTU/$ft^2 sec\,^oF$.

1.4.2 Frequency spectra of waves

Another possible approach to determining the velocity of propagation and change in shape of a pressure wave in a two-phase system is to consider the frequency spectra of the wave. Fig. 3.2 shows the frequency spectra of a step wave and an impulse wave (which is the limiting case of the triangular wave previously analyzed).

A step wave can be seen to have mainly low frequency components and hence will be expected to propagate at a speed characteristic of low frequency waves.

The frequency spectrum of an impulse wave is a straight line indicating equal proportions of all frequencies.

However the attenuation of a sinusoidal pressure wave has been found to increase with frequency (chapter 4) and hence the higher frequencies will have little effect after the wave has travelled a short distance. Comparing the two frequency spectra shown in Fig. 3.2 and assuming the corresponding step and impulse waves (of equal initial amplitude) to have propagated sufficient distance to make all frequency components above f′ negligible, then it can be seen that the "bulk" of the impulse wave will travel at a higher velocity than the "bulk" of the step wave, since a greater proportion of the wave amplitude consists of frequency components approaching f′.

In a two-component (air/water) system the variation of sonic velocity with wave frequency is small (section 1.1) and so wave dispersion due to the above effect will be much less than in a one-component (steam/water) system.

It is considered that before this method of estimating the propagation velocity of pressure waves in a two-phase system can give reliable results, more accurate knowledge must be gained of the attenuation of sinusoidal pressure waves in such systems.

1.4.3 Experimental verification of theoretical approach

Equation 1.29 and 1.30 are only valid for small pressure waves which are less than required to condense all of the vapour phase and therefore cannot be used to predict the results of Karplus (15). This condition also means that in very low quality media the equations are probably more applicable to rarefaction waves. The reason for this is probably that the variation of sonic velocities, characteristic of the range of voidages, which exist within the wave

approaches zero. This will lead to large distortion of the wave due to "compressibility" effects which are not included in the analysis.

The propagation velocities of rarefaction step waves in steam/water mixtures were measured by Barclay [5]. Equation 1.29 can be re-written as

$$U_{STEP} = \frac{(0.92\, C_{NMT})^2}{b\ell} \qquad 1.31$$

U_{STEP} now represents the velocity of the wave at a distance ℓ along the flow, the wave having the form of a pure "step" wave at the position $\ell = o$. The velocities measured experimentally [5] were the average over the first 1.5 ft. of the distance travelled by the wave. Fig. 4 shows the experimental results together with velocities predicted using the above equation at $\ell = 0.75$ ft. and atmospheric pressure. The value of h giving the best correlation was between 0.5 and 1.0 $BTU/ft^2 sec\,^oF$.

The equation for the velocity of a triangular wave in a two-phase one-component medium (equation 1.30) may similarly be written:-

$$U_{TRI} = \frac{2(C_{NMT})^2}{b\ell} \qquad 1.32$$

In the present experimental system (section 3.1) the velocity of a wave was measured over a fixed length of 9 inches which was approximately 6 inches from the point where the generated waveform entered the two-phase mixture. This implies that the wave had propagated a distance of approximately 9 inches before the velocity was measured.

Substituting this value of ℓ into the above equation yields the curve shown in Fig. 4. Experimental measurements of the velocities of rarefaction peaks are also shown. For reasons which will be discussed in chapter 3, a significant spread of data was obtained. Nevertheless the measured velocities are of the same order as predicted by equation 1.32 with h = 0.5 BTU/ft^{2}sec^{o}F.

Experimental verification of equation 1.25 for the velocity of sinusoidal pressure waves in a two-phase steam/water mixture constitutes the major part of the experimental work reported within this thesis.

2. EXPERIMENTAL MEASUREMENT OF THE PROPAGATION VELOCITY OF SMALL AMPLITUDE WAVES IN AIR/WATER BUBBLY MIXTURES

2.1 Sinusoidal pressure waves

This experimental work was carried out principally to develop techniques of propagating and detecting sinusoidal pressure waves through a two-phase mixture, in order to apply the systems to the steam/water experimental apparatus which will be described in chapter 3. Also the results obtained enable a distinction to be made between compressibility and mass-transfer effects occurring within a steam/water mixture.

Silberman[13] and Karplus[10] measured the sonic velocity in air/water mixtures using standing wave tubes. The methods involved the use of an accelerometer or pressure transducer which could be moved through the medium in order to detect the nodes of vibration. Measurement of the wave length yielded the phase velocity for a given frequency wave. Due to the high attenuations experienced in two-phase media, the method was only of use at very low voidages. However, Karplus[10] measured wave velocities at higher voidages by varying the distance between the wave transmitter and detector until the signals from both displayed on a C.R.O. resulted in a collapsed Lissajou figure. This indicated that a distance of one wave length existed between the two transducers.

Silberman[13] detected no change in the sonic velocity within the range of frequencies 100 - 1,000 cps at very low voidages, whereas Karplus[10] detected variations in velocity of up to 20%, over the same range of frequencies at higher voidages. This was assumed to be due

to the presence of detergent within the flow, which was added to maintain the bubbly characteristics of the flow, in the latter experimental work. It should be noted that although Silberman worked with very low voidage flows, the average bubble size was much larger than used by Karplus.

The present air/water investigation will endeavour to reproduce the results of these previous authors and indicate that a variation of propagation velocity of a sinusoidal wave with frequency is the result of the change in behaviour of the gas phase from isothermal to adiabatic, as previously proposed in section 1.1.2.

2.2 Experimental apparatus

A diagram of the apparatus is shown in Fig. 5.1. Known mass flow rates of air and water were supplied to the mixing section. Within this section the air passed through a porous cylinder into the main water flow. This was found sufficient to provide a homogeneous distribution of bubbles of approximately uniform size (Fig. 6.1). The main section, a vertical $1\frac{1}{2}$" O.D. perspex tube, had affixed two crystal pressure transducers spaced a distance of 2 ft. apart. A short branch tube 1" O.D. connected the vibrating system to the main section. To prevent bubbles from accumulating in the branch tube, it was inclined at an angle to the main section. Having passed through the test section, the mixture was separated and the water recirculated.

2.2.1 Generation of wave

A vibrating system was required capable of producing fluid displacement amplitudes up to 0.1" on account of

the ranges of voidage and wave frequency (30 - 100 cps) to be investigated. This eliminated the possibility of using an electromagnetically driven diaphragm as used by Silberman [13] and Karplus [10].

The system shown in Fig. 5.2 was devised. A light aluminium piston in a brass cylinder of equal diameter to the branch tube, the piston being driven by an electro-mechanical vibrator. To prevent the fluid pressure on the piston from inhibiting the sinusoidal motion of the vibrator, a spring was inserted behind the piston. Once the required voidage was obtained in the main section, the piston settled to an equilibrium position determined by the characteristics of the spring. On connecting the vibrating system the piston moved about this equilibrium position. The spring was made so as to ensure a low natural frequency and hence minimal effect on the vibrator. A build up of pressure behind the piston was prohibited by attaching a small bleed line.

The whole vibrating system was connected to the branch arm of the main section with a thin rubber sleeve, so inhibiting vibrations from travelling through the perspex walls of the main section to the pressure transducers. The effectiveness of this could be verified by lowering the water level below the upper pressure transducer so causing the transducer signal to disappear and indicating

that the pressure waves were confined to travel within the fluid.

During these experiments, standing waves did not occur within the test section. This was probably due to the large attenuations of pressure waves, which occur in a two-phase mixture within the range of working voidages.

2.2.2 Detection and measurement of wave velocity

Signals from the two pressure transducers could be displayed simultaneously on either a C.R.O. or U.V. recorder. Measurements from the display on the C.R.O. required the use of a camera and trigger mechanism. Although this produced acceptable results, sample photographs being shown in Fig. 7.1, the U.V. recorder was favoured as a greater lateral spread of the transducer signals was possible. However, variations in the paper speed of the recorder resulted in some loss of this accuracy.

The majority of results shown in the following sections were obtained using a storage C.R.O. This allowed for easier, faster and more accurate measurements to be made. Unfortunately no camera was available with which to photograph the screen of this C.R.O. and hence permanent records (i.e. Figs. 10 and 22) were traced manually from the screen.

Measurement of the phase shift between the two sinusoidal signals gave a direct indication of the velocity of the pressure wave along the test section. Due to the possibility of phase shifts greater than one wave length, a system of identifying a given pressure

wave had to be developed.

Two sinusoidal input signals of near equal frequency applied to the vibrator resulted in an output sinusoidal pressure wave, the amplitude of which varied at a frequency equal to the difference of the two input signals. This system was rejected as, in order to detect a given wave, the "beat" frequency was required to be at least one tenth of the main wave frequency. It was thought that this may influence, significantly, the wave propagation velocity.

It was found that by switching off the vibrator, the resulting attentuation of the pressure wave was sufficient to identify the same pressure wave on both transducer signals. A typical photograph of the C.R.O. trace is shown in Fig. 7.2.

2.2.3 Voidage measurements

The voidage was measured using γ-ray attenuation. A single shot, split beam technique was used and found to give a good estimate of voidage regardless of radial variations of bubble density. A detailed description of the system is given in references 24 and 25.

Knowing the specific mass flow rates of the air and water, the liquid velocity and the slip velocity ratio could be calculated using the voidage measurement.

2.3 Factors affecting velocity of pressure wave measurements

2.3.1 Velocity of sound in a moving fluid

It has been shown (11) that a pressure wave moves through a stratified two-phase flow at a velocity relative to a weighted mean velocity of the fluid.

i.e $$U_{WAVE} = \bar{U} \pm C_{STRAT} \qquad (\bar{u} \ll c) \qquad 2.1$$

where $$\bar{u} = \frac{u_a \rho_a (1-\alpha) + u_w \rho_w \alpha}{\rho_a (1-\alpha) + \rho_w \alpha}$$

However, the validity of defining a sonic velocity in a stratified flow ($C_{STRAT.}$) has been questioned and it appeas likely that a pressure wave will move independently through each phase. Nevertheless, if the two-phase fluid is completely homogeneous with both phases moving at equal velocities it may be expected that

$$U_{WAVE} = \bar{u} \pm C_{HOMO} \qquad 2.2$$

It has been assumed in the present work that $\bar{u}$ can be replaced by the liquid velocity U_w.

Voidage and flow quality measurements in the vertical air/water flow used in this experimental work have indicated slip velocity ratios, between the phases, up to 1.5. By comparing equations 2.1 and 2.2, this may lead to maximum errors in the measured propagation velocity of U_W (σ -1)ft./sec. (when α is small). The maximum fluid velocities used in the present series of experiments were of the order of 3 ft./sec., hence maximum errors of 2 ft./sec. may be obtained by assuming pressure waves to travel relative to the liquid phase velocity.

2.3.2 Velocity of pressure waves in tubes

The velocity of sound in a fluid confined to a pipe is lower than the sonic velocity in an infinite medium [22]. Based on work by Lin and Morgan, Silberman [13] suggests that sound waves can be considered plane if the wave length is greater than twice the pipe diameter. At wave frequencies of 100 cps the velocities of sound measured in this experimental investigation were greater than 100 ft./sec. Therefore the minimum wave length is given by

$$\lambda = U/f > 1{\cdot}0 \text{ ft.} \qquad 2.3$$

The effect of viscosity, near the tube walls, on the propagation velocity of a wave has been shown by Rayleigh (27) to be

$$U_{PIPE} = U_\infty'\left(1 - \frac{1}{D}\sqrt{\frac{\mu}{\pi f \rho}}\right) \qquad 2.4$$

In a two-phase system, the average viscosity and density can be defined as

$$\mu_{TP} = \mu_W(1 + 2{\cdot}5\alpha) \qquad \text{(ref. 28)}$$

$$\rho_{TP} = \alpha\rho_n + (1-\alpha)\rho_W$$

Substituting the relevant values for an air/water system at atmospheric pressure it can be shown that:-

$$\frac{1}{D}\sqrt{\frac{\mu}{\pi f \rho_{TP}}} \approx 10^{-3} \qquad f = 10 \text{ cps}$$

Hence this effect is considered negligible.

It is therefore concluded that the measured propagation velocities of small amplitude waves in the present apparatus will be essentially the same as in an infinite medium.

2.3.3 Surface tension effects

It was supposed by Karplus (10) that the variation of sound velocity with frequency, which he detected, may have been the result of surface tension effects induced by the addition of detergent to the flow.

Theoretically McWilliams and Duggins (29) studied the effect of surface tension on the speed of sound in bubbly mixtures and concluded that for bubbles of radii greater than 10^{-2} inches this effect was negligible. It is therefore possible that Karplus was correct in his supposition as bubbles of average radius 2×10^{-3} inches were used in his work. In the present experimental work

the bubbles can be seen (Fig. 6) to be of the order of 10^{-1} inches and hence it is assumed that surface tension has no significant influence on the measured velocity of pressure waves through the medium.

2.3.4 Bubble resonance frequency

It has been found that the natural vibrations of the bubbles in a two-phase mixture have a marked effect on the velocity at which a pressure wave is transmitted, particularly when the wave frequency approaches the resonance frequency of the bubbles [13]. If the wave is 180^{o} out of phase with the oscillations of the bubble and of the same amplitude, then it is possible that the fluid will become virtually incompressible and hence an infinite velocity of sound will be recorded [30].

The experimentally proved formula for the resonance frequency of a spherical bubble [31] is

$$2\pi f_R = \left(\frac{3\gamma P_e}{\rho r^2}\right)^{\frac{1}{2}} \qquad 2.5$$

For an air bubble in water at atmospheric pressure and under isothermal conditions, this reduces to

$$f_R = 18/d \qquad \text{(where d is measured in ft.)}$$

The average size of bubbles shown in Fig. 6.1 is 0.1", or approximately 10^{-2} ft., in diameter and hence the resonance frequency of these bubbles will be of the order of 2,000 cps. The natural vibrating frequency of spheroidal gas bubbles and of spherical bubbles close to a rigid surface have been shown to be greater than the resonance frequencies previously discussed [32]. For spherical bubbles in contact with the pipe wall, it

appears from these results that bubble pulsation frequencies 50% greater than given by equation 2.5 may be experienced.

2.3.5 Tube radial vibrations

In the present air/water experiments, the pressure waves were transmitted along a fluid flowing in a perspex pipe, hence the elasticity of the pipe was such that it may be necessary to apply a correction to the measured propagation velocity of the wave.

This correction is given by (13)

$$U_{MEASURED} = U'_{\infty}\left(1 + \frac{D}{y}\frac{E_M}{E}\right)^{-1/2} \qquad 2.6$$

when E_M is the average bulk modulus of elasticity of the fluid (given approximately by equation 1.4) and E the modulus of elasticity of the perspex tube wall. D and y are the flow tube diameter and wall thickness respectively.

Assuming that the bulk modulus of the liquid phase is much greater than that of the gas phase, equation 1.4 reduces to

$$E_M \simeq \frac{1}{\alpha n P} \qquad \text{(P is the absolute pressure)}$$

On obtaining Young's modulus for perspex (22) it can be shown that in the present system

$$\frac{E_M}{E} \sim O(10^{-5}) \qquad [\text{ie. of the order of } 10^{-5}]$$

From the dimensions of the test section $\frac{D}{y} \sim O(10)$

Hence from equation 2.6 it is unlikely that radial vibrations of the tube walls will significantly affect the propagation velocity of a pressure wave through the mixture.

2.3.6 Tube transverse vibrations

During the measurement of the propagation of a sinusoidal pressure wave, the main bubbly flow was subjected to vibrations of known frequency via a small branch arm

(section 2.2). It was, therefore, possible that the test section would vibrate transversely giving a false indication of wave shape and velocity on the pressure transducers. This was most likely to occur when the frequency of vibration coincided with the natural frequency of a length of test section between supports. This effect was avoided by securing the test section, at four points along its length, to a vibration free Rolled Steel Joist. With the aid of the storage C.R.O. it was verified experimentally that the natural frequencies of all the sections of the apparatus, likely to affect the transducer readings, were much higher than the range of wave frequencies investigated.

2.4 Experimental results

The experimental data showed a variation of propagation velocity of sinusoidal pressure waves with frequency (Fig. 8). However, the range of velocities measured was greater than predicted by the theory given in section 1.1.2 which indicates that this effect is not due entirely to the variation of polytropic index of the gas phase.

The maximum wave frequency for which the propagation velocity could be measured was determined by the wave attenuation. At voidages above 20% this maximum was 100 cps. At lower voidages no significant increase in velocity was measured for wave frequencies between 100 - 150 cps.

It was suggested by Mawardi[14] that the transition from isothermal to adiabatic behaviour of an enclosed volume of gas occurs within the frequency range

$$0{\cdot}1 < \sqrt{F}\,\frac{V}{S} < 10 \qquad \text{(V and S measured in c.g.s. units)}$$

where S denotes the surface area of the enclosure containing a volume V of gas.

For a spherical bubble $\frac{V}{S} \approx \frac{r}{3}$ (r in cms.)

Hence for bubbles of diameter 0.1 inches the frequency range suggested is

$$5 < f < 500$$

For smaller bubbles, as used by Karplus[10], the transition is expected to occur within a higher frequency range, and therefore may be one of the reasons for the measured variation of sonic velocity with frequency (Fig. 1). However, it has been shown in section 2.3.3 that surface tension could also account for this variation.

In the present experimental work propagation velocities higher than the "adiabatic" sonic velocity were measured (Fig. 9) indicating the effect of some phenomena other than the variation of polytropic index of the gas phase.

The fluid pressure mid-way between the two pressure transducers on the main section of the apparatus was determined using a water manometer. This was taken to represent the mean pressure of the mixture within the test section and indicated an average pressure of 17 p.s.i. varying $\pm$ 1 p.s.i. with flow rate (3 ft/sec) and voidage.

At low voidages changes in wave amplitude resulted in a maximum variation of propagation velocity of 5%. At higher voidages such measurements were not possible as the waves were restricted to a small range of

amplitudes, determined by the wave attenuation and the maximum permissible amplitude of the vibrating system.

Each data point in Fig. 9 represents the measured propagation velocity of a wave with initial amplitude such that it was just detectable at the upper transducer. Slight distortion of the waveform was observed particularly at high voidages and high wave frequencies where increased wave attenuation required a larger initial wave amplitude. The magnitude of the pressure waves was in all cases much less than 1.0 psi and hence it is improbable that this is the cause of the high measured velocities.

In order to investigate, further, possible causes why the measured propagation velocities are higher than the theoretical "adiabatic" sonic velocity, the propagation of small impulse (or triangular) pressure waves through the same medium were studied. These waves were expected to travel at the adiabatic sonic velocity.

2.5 Finite impulse pressure and rarefaction waves

In a compressible single phase medium it is known that a finite pressure wave will steepen [33] and eventually become a "shock" wave, which propagates at a speed greater than the sonic velocity within the fluid.

Campbell and Pritcher [34] showed analytically that within a two-phase two-component mixture "shock" waves travel at a speed given by

$$U^2_{shock} = \frac{P_1}{P_2} C^2 \qquad 2.7$$

where P_1 and P_2 represent the fluid pressure on either side of the wavefront. This has been verified experimentally [34][35]

(Fig. 12). In the present investigation impulse waves have been generated instead of "step" waves as studied by other authors. These impulse waves have been of relatively small amplitude (<1 p.s.i.) and so will not propagate at a velocity significantly greater than the sonic velocity in the medium. It is, therefore, anticipated that the velocity of this type of wave will verify the adiabatic velocity of sound as predicted by equation 1.15.

2.5.1 Modifications to wave generator

The cylinder/piston system as described in section 2.2.1 was modified to enable the generation of both presure and rarefaction impulse waves.

The electro-mechanical vibrator was disconnected and the piston support spring, as shown in Fig. 5.2, replaced by a considerably stiffer one. To generate the wave, the piston rod was pulled manually to compress the spring and then released.

For the propagation of a rarefaction wave the spring was placed around the piston rod against the back surface of the cylinder and hence the reverse action was obtained.

As these systems were manually operated, the amplitude and steepness of the wave could not be determined before the wave was detected by the lower pressure transducer.

2.5.2 Shape of waves

Sample traces from the C.R.O. screen indicating the change in shape and the velocity of the pressure impulse and rarefaction impulse waves are shown in Fig. 10.

The wave shape is basically triangular, the height or amplitude representing pressures less than 1 p.s.i. above the ambient pressure and the wave "thickness" representing a time interval of approximately 4 m/secs.

Slight changes in wave shape were detected as the waves progress along the flow, the pressure waves steepening and the rarefactions becoming less steep. However, as can be seen from the results (Fig. 11) this did not significantly affect the measured wave velocity.

The principal impulse waves were followed by a smaller wave of the opposite sense. When the pulse was generated in a single phase liquid medium, the main wave and the trailing wave were of the same magnitude, indicating that this is caused by the action of the wave generator. The fact that the trailing wave became less significant with increasing voidage is probably due to an effect of the compressibility of the medium.

This point will be discussed in section 3.5 when the shape of an impulse wave in a steam/water medium is examined.

2.5.3 Experimental results

Experimentally measured propagation velocities are shown in Fig. 11 for varying flow voidage. Within the spread of experimental data, inherent in these types of measurement, (Figs. 11 and 19) no significant velocity variation was detected with changes of wave amplitude or fluid velocity. Also pressure and rarefaction impulse waves were found to propagate at approximately the same velocity.

The results can be seen to be noticeably higher

than predicted for the adiabatic velocity of sound (equation 1.15) at a fluid pressure of 17 p.s.i.

The distribution of experimental points relative to this sonic velocity curve appears to indicate that the fluid pressure has been underestimated. As mentioned previously, the pressure within the test section was found to vary by less than $\pm$ 1.0 p.s.i. for varying flow rates and voidages.

By considering the mechanics by which a pressure wave steepens and a rarefaction wave becomes less steep when travelling through a compressible medium[33], the velocity calculated by measuring the displacement between the "peaks" of pressure waves, (either impulse or sinusoidal, Fig. 7, 10) will be the sonic velocity corresponding to the fluid pressure of $P + \Delta p$, where P is the initial or ambient fluid pressure and Δp is the amplitude of the pressure wave. In the present experiments the wave amplitudes were less than 1 p.s.i. and so this may account for small deviations from the sonic velocity curve, but not the large deviations measured.

When considering the propagation of waves through a homogeneous bubbly mixture, if the two phases are at different pressures, it is probably the pressure of the gas phase which determines the wave velocity. This is because the properties of the gas phase are more pressure dependent than the liquid phase, which is generally assumed incompressible.

Although an excess pressure within the bubbles would account for the measured discrepancy between theoretical and experimental results, it is difficult to

explain such a pressure difference, for as noted in section 2.3.3, the bubbles within the present system were sufficiently large to neglect surface tension effects.

The same deviation of experimentally measured velocities of "shock" waves from theoretical predictions was noted by Hamilton Nyer and Schrock[35] (Fig. 12). The apparatus used to obtain experimental data was similar to the present system inasmuch as the bubbly air/water mixture was flowing vertically under steady conditions and the voidage measured using γ-ray attentuation techniques. This suggests that the discrepancy between experiment and theory at higher voidages is caused by the properties of the flow.

The accuracy of voidage measurements using the present system (section 2.2.3) has been checked by comparing with results obtained using a double valve technique[25]. It is indicated that errors of up to 5% voidage may be incurred, which possibly explains the spread of results, particularly at low voidages. A similar error will also occur in estimating the flow velocity, as this was obtained from the water flow rate using the equation:-

$$G_w = U_w \rho_w (1 - \alpha) \qquad 2.8$$

Due to the small liquid velocities used in the present work the error in U_w will be negligible when compared to the measured wave propagation speeds.

It was considered that the existence of a slip velocity ratio between the phases may effect the wave velocity. As the experimental points in Fig. 11 show no noticeable variation with fluid velocity and hence

slip velocity ratio (Chapter 6), this effect must be small.

The two-phase flow in the test section was observed to be bubbly for voidages up to 30%, however at the higher voidages, pulsations of the flow were noted. It is probable that under such conditions the visible bubbly flow near the tube wall concealed "slug" formation in the tube centre. The range of flow properties (mass flow rate and quality) used in these experiments are shown in the flow map for vertical air/water systems (Fig. 36.2). It can be seen that "slug" flow may occur at the larger voidages.

The velocity of sound in a two-component "slug" flow is given by [12].

$$C_{SLUG} = \frac{C_W C_A}{(1-\alpha)C_A + \alpha C_W} \qquad 2.9$$

Hence $$C_A < C_{SLUG} < C_W$$

The derivation of the above equation was based on a flow pattern consisting of alternate regions of gas phase and liquid phase. If the flow pattern is alternate regions of high (MAX) and low (MIN) voidage, such as occurs in the observed pulsating flow, and if it is assumed that each region is equal in length, then equation 2.9 can be written:-

$$C_{MEAN} = \frac{C_{MAX}\, C_{MIN}}{C_{MAX} + C_{MIN}} \qquad 2.10$$

In this case the γ-ray technique for measuring voidage will record $\bar{\alpha}$, where

$$\bar{\alpha} \simeq \frac{\alpha_{MAX} + \alpha_{MIN}}{2}$$

However, due to the non-linearity of the variation of sonic velocity with voidage, the velocity of a wave passing through the medium will be greater than the sonic velocity corresponding to a **homogeneous voidage** $\bar{\alpha}$.

The presence of non-homogeneities within a visibly bubbly flow will, therefore, increase the propagation velocity of a wave significantly and is probably the reason why velocities greater than the adiabatic sonic velocity in a homogeneous mixture were measured in the present experimental work.

2.6 Summary of experimental results obtained using air/water systems

The variation of propagation velocities of small amplitude sinusoidal waves were measured, with frequencies from 30 c.p.s. to 100 c.p.s. Within the range of experimental accuracy, at low voidages ($<10\%$) the measured velocities were between the "adiabatic" and "isothermal" sonic velocities of the medium. This indicates that the variation of polytropic index of the gas phase with wave frequency may be an important factor when predicting the velocity of sound in two-phase media.

At voidages greater than 10%, it is possible that non-homogeneity of the mixture resulted in the high propagation velocities measured in this experimental work and also that of other authors (35).

A study of the velocity of small amplitude impulse waves through the media, reinforced the above conclusion and also indicated no significant difference between the behaviour of impulse and step waves (Fig. 11 and 12).

The systems for generating, detecting and recording the pressure waves, in this series of experiments, were considered satisfactory and were hence transferred to the steam/water system described in the following chapter.

3. EXPERIMENTAL MEASUREMENT OF THE PROPAGATION VELOCITY OF SMALL AMPLITUDE WAVES IN STEAM/WATER BUBBLY MIXTURES

Many of the previous experimental studies into the sonic velocity in two-phase one-component mixtures have been carried out using wet steam or at least very high quality mass flows. In such media the mixture can generally be assumed to be in thermodynamic equilibrium (36)(37)

The present experimental programme deals with low quality steam/water flows where the vapour phase is distributed as bubbles within the liquid phase. Previous measurements of the velocity of a pressure wave in a liquid continuous, steam/water flow have shown that this medium may or may not be in equilibrium (5)(15)(21), possibly depending on the shape of the wave.

In section 1.2 it was hypothesised that the velocity at which a wave is transmitted through a medium depends upon the degree of equilibrium or 'fraction of equilibration' attained by the fluid within the wave, this being controlled by the rate of heat transfer between the liquid phase and the bubble surface.

This experimental work is intended to verify this approach to the problem of thermodynamic non-equilibrium in bubbly one-component flows and hence lead to a better understanding of the heat transfer coefficient of the bubble/liquid interface.

3.1 Description of steam/water apparatus

The basic requirement of the apparatus was that it should produce a homogeneous bubbly mixture in thermodynamic equilibrium. A flow of near saturated water

which flashed due to the pressure gradient along a pipe provided the homogeneous mixture, the flow rate being sufficiently high to prevent phase separation.

The flow map shown in Fig. 36.1 indicates that in a horizontal steam/water system, at atmospheric pressure, the required specific mass flow is greater than 700 lb/ft^2 sec, however due to the inclination of the test section it was found that a flow rate of approximately 500 $lb/ft^2 sec$ maintained a homogeneous distribution of bubbles.

Thermodynamic equilibrium was ensured by inclining the test section to the horizontal such that the two-phase frictional pressure drop became equal to the static pressure rise, resulting in zero pressure drop along the section.

Using the empirical equation for the two-phase frictional pressure drop (equation 7.15), this condition can be written

$$\frac{\Delta p}{\Delta \ell} = 0 = \rho_f (1-\alpha) g \sin\theta - \frac{4f}{2D} U_o^2 \rho_f \left(1 + \frac{m\alpha}{1-\alpha}\right) \qquad 3.1$$

Hence, for a given angle, θ, there is a unique value of voidage which can be obtained for a given initial fluid velocity (U_o).

By substituting approximate expected values of the variables into the above equation it can be shown that a near vertical test section is required to satisfy this condition. In practice, it was found that a test section angled at 70° to the horizontal provided a sufficient range of 'equilibrium' voidages. It must therefore be

assumed that the expression for the frictional pressure drop may not be accurate for very low voidage flows.

A further advantage of the angled test section was to reduce the slip velocity ratio to near unity. Comparison with predicted values in an air/water system (section 6.4, Fig. 31) shows that in flows angled at 70^{o} down from the horizontal the slip velocity ratios are small and possibly less than unity. In view of this it was considered that the flow was completely homogeneous.

A diagram of the apparatus is shown in Fig. 13. Water, driven by the centrifugal pump, flowed through the heater and flashed as the flow passed through the wire mesh at the top of the test section. Flashing was initiated either by the pressure drop across the mesh or the turbulence induced within the flow by the mesh. The inclination of the test section, as previously discussed was such that no further flashing took place until the flow entered the condenser, after which the water was recirculated.

The test section was the same in principle as the air/water apparatus, (section 2.2) although it should be noted that the pressure wave travels in the opposite direction to the fluid flow, increasing the effective distance between the transducers.

Copper tube $\frac{5}{8}$" I.D. was used in the construction of the test section, the pressure transducers being mounted on the tube a distance 9.25" apart. The high attenuations experienced by a wave in a steam/water medium made this distance the maximum which enabled detection of the pressure

wave at the upper transducer, over an acceptable range of voidages. A 6" length of glass tubing was inserted between the transducers to allow for observation and photography of the flow.

It has been suggested[16] that vaporization and condensation within a bubbly steam/water mixture occurs at different rates, malproducing an accumulation of our may acvapourate within the branch arm of the main section so greatly increasing the attenuation of the wave. To prevent this, cold water was continuously injected into the system. This flow rate of water was kept very low so as to have a negligible effect on the pressure drop along the main section. A drain was installed to maintain a constant level of water in the condenser.

Water manometers were used to detect any change in the pressure drop and hence variations of voidage along the test section. Bubbles were regularly expelled from the manometers by applying pressure to the open ends. The accuracy of these pressure readings are discussed in section 3.1.5.

3.1.1 Generation and detection of wave.

The systems described in sections 2.2 and 2.5.1 were used, except that due to the increased attenuation effects, a larger electro-mechanical vibrator was necessary giving a maximum amplitude of 0.3" at a frequency of 30 cps. A storage oscilloscope was used to record the transducer signals.

3.1.2 Voidage measurements

The range of working voidages was restricted by the

attenuation of the waves and the coalescing of the bubbles to form 'plugs'. The latter was found to be more restrictive at velocities of 10 ft/sec and permitted a maximum working voidage of approximately 5% (Fig. 14).

At such low voidages the γ-ray technique (section 2.2.3) proved unsuccessful in estimating the voidage, probably due to the small dimensions of the test section.

Measurement of the liquid temperature loss between a point in the flow before the mesh and a point within the test section would yield an estimate of the flow quality. Neglecting increases in kinetic energy of the fluid, from the energy equation (7.22)

$$\Delta x = \frac{C_w}{h_{fg}} \Delta T \qquad 3.2$$

At atmospheric pressure using equation 5.4, and neglecting any slip velocity between the phases in a steam/water medium, a voidage of 5% corresponds to a quality of $\simeq 10^{-5}$. Hence the liquid temperature drop due to the formation of this amount of vapour is 10^{-2} °F. No equipment was available with which to measure temperature differences of this order.

It was thought possible to estimate the voidage by noting the change of pressure drop along the test section as the fluid commenced to flash. However, as previously noted, the accuracy of the empirical formula for two-phase frictional pressure drop (7.15) is unknown at low voidages.

Other methods, making use of the refractive index [38] and electrical impedance [39] of the mixture were considered unsuitable for measuring the voidage in the present system [40].

A photographic method was finally used to estimate the voidage. At low voidages the bubbles were separated sufficiently to enable the approximate number of bubbles present in a pound of fluid to be determined. It was confirmed that the camera detected all of the bubbles by varying the focal plane. In all cases the number of bubbles/lb of fluid was estimated at 20,000. The Polaroid oscilloscope camera used for this work had a restricted depth of field within which the bubbles were in focus, and so, although all the bubbles could be detected, the dimensions of many were indeterminate. It was assumed that the distribution of bubble sizes throughout the flow could be characterized by the bubbles in focus. To enable the largest sample of bubbles to be measured the focal plane was fixed at the centre of the test section. This can be seen from the photographs (Fig. 15) where the bubbles at the wall of the tube are in focus. The fact that, in these photographs, the tube wall is not visible indicates that, due to the refraction of the light in passing through the glass/water cylindrical lens, a magnification of the bubbles is observed. From the photographs it can be seen that, in the mid-plane of the tube, the inner diameter of the glass section is magnified so as to equal the outer diameter. The glass section was of radial dimensions $\frac{5}{8}$" I.D. and $\frac{3}{4}$" O.D. and hence the magnification factor is 1.2. This was verified by photographing a rod of known diameter in a similar glass section.

At voidages approaching 5% slight bubble amalgamations were observed resulting in a few larger non-spherical

bubbles. Although this was considered not to cause major deviations from the spherical bubble assumption made in the theory, the volume of these bubbles could not be estimated as only two-dimensions could be measured. It was therefore assumed that these non-spherical bubbles were made up of spherical bubbles of the same size distribution as the remainder of the flow.

For accurate measurement of the bubbles, the photographs were analyzed on a projector giving x 15 magnification.

3.1.3. Experimental procedure.

On heating the water to approximately its saturation temperature, the flow rate was set such as to give a small pressure change along the test section. Heat was then applied until sufficient flashing occurred to reduce the pressure difference to zero. Small adjustments were made to maintain stable conditions. This procedure took sufficient time to ensure that excess air in the water was eliminated. The importance of this was due to the possibility of obtaining a low quality flow within the test section before saturation conditions were attained by the liquid. In this case one would have probably measured the no-mass transfer sonic velocity for all frequency waves. Once steady conditions were obtained, results were taken and the voidage checked intermittently by photographing the flow.

3.1.4. Background noise within a flashing two-phase system.

Pressure fluctuations are known to be prominent in two-phase flows and have been used to analyze flow patterns [41]. However, during preliminary tests with the

present steam/water apparatus, the transducers detected a significant amount of background noise which had to be reduced in order to identify clearly the generated sinusoidal waves.

Prior to the initiation of flashing a considerable amount of noise, thought to be due to the main pump, was detected. This fortunately disappeared as soon as flashing commenced probably due to the attenuation of the noise in passing through the two-phase mixture between the mesh and upper transducer. The effect of turbulence was also noted mainly on the lower transducer, this was reduced by careful alignment of the test section and by ensuring that the sensitive surfaces of the pressure transducers were positioned in line with the pipe inner wall.

As the liquid neared the saturation temperature corresponding to the fluid pressure in the test section, boiling occurred in the condenser resulting in high frequency noise being transmitted up the flow to the transducers. Maintaining a water level in the condenser, which allowed the formation of a free jet at the outlet of the test section, reduced this noise to negligible proportions.

At the higher voidages, sharp peaks in the upper transducer signal were detected, this was thought to be caused by cavitation or the impaction of bubbles on or near the transducer face. However, this occurred outside the range of voidages, permitted by the wave attenuation, in which measurements could be made.

It was noted that while results were being taken the signal to noise ratio of the system was of the order 5:1.

While the background noise may cause appreciable error in measuring both wave velocity and attenuation it was considered that as the noise was apparently completely random these errors would represent a spread, rather than a shift, of experimental data.

3.1.5. Accuracy of measurements.

Difficulty was experienced in maintaining steady flow conditions within the test section. A pressure regulating valve was introduced to enable finer control of the steam supply to the heater but, nevertheless it was generally not possible to keep the pressure drop along the test section exactly zero for any length of time. In many cases it varied by $\pm \frac{1}{2}$" of water. This was unlikely to cause significant departures from thermodynamic equilibrium within the mixture, however it probably caused slight increases or decreases in voidage along the flow.

From equation 3.1 it can be shown that for a small change in pressure gradient along the test section

$$\Delta\left(\frac{\Delta p}{\Delta \ell}\right) = -\Delta\alpha\rho_f\left(g\sin\theta + \frac{4f}{2D}U_o^2\frac{m'}{(1-\alpha)^2}\right) \qquad 3.3$$

A variation in pressure drop, between the manometer tappings, of $\pm \frac{1}{2}$" of water corresponds to a pressure gradient of $\pm$ 45 pdls/ft^2. Substituting the relevant parameters into the above expression results in a maximum change of voidage of $\pm$ 0.5%. The glass section at which photographs were taken was situated midway between the transducers and hence in some cases the measured voidage represents a mean value.

The displacement between the transducer signals were

measured directly from the C.R.O. screen. In theory it was possible to elongate the time scale of the oscilloscope to enable very accurate measurement, however this was impractical as the position of the wave peak then became a matter of conjecture, particularly at low wave frequencies. Generally a time scale was used which would allow the time displacement to be measured within 0.5 ms. This represents a possible error of 6% in measuring velocities of 100 ft/sec and 10% error in velocities of 200 ft/sec.

The wave amplitudes were restricted to be as small as possible to prevent excessive wave distortion. However, in some cases, distortions were unavoidable and detected by the discrepency in time displacement between the peaks and troughs of each wave trace. This led to errors in measuring the velocity of the wave which will be discussed in section 3.3.

Of the phenomena described in section 2.3, only surface tension proved to have a possible effect on the propagation speeds in the present system.

Except at very low voidages, the measured bubble radius was greater than 10^{-2} inches and hence the effect of surface tension is negligible [29]. However, the velocity of wave propagation may be increased at low voidages due to the pressure which exists within the bubbles, this being greater than the liquid pressure.

Using the well known formula

$$\Delta p = \frac{2\sigma}{r} \qquad 3.4.$$

the excess bubble pressure can be calculated. If 20,000

bubbles/lb exists in a medium of voidage of 1% then the average diameter of the bubbles is 6.7×10^{-3} inches. From equation 3.4 the pressure difference between the phases is of the order 0.2 psi. Comparing this with the maximum wave pressure of 1.5 psi it can be seen that surface tension is unlikely to have a measurable effect.

3.2. Experimental results.

A significant spread in the measured velocities was obtained probably due to the difficulty in maintaining a constant voidage within the test section. This was further emphasised by the large variations in sonic velocity for small voidage changes, over the working range of voidage. (Fig. 2). Understandably the spread of experimental data decreased with increasing voidage.

A variation in the velocity of propagation with the wave frequency was detected (Fig. 16,17). This behaviour has been predicted successfully using the theory (appendix A) and a constant value of the heat transfer coefficient $h = 0.5$ BTU/ft^{2}sec^{o}F. The variable value of h suggested in section 7.5.2 was found to predict smaller velocity variations then measured experimentally.

It was indicated by Collier and Wallis[11] that for a stationary bubble within a liquid, the heat transfer coefficient is given by Nu = 2.0.

For bubbles of diameter 10^{-3} ft and assuming the thermal conductivity of the water phase to be 10^{-4} BTU ft/ft^{2}sec^{o}f, and using the definition of Nusselt number[85], $Nu = {}^{hD}/_{K}$, then Nu = 2.0 implies that h = 0.2 BTU/ft^{2}sec^{o}F. In the present experimental system very

little relative velocity existed between the phases, it is therefore not unexpected that the value of h suggested by comparison of theoretical and experimental results, is of this order.

At low frequencies, wave velocities significantly higher than theoretically predicted were measured. The linearisation used in the analysis was $\Delta p/p \ll 1.0$ where Δp is the amplitude of the pressure wave. This condition was satisfied in the present work as wave amplitudes between 0.5-1.5 p.s.i. were generated. Depending on the rate of mass transfer between the phases, Δp may be sufficient to condense all of the vapour phase. This is most likely to occur at low wave frequencies, where conditions will more nearly obtain equilibrium, and at low voidages, where the required Δp is small. In these cases the wave amplitude can no longer be considered infinitesimal.

3.3. The propagation velocity of finite amplitude sinusoidal waves.

In a single phase compressible medium a pressure wavefront tends to steepen and a rarefaction becomes less steep as a result of the variation of compressibility and density of the medium with pressure (33). The effect will be more significant in a two-phase one-component medium where changes in pressure may cause evaporation or condensation to occur producing a variation of voidage throughout a wavefront. The velocities of various portions of the wave will differ significantly depending on the local value of pressure and voidage.

In the present experimental work it was attempted to restrict the amplitude of the sinusoidal pressure waves

so as to reduce wave distortion to negligible proportions. However, owing to the initial wave amplitudes required to overcome attenuation effects, distortions were unavoidable in some cases.

Fig. 18.1 shows a trace from the U-V recorder showing a change in shape of a finite amplitude wave. The pressure peaks have been displaced to the left, an effect which is more noticeable on the upper trace as this represents the wave shape a further 9" along the test section. The distance between corresponding pressure peaks in each trace was taken to be a measure of the propagation velocity of the wave, therefore, in the case shown in the figure, the measured velocity is significantly greater than for a smaller amplitude wave.

Neglecting attenuation effects, and assuming the sonic velocity in a medium to be directly proportional to the liquid pressure, the idealised change in shape of a sinusoidal wave is shown in Fig. 18.2. After some time the wave becomes a 'saw tooth' shape and eventually, it is anticipated that, the distorted 'shock' type of wave will 'overtake' the preceding rarefaction, thus eliminating the pressure wave. This will be discussed further in section 3.5.2.

3.4. The propagation velocity of finite amplitude step and impulse waves.

The velocities of propagation of step pressure waves with sufficient amplitude to condense all of the vapour phase, were measured by Karplus (15). However, the wave-fronts were found to become less steep as they progressed

through the fluid, indicating that the mixture may not have been in a state of thermodynamic equilibrium before the application of the pressure pulse (section 3.5.1).

Similar experiments were made by Barclay[5] who found the waves to change in shape according to compressible flow theory. A discrepancy was detected between the velocities of pressure and rarefaction step waves, this being possibly due to the effect of large wave amplitudes and the change in shape of the wavefronts as similar variations were measured by Dejong and Firey[37] when examining the sonic velocity in air. In a two-phase, liquid continuous medium, no difference in propagation velocity of the two types of wave could be detected[37]. This was also found by Grolmes and Fauske[21], their results being shown in Fig. 19.

The wave generating system described in section 2.2.1 was more adaptable to the propagation of impulse waves rather than step waves as investigated by other authors.

From the frequency spectra of step and impulse waves shown in Fig. 3.2, both waves can be seen to contain high frequency components which, from the theory given in section 1.3, are predicted to travel at the no-mass transfer sonic velocity. If the minimum frequency component which propagates at this velocity is denoted by f' then providing the step and impulse waves have not propagated sufficient distance to make all frequency components above f' negligible due to attenuation, the velocity of the leading point or "foot" of both step and impulse waves may be expected to travel at the same velocity.

As previously noted in section 1.42, the "bulk" velocities of these waves will be significantly different and this will result in differing rates of steepening of the wavefronts.

The above analysis cannot be applied to perfectly formed step and impulse waves as these are categorized as "shock" waves and require a separate treatment (97).

3.4.1 Present experimental investigation

As in the experiments with air/water mixtures, the wave generating system was modified as indicated in section 2.5.1 to enable the propagation of small amplitude pressure and rarefaction impulses.

Although these waves will be referred to as impulses they would be more accurately described as "thin" triangular waves. The time "thickness" of the waves was of the order of 4 ms making the wave similar in form to one cycle of a 250 cps sinusoidal wave.

As the wave velocity was assumed to be characterised by the velocity of the foot of the wave, various degrees of steepening of the wavefront did not affect the results. Wave amplitudes of 1-3 p.s.i. were generated, but this also did not significantly vary the velocity of wave propagation.

Experimentally determined velocities are compared to the no-mass transfer sonic velocity in Fig. 20. Rarefaction and pressure impulses were found to travel at approximately the same velocity.

Simultaneous photographing of the flow and generation of the wave allowed more consistent estimates of voidage to be made than in the previous experimental programme.

The results indicate that within the leading part of a wave of this type no mass transfer occurs and hence the velocity of the 'foot' of the wave will be independent of the following waveform, providing a pressure discontinuity does not occur.

3.5. Analysis of waveforms.

As a wave progresses through a two-phase medium, the shape changes continuously. Generation of the wave in a single phase water medium showed the initial shape of an impulse wave to be closely approximated by two triangular waves of opposite sense. Due to compressibility and mass transfer effects within the steam/water mixture, the wave profile had significantly changed by the time the wave reached the first transducer and a further change was detected by the second transducer. Ideally for an investigation of this sort, more pressure transducers should be equally spaced along the test section giving a detailed indication of variations in waveform. Although in the present experimental apparatus only two transducers were available, with the knowledge of the initial waveform a few tentative conclusions can be drawn.

In the following analysis it is convenient to divide the waveform into two portions, the wavefront and the 'trailing' wave.

3.5.1. Change in shape of the wavefront.

The wavefront is defined as the initial variation of pressure from the ambient fluid pressure to the maximum (or minimum in the case of a rarefaction) wave pressure. This may be expected to behave in a similar way to the

wavefront of a step wave as investigated by other authors.

Fig. 22 indicates a steepening of the front of a pressure impulse caused by the pressure peak travelling at a higher velocity than the 'foot' of the wave. For similar reasons the wavefront of a rarefaction decreased in steepness (Fig. 23). This is in agreement with compressible flow theory [33] [5][21] and previous experimental work [15]

Karplus found that pressure wavefronts became less steep in steam/water mixtures, however it was observed that vapour bubbles continued to grow in the initial part of the wave, with complete condensation occurring behind the wave. This would indicate that the mixture was not initially in thermodynamic equilibrium. With the present experimental system it was possible to adjust the flow conditions such that either condensation or vaporization occurred along the test section. Impulse waves were, therefore, propagated through mixtures of approximately the same mean voidage for pressure variations along the test section of 0, $+\Delta p$ and $-\Delta p$.

Fig. 21 shows sample wave profiles obtained in these three cases. It can be seen that if vaporization occurs along the test section (i.e. the wave propagates through a medium of decreasing voidage) it is possible that a pressure wave will become less steep. Similarly if condensation occurs within the fluid, the pressure wave becomes much steeper than expected from compressibility considerations. Rarefaction waves may also be found to steepen while passing through a medium of increasing voidage (condensation

occurring in a direction opposite to the wave motion).

Although the above wave characteristics were observed to occur regularly, they were not general. Since the sonic velocity in a steam/water mixture depends on the value of $\partial x/\partial p$ (equations 1.13 and 1.16) which includes the rate of vaporization in the initial fluid and the wave shape, it is suggested that only certain combinations of these two factors will result in the above wave characteristics.

3.5.2. Trailing pressure wave.

As previously noted, each impulse wave was followed by a similar wave, opposite in sense. This occurred at all amplitudes and is probably due to the action of the wave generating system. Such a waveform was thus taken to be the initial shape of the wave propagating through the steam/water mixture. Figs. 22 and 23 give an indication of how the waveforms varied while progressing along the flow. The variation was found to occur more quickly at higher voidages suggesting that the principal cause is mass transfer between the phases, this being dependent on the inter-phase surface area.

Each point on the wave may be assumed to travel at the sonic velocity corresponding to the local pressure, quality and the rate of change of quality with pressure (equations 1.13 and 1.16). As little distortion of similar waves was found to occur in air/water mixtures (Fig. 10) and the generated waves were generally of small amplitudes (<1.5 p.s.i.), it is likely that the variations of sonic velocity with local wave pressure and hence changes in compressibility of the medium can be neglected.

The rarefaction which trails the pressure impulse, quickly elongates and reduces in amplitude,as can be seen in the traces (fig. 22), and gives the appearance of having disappeared completely. However during the propagation of the wave, vaporization was observed to take place indicating the continuous presence of a rarefaction.

The profile of the rarefaction impulse and trailing pressure wave is more complex, (Fig. 23) the change in shape of the latter portion of the trough being of particular interest, as this is the position where the lowest wave velocities are measured and, it is also likely that the position of maximum wave voidage will be in this region. If the point of maximum voidage within the wave could be determined accuractely, an estimate of the rate of vaporization within the mixture could be made. Since the velocity of each portion of the wave depends on the local rates of change of pressure and quality, an elementary analysis indicates that the point of maximum voidage lies to the left of the point of minimum wave velocity (Fig. 23).

The above type of wave analysis can only be valid for small distortions of the wave shape. Larger distortions may be expected due to the trailing pressure wave "overtaking" the preceding rarefaction, resulting in a pressure between the rarefaction minimum and pressure maximum. At higher voidages the trailing pressure wave did not occur, possibly because the rarefaction and pressure portions of the wave had combined leading to the exceptionally large measured attenuation of the rarefaction. It is also possible that due to the evaporation which takes place within the mixture during the passing of the rarefaction, the following pressure wave becomes less

steep (section 3.5.1) and eventually disappears.

From the above discussion it can be seen that, if the wave velocity is defined as the velocity of a given point on the wave profile, then changes in wave shape are important, even when considering small amplitude waves in two-phase one-component mixtures. The rate of mass transfer appears to be one of the most important factors governing the variation of waveform, this being dependent on quality and phase distribution.

3.6. Summary of results.

Experimental results have shown that the velocity of propagation of sinusoidal waves in two-phase steam/water bubbly mixtures can be predicted using the theoretical analysis (appendix A) based on conduction controlled mass transfer between the phases. The results indicate a value of the heat transfer coefficient (h) of 0.5 $BTU/ft^2 sec\,^oF$, which compares favourably with the findings of other experimenters [23].

Due to the large wave attenuations which occur in such media, distortion of the waves was inevitable in certain cases and gave rise to higher measured velocities.

The foremost point of small amplitude impulse (or triangular) pressure and rarefaction waves were found to travel at approximately the no-mass transfer sonic velocity through a mixture initially in thermodynamic equilibrium, thus behaving similarly to a step pressure wave [21].

Again wave distortion was found to be significant when considering the velocity of the 'bulk' of the wave. The change in shape of the wavefront was shown to be dependent

upon the initial thermodynamic state of the medium, indicating a possible explanation of previous experimental observations [5][15].

4. ATTENUATION OF PRESSURE WAVES IN A TWO-PHASE MEDIUM

When an infinite fluid medium is made to vibrate, energy losses occur due to thermal conduction and viscous effects, these mechanisms being generally termed, internal friction [42]. Very little is known about this phenomenon in a two-phase mixture. However, a measure of the energy loss of a wave, which is propagating through a medium can be gained by considering the impedance of the medium or, alternatively, the amplitude attentuation of the wave in travelling a known distance through the medium.

The attentuation constant is generally measured in nepers/unit length [22].

i.e. $$k = \frac{1}{2d} \text{Log}_e \frac{A_0}{A_d} \frac{I_0}{I_d} \qquad 4.1$$

where A_0 and A_d are the wave ~~amplitudes~~ intensities at points $\ell = o$ and $\ell = d$ in the medium.

Sometimes the attentuation is referred to in decibels/unit length in which case

$$k' = \frac{10}{d} \text{Log}_{10} \frac{A_0}{A_d} \qquad 4.2$$

and $$k' = 8{\cdot}68\, k \qquad 4.3$$

The characteristic impedance of a medium [26] is defined by the equation:-

$$Z = \rho C \qquad 4.4$$

where C is the sonic velocity in the medium of density ρ.

Using the definition of sonic velocity (equation 1.13)

$$Z = \left[-\left(\frac{\partial P}{\partial V}\right)\right]^{1/2} \qquad 4.5$$

When the medium is restricted to a tube it is possible that viscosity has a dominant effect on wave attenuation. For laminar fluid flow in a small diameter tube, it has been suggested that the impedance is given by Poiseuilles' coefficient.

$$Z_T = \frac{8\mu c}{R^2 \omega} \qquad 4.6$$

For larger flow tubes, across which the fluid velocity can be considered constant except for a small annulus near the tube wall, it was indicated (43) that the impedance is equal to:-

$$Z_T = \frac{c}{R}\sqrt{\frac{2\rho\mu}{\omega}} \qquad 4.7$$

For large tubes satisfying the condition $R \gg (\mu/2\omega\rho)^{1/2}$, the impedance and attenuation of the medium are related by the equation

$$k_T = \frac{Z_T \omega}{2\rho c^2} \qquad 4.8$$

Hence for waves propagating in a tube, the wave attenuation due to viscous effects near the tube wall is given by:-

$$k_T = \frac{1}{RC}\left(\frac{\omega\mu}{2\rho}\right)^{1/2} \qquad 4.9$$

This equation does not include the effect of heat conduction across the wall of the tube, however, it has been suggested that such losses have an equivalent effect on the attenuation of a wave, to an increase in the viscosity of the medium. The "effective viscosity may be given by (43) :-

$$\mu' = \mu\left[1 + (\gamma - 1)\left(\frac{K}{\mu C_p}\right)^{1/2}\right]^2 \qquad 4.10$$

Equation 4.9 indicates the additional attenuation experienced by a wave in a tube, over a similar wave in an infinite medium, and so does not predict internal friction effects. There appears to be no general theory for predicting the attenuation of waves in an infinite medium, particularly two-phase mixtures.

A perturbation technique (as used in appendices A and B) for investigating the propagation of small amplitude waves in a homogeneous two-phase bubbly mixture, yields no solution for the attenuation constant if heat transfer and viscosity effects are omitted from the theory. As little is known about these effects in an air/water mixture, this approach is fruitless.

In the theory given in Appendix A, it is assumed that in a steam/water mixture, heat is transferred between the phases at a rate determined by the heat transfer coefficient of the bubble surface, and the analysis predicts an attenuation constant given by:-

$$k = -\frac{\omega}{\sqrt{2}\lambda}\left(\varkappa\left|\frac{\partial V_g}{\partial p}\right| + \frac{mq_-}{m^2+n^2}\right)^{\frac{1}{2}}\left\{\sqrt{1+\left(\frac{nq_-}{\varkappa\left|\frac{\partial V_g}{\partial p}\right|(m^2+n^2)+mq_-}\right)^2}-1\right\}^{\frac{1}{2}} \qquad 4.11$$

This expression probably does not represent the total energy loss, as further losses occur through viscous effects (equation 4.9) and other effects similar to those occurring in air/water mixtures which are not accounted for within the theory.

4.1 Attenuation in air/water bubbly mixtures

Carstensen and Foldy [31] devised a theory for the attenuation of sinusoidal pressure waves in an air/water

bubbly mixture, with wave frequencies of the same order as the resonance frequency of the bubbles. Their predictions were verified experimentally [44]. The theory is not applicable to low frequency waves, as the calculated attenuation of a 100c.p.s. wave in a 10% voidage medium, is an order of 10 higher than measured in the present experimental work.

Further experimental studies have been carried out on this subject, but have been restricted to high frequency waves [13] [30].

Karplus [10] noted that the impedance of a two-phase mixture lay between the two limiting values 3.12×10^5 lb/ft^{2}sec in water and 82.5 lb/ft^{2}sec in air. Experimental verification of this requires only the measurement of sonic velocity for varying voidage.

A further analytical solution for the attenuation of pressure pulses in an air/water mixture was noted by Gibson [45]. The ratio of wave pressure in a two-phase mixture to that in single phase water, was indicated to be a function of the wave velocity and properties of the fluid and flow tube. As a characteristic length through the fluid is not included in the expression, it cannot be generally used to predict the attenuation constant in such media.

The present experimental investigation indicated that the wave attenuation varied with voidage as shown in Fig. 24. The spread of data points is probably caused by the effects of background noise within the apparatus and also wave distortion (section 4.2). As discussed in

chapter 2, these effects were minimised.

By extrapolating the graph shown in Fig. 24, it can be seen that the attenuation constant in a single phase water medium is of the order 0·05 nepers/ft. Equation 4.9 predicts the attenuation, due to viscous effects near the pipe wall, to be of the order 10^{-4} nepers/ft. in a water medium. It is suggested that the high attenuation measured in the single phase is due to wave dispersion caused by various components of the frequency spectrum (section 1.4.2) of the wave travelling with differing velocities and attenuations. Although water is not a dispersive medium, it has been shown (46) that the presence of pipe walls will have this effect.

4.2 Attenuation of sound in steam/water bubbly mixtures

The attenuation of sinusoidal pressure waves in a steam/water mixture was found experimentally to be considerably larger than in an air/water mixture. The reason for this is not clear as the two systems differ significantly only due to the fact that mass transfer occurs in the former mixture. If the rates of condensation and evaporation are equal, the phase change processes are reversible and will therefore not influence the wave attenuation. A difference in the rates of condensation and evaporation would result in an overall increase or decrease in voidage of the mixture during the wave propagation which was not observed in practice.

Equation 4.11 represents the attenuation of a sinusoidal pressure wave in a low quality two-phase mixture according to the theory described in Appendix A.

From equation A.20, the relation between the wave velocity and attenuation can be written:-

$$k = \frac{U_{SINE}\, \rho^2 h A V_g (\partial T_s/\partial p)}{2 h_{fg} \left[\left(\frac{hA}{\omega C_w}\right)^2 + 1\right]}$$

When the wave frequency is high and no-mass transfer occurs, this reduces to

$$k_{NMT} = \frac{U_{SINE}}{2} \frac{\rho^2 h A V_g (\partial T_s/\partial p)}{h_{fg}}$$

This analysis predicts no attenuation of low frequency waves within which thermodynamic equilibrium is maintained.

It is possible that a two-phase one-component mixture may act in a similar way to a visco-elastic medium as described by the mechanical model shown in Fig. 25.1. The spring A represents the compressibility of the medium and hence may be used to describe a simple air/water bubbly mixture. Mass transfer in a one-component medium is represented by the spring B and dashpot in parallel. Such a model has been analyzed by Kolsky (42) and shown to give results (Fig. 25.2) comparable to the predictions of the theory given in appendix A. The attenuation is seen to increase with frequency and the internal friction (defined as k/f) to exhibit a maximum value. The variables used plotting the shown graphs, C_o and τ, may be considered as constant, C_o being the wave velocity at zero frequency and τ, the "time of retardation" (42) of the spring (B) and dashpot, which is probably related to the rate of mass transfer in a one-component system.

The experimental results show the same variation with voidage and frequency as predicted by the theory (Figs. 26 and 27). However, the measured attenuation constants are consistently lower than predicted. The probable cause of this is wave distortion.

An estimate of the variation of the maximum pressure of a wave due to distortion can be obtained by considering the energy of a wave. In a progressive wave, of any type, the total energy is half potential and half kinetic [27], therefore only the kinetic energy of a wave need be considered, which is given by:-

$$K.E. = \tfrac{1}{2}\rho \iiint u^2 \, dv \qquad 4.13$$

If the wave is assumed plane and travels along a pipe of constant cross sectional area, A, the energy in the positive half of a periodic wave is:-

$$K.E. = \tfrac{1}{2}\rho A \int_0^{\lambda/2} u^2 \, d\ell \qquad 4.14$$

where $d\ell$ is the incremental distance in the direction of wave propagation.

Considering two pressure waves of equal energy, but one having a sinusoidal form and the other a sawtooth shape (Fig. 18.2), the velocity of elements of fluid within the wave may be considered to vary in a way similar to the pressure, the fluid velocity over half of a wavelength being given by:-

$$u_{SINE} = u_m \sin \frac{2\pi\ell}{\lambda}$$

and

$$u_{TRI} = \frac{2u_m'\ell}{\lambda}$$

Substituting these expressions into equation 4.14 and equating the resulting wave energies, results in

$$U_M' = \sqrt{3}\ U_m$$

For a sinusoidal wave the maximum fluid pressure and velocity are related by (43)

$$P_M = a\ \rho\ U_m$$

where a is the displacement amplitude of vibration.

As a triangular wave may be considered as an infinite sum of sinusoidal waves, it is likely that the above relation also holds for this type of wave. Therefore

$$P_M' = 1.7\ P_M$$

Hence the distortion of a sinusoidal wave to a triangular wave, with the same energy, may result in the maximum wave pressure being overestimated by a factor of 1.7.

From Figs. 26 and 27, the approximate deviation of experimental data from the theoretical curves is 0.25 nepers/ft. For initial wave amplitudes of 1.5 p.s.i., and an actual attenuation of 0.75 nepers/ft, this deviation represents a variation of the measured wave amplitude, as detected by the upper transducer, of approximately 50%. This is possibly accounted for by wave distortion as shown in the above analysis.

5. THE PHENOMENA OF CRITICAL OR CHOKING FLOW IN PIPES

5.1 Introduction

As is well known, when a single phase fluid flows from a reservoir in which the conditions are fixed, the mass flow rate at first increases as the downstream pressure is reduced, but eventually reaches a maximum value, thereafter further reductions in downstream pressure produce no change in mass flow rate and a pressure discontinuity occurs at the outlet. In this condition the flow is said to be "choked" or "critical" and the one dimensional analysis indicates that the Mach number reaches unity at the outlet. Boundary layer effects modify the phenomena but for many fluids the simple theory gives good agreement with experimental results.

In a two-phase medium the one-dimensional approximation is only valid for well mixed fluids such as can arise in "bubbly" flow or "mist" flow. For "annular" and "slug" flow such an approximation is clearly not appropriate. In general the phases do not move at the same velocity and departures from thermodynamic equilibrium may lead to a lack of symmetry between rarefaction and compression waves and also time rate of change effects. For these reasons a unique sonic velocity does not exist in two-phase systems and some experimental work suggests that a critical flow does not exist either. Certainly in one-component systems it cannot be defined in terms of the upstream reservoir conditions alone since the subsequent behaviour is very sensitive to nucleation phenomena. Because the

number of variables has been increased in the two-phase system, many authors have produced theoretical models to account for the phenomena and the following literature survey attempts to outline the progress of these approaches to a mathematical description of a two-phase one-component critical flow.

5.2 A survey of previous theories for choking flow in pipes.

The first model for critical flow in a two-phase system was based upon that for a single phase, and is known as the Homogeneous equilibrium (H.E.) model.

Assuming the two-phases to be homogeneously dispersed, moving with the same velocity and in thermodynamic equilibrium, the critical specific mass flow rate is given by:-

$$G^2_{CRIT} = -\left(\frac{\partial P}{\partial V}\right)_s \qquad 5.1$$

where the pressure is measured in absolute units.

This, together with the definition of specific volume in a homogeneous mixture

$$V = (1 - x)V_f + xV_g \qquad 5.2$$

enables the critical flow rate to be calculated for a given outlet pressure and quality.

The method of evaluating $\left(\frac{\partial V}{\partial P}\right)_s$ has been outlined by Fauske (50). Assuming a pressure and quality, the entropy of a two-phase mixture is given by:-

$$S = S_f(P) + S_{fg}(P)\,x \qquad 5.3.1$$

where S_f and S_{fg} are obtained from thermodynamic tables.

If the process is isentropic, a small variation in pressure implies that:-

$$S = S_f'(P+\Delta p) + S_{fg}'(P+\Delta p)\,x' \qquad 5.3.2$$

Similarly, the specific volumes of the mixture at these pressures are:-

$$V = V_f(P) + x\,V_{fg}(P) \qquad 5.3.4$$

$$V' = V_f'(P+\Delta p) + x'\,V_{fg}(P+\Delta p) \qquad 5.3.5$$

Values of x' computed from equations 5.3.2 and 5.3.1 can be used in equation 5.3.5, and hence a graph of V against P, within the vicinity of P, may be drawn and the gradient $\frac{dV}{dP}$ measured.

Fig. 28 shows the calculated critical specific mass flow rate for varying quality, at pressures of 50 psi. and 14.7 psi. The former pressure allows comparison with the experimental results of Faletti, Moy, Fauske and Henry [55]. The latter pressure is more relevant to the work covered in this report.

It can be seen that the predicted results using the H.E. model underestimate the critical flow rate, except at high qualities where the model more accurately describes the physical "mist" flow.

At very low qualities, within the bubbly flow regime, although the flow homogeneity is maintained, the model still underestimates the flow rate since thermodynamic equilibrium does not then exist between the phases.

The existence of a slip velocity ratio implies that the voidage and quality are independent variables related by the following expression

$$\sigma = \frac{(1-\alpha)}{\alpha}\frac{x}{(1-x)}\frac{V_g}{V_f} \qquad 5.4$$

Hence, a correlation between α and x yields values of the

slip velocity ratio. Correlations made empirically by Lockhart and Martinelli[47] and Armand[48] will be discussed more fully in section 6.1.

The fact that the phases move with different velocities also leads to three possible definitions of specific volume.

An area average specific volume:-

$$V_A = \left(\frac{1}{A}\int_A \rho \, dA\right)^{-1} \qquad 5.5.1$$

a momentum average

$$V_M = \frac{1}{G^2 A}\int_A \rho u^2 \, dA \qquad 5.5.2$$

and a kinetic energy average

$$V_{KE} = \left(\frac{1}{G^3 A}\int_A \rho u^3 \, dA\right)^{-\frac{1}{2}} \qquad 5.5.3$$

Using the definition of specific flow rate

$$G = (1-x)G + xG$$

$$= \frac{(1-\alpha)u_f}{V_f} + \frac{\alpha u_g}{V_g} \qquad 5.6$$

The three specific Volumes can be rewritten as

$$V_A = \frac{1}{(1-\alpha)\rho_f + \alpha\rho_g} \qquad 5.7.1$$

$$V_M = \frac{x^2 V_g}{\alpha} + \frac{(1-x)^2 V_f}{1-\alpha} \qquad 5.7.2$$

$$V_{KE} = \frac{x^3 V_g}{\alpha^2} + \frac{(1-x)^3 V_f}{(1-\alpha)^2} \qquad 5.7.3$$

In the case where the slip velocity ratio is unity, it can be seen that, the above three definitions of specific volume reduce to equation 5.2.

By applying a momentum balance to a separated flow model, Isbin, Moy and Da Cruz[49] derived equation 5.1, and

using the momentum average specific volume (equation 5.7.2) together with a relation between the voidage and quality given by the Lockhart-Martinelli correlation, obtained improved theoretical predictions for the critical mass flow rates at qualities above 0.4.

Massena [52], using the same principle, but the Armand correlation obtained results similar to those of the Isbin momentum model.

The next major advance in the theory of critical two-phase flow was made by Fauske [50]. Using a separated, thermodynamic equilibrium model, he derived momentum equations for both phases. These led to the equation of motion similar to that for a single phase fluid flowing through a conduit:-

$$G^2\left(dV_m + \frac{f V_m}{2D}\,dl\right) + dp = 0 \qquad 5.8.1$$

His assumption that dp/dl attained a maximum value at the critical condition, for a given G and x, implied that:-

$$\frac{\partial}{\partial \sigma}\left\{G^2\left(\frac{dV_m}{dl} + \frac{f V_m}{2D}\right)\right\} = 0 \qquad 5.8.2$$

since the slip velocity ratio is the only independent variable occurring in equation 5.8.1.

Equation 5.8.2 then leads to the condition

$$\frac{d}{dl}\left(\frac{\partial V_m}{\partial \sigma}\right) + \frac{V_m}{2D}\left(\frac{\partial f}{\partial \sigma}\right) + \frac{f}{2D}\left(\frac{\partial V_m}{\partial \sigma}\right) = 0 \qquad 5.8.3$$

If the flow is considered non-isentropic, where f is not zero, this has a solution when

$$\frac{\partial V_m}{\partial \sigma} = 0 \qquad 5.8.4$$

and

$$\frac{\partial f}{\partial \sigma} = 0 \qquad 5.8.5$$

From equations 5.7.2 and 5.8.4 the limiting value of the slip velocity ratio is found to be

$$\sigma = \left(\frac{V_g}{V_f}\right)^{1/2} \qquad 5.9$$

Equation 5.8.1 can be rearranged into the form of equation 5.1, and the critical flow rate found using 5.7.2 and 5.9.

As the process is assumed isenthalpic, the partial derivatives $\partial V_g/\partial p$ and $\partial V_f/\partial p$ are evaluated using thermodynamic steam tables, and $\partial x/\partial p$ can be defined as:-

$$\frac{\partial x}{\partial p} = -\frac{1}{h_{fg}}\left(\frac{\partial h_f}{\partial p} + x\frac{\partial h_{fg}}{\partial p}\right)$$

which is also obtainable from standard tables.

This theory shows excellent agreement with experimental values of G_{CRIT} (Fig. 28) but the predicted value of slip velocity ratio at the critical condition, is much larger than have been measured experimentally. There also appear to be errors in the mathematics of the theory, which were pointed out by Cruver and Moulton (51). Equation 5.8.2 has been shown to represent a minimum value of the pressure gradient instead of a maximum as assumed by Fauske. Also equations 5.8.4 and 5.8.5 do not necessarily represent a solution of equation 5.8.3 as:-

$$\frac{\partial V_m}{\partial \sigma} = 0 \quad \text{does not imply} \quad \frac{d}{d\ell}\left(\frac{\partial V_m}{\partial \sigma}\right) = 0$$

Due to the separated flow model used in the analysis, very little exchange of momentum occurs between the phases caused by the viscous shear stresses at the inter-phase surface, which probably results in the large predicted values of slip velocity ratio. Clearly in a low quality

bubbly flow this momentum exchange is considerable and hence slip velocity ratios of the order indicated by equation 5.9 are unrealistic.

Equation 5.1 was derived by the previous authors using the continuity and momentum equations. Moody [52] derived an alternative expression for the critical mass flow rate by considering the continuity and energy equation, the theory being applied to a short converging nozzle.

Assuming the flow to be isentropic

$$h_o = x\left(h_g + \frac{U_g^2}{2J}\right) + (1-x)\left(h_f + \frac{U_f^2}{2J}\right) \qquad 5.10.1$$

where h_o is the initial liquid enthalpy.

Also

$$S_o = x S_{fg} + S_g \qquad 5.10.2$$

So being the initial liquid entropy.

The phase velocities were eliminated from equation 5.10.1 by using the continuity equation (equation 5.6)

$$G = \frac{\alpha U_g}{x V_g} = \frac{(1-\alpha) U_f}{(1-x) V_f} \qquad 5.10.3$$

x and α were then eliminated from the resulting expression by using equations 5.4 and 5.10.2.

On assuming the fluid to remain in thermodynamic equilibrium, the flow properties s, h and v are functions of pressure only and obtainable from standard tables.

G is thus shown to be a function of pressure and slip velocity ratio (σ) only, having a maximum value when

$$\left(\frac{\partial G}{\partial \sigma}\right)_p = 0 \qquad 5.10.4.$$

$$\left(\frac{\partial G}{\partial P}\right)_\sigma = 0 \qquad 5.10.5$$

The application of condition 5.10.4 showed that the maximum flow rate occurred when the slip velocity ratio attained the value

$$\sigma = \left(\frac{V_g}{V_f}\right)^{1/3} \qquad 5.11$$

It was assumed that this value of σ, when substituted into the main equation for G automatically implied the condition 5.10.5.

The agreement of the predictions of this theory with experiment are good for long cylindrical nozzles. However its inability to successfully predict conditions in a short nozzle implies the existence of metastable effects which are not taken into account within this theory. Cruver and Moulton (51) also using a separated equilibrium model, assumed that choking occurred when the flow reached a state of maximum entropy. This was found to occur when the kinetic-energy-average specific volume, (defined by equation 5.7.3) minimised with respect to the slip velocity ratio, and the value of the slip became $\left(\frac{V_g}{V_f}\right)^{1/3}$. (as in equation 5.11.). The critical flow rates resulting from the theory are low at high qualities and high at low qualities compared to experimental results, indicating that the slip velocity may have been overestimated at high qualities and suggesting the presence of non-equilibrium effects at lower qualities.

A numerical treatment was given to the problem by Linning, Alderson and Pexton (53), assuming a separated equilibrium model, a set of differential equations was

derived and solved using a step by step integration technique. Choking was assumed to occur when any further expansion of the fluid required a kinetic energy increase greater than that available from the internal energy of the system, i.e. when the equations became inconsistent. The predicted value of critical flow rate for a given initial pressure was lower than found in experiment, indicating possible metastable or non-equilibrium effects at the beginning of the flow.

Katto[54] assumed choking to occur when the pipe frictional force was reduced to zero. This enabled the solution of equations derived from a separated equilibrium flow model. The results compare favourably with experiment within the range $0.02 < x < 0.5$. At qualities above 0.5, however, the theory indicates that condensation begins to occur at the choking pipe outlet, also, at low qualities the predicted critical flow rate exhibited a maximum at a quality of approximately $x = 0.01$. Neither of these phenomena have been found to occur in practice.

Henry[55] carried out both experimental and theoretical work with low quality two-phase one-component flow. Recognising the fact that non-equilibrium effects may occur in low quality flow, he assumed the quality at any point along the pipe to be:-

$$\chi = \sigma N' \chi_{EQ} \qquad 5.12$$

where the value of N' was derived empirically from experimental work, and χ_{EQ}, the quality that would exist were the fluid in thermodynamic equilibrium.

A comparison between equation 5.12 and 5.4 shows that if $x \ll 1.0$, then -

$$N' = \frac{\alpha V_f}{X_{EQ}(1-\alpha)V_g} \qquad 5.12.1$$

As the variables on the R.H.S. could be measured experimentally the variation of N′ along the flow was determined. It was found that N′ remained constant over the latter part of the choking flow.

$$\text{i.e.} \quad \left.\frac{dN'}{\partial \ell}\right]_{EXIT} = 0 \qquad 5.12.2$$

Henry suggested that a linear relation existed between N′ and x_{EQ} at the exit of the flow and the equation

$$N' = 20\, x_{EQ} \qquad 5.12.3$$

was found to agree with experimental data. Within the accuracy of experimental measurement, equation 5.12.3 was found to be independent of pressure.

The slip velocity ratio at the exit of the flow could only be measured by assuming equilibrium conditions, which resulted in values of slip between 1.3 and 8.0. It was suggested that as thermodynamic equilibrium did not exist, the actual slip velocity ratio was of the order 1.3→2.0.

This thermodynamic non-equilibrium approach yielded critical flow rates which were in good agreement with Henry's own experimental work, at qualities down to 5×10^{-3} (Fig. 28).

It was assumed by Edwards[56] that the deviation of experimental results at low qualities, within the bubbly regime, from the predictions of the H.E. model was due entirely to non-equilibrium effects, the rate of vaporisation, or increase in quality along a flow being controlled by the

heat conduction through the fluid shell surrounding each individual bubble. This flow of heat to the bubble surface was calculated using the numerical method of Dusinberre[57]. The predictions of this theory were understandably dependent on the number of bubbles per unit mass of fluid, however, the critical flow rates at high pressures in short pipes were successfully predicted assuming 10^9 - 10^{10} bubbles per pound of two-phase fluid. Photographs taken of a two-phase flashing flow (Fig. 14.1) suggest that the number of bubbles present in a pound of untreated water is of the order 10^4 - 10^5 hence the number assumed by Edwards may be an overestimate. Also, the heat transfer from the liquid phase to a bubble is greatly enhanced if the bubble is moving relative to the liquid (section 7.5.1). An assumption of no slip velocity between the phases as made by Edwards, may therefore lead to a lower rate of heat transfer between the bubble and the liquid phase, than actually occurs in the physical system.

It is possible that an overestimate of bubble population and a low heat transfer coefficient result in the correct predictions obtained.

The preceding survey has shown how the understanding of a two-phase one-component critical flow has progressed from a Homogeneous equilibrium model to a model in which the slip velocity ratio is an important factor and eventually to a model where the major effect is that of thermodynamic non-equilibrium. It can also be seen how each model successfully describes the flow over a restricted range of qualities, the H.E. model being applicable at very

high qualities, the "slip" model at medium qualities and a "non-equilibrium" model at low qualities.

6. SLIP VELOCITY RATIO

The importance of the ratio of phase velocities in the analysis of two-phase critical flow is apparent from the previous chapter. The present concern is with bubbly mixtures within which it has generally been found that the relative velocity between the phases is small, with the result that it has been neglected in comparison to the effect of departures from thermodynamic equilibrium within the mixture.

Many chemical engineering problems, involving bubbles within a liquid, have revealed a significant dependence on bubble motion of the processes which occur at the bubble surface. It, therefore, appears that the principal effect of slip velocity in a steam/water bubbly system will be in the thermodynamics rather than the mechanics of the flow. The success of a non-equilibrium model in describing a two-phase choking flow will depend, to a great extent, on the correct prediction of the rate of vaporization which occurs within the mixture and this will be governed significantly by the slip velocity ratio.

Previous studies have resulted in empirical expressions for the slip velocity ratio. However, observations of the two-dimensional effects existing within a two-phase flow have indicated that these expressions do not accurately represent the physical system.

A model is proposed, based on a balance of the forces acting on an individual bubble, with which to predict the relative motion between a bubble and the contiguous liquid.

6.1 Literature Survey

Separated flow models as used by Fauske[50] and Cruver and Moulton[51] have resulted in slip velocity ratios at the exit of a critical flow, significantly higher than those measured in experiment. This is probably due to an underestimate of the exchange of momentum between the phases. Clearly this type of model cannot be applicable to a flow which remains in the bubbly regime as the exchange of momentum between a bubble and the surrounding liquid, due to the drag forces acting on the bubble, is very great.

Also using a separated flow model, Levy[58] derived the expression for the slip velocity within a steam/water flow:-

$$\sigma = \left(\frac{\rho_f}{\rho_g}\right)^{1/2} (2\alpha)^{1/2} \qquad 6.1$$

This was found to agree with experiment, but as both the theoretical derivation and the experimental measurement of quality were based on the concept of thermodynamic equilibrium, equation 6.1 may not accurately represent the physical system.

Several empirical correlations for the slip velocity ratio have agreed well with experiment for qualities above 10^{-2} and pressures greater than 5 atmospheres. The most widely used correlation is probably that of Lockhart and Martinelli[47] who assumed the voidage to be a function of the non-dimensional parameter defined as:-

$$\left(\frac{A}{\pi D}\right)^{m+n} \frac{C_f}{C_g} \frac{W_f^{2-m}}{W_g^{2-n}} \frac{\rho_g}{\rho_f} \frac{\mu_f^n}{\mu_g^m} \qquad 6.2$$

where the friction factor for each phase is given by the Blasius expression:-

$$f_g = C_g (R_{eg})^{-m} \qquad 6.3$$

$$f_f = C_f (R_{ef})^{-n}$$

The voidage was correlated to the function (6.2) using the values of C_g, C_f, m and n, appropriate to given types of flow (47).

Marchaterre and Hoglunds (59) correlated the measured slip velocity ratio in a vertical steam/water flow with the parameter

$$\frac{x}{(1-x)} \frac{\rho_f}{\rho_g} \qquad 6.4$$

and found a dependence of slip on Froude No.

A linear relation between the slip velocity ratio and quality was assumed by Haywood et al. (60)

$$\sigma = 1 + Ax \qquad 6.5$$

where A was correlated to $\frac{V_g - V_f}{V_f}$

Although the work of Marchaterre (59) and Haywood (60) give reasonable agreement with high quality, high pressure steam/water flow, as the measurement of quality in experiment relies on the assumption of thermodynamic equilibrium, its relevance to a system which is not in equilibrium must be suspect.

All of the above correlations overestimated the slip velocity ratio in low quality steam/water and air/water flows. It appears that for a flow which remains

in the bubbly regime, another model is required to predict the slip velocity ratio.

In a very low quality bubbly vertical two-phase flow it is likely that the slip velocity ratio is closely related to the terminal velocity of an individual bubble in a stationary liquid.

This approach to the problem was made by Collier (11) and Wallis who assumed

$$\sigma = 1 + \frac{U_\infty}{U_w}(1-\alpha)^m \qquad 6.6$$

where $0.5 < m < 1.0$ according to the bubble size regimes defined by Peebles and Garber (61).

For air bubbles exceeding 1.2×10^{-2} ft. in radius, it was suggested by Zuber that

$$\sigma = 1 + \frac{U_\infty}{U_w(1-\alpha)} \qquad 6.7$$

Simpson and Rooney (63) assumed that the mean gas velocity was given by:-

$$U_a = U_{homo} + U_{Rel} \qquad 6.8$$

where U_{homo} represents the mean velocity, if the fluid were flowing homogeneously ($= G\left[xV_a + (1-x)\ V_w\right]$); and U_{Rel} is the relative velocity of the bubble to this homogeneous velocity. U_{Rel} was assumed to be the terminal velocity of a bubble within the bubble churn-turbulent regime defined in reference (61). After some algebraic manipulation it can be seen that equation 6.8 reduces to the form of equation 6.7.

Equations 6.6 and 6.7 predict slip velocity ratio, much smaller than have been measured in vertical air/water flows (25).

Bankoff[67] suggested that no actual slip velocity ratio occurred between a bubble and the surrounding liquid, the measured values of slip velocity being due entirely to voidage and velocity variations across a section of the flow. Such voidage and velocity profiles have been noted in experiment.[64] [65]

Assuming power law distributions of voidage and velocity, Bankoff derived the expression for the apparent slip velocity ratio in a horizontal two-phase flow

$$\sigma_{app} = \frac{1-\bar{\alpha}}{K-\bar{\alpha}} \qquad 6.8$$

$\bar{\alpha}$ being the mean voidage across a section, and K, a distributional parameter, depending on the form of the profiles, and having a value $0.5 < K < 1.0$.

K was assumed to be linearly dependent on the fluid pressure

$$\text{ie.} \quad K = 0{\cdot}71 + 0{\cdot}0001P \qquad 6.9$$

(where P is measured in p.s.i.)

This theory showed reasonable agreement with the Lockhart-Martinelli[47] correlation for pressures above 100 p.s.i., with K equal to an average value of 0.89.

It was pointed out by Zuber[66] that the parameter K could be replaced by the Armand[48] correlation constant

$$C = \frac{\alpha}{\beta} \approx 0{\cdot}833 \qquad 6.10$$

which enabled equation 6.8 to successfully predict Russian experimental results.

Neal and Bankoff[69] modified equation 6.8 by assuming a constant "local" slip velocity σ between the bubble and its surrounding liquid, resulting in the expression

$$\sigma_{app} = \sigma\left(\frac{1-\bar{\alpha}}{K'-\bar{\alpha}}\right) \qquad 6.11$$

K' being another distributional parameter equal to K when $\sigma = 1.0$. For vertical flow, σ was assumed to be given by an equation of the form 6.7.

It was assumed by Levy[70], that the local velocity of the gas phase was proportional to the local flow velocity $\bar{u}$

$$\left(u_g = \alpha u_g + (1-\alpha)u_w\right)$$

$$\text{i.e.} \quad u_g = k\bar{u} \qquad 6.12$$

This led to the expression for the apparent slip velocity ratio of

$$\sigma = \left(\frac{1-\bar{\alpha}}{\frac{K}{k}-\bar{\alpha}}\right) \qquad 6.13$$

The value of k was derived from experimental work and for small voidage became equal to K resulting in an apparent slip of unity.

In order to include the effect of velocity and voidage profiles, Zuber[68] modified equation 6.7 to

$$\sigma(1 - C_o\alpha) = C_o(1-\alpha) + \frac{u_\infty}{u_w} \qquad 6.14$$

where C_o is a distributional parameter equivalent to the reciprocal of K (the Bankoff distributional Parameter). The value of $C_o = 1.2$ gave good agreement with experimental work for a vertical churn-turbulent flow of air bubbles with radius $> 1.2 \times 10^{-2}$ ft.

It will be noted that the accuracy of the above theories depend critically on the value of the distributional parameter. This parameter, being a function of the shape of velocity and voidage profiles across a section of the flow, will probably vary significantly along the flow. Hence in a flashing flow, if the nucleation is assumed to occur homogeneously, the distributional parameter will have an initial value of unity and will then decrease due to bubble migration towards the centre of the tube and the resulting change in velocity profile. This will be discussed more fully in section 6.5.

Simultaneous measurement of voidage and velocity profiles within a flow will yield the value of the distributional parameter at a given position in the flow. Such measurements are difficult to make in a two-phase system. Haywood [60] measured the variation of voidage profile shape with gas velocity, quality and pressure. Using a γ-ray attenuation technique and assuming the flow to be axi-symmetric about the centre of a vertical flow tube, the profiles shown in Fig. 33 were obtained. At low pressure the voidage profile was found to be parabolic in shape, thus verifying the approach of Bankoff [67]. An approximate linear variation of voidage with radial position was found at intermediate pressures of about 600 p.s.i. Above this pressure, the profile exhibited a maximum value at a position other than the tube centre. Profiles of the latter form have also been measured by Hammitt [64]. Decreases in quality were found to make the voidage profile less prominent indicating that in the limit as $x \to 0$ the voidage is constant across the flow.

In dealing with critical flow in a two-phase system which remains in the bubbly regime, large specific mass flow rates and very small qualities within the major portion of the flow are expected and hence deviations of the velocity and voidage profiles from a plane have been neglected in this analysis (chapter 7). Radial bubble distributions probably become significant in the latter portion of a choking flow and this effect is discussed in section 8.5.

It is expected that one of the major effects of the slip velocity ratio in a critical flow is to increase the flow of heat between the phases. When used in this context, a "local" slip velocity ratio must be defined as the ratio of the bubble velocity to the velocity of the surrounding liquid, which will be independent of any two-dimensional profiles which may exist.

Before an analysis of the critical flow phenomena in a bubbly two-phase one-component flow can be undertaken, it is necessary to obtain an estimate of the magnitude of the "local" slip velocity ratio which exists in such media.

6.2 Dynamics of a bubble accelerating through a two-phase

The problem of predicting the motion of a bubble in a two-phase medium is one of viscous fluid flow which cannot be solved directly. However, the drag on a bubble can be regarded as a combination of tangential stresses and normal stresses, i.e. viscous drag and "form" drag. Tangential forces at the bubble surface can only arise from a non-uniform surface tension, due to the presence of

impurities, or the existence of circulation of the gas within the bubble. Neither of these effects is expected to be large. The "form" drag arises from the energy dissipation in the bulk of the fluid surrounding the bubble and is the most important.

6.2.1 Form drag force

Fig. 29.1 shows the variation of terminal velocity of an air bubble in water with bubble radius, according to Peebles and Garber[61]. Four regimes of bubble behaviour were noted. Very small bubbles behaved in the way predicted by Stokes[71]. In the second regime, bubbles up to a radius of 3.25×10^{-3} ft., acted as solid spheres. Between the radii 3.25×10^{-3} and 1.2×10^{-2} ft. the bubbles were found to deform slightly, hence increasing the viscous drag force. A constant terminal velocity was found in region four, where the bubbles were hemispherical in shape. The last regime will not be used in this theory, as gas bubbles of this size and shape, within a two-phase flow, have been categorized as "Taylor" slugs[74] and require a separate theoretical treatment.

The terminal velocity of a bubble in a stationary liquid represents a balance of the buoyancy and drag forces, hence from Fig. 29.1 a further graph can be drawn of the drag coefficient, C_D, against bubble radius (Fig. 29.2). The drag coefficient is defined by the equation

$$\text{Drag force}\,(d) = \frac{C_D}{2}\,\pi r^2 U_\infty^2 \rho_w \qquad 6.15$$

To enable the graph shown in Fig. 29.2 to be used in numerical computations, two empirical curves were

fitted either side of the minimum value of C_D at r = 3.25 x 10^{-3} ft. This ensured maximum accuracy of values of the drag coefficient, for bubbles of radii between 10^{-3} and 10^{-2} ft.

The values of C_D were found to be given by the equations:-

$$C_D = \frac{0.834 \times 10^{-3}}{r} + \frac{0.4 \times 10^{-6}}{r^2} - 0.064 \qquad r < 3.25 \times 10^{-3} \text{ ft}$$

$$C_D = 2.42 \times 10^{4} r^2 - 80.0 r - 0.24 \qquad r > 3.25 \times 10^{-3} \text{ ft.} \qquad 6.16$$

6.2.2 Displaced mass drag force

When a spherical bubble accelerates through a medium, it is subject to a further force retarding the motion (71) equal to:-

$$\frac{M'}{2} \frac{du}{dt} \qquad 6.17$$

where M′ is the mass of liquid displaced by the bubble. For a bubble moving within a two-phase mixture, it is assumed that this force will be of the form

$$\frac{2}{3}\pi r^3 \rho_w (1-\alpha) \frac{d}{dt}(U_A - U_W) \qquad 6.18$$

(where $\rho_w(1-\alpha)$ is the average density of the surrounding fluid) although this expression may be modified due to the close proximity of other bubbles.

6.3 Equation of motion of the bubble

The motion of a spherical bubble in a fluid is determined by the action of drag forces, buoyancy force and the pressure gradient in the direction of flow.

The momentum equation of the gas phase in a two-component bubbly mixture has been derived in appendix D (equation D.10).

$$\rho_A U_A \frac{dU_A}{d\ell} = -\frac{dp}{d\ell} - N D_o \rho_w \left(\frac{1-\alpha}{\alpha}\right)$$

From equations 6.15 and 6.18

$$D_o = d + \frac{2}{3}\pi r^3 \rho_w (1-\alpha) \frac{d}{dt}(U_R - U_W) \qquad 6.19$$

using equations 5.4 and 7.45, and assuming $\sigma(1-\alpha)\rho_w/2\rho_R \gg 1.0$, the equation of motion for the gas phase can be shown to be

$$\sigma\left(\frac{1-\alpha}{2}\right)\rho_w\left(U_R\frac{\partial U_R}{\partial \ell} - U_W\frac{\partial U_W}{\partial \ell}\right) = -\frac{\partial P}{\partial \ell} - \sigma\frac{dN}{x}\rho_R + \rho_w g \sin\theta \qquad 6.20$$

$$\text{where} \qquad d = C_D \pi r^2 (U_R - U_W)^2 \rho_w \qquad 6.21$$

and θ is the inclination of the flow to the horizontal.

6.4 Slip velocity ratio in an air/water bubbly mixture

In order to investigate the behaviour of the slip velocity ratio in an air/water system, the relevant equations will be stated here. The derivation will be given in chapter 7.

Momentum equation for the liquid phase

$$\left(U_R\frac{\partial U_R}{\partial \ell} - U_W\frac{\partial U_W}{\partial \ell}\right)\left(1 + \frac{(1-\alpha)}{2}\frac{\rho_w}{\rho_R}x\right) = \frac{1}{\rho_w}\frac{\partial P}{\partial \ell} + U_R\frac{\partial U_R}{\partial \ell} - Nd + \frac{4f}{2D}U_S^2\left(1 + \frac{n\alpha}{1-\alpha}\right) + g\sin\theta \qquad 6.22$$

Continuity of mass:-

$$\frac{\partial U_W}{\partial \ell} = -x\frac{\rho_w}{\rho_R}\frac{U_W^2}{U_R}\left(\frac{1}{nP}\frac{\partial P}{\partial \ell} + \frac{1}{U_R}\frac{\partial U_R}{\partial \ell}\right) \qquad 6.23$$

where the compression and expansion processes within the gas phase are assumed to be polytropic with index n. In the calculations, these processes are assumed isothermal ($n = 1.0$), to agree with the observations made by Huey and Bryant[72].

Equations 6.20, 6.22 and 6.23 represent the motion of a two-phase air/water system as a set of

simultaneous non-linear differential equations. The solution was computed numerically using a forward integration technique. Assuming the existence of bubbles of a finite size with a slip velocity ratio of unity at the initiation of the two-phase flow, the flow properties could be determined at all positions along the pipe.

Fig. 30.1 shows the increase in slip velocity ratio as the bubble progresses along the pipe. The bubble accelerates from the imposed initial condition until a more stable situation is reached, after which the slip velocity increases slowly. During the initial bubble acceleration, the voidage decreases to a minimum and thereafter increases due to bubble expansion. It is the value of the slip velocity ratio at the position of maximum voidage which is shown in the subsequent figures.

The influence of bubble radius on the slip velocity ratio was found to be greater than that of the bubble population or voidage. This can be seen by comparing Figs. 30.2 and 30.3.

Fig. 30.4 shows the variation with velocity, for constant bubble size, the slip velocity ratio being almost independent of velocity in a horizontal flow. This has been noted in experimental work (25).

At high liquid velocities, the slip velocity ratios are of the same order in both vertical and horizontal flow. Fig. 31 shows the variation of slip with the angle of inclination to the horizontal of the flow, for various velocities. As expected, in low

velocity inverted flow the slip velocity ratio becomes less than unity, resulting in an increase in voidage and a possible change of flow regime.

It was assumed by Bankoff[67] that no actual slip existed between a bubble and its surrounding liquid in a horizontal two-phase bubbly flow. However, this analysis indicates the existence of a slip velocity ratio of approximately 1.05 in such a system, the result being independent of liquid velocity and varying slightly with bubble radius.

In a vertical system, this theory compares favourably with the expressions assumed by Zuber[68] and Collier and Wallis[11], all three exhibiting the same variation with liquid velocity (Fig. 32.1).

The variation of slip velocity ratio with voidage predicted by this theory is of the same form as the predictions of Collier and Wallis. However, the absolute value is found to be higher (Fig. 32.2). This is probably due to the assumption made by Collier and Wallis that at very low voidages the relative velocity of the bubble with respect to the liquid phase is equal to the terminal velocity of a single bubble in a stationary liquid.

The terminal velocity of a bubble in a stationary liquid is determined by the balance of drag forces and buoyancy forces. In a moving system there exists a larger variation of pressure around the bubble surface and as it is this pressure which must be integrated over the bubble surface to determine the buoyancy force, a larger "terminal" velocity will result.

Using the same reasoning, it may be expected that the slip velocity ratio will increase with the fluid velocity. However, an increase in pressure gradient will result in a larger relative velocity between the phases and not, necessarily, a higher slip velocity ratio.

In view of the small values of slip predicted by the theory, it appears that the values of drag coefficient implied by experimental measurement of slip [25] are inconsistent with those calculated from the work of Peebles and Garber [61].

As suggested by Bankoff [67] the experimentally measured slip velocity ratios in a two-phase bubbly mixture are principally the result of voidage and velocity variations within the flow. In order to compare the calculated values of the "local" slip velocity ratio with measured values, it is necessary to consider these two-dimensional effects.

6.5 Effect of voidage and velocity profiles

When a bubbly two-phase mixture flows along a tube it has been observed [60] that the bubbles have a velocity component in a direction perpendicular to the tube walls. The actual flow mechanisms which initiates this bubble migration is unknown, but it appears from existing literature, to be due to a combination of the "Magnus" effect and the "Bernoulli" effect. The former, due to rotation or circulation around the bubble probably induced by the large velocity gradients which exist near a solid boundary, produces a "lift" force acting away

from the boundary. The "Bernoulli" effect, being due to the velocity and hence pressure distributions around a bubble situated near a boundary, gives rise to a force on the bubble acting towards the surface. It is therefore a balance of these forces which produces the distribution of bubbles, or voidage profiles, which have been reported by several authors [64][65] (Fig. 33). This variation in fluid density across the flow area will lead to fluid velocity profiles which are expected to deviate significantly from the usual 1/7 power profile found in turbulent single phase flows.

The following analysis is intended to give a guide as to the effect of such voidage and velocity profiles on the values of the slip velocity ratios measured in experiment.

Assume that the local voidage and liquid velocity are symmetrical about the pipe axis, and that there exists a constant "local" slip velocity of σ .

Considering an elementary annulus of flow area, thickness dr, at a radius r from the tube centre. The mass flow through this annulus is:-

$$\Delta W = 2\pi r\,dr\,(\alpha U_A \rho_A + (1-\alpha) U_w \rho_w) \qquad 6.24$$

If U_w and α are functions of r only, this can be integrated, hence

$$W = 2\pi\left[\rho_w \int_0^R r\,U_w(r)(1-\alpha(r))\,dr + \sigma\rho_A \int_0^R r\,U_w(r)\alpha(r)\,dr\right] \qquad 6.25$$

For an air/water system, the mass flow rate of each phase is constant.

$$\text{i.e.} \quad 2\pi\rho_w \int_0^R r\,U_w(r)(1-\alpha(r))\,dr = \pi R^2(1-\bar{\alpha})\,\bar{U}_w \rho_w \qquad 6.26$$

$$2\pi\rho_A \sigma \int_0^R r\, U_w(r)\alpha(r)\, dr = \pi R^2 \bar{\alpha}\, \overline{U_w}\, \bar{\sigma}\rho_A \qquad 6.27$$

Also the average voidage across a flow section is given by

$$\alpha = \frac{2r}{A}\int_0^R r\,\alpha(r)\,dr \qquad 6.28$$

Assuming the voidage and velocity profiles to be given by

$$\alpha = \alpha_M\left(1 - r/R\right)^n \qquad 6.29$$

$$U_w = U_M\left(1 - r/R\right)^m \qquad 6.30$$

equation 6.27 can then be written

$$2U_M\alpha_M\sigma\int_0^R r\left(1 - r/R\right)^{m+n} dr = R^2\bar{\alpha}\sigma\overline{U_w}$$

Evaluation of the integral results in the expression

$$\frac{\alpha_M U_M \sigma}{(m+n+1)(m+n+2)} = \frac{\bar{\alpha}\bar{\sigma}\overline{U_w}}{2} \qquad 6.31$$

It can be shown that equation 6.26 and 6.28 reduce to-

$$\overline{U_w} = \frac{U_m}{(1-\bar{\alpha})}\left[\frac{2}{(m+1)(m+2)} - \frac{\alpha(n+1)(n+2)}{(m+n+1)(m+n+2)}\right] \qquad 6.32$$

and

$$\bar{\alpha} = \frac{2\alpha_M}{(n+1)(n+2)} \qquad 6.33$$

Combining equations 6.31 - 6.33, the following result is obtained

$$\frac{\bar{\sigma}}{\sigma} = \frac{1-\bar{\alpha}}{K-\bar{\alpha}} \qquad 6.34$$

where $$K = \frac{2(m+n+1)(m+n+2)}{(m+1)(m+2)(n+1)(n+2)} \qquad 6.35$$

This result is similar to that obtained by Bankoff (67).

The values of m and n will probably vary considerably as the flow progresses along the pipe, particularly near the pipe inlet before the flow has fully developed. However, Bankoff

suggested a value of K of 0.89 and it was confirmed by Zuber[66] that this value gave good agreement with available experimental data.

A theoretical indication of the value of distributional parameter, K, can be gained by considering two further elementary flow models.

If the bubbles are distributed homogeneously within the flow except for a small annulus of flow area, thickness δ , next to the pipe wall where the voidage is zero.

$$\begin{aligned} \alpha &= \alpha_m \quad ; \ 0 < r < R-\delta \\ \alpha &= 0 \quad ; \ R-\delta < r < R \end{aligned} \qquad 6.36$$

Assuming the velocity profile to be as previously discussed, and described by equation 6.30, equations 6.26 - 6.28 again result in the ratio of "apparent" slip velocity ratio to "local" slip velocity ratio being defined by equation 6.34, with

$$K = \frac{\left(1 - \frac{\delta}{R}\right)^2}{(m+1)\left(\frac{\delta}{R}\right)^{m+2} - (m+2)\left(\frac{\delta}{R}\right)^{m+1} + 1} \qquad 6.37$$

If m is assumed to be 1/7, which is the approximate value for a single phase turbulent flow, $R_e \geq 2{,}000$, and δ is 10% of the tube diameter, evaluation of 6.37 gives

$$K = 0.916$$

A linear voidage profile and "power law" velocity profile given by

$$\begin{aligned} \alpha &= \alpha_M - (\alpha_M - \alpha_o)\frac{r}{R} \\ U_{vl} &= U_M \left(1 - \frac{r}{R}\right)^m \end{aligned} \qquad 6.38$$

results in the expression for K

$$K = \frac{m+3}{m\frac{\alpha_m}{\bar{\alpha}} + 3} \qquad 6.39$$

The maximum value of $\alpha_m/\bar{\alpha}$ occurs when the voidage at the tube wall α_w is zero, i.e. $\alpha_m/\alpha = 3.0$ Evaluating 6.39, again with m = 1/7 gives the minimum value of K as 0.92.

6.6 Comparison of theoretical predictions of slip velocity ratio with experiment

In this comparison of the results of the theory, (section 6.4) for the slip velocity ratio in an air/water system, with experimental data, the effects of two-dimensional distributions of velocity and voidage have been taken into account.

The "local" slip velocity ratios predicted in the preceding sections are based on a one-dimensional model and it is probable that due to variations of velocity and voidage, a slip velocity ratio profile will also exist across the section of a flow tube. As the exact form of these profiles are unknown, it is assumed in the following correlations that the apparent or measured value of the slip velocity, is given by

$$\sigma_{APP} = \sigma\left(\frac{1-\bar{\alpha}}{K-\bar{\alpha}}\right) \qquad 6.36$$

where σ is the local slip velocity ratio characteristic of the mean voidage ($\bar{\alpha}$) and the mean fluid velocity of the two-dimensional flow, as predicted by the theory (section 6.4). K is a distributional parameter assumed to be approximately 0.9.

Herries[25] measured the slip velocity ratio in both vertical and horizontal air/water systems. Over the range of liquid velocities and bubble sizes used, equation 6.36 gives reasonable agreement with these results (Fig. 34). It should be noted that the same value of distributional parameter was used to predict σ_{APP} in both horizontal and vertical flows, indicating the same form of voidage and velocity profiles in each case.

Fig. 35 shows experimental data[68] for a vertical flow of air bubbles in water. The importance of a correct estimate of K can be seen from the various predictions shown in this figure.

It is concluded therefore that the measured values of slip velocity ratio in the bubbly regime of a two-phase flow are mainly a result of voidage and velocity profiles which exist within the flow. In this chapter, it has been proposed that a small "local" slip velocity ratio exists between a bubble and its surrounding liquid, and that this will be an important factor in the following analysis of a choking two-phase one-component flow. because of the presence of large pressure gradients such as occur near the outlet of a choked flow, this small "local" slip may become quite large.

7. ANALYSIS OF TWO-PHASE CRITICAL FLOW

The object of this analysis is to produce a rational theory for the choking phenomenon in a one-component bubbly mixture, which includes both the effects of a slip velocity between the phases and a finite rate of vaporization.

The slip velocity ratio in such media has been discussed in the previous chapter and appears to be considerably smaller than suggested by previous critical flow models [50][52]. However, it cannot be neglected in the present model as, together with the inter-phase surfact area and its heat transfer coefficient, the slip represents one of the major parameters upon which the finite rate of vaporization depends.

Several empirical formulae for the heat transfer coefficient of a vapour bubble surface will be surveyed in section 7.6.1. However, due to the unknown influences of voidage and bubble size, the determination of h_i will generally be through correlation with experimental data.

The bubble/liquid surface area is dependent on the number and size of bubbles per pound of flashing liquid (N) and represents one of the most important unknown variables. Previous authors have suggested values of N between 500 - 10^{10}, the former being probably measured after considerable coalescing of the bubbles had taken place and the latter is likely to be an overestimate as this number of bubbles in a 50% voidage mixture implies an average bubble radius of less than 10^{-4} ft. The

number of nucleation sites within a liquid will vary significantly, with undissolved gas content and other impurities, and it is not possible to obtain a value of N applicable to all systems. By photographing a flashing system (Fig. 14.1), it was estimated that of the order of 20,000 bubbles existed in a pound of untreated water, and it is this value which has generally been used in the following chapters.

In choking flow experiments, it is required to know the length of pipe in which flashing is occurring, hence a position where flashing is said to commence must be defined. This point is generally where the bubbles become visible to the naked eye. In this case a finite initial value of the flow quality exists and this is referred to as x_o in the calculations. Due to the speculative definition of the initiation of flashing, x_o represents another major variable in the calculations. From the photographs shown in Fig. 14.1, the smallest bubbles which can be detected are of the order 10^{-3} ft, with 20,000 bubbles/lb. of fluid. This represents a quality of approximately 10^{-6}.

As noted above the variables N and x_o may be estimated for a given system by photographic methods, and a value of h determined by correlating theoretical and experimental results. An experimental programme is underway at the Heriot-Watt University to produce measurements of these relevant variables.

7.1 Mathematical model describing a critical two-phase one-component flow

A one-dimensional theory for a two-phase flow, with a homogeneous distribution of equal sized bubbles, the existence of a slip velocity ratio and non-equilibrium effects will be described in the following chapters.

Previous authors have used one-dimensional models and it is probably sufficient to describe the major part of a homogeneous two-phase critical flow. However at the outlet of the flow tube, once the critical condition has been reached, two-dimensional effects could be important [55]. The consequence of radial variations in fluid velocity and bubble distribution will be discussed in section 8.5.

Surface tension can be a major cause of non-equilibrium in a two-phase flow [50]. Such an effect can only cause significant departures from equilibrium at the initiation of flashing when the bubbles are small. In the present model it is assumed that non-equilibrium exists because of the time required for heat to be conducted from the bulk of the liquid phase to the bubble surface, or in other words the vapour formation is heat transfer limited.

As this approach to the problem is only applicable to a two-phase flow which is in the bubbly regime, it is necessary to determine the maximum values of flow quality and voidage which are permissible within this regime.

7.1.1 Flow regime maps

When two phases flow simultaneously through a pipe, the gas or vapour phase may be distributed in different ways within the liquid phase [73]. This distribution or "flow regime" will depend principally upon the voidage, the relative motion of the phases and the specific mass flow rate. For this reason the flow regime maps shown in Fig. 36 have been transformed from the original axes to a G/x system which also enables comparisons to be made between the maps.

A study of the relevant flow properties which determine the flow regime [73] reveals that for pressures higher than one atmosphere, the maximum quality at which a bubbly flow exists is increased for a given specific mass flow rate.

The flow maps are purely experimental and therefore represent only approximate boundaries. No theoretical analysis exists to accurately predict these boundaries although it is likely that surface tension and viscosity are important.

In most cases the flow regime was categorized by visual observation of the flow, which represents a possible source of error as recent X-ray photographic techniques [76] have shown that some visibly bubbly flows conceal vapour cores or slugs.

In a horizontal steam/water flow with specific mass flow rates greater than 1,000 lb./ft.^{2}sec., it can be seen from Fig. 36.1 that the bubbly regime exists up to a quality of 10^{-2}. At atmospheric pressure and assuming an

average slip velocity ratio of 1.5[25], this corresponds to a voidage of 70%. This value is probably an over-estimate as the maximum voidage possible with closely packed equal spherical bubbles is 0.74[77].

It is assumed in this work that once the voidage becomes greater than 0.5, the bubbles have deformed sufficiently for the mathematical model to be no longer applicable.

7.1.2 Basic assumptions

In the following analysis of the critical flow of a two-phase one-component medium in a cylindrical tube, it is assumed that:

(i) A homogeneous distribution of equal sized bubbles exists within the flow.

(ii) The bubbles move relative to the liquid, the magnitude of this slip velocity depending on the drag force acting on an individual bubble as described in section 6.2, and the pressure gradient which produces the driving force.

(iii) The flow is basically turbulent and hence the pressure and fluid velocities are approximately constant across a section of the flow tube.

(iv) No bubbles are in contact with the pipe wall, so that the wall friction forces act only on the liquid phase.

(v) The fluid departs from a state of thermo-dynamic equilibrium owing to the time taken

for heat to be conducted from the liquid phase to each bubble.

(vi) The liquid phase is incompressible.

(vii) The thermodynamic properties h_{fg} and C_w are constant.

Derivation of equations describing a two-phase one-component flow

7.2 Momentum equation for the liquid phase

The momentum equation for the liquid-phase in a two-phase one-component flow is derived in appendix D (equation D.9). For a horizontal evaporating flow it reduces to

$$\rho_f u_f \frac{du_f}{dl} = -\frac{dp}{dl} - \frac{\Delta p}{\Delta l}\Big]_{TP} + N D_o \rho_f \qquad 7.1$$

where D_o is the drag force acting on an individual bubble. In chapter 6, D_o is shown to be given by

$$D_o = C_D \pi r^2 (u_g - u_f)^2 \rho_f + \frac{2}{3}\pi r^3 \rho_f (1-\alpha)\left(u_g \frac{du_g}{dl} - u_f \frac{du_f}{dl}\right) \qquad 7.2$$

It thus remains to choose an empirical expression which describes the pressure drop in a two-phase flow.

7.2.1 Two-phase frictional pressure drop

The pressure drop which occurs when a two-phase mixture flows along a pipe has been the subject of much literature. In the present work an empirical equation is sought which describes the pressure drop in low-quality two-phase one and two-component flows and it is therefore necessary to review a few of the correlations and empirical formula derived by previous authors.

The correlation of Lockhart and Martinelli[47] is probably the most widely used method for predicting the pressure drop in a two-component system. Experimental measurements of the ratio of pressure drops $dP]_{TP}/dP]_{SPL}$ were correlated to the non-dimensional variable described in chapter 6 (equation 6.2). The resulting relation has been used with reasonable success over the complete range of qualities and pressures. However it has been pointed out by Chisholm[78] that the correlation was developed mainly for horizontal two-component flow at atmospheric pressure and hence applications at higher pressures or to a one-component mixture may result in an appreciable error.

Chisholm[78] suggested that for an air-water system the two-phase frictional pressure drop may be estimated using the equation

$$\frac{dP]_{TP}}{dP]_{SPL}} = 1 + c\sqrt{\frac{dP]_{SPG}}{dP]_{SPL}}} + \frac{dP]_{SPG}}{dP]_{SPL}} \qquad 7.3$$

where

$$\frac{dP]_{SPG}}{dP]_{SPL}} = \left(\frac{\alpha}{1-\alpha}\right)^{1.75} \qquad 7.4$$

The value of the constant c was found to lie between 5 and 21 depending on the absolute pressure and the type of flow regime as described by Lockhart and Martinelli[47].

It was recommended by Chisholm and Laird[79] that for general engineering work the expression

$$\frac{dP]_{TP}}{dP]_{SPL}} = \frac{0.8}{(1-\alpha)^{1.75}} \qquad 7.5$$

should be used to obtain an estimate of the two-phase frictional pressure drop.

For a bubbly air/water mixture Wallis[80] found that the formula

$$\frac{dP]_{TP}}{dP]_{SPL}} = 1 + 3.0\,\frac{Q_g}{Q_f}\,(G \times 10^{-6})^{\frac{1}{3}} \qquad 7.6$$

[G] = lbs/ft²hr.

although dimensionally inconsistent, successfully predicted the pressure drop in pipes of up to 1" in diameter.

Martinelli and Nelson[81] correlated the two-phase pressure drop in a steam/water system with the non-dimensional variable

$$\chi = \left(\frac{\rho_g}{\rho_f}\right)^{0.572}\left(\frac{\mu_f}{\mu_g}\right)^{0.143}\frac{W_f}{W_g} \qquad 7.7$$

This yielded a similar result to the Lockhart-Martinelli correlation.

A similar equation to 7.3 was derived by Chisholm for application to a steam/water mixture. However good agreement with the Martinelli-Nelson correlation was only obtaincd at pressures nearing the critical pressure.

From shear stress considerations, Levy[58] derived the approximate expression for the two-phase pressure drop

$$\frac{dP]_{TP}}{dP]_{SPL}} = \left(\frac{1}{1-\alpha}\right)^2 \qquad 7.8$$

which was found by Chisholm[82] to give a good correlation with experimental data for pressure gradients below 60 lb./ft.^{3}.

The pressure drop "ratios" so far discussed represent pressure losses measured over an infinitesimal small length of pipe such that the flow properties retain

a constant value. Hence they can be applied directly to a non-accelerating air/water system where the voidage and quality do not vary significantly along the length of the flow. In a flashing or accelerating system, the voidage and quality continuously change and therefore the total pressure drop along a given length of pipe must be given by

$$\frac{\Delta p]_{TP}}{\Delta p]_{SPL}} = \frac{1}{x_E}\int_0^{x_E} \frac{dp]_{TP}}{dp]_{SPL}}\, dx \qquad 7.9$$

where x_E is the quality at the exit of the pipe.

If $dp]_{TP}/dp]_{SPL}$ is known as a function of the voidage then equation 7.9 may similarly be written in terms of the exit voidage α_E.

For this approach to give satisfactory results the variation of flow quality or voidage along the flow must be known.

Martinelli and Nelson (81) assumed a linear relation between x and distance along the flow, and together with their correlation previously noted, were able to estimate the pressure drop in an evaporating system.

Experimental work was carried out by Wallis (80) with an accelerating bubbly flow. Air bubbles were continuously injected into a flow of water through the pipe walls which were of a porous material. The two-phase pressure drop was correlated with the non-dimensional parameter $\frac{q}{\bar{u}}$ where q represents the radial air flux at the pipe wall and $\bar{u}$ the liquid velocity. The correlation suggested the empirical equation

$$\frac{\Delta p]_{TP}}{\Delta p]_{SPL}} = 1 + \left(\frac{n\,\dot{Q}}{\bar{u}}\right)^{m} \qquad 7.10$$

where m and n took on various values according to the pipe size. For the application of this correlation to a flashing system it was assumed that $\dot{Q}$ could be regarded as the rate of vapour formation on the tube walls. Hence $\dot{Q}/\bar{u}$ is proportional to the flow quality at the pipe exit and equation 7.10 is similar to the equation derived by Jakob (80).

$$\frac{\Delta p]_{TP}}{\Delta p]_{SPL}} = 1 + K x^{1.17} \qquad 7.11$$

If, as assumed by Martinelli, x varies linearly along the pipe length and flashing commences at the pipe entrance, the average quality within the flow is $x_E/2$ and equation 7.11 is of the form

$$\frac{\Delta p]_{TP}}{\Delta p]_{SPL}} = 1 + K'\left(\frac{\alpha}{1-\alpha}\right)^{1.17} \qquad 7.12$$

where K′ is a constant only if the slip velocity ratio is considered to have a constant value along the flow.

From these previous theories it is evident that the non-dimensional parameter $\frac{\alpha}{1-\alpha}$ may be sufficient to correlate with the two-phase frictional pressure drop. The analysis gives in appendix C, which is similar to that presented by Chisholm (78) shows that the pressure drop in a two-phase flow may be given by

$$\frac{dp]_{TP}}{dp]_{SPL}} = \left(1 + \frac{\alpha}{1-\alpha}\right)^{2-n} \qquad 7.13$$

where n has an approximate value of 0.25 depending on the pipe inner surface.

For small voidages, this can be approximated to

$$\frac{dP]_{TP}}{dP]_{SPL}} = \left(1 + \frac{m'\alpha}{1-\alpha}\right) \qquad 7.14$$

where m = 1.75, although experimental work with air/water bubbly mixtures [25] indicates that for voidages up to 30% an equation of this form (7.14) will successfully predict the pressure drop in a horizontal flow with m' = 3.0.

Equation 7.14 is compared to the predictions of other authors in Fig. 37. The curves are plotted over the range of voidages with which this report is most concerned, and at a pressure of one atmosphere. For an air/water system under these conditions it can be seen that Chisholm (equation 7.3) predicts pressure drops much larger than those suggested by the Lockhart-Martinelli correlation. The general equation (7.5) for all flow regimes predicts low values for the pressure drop in the low quality regime considered here.

The dependence on flow rate is made clear by the results of Wallis (equation 7.6). Experimental verification of equation 7.14 [25] was carried out with specific mass flow rates of 100 - 300 lb./ft.^{2}sec. which probably accounts for the agreement between equations 7.6 and 7.14 shown in the figure (37.1). However it is possible that higher flow rates result in larger values of the two-phase frictional pressure drop than will be predicted by equation 7.14.

For a steam/water flow, Fig. 37.2 shows good

agreement between the Martinelli-Nelson correlation, the equation of Levy and equation 7.14. The equations due to Wallis (7.10) and Jakob (7.11) were evaluated with the constant $K' = 3.0$ which gave best agreement.

It has been shown in this section that equation 7.14 can be used to give an acceptable estimate of the two-phase frictional pressure drop in both air/water and steam/water horizontal systems and hence will be used in this analysis.

Using equation C.1 (Appendix C) for the frictional pressure drop in a single phase flow, together with equation 7.14 gives

$$\left.\frac{dP}{d\ell}\right]_{TP} = \frac{4f}{2D} U_o^2 \rho_f \left(1 + \frac{m'\alpha}{1-\alpha}\right) \qquad 7.15$$

Equations 7.15 and 7.2 are hence substituted into the momentum equation for the liquid phase (7.1).

Assuming the flow to be steady, the momentum equation for the liquid phase of a two-phase bubbly flow becomes:-

$$U_f \frac{dU_f}{d\ell} = -\frac{1}{\rho_w}\frac{dP}{d\ell} + Nd + \frac{(1-\alpha)}{2}\frac{\rho_\ell}{\rho_g} \propto \left(U_g \frac{dU_g}{d\ell} - U_f \frac{dU_f}{d\ell}\right) - \frac{4f}{2D} U_o^2 \left(1 + \frac{m'\alpha}{1-\alpha}\right) \qquad 7.16$$

d being defined by equation 6.21.

7.3 Momentum equation for the vapour phase

For a horizontal evaporating one-component bubbly flow, the momentum equation of the vapour phase has been shown to be: (appendix D, equation D.10).

$$\rho_g U_g \frac{dU_g}{d\ell} = -\frac{dP}{d\ell} - N D_o \rho_f \frac{(1-\alpha)}{\alpha}$$

Substituting for D_o from equation 7.2 and making the approximations indicated in section 6.3, this can be written

$$\sigma(1-\alpha)\,\rho_f\left(u_g\frac{du_g}{d\ell} - u_f\frac{du_f}{d\ell}\right) = -\frac{dp}{d\ell} - \sigma\frac{dN}{x}\rho_g \qquad 7.17$$

7.4 Continuity equation (conservation of mass)

For a single phase one dimensional compressible fluid flow the continuity equation is

$$\frac{d\rho}{dt} + \rho\frac{\partial u}{\partial \ell} = 0 \qquad 7.18$$

Assuming the flow to be steady and within a constant area pipe, this reduces to

$$\frac{\partial(\rho u)}{\partial \ell} = \frac{\partial G}{\partial \ell} = 0 \qquad 7.19$$

In a two-phase system, the specific mass flow rate can be written

$$G = \alpha u_g \rho_g + (1-\alpha) u_f \rho_f \qquad 7.20$$

Combining equations 7.19 and 7.20 results in

$$\frac{\alpha V_g}{u_g}\frac{du_g}{d\ell} + \frac{V_f \sigma}{u_f}\frac{du_f}{d\ell} - \alpha\left(\frac{\partial V_g}{\partial p}\right)\frac{dp}{d\ell} = V_g\frac{dx}{d\ell} \qquad 7.21$$

7.5 Energy equation

The steady flow energy equation for a horizontal adiabatic two-phase system is shown, in appendix E, to reduce to:-

$$h_{fg}\frac{dx}{d\ell} = -c_w\frac{dT}{d\ell} - \frac{u_f}{J}\frac{du_f}{d\ell} \qquad 7.22$$

7.6 Rate of vaporization equation

The idealized model from which the rate of vaporization equation is derived assumes no temperature gradients to exist within the bubble, the bubble

temperature being the saturation temperature corresponding to the local fluid pressure. The vapour/water interface is also at the saturation temperature, but the bulk water temperature is independent of the pressure. Therefore a temperature gradient exists within a spherical shell of liquid surrounding the bubble, and it is this which denotes a departure from thermodynamic equilibrium.

The rate of heat transfer from the liquid phase across the bubble surface is given by

$$\frac{dQ}{dt} = KA\left(\frac{dT}{dr}\right)_{\text{BUBBLE SURFACE}} \qquad 7.23$$

and hence the rate of vaporization can be written as

$$h_{fg}\frac{dx}{dt} = KA\left(\frac{dT}{dr}\right)_{bs} \qquad 7.24$$

where K is the thermal conductivity of the liquid and A is the liquid/vapour interface area per pound of fluid.

The radial temperature gradient $(dT/dr)_{bs}$ depends not only on the temperature difference between the phases but also upon the time which has elapsed since the initiation of the flow, i.e. the flow "history". The evaluation of (dT/dr) also relies upon the geometry of a system and hence a simple one-dimensional approach will only give a realistic value for the temperature gradient at the surface of a large bubble. For smaller bubbles it was suggested by Edwards (56) that the effect of spherical geometry is to increase the

heat transfer across the surface by a factor of $\sqrt{3}$.

7.6.1 Evaluation of $(dT/dr)_{BS}$ as applied to critical flow

Carslaw and Jaeger[83] derived an analytical solution for the temperature field within a semi-infinite medium, the boundary of which is subject to known temperature variations T(t).

Neglecting spherical geometry effects, the above approach is applicable to a vapour bubble in an infinite liquid, only if it is assumed that the bubble remains in contact with the same particles of fluid.

With these restrictions, the solution suggested by the results obtained by Carslaw and Jaeger, for the temperature field within a liquid surrounding a bubble of temperature $T_s(t)$ is

$$T]_{\text{AT DISTANCE } y \text{ FROM BS}} = \frac{-y}{2(\pi\kappa)^{1/2}} \int_0^t T_s(\lambda) \frac{e^{-\frac{y^2}{4\kappa(t-\lambda)}}}{(t-\lambda)^{3/2}} \, d\lambda \qquad 7.25$$

Unfortunately, in a critical two phase flow, $T_s(t)$ is not known explicitly. Therefore an exact solution of equation 7.25 is not possible.

An approximate solution may be obtained by assuming T = kt (k a constant). This yields

$$\left(\frac{dT}{dr}\right)_{BS} = \left(\frac{dT}{dy}\right)_{y=0} = \frac{2(T - T_s)}{(\pi\kappa t)^{1/2}} \qquad 7.26$$

Edwards[56] considered the effects of bubble growth in a constant pressure field. By using the results of Plesset and Zwick[84] the expression derived for the bubble surface temperature gradient was

$$\left(\frac{dT}{dr}\right)_{BS} = \frac{\sqrt{3}\,(T - T_s)}{(\pi \kappa t)^{1/2}} \qquad 7.27$$

The assumption that the same liquid particles remain in contact with the bubble surface will almost certainly not occur in practice. Due to bubble growth, the existence of a slip velocity ratio and turbulence within the flow, the liquid in contact with the bubble is continuously changing, leading to an effective heat transfer coefficient larger than indicated by equations 7.26 and 7.27.

The effect of a relative velocity occurring between a bubble and its surrounding liquid, on the collapse of vapour bubbles have been noted by Wittke and Chao[88].

Ruckenstein[85] considered the heat transfer between a liquid at rest and a bubble of constant radius moving through the liquid with constant velocity U. Using spherical geometry he derived the rate of heat transfer across the bubble surface as

$$\frac{dQ}{dt} = h A (T_\infty - T_s) \left[-h_{fg} \frac{dx}{dt}\right] \qquad 7.28$$

where h, the effective heat transfer coefficient, is given by the expression

$$h = \frac{\sqrt{2}\,K}{\sqrt{\pi \kappa}} \cdot \sqrt{\frac{U}{r}} \qquad 7.29$$

In a later paper Ruckenstein and Davis[86] modified the above theory and obtained a more widely applicable equation

$$h = \frac{\sqrt{3}}{2\sqrt{2}} \frac{K}{\sqrt{\pi K}} \left(\frac{U}{r}\right)^{1/2} w(t,r) \qquad 7.30$$

Value of the function w(t, r) tabulated in reference [87] indicate that for $\frac{3}{2}\frac{Ut}{r} \gg 1.0$, w takes on the constant value of 3.3, in which case equation 7.30 reduces to equation 7.29. The effect of the condition $3Ut/2r \gg 1.0$ is to neglect transient variations at small time.

Bubble velocity was shown to have the maximum effect on bubble growth for $N_{JA} < 50$, where N_{JA}, the Jakob number is defined as

$$N_{JA} = C_w \frac{(T_F - T_S)}{h_{fg}} \frac{\rho_f}{\rho_g} \qquad 7.31$$

For a steam/water system at atmospheric pressure, $N_{JA} = 1.6\ (T_F - T_S)$. Hence for superheats less than $30^{\circ}F$ it is considered that an equation of the form 7.29 must be used in the present analysis for two-phase one-component critical flow.

A lack of experimental data prevented Ruckenstein from rigorously verifying equation 7.29. However it was shown to give values of h of the same order as measured experimentally by Fritz and Ende [85].

In his analysis, Ruckenstein makes three assumptions which make doubtful the direct application of equation 7.29 to a two-phase flow. These assumptions were to neglect the effects of

(1) Bubble growth

(2) Turbulence

(3) Presence of other bubbles

At the front stagnation point of a bubble moving through a liquid, bubble growth will result in increasing the effective bubble velocity and hence the heat transfer coefficient at that point. It may be expected that a corresponding decrease in heat transfer coefficient will occur at the rear stagnation point. However, the increase in thickness of the thermal boundary layer towards the rear of the bubble [86][88] will limit this effect. It is therefore probable that bubble growth will continually move the bubble surface into regions of higher liquid temperatures and increase the heat transfer across the bubble surface.

The effect of turbulence within a fluid flowing next to a plane surface is to increase the effective heat transfer coefficient at the surface [11], and hence it is likely that turbulence within a fluid flowing around a bubble will have a similar effect.

The Ruckenstein theory is valid for independent bubbles which, it was suggested, should be separated by a distance of at least 4r. This implies that for equally spaced spherical bubbles, the maximum voidage obtainable under this restriction is less than 10%.

A change in the heat transfer coefficient at a bubble surface due to the presence of other bubbles may only be expected if its temperature field "overlaps" the temperature field of a nearby bubble. This effect has been indicated experimentally by Calderbank and Moo-Young [11].

Equation 7.29 can be written for a steam/water mixture in the form

$$N_u = 1{\cdot}13\,(P_e)^{1/2} \qquad 7.32$$

Collier and Wallis[11] noted that the majority of experimental data for the heat transfer coefficient of a single spherical body in an infinite fluid could be correlated using the expression

$$N_u = 2 + 0{\cdot}7\ P_r^{1/3} R_e^{1/2} \qquad 7.33$$

where the first term on the R.H.S. represents the solution for a stagnant fluid.

Grigull[83] recommended the use of the expression

$$N_u = 0{\cdot}37\ P_r^{1/3} R_e^{0{\cdot}6} \qquad 7.34$$

Experimental work on bubble dispersions have shown that the effect of voidage is to lower the heat transfer coefficient at the bubble surface[11]. For small spherical bubbles it was found that the data approximately satisfied

$$N_u = 0{\cdot}81\ P_r^{1/3} R_e^{1/3} \qquad 7.35$$

The Prandtl No. (P_r), Reynolds No. (R_e) and Péclet No. (P_e) are related by

$$P_e = P_r\ R_e$$

For a steam/water mixture the Prandtl number has a value of approximately 0.2. Hence equations 7.33 – 7.35 can be written in terms of P_e. A comparison between the predictions of the above expressions are shown in Fig. 38.

As can be seen from the previous discussion, it is likely that the heat transfer across a bubble surface

which is moving within a turbulent bubbly mixture can be represented by an equation of the form recommended by the Ruckenstein model (equation 7.29 and 7.28). It is therefore proposed that the effective heat transfer coefficient in a flashing two-phase one-component flow can be written in the form

$$h = \eta_o \left[\frac{u_f(\sigma-1)}{r}\right]^{1/2} \qquad 7.36$$

where η_o is a constant possibly determined from experimental data.

The value of η_o suggested by the Ruckenstein model for a steam/water system is 0.07 BTU/ft.^{2} sec.$^{\frac{1}{2}}$ F.

Equation 7.28 and 7.36 constitute the rate of vaporization equation which is used in the computation described in chapter 8.

7.6.2 Evaluation of $(dT/dr)_{BS}$ as applied to velocity of pressure wave calculations

In both the theoretical analysis and experimental work on the propagation velocity of pressure waves in a two-phase one-component media, the fluid is assumed to be homogeneous with both phases moving with the same velocity. Hence the solution for the temperature field about a stationary bubble is applicable.

Using equation 7.25, given by Carslaw and Jaeger, the surface temperature variation is given by

$$T_s(t) = T_f + \Delta T \cos \omega t \qquad 7.37$$

Neglecting any transient variations of temperature caused by the initiation of the surface temperature

disturbance, the solution of the integral (7.25) yields

$$T = \Delta T\, e^{-y\left(\frac{\omega}{2\kappa}\right)^{1/2}} \cos\left[\omega t - y\left(\frac{\omega}{2\kappa}\right)^{1/2}\right] \qquad 7.38$$

which implies

$$\left(\frac{dT}{dy}\right)_{y=0} \equiv \left(\frac{dT}{dr}\right)_{BS} = \Delta T\left(\frac{\omega}{2\kappa}\right)^{1/2} (\sin \omega t - \cos \omega t) \qquad 7.39$$

ΔT, the amplitude of the temperature variation is $T_F - T_{SM}$ where T_{SM} is the saturation temperature corresponding to the ambient pressure plus the maximum wave pressure, and T_F is the liquid temperature which, if the mixture is assumed to be initially in thermodynamic equilibrium, is equal to the saturation temperature corresponding to the ambient fluid pressure.

It is unnecessary to use the continuous expression for the temperature gradient (equation 7.39) in the analysis of the propagation velocity of sinusoidal waves. In view of the approximations already made it is considered sufficient to obtain the average temperature gradient for a given frequency. This involves integrating equation 7.39 over one cycle. As the integrand is periodic, the solution over an integral number of cycles is zero. Hence equations 7.24 and 7.39 indicate that any difference between the rate of vaporization and the rate of condensation in this theory, is due only to the variations of bubble surface area.

The mean value of $(dT/dr)_{BS}$ over the positive half of a cycle is given by

$$\left(\overline{\frac{dT}{dr}}\right)_{BS} = 2f \int_{f/2}^{5f/8} \left(\frac{dT}{dr}\right)_{BS} dt \qquad 7.40$$

Hence from equation 7.39

$$\left(\frac{dT}{dr}\right)_{os} = \frac{2\sqrt{2}}{\sqrt{\pi K}} (T_{SM} - T_F) f^{1/2} \qquad 7.41$$

Combining this temperature gradient with equation 7.24, it can be seen that the rate of vaporization equation can be written in the form

$$\frac{dx}{dt} = \frac{hA}{h_{fg}} (T_{SM} - T_F)$$

where

$$h = \frac{2\sqrt{2}}{\sqrt{\pi K}} K f^{1/2}$$

or in terms of the instantaneous temperature difference between the phases, $(T - T_s)$

$$\frac{dx}{dt} = \frac{hA}{h_{fg}} (T - T_s) \qquad 7.42$$

where

$$h = \frac{\sqrt{2\pi}}{\sqrt{K}} K f^{1/2} \qquad 7.43$$

or $h = \eta_s f^{1/2}$ where η_s is an empirical constant to be determined experimentally, and having a probable value of $\approx$ 0.2 BTU/ft.^{2} sec.$^{\frac{1}{2}o}$ F for a steam/water mixture.

7.7 Supplementary Equations

The area of the liquid/vapour interface per unit mass of the fluid is given by the equation

$$A = 4\pi r^2 N/\sigma \qquad 7.44$$

Eliminating the bubble radius by using the expression

$$x = \frac{4}{3}\pi r^3 N \rho_g \qquad 7.45$$

yields the result

$$A = \frac{4.83}{\sigma} \left[N (V_g x)^2\right]^{1/3} \qquad 7.46$$

The equation relating the voidage, quality and slip velocity ratio (equation 5.4) is re-written here for convenience

$$\sigma = \left(\frac{1-\alpha}{\alpha}\right)\left(\frac{x}{(1-x)}\right)\frac{V_g}{V_f}$$

To enable numerical computation, empirical curves were fitted to data obtained from standard steam tables giving the saturation temperature and the specific volume of the vapour phase as functions of pressure.

$$V_g = \frac{403.0}{P} - \frac{166.0}{P^2} \qquad P < 12.0 \text{ P.S.I.}$$

$$V_g = \frac{423.7}{P} - \frac{489.7}{P^2} + 0.242 \qquad P > 12.0 \text{ P.S.I.} \qquad 7.45$$

$$T_s = 59.3\sqrt{P} - 4.59\,P + 52.5 \qquad P < 14.7 \text{ P.S.I.}$$

$$T_s = 30.76\sqrt{P} - 0.866\,P + 106.8 \qquad P > 14.7 \text{ P.S.I.}$$

These empirical equations were differentiated to give values of $\left(\partial T_s/\partial P\right)_{SAT}$ and $\left(\partial V_g/\partial P\right)_{SAT}$

The accuracy given by the above formulae is better than 1% of the tabulated values over the range of pressures 4 p.s.i.→100 p.s.i. At atmospheric pressure the accuracy is within 0.2%.

The values of T_s are most important in the calculation of the rate of increase of quality. The errors incurred by the use of the empirical equations will depend on the absolute values of $T_F - T_S$ (equation 7.28) and hence will be greatest at the initiation of a flashing system. For the major part of such a flow it is expected that, within the bubbly flow regime, the effect of thermodynamic non-equilibrium will be to increase the value of $(T_F - T_S)$ so minimising the error. For example, at the exit of a choking flow, assuming the pressure ratio to be $\frac{1}{2}$ [91], if the exit pressure is atmospheric, the value of $T - T_S$ at the exit may be of the order of $30^{\circ}F$.

In this case the error will be less than 2%.

The maximum effect of errors in $(\partial V_g/\partial p)_{sm}$ will be evident in the calculation of sonic velocity. At atmospheric pressure, the error in the calculated value of the compressibility term will be 3%, which will lead to errors in the evaluation of sonic velocity of < 2%.

Clearly the accuracy of the values of T_S and V_g given by equations 7.45 are important in the calculation of the critical flow condition and sonic velocity in a two-phase one-component mixture. It is possible that an alternative method of storing the tabulated values of these variables in a computer would be preferable. However such a facility was not available on the computer used for the present calculations.

8. THEORETICAL PREDICTIONS OF CRITICAL FLOW

8.1 Numerical Computation

Equations 7.16, 7.17, 7.21, 7.22, 7.28 and 7.32 represent the flow of a two-phase one-component mixture along a pipe, as a set of simultaneous, first order, differential equations, the numerical solution of which involved the use of a forward "step by step" integration technique (89).

Knowing the fluid properties F_o at the initiation of the two-phase flow ($\ell = o$), the axial gradient of each fluid property can be determined using the basic equations, which can be rearranged to the form:-

$$\frac{dF_o}{d\ell} = Q(F_o) \qquad 8.1$$

The value of the fluid property at a distance $d\ell$ downstream of the initial point is therefore given by

$$F]_{\ell=d\ell} = F_o + Q(F_o)\, d\ell = F_1 \qquad 8.2$$

This process can be repeated using F_1 as the "initial" value, hence the fluid properties at all points along the flow can be computed.

The accuracy of such a method clearly depends on the axial step length $d\ell$, and as equation 8.2 represents the first two terms of a Taylor expansion, the errors incurred are of the order $\left(\frac{d\ell}{\ell}\right)^2$

Several modifications have been made to this basic technique to improve the accuracy. The most popular of these are probably the Runge-Kutta methods of forward integration (89) which give maximum errors of the order $\left(\frac{d\ell}{\ell}\right)^5$

However, because of the simplicity of the

method and the nature of the expected solution of the equations, the basic method was used in the present numerical computations.

In a choking two-phase one-component flow, the fluid properties are expected to change slowly during the initial part of the flow and at a near infinite rate towards the flow exit. For the maximum accuracy to be obtained, within an acceptable length of computation time, a variable axial step length was introduced, this being proportional to the local pressure gradient. Hence the integration step length commenced at a value of 10^{-3} ft. and decreased to a value of approximately 10^{-5} ft. at the pipe exit.

Smaller step lengths were also used, but no significant change in the results were obtained.

8.1.1 Initial conditions

To enable the present mathematical model to simulate flashing in a constant area pipe for a given mass flow, an initial pressure was chosen and the initial liquid temperature set at the corresponding saturation temperature, indicating zero superheat.

It can be seen from the rate of vaporization equation (7.28, 7.46) that a finite value of the flow quality is required for the initiation of the flashing. This initial quality may physically be representative of small bubbles of air or vapour which exist within the system prior to the position where, experimentally, flashing is observed to commence (section 7). The effect of

air-bubbles in a flashing flow have been noted by Henry (55).

It is possible numerically, to initiate flashing from zero quality by considering further terms in the Taylor expansion (equation 8.2). However, this method offered no significant advantage.

8.1.2 Exit Conditions

As previously noted, the step lengths of integration used within the computation were dependent on the axial pressure gradient. Hence near the choked outlet of the pipe, where the pressure gradients are very large the integration step lengths were very small. This enabled the critical pipe length for a given inlet pressure and specific mass flow rate to be determined accurately.

The computation was halted when the pressure gradient became sufficiently large such that the theoretical pressure became negative. This is when the mathematical equations are inconsistent with the physical system. The computed values of the flow properties immediately prior to this condition were assumed to be the critical flow properties.

It was found that the "critical" outlet pressure and the exit flow properties X_{EQ} ; T_s and α were particularly dependent on the step length of integration as the axial gradients of these properties were near infinite at the pipe exit. Although in the majority of cases the variation of such a fluid property over the last integration step length was $< 2\%$, it has

nevertheless been denoted by a "bar" in the figures.

The other flow properties χ and σ , were less dependent on sudden pressure changes and varied by < 1% over each computation step length near the flow exit.

8.2 Survey of experimental techniques used to investigate a critical flow

Experimental investigations into the critical flow phenomena within a two-phase one-component mixture, have been carried out by many authors [50][70]. Unfortunately the majority of this experimental work dealt with high quality flows, possibly not within the bubbly regime, and therefore the results are not directly comparable to the theory presented in the previous chapters.

However the techniques used to measure the flow properties in this experimental work will probably also be applicable to choking flow experiments within the bubbly regime. Hence a study of these measuring techniques will enable the most relevant parameters to be chosen from the critical flow theory, with which to describe a two-phase critical flow.

A two-phase steam/water flow can be obtained experimentally in two ways. Firstly the liquid phase, being near the saturation temperature, can be flashed [55], or secondly the two-phases can be mixed using a system of nozzles [93][49]. In both cases the initial flow properties can be determined, in the former by monitoring the single phase and in the latter case by monitoring each phase individually before the mixing process.

The pressure along the main flow pipe is usually measured using a series of manometers and the choking

condition can be detected by reducing the downstream pressure, until a further reduction does not result in a change of the pressure profile along the pipe axis. This condition was difficult to obtain in practice (49)(70), the manometer nearest the pipe exit invariably changing with further variations of downstream pressure. Isbin (49), suggested that this was due to the non-uniform distribution of the phases, the pressure being transferred upstream via a liquid annulus. Henry (55) showed that another possible cause was the effect of the two-phase jet emerging from the pipe exit and by attaching a diverging nozzle to the end of the pipe, to restrict the expansion of the jet, he obtained "complete" choking.

If experimental results are to be compared to a theoretical analysis, the fluid pressure at the exit of the flow must be determined. Theoretically, the pressure gradient at the exit of a choking flow is infinite, hence difficulty was experienced in measuring this "critical" pressure. Isbin, Moy and Da Cruz (49) obtained the critical pressure by extrapolating the axial pressure profile, indicated by the manometers, to the pipe exit. The accuracy of this method is clearly dependent on the distance of the downstream manometer from the pipe exit. The same method was used by Zaloudek, his manometers being closer to the pipe exit, and the results obtained implied exit qualities 50% higher than those measured by Isbin. Fauske used a manometer situated one pipe diameter from the pipe exit

to determine the critical pressure.

Uchida and Nariai[91] placeda manometer at the end of the pipe such that the centre line of the manometer tapping coincided with the exit plane of the pipe. An annular flow tube was used by Faletti and Moulton,[92] which enabled the pressure at the mid-point of the exit plane to be measured via the centre core.

It is probable that the effects of the fluid jet at the pipe exit, as described by Henry[55], were significant in the last two methods.

The importance of an accurate measurement of the critical pressure is further emphasised by the method generally used to determine the exit flow quality.

Assuming the fluid to be in thermodynamic equilibrium, the exit quality was calculated using the energy equation

$$\text{Total Energy} = h_f + x h_{fg} + \frac{(V_f + x V_{fg})^2 G^2}{2J} \qquad 8.3$$

Hence, knowing the inlet fluid enthalpy, specific flow rate and the critical pressure, the exit quality could be determined.

In a flow where thermodynamic equilibrium does not exist, this method of measuring the exit quality can no longer be used. If the energy equation is written in the form of equation 7.22 it can be seen that if the increase in kinetic energy of the fluid can be neglected, the change in quality between two points within the flow is proportional to the liquid temperature drop.

Therefore, if x_o and T_o are the initial quality and liquid temperature of a flashing flow, then at any point along the flow, x and T are related by :-

$$x - x_o = \frac{c_w}{h_{fg}}(T_o - T) \qquad 8.4$$

Hence, by measuring the temperature loss of the liquid phase in passing along a choked flow, the resulting exit quality can be estimated.

Such temperature measurements have been made (25) with limited success. However these were not in a critical flow and the application of such measurements at the exit of such a flow may be less satisfactory.

As discussed in chapter 5, Henry (55) estimated the exit quality of a choking flow, by introducing an empirical relation

$$x = \sigma N' x_{EQ} \qquad 8.5$$

where N' could be calculated throughout the flow directly from pressure measurements. The quality is seen to be dependent on the slip velocity ratio which was estimated at 1.3 for low quality flows, possibly in the bubbly regime.

It can be seen from the above brief survey that a limited number of fluid properties can be measured at the exit of a choking flow.

The fluid pressure can be determined at a distance upstream of the exit and depending on this distance this measured pressure can be assumed to be the critical pressure (50) or the approximate critical pressure can

be extrapolated[49][70].

Assuming thermodynamic equilibrium to exist, the exit quality can be determined directly from the knowledge of the critical pressure. The exit voidage can be determined using γ-ray attenuation techniques[25][55] and using the general equation relating quality, voidage and slip (equation 5.4), the "equilibrium" slip velocity ratio can be determined.

The deviation of the physical system from a flow which is assumed to remain in thermodynamic equilibrium, can be denoted by the variable

$$\beta = \frac{x}{x_{eq}} \qquad 8.6$$

This is equivalent to the group of variables $\sigma N'$ as used by Henry[55].

If the small kinetic energy terms are neglected in the energy equation (7.22), it can be seen that

$$\frac{x}{x_{eq}} = \frac{T_o - T}{T_o - T_s} = \beta \qquad 8.7$$

which is a variable first introduced by Silver[7] and is known as the "fraction of equilibration".

It is suggested that the most important parameters with which to describe a choking flow, knowing the specific mass flow rate and initial fluid pressure, are the exit "equilibrium" quality (x_{eq}), the fraction of equilibration (β), the exit voidage (α_E) and the critical length of pipe within which choking occurs (L_c).

8.3 Theoretical Results

The equations described in chapter 7 were solved using the numerical method outlined in section 8.1 on an

Elliot 903 computer and the results are shown in Figs. 39 - 42.8. Before these predictions are discussed, the effect of parameters, which do not necessarily occur, within the physical system, must be noted. These are the integration step length ($d\ell$) and the initial quality (x_o) The following table shows the maximum change in the critical exit flow properties when $d\ell$ is decreased from 10^{-2} to 10^{-3} (ft.) and x_o from 10^{-5} to 10^{-6}.

	β	x	x_{EQ}	α	σ	L_c
$10^{-2} \rightarrow d\ell. \rightarrow 10^{-3}$	4%	1%	5%	3%	0.5%	3%
$10^{-5} \rightarrow x_o \rightarrow 10^{-6}$	20%	20%	6%	12%	1%	40%

Understandably, a knowledge of x_o is required before an accurate prediction can be made of the critical flow properties. As previously noted in section 8.11, x_o may vary considerably in different experimental systems, with the result that when this theory is being applied to a particular system (section 8.4) the relevant value of x_o must be estimated.

Fig. 39 shows typical axial profiles of flow properties along the length of a choking flow. Pressure variations are slow initially, increasing quite suddenly near the pipe exit. The voidage profile also has this characteristic, unlike the theory of Linning[53] which predicts a sudden increase in voidage within the first part of the flow.

It can be seen that at the choking exit, the slip velocity ratio attains a value of approximately 1.2 which is of the same order as those indicated experimentally in low quality choking flows[55].

The axial gradient of the quality at the pipe exit, $\left(\frac{dx}{dp}\right)_E$ is shown to be finite indicating that the mixture is not in thermodynamic equilibrium.

Due to the initial condition imposed on the solution (section 8.1.1), that the fluid is initially in thermodynamic equilibrium (hence neglecting any effect of surface tension, section 5.3), the fraction of equilibration β has an initial value of unity and then decreases because of the small interphase surface area available for vaporization to occur. As this area and the time since the initiation of the flow increase, the fluid tends towards equilibrium (i.e. β exhibits a minimum) until the "choking" pipe exit is reached where, because of the large pressure gradient and the finite rate of vaporization, β decreases suddenly.

The variation of β with η_o is shown in Fig. 40. An increase in the value of η_o results in a smaller critical pipe length (L_c), for a given mass flow and initial pressure, and also a higher maximum value of β within the pipe.

The friction factor and pipe diameter appear in the basic equations as the ratio f/D, hence a decrease in D or increase in f have equivalent effects on the computed results.

The number of bubbles per unit mass of fluid (N) and the parameter η_o both directly affect the rate of vaporization and hence the critical pipe length.

Variations of the predicted results with changes in the parameters f/D, N and η_o are shown in Fig. 41

and it can be seen that they only marginally affect the exit flow properties at low pressures, the exit liquid velocity being mainly dependent on the exit voidage and quality irrespective of the flow "history". This is probably because of the relatively small maximum value of the slip velocity ratio. The major effect of changing the parameters f/D, N and η_o is in the calculation of the critical pipe length and fraction of equilibration as illustrated in Fig. 41.2.

Figs. 42 show computed flow properties at the exit of a choking stream/water bubbly mixture, calculated using the parameters f/D = 0.05 ft^{-1}; N = 20,000/lb.; $x_o = 10^{-5}$ and η_o = 0.1 BTU/ft.^{2}sec.$^{\frac{1}{2}o}$F.

The "critical" lengths of pipe (L_c) within which a given specific mass flow will choke for given inlet pressures (P_I) are shown in Fig. 42.1. By considering the P_I = 2ar. curve, it can be seen that a specific mass flow rate of 4,000 lb./ft.^{2}sec. will choke in a pipe of length 0.5 ft. In a shorter pipe this flow will not be choked as the critical flow rate is greater than 4,000 lb./ft.^{2}sec.; and similarly this flow cannot exist in a pipe of length greater than 0.5 ft., as it exceeds the critical flow rate. The broken portions of the curves (Fig. 42.1) indicate flows in which the exit voidage is greater than 50% and the flow regime is probably not bubbly.

The predicted quality at the exit of a choking flow (Fig. 42.2) shows the same variation with specific

mass flow rate as the experimental data of Henry[55]. However, due to departures from thermodynamic equilibrium within the mixture, the flow qualities predicted by this theory are less than those shown in Fig. 2 8.

Fig. 42.4 indicates that the pressure ratio is independent of flow rate and has a value between 0.35 and 0.4, varying with pressure, which compares with experimental results of Uchida and Nariai[91] who measured pressure ratios between 0.3 and 0.6 in a critical "mist" flow.

The fraction of equilibration which exists at the exit of a choking flow is shown in Fig. 42.5 for varying exit "equilibrium" qualities. It was suggested by the experimental work of Henry[55] that these variables should satisfy

$$\beta = 20\,\sigma\,x_E \qquad 8.8$$

Clearly this is not the case in Fig. 42.5. However, it is possible that experimentally the maximum values of β just upstream of the exit were measured, hence bringing the predictions of the present model more in line with equation 8.8. A full comparison with the experimental data of Henry[55] will be made in the following section.

The slip velocity ratios shown in Fig. 42.7 are higher than those predicted in chapter 6 for a horizontal air/water system with similar flow rates and voidages. This is due to the large pressure gradients and fluid accelerations which occur in the latter part

of a choking flow. As noted in section 6.5, the calculated slip velocity ratios do not include the effects of two-dimensional voidage and velocity profiles and may therefore under-estimate measurements made in any flow which is not completely homogeneous. This will be dealt with more fully in section 8.5.

The above discussion has indicated the principal effects of various flow parameters on a "critical" two-phase flow. When comparing the predictions of this theoretical approach to experimental data, the parameters f/D, N and x_o must be estimated for the particular experimental system. The correlation will then result in an estimate of the parameter η_o and hence the heat transfer coefficient of a bubble surface in a two-phase one-component flowing mixture.

8.4 Application of critical flow model to predict experimental results

Temperature measurements in a flashing horizontal steam/water bubbly flow enabled Herries [25] to determine the flow quality and make an estimate of the fraction of equilibration. The number of bubbles per pound of fluid was estimated at 500 which is considerably less than noted in the present experimental work (Fig. 14.1), and is probably due to bubbles coalescing shortly after nucleation. The other flow parameters in these experiments were D = 0.531", f = 0.0053; P_I = 1 AT, and specific mass flow rates of 260 - 370 lb./ft.^{2}sec. Difficulty was experienced in determining the exact position where the flashing commenced and therefore in

describing this flow theoretically the initial quality (x_o) was set at an average value of 10^{-5}. Best agreement between the experimental results and theoretical predictions using the present model was obtained with the parameter η_o = 0.2 BTU/ft.^{2}sec.$^{\frac{1}{2}o}$F (Fig. 43). The largest deviations between the two sets of results occurred at the higher mass flow rates where it was noted during the experiment that the flow regime deviated from bubbly, which would probably account for the larger values of β and the lower measured values of the liquid temperature.

Fauske[93] investigated two-phase steam/water choking flow in short cylindrical nozzles, the flashing occurring as the fluid passed from a reservoir into the nozzle. The results were successfully predicted by Edwards[56] who considered various regimes of bubble growth within the vena-contracta which existed at the nozzle entrance. It is proposed that the present critical flow model can predict the results of Fauske by assuming the flashing to occur in a constant area duct and applying a large initial superheat to the flow.

If the liquid within the reservoir is saturated and at a pressure P_R and temperature T_R, the pressure at the nozzle entrance P_I is given by the equation

$$P_I = P_R - G^2/2\rho_f$$

where G is the specific mass flow rate through the nozzle. As soon as nucleation occurs it is assumed that due to the very fast growth rate of the bubbles up to a critical radius[84] the bubbles immediately attain the saturation temperature corresponding to the local fluid pressure P_I.

Therefore the initial superheat is given by

$$\Delta T = T_R - T_s]_{p=p_i}$$

The experimental results, together with the predictions of Edwards, are shown in Fig. 44. An extrapolated curve corresponding to a reservoir pressure of 100 p.s.i. has been compared to the results of the present critical flow theory. (Flow parameters:— f = 0.01; D = 0.0208 ft.; N = 10^5/lb.; $x_o = 10^{-5}$ and η_o = 0.2 - 0.3 BTU/ft.^{2}sec.$^{\frac{1}{2}o}$F.) Agreement is not good for very small pipe lengths where it is likely that the effect of the vena-contracta dominates in the physical system.

Choking flows in low quality steam/water mixtures were investigated by Henry (55). Water of known initial enthalpy was flashed in cylindrical pipes at a mass flow rate such that choking occurred at the pipe exit. The axial pressure profiles were measured, which enabled the approximate deviation of the mixture from thermodynamic equilibrium to be determined (section 8.2). Although the pipe lengths were of the order of 30", the liquid did not attain the saturation condition until the flow approached the pipe exit and hence the present theory can only be applied to the latter part of these flows. Bubbles were observed along the total pipe length, which were assumed to be due to the pressure of undissolved gas within the water phase, and therefore an initial quality (x_o) of 10^{-4} was used in the present computations to describe this flow.

The theoretical pressure profiles agree well with the measured pressures (Fig. 45). However a discrepancy arises between the physical pipe exit and computed exit, which is probably due to the two-dimensional effects that occur near the pipe exit preventing the flow from choking in the way predicted by the theory. To eliminate these effects a diverging nozzle was placed at the pipe exit [55], the pressure measurements and theoretical predictions being shown in Fig. 45.3. The addition of the nozzle appears to initiate choking at a higher exit pressure, as it is noticeable that in this series of experiments the critical pressure ratio has a value of >0.9, whereas other authors have noted a value of approximately 0.5 [91].

The computed flow properties at the physical pipe exit are compared to the measured values (Figs. 45) and it can be seen that the predicted fraction of equilibration is lower than the measured value of N' (equation 5.12.1). The two variables β and N' differ by a factor of σ, the slip velocity ratio, and this was estimated at 1.3 for the majority of the experimental runs. The flow parameters used in the above computations were $f = 0.01$; $D = 0.313"$; $N = 10^6$/lb. and $\eta_o = 0.25$ BTU/ft.^{2}sec.$^{\frac{1}{2}o}$F.

From the above comparison with experimental data it can be seen that the present critical flow model may be used to give an estimate of the flow properties occurring in the choking flow of a steam/water bubbly mixture and it is likely that the parameter controlling

the rate of vaporization (η_o) has a value of approximately 0.2 - 0.3 BTU/ft.^{2}sec.$^{\frac{1}{2}o}$F.

8.5 Two-dimensional effects in two-phase critical flow

The cross section velocity profile of a saturated turbulent liquid flowing along a pipe is known to approximately satisfy a 1/7 power law [71]. When nucleation occurs it has been observed [64][65] that the bubbles which are formed, move towards the centre of the tube (chapter 6). This results in a less dense medium flowing within the centre of the tube, hence exaggerating the velocity profile and causing the rate of vaporization to be greater in the centre of the flow than at the pipe wall. Under these conditions the flow will quickly tend to an annular flow pattern.

A complete study of these effects would demand an accurate knowledge of bubble migration, shear stresses in a two-phase medium and a complex numerical computation. However an indication can be gained by considering the following bubbly/annular flow model.

8.5.1 Bubbly/annular critical flow model

Consider an annulus of water within which no nucleation occurs, surrounding a bubbly two-phase core. The equations describing the motion of the core are very similar to thosederived in chapter 7, except for two major modifications.

The continuity equation for a variable area flow tube is

$$\frac{d(GA)}{dl} = 0 \qquad 8.8$$

using equation 7.20 to define G, this reduces to

$$\frac{1}{A}\frac{dA}{d\ell}(xV_g + \sigma V_f) + \frac{x V_g}{u_g}\frac{du_g}{d\ell} - x\left(\frac{\partial V_g}{\partial P}\right)\frac{dP}{d\ell} + \frac{\sigma V_f}{u_f}\frac{du_f}{d\ell} - V_g\frac{dx}{d\ell} = 0 \qquad 8.9$$

and $A = \frac{\pi(D-2\lambda)^2}{4}$ where λ is the thickness of the liquid annulus.

The effect of wall friction is also replaced in the momentum equation for the liquid phase (equation 7.16) by a force based on shear stress considerations.

In section 7.12 it was shown that the term,

$$\frac{4f}{2D}\,u_o^2\left(1 + \frac{m'\alpha}{1-\alpha}\right) \qquad 8.10$$

represents the effect of the two-phase frictional pressure drop in the momentum equation for the liquid phase of a bubbly flow within a pipe, and therefore in this present model

$$\frac{4f}{2D}\,u_o^2\left(1 + \frac{m'\alpha_T}{1-\alpha_T}\right) \qquad 8.11$$

is the force acting on a unit mass of the fluid (α_T being the total voidage including both annulus and core).

The shear stress at the pipe wall is given by

$$\tau = \frac{\text{Force}/\text{unit mass}}{\pi D\, \ell_o} \qquad 8.12$$

where ℓ_o is the length of tube containing a unit mass of fluid.

Hence, eliminating ℓ_o and using the expression 8.11 yields

$$\tau]_{WALL} = \frac{f}{2D}\,u_o^2\left(1 + \frac{m'\alpha_T}{1-\alpha_T}\right)\rho_w(1-\alpha_T) \qquad 8.13$$

Assuming the shear stress to be linear throughout the thickness of the annulus, then

$$\tau]_{\text{CORE/ANNULUS INTERFACE}} = \left(\frac{D-2\lambda}{D}\right) \tau]_{\text{WALL}} \qquad 8.14$$

and the core/annulus interfacial force acting on a unit mass of the core can be seen to equal:-

$$\frac{2f}{D} U_o^2 \left(\frac{1-\alpha_T}{1-\alpha}\right)\left(1 - \frac{m'\alpha_T}{1-\alpha_T}\right) \qquad 8.15$$

This replaces the expression 8.10 in the momentum equation for the liquid phase within the core (equation 7.16).

The force per unit mass acting on the liquid annulus is derived from equations 8.12, 8.13 and 8.14 and assuming the annulus thickness to be small, it is found to be

$$\frac{2f}{D} U_o^2 (1-\alpha_T)\left(1 + \frac{m'\alpha_T}{1-\alpha_T}\right) \qquad 8.16$$

The equations describing the motion of the liquid annulus are therefore:-

$$U_A \frac{dU_A}{d\ell} = -\frac{1}{\rho_F}\frac{dP}{d\ell} - \frac{2f}{D} U_o^2 (1-\alpha_T)\left(1 + \frac{m'\alpha_T}{1-\alpha_T}\right) \quad \text{(momentum)} \qquad 8.17$$

$$\frac{d(\lambda U_A)}{d\ell} = 0 \quad \text{(continuity)} \qquad 8.18$$

The relation between the local voidage within the bubbly core (α) and the total voidage across a pipe section (α_T) is

$$\alpha_T = \alpha \left(\frac{D-2\lambda}{D}\right)^2 \qquad 8.19$$

The solutions of the modified sets of equations are obtained by the method outlined in section 8.1. Two further initial conditions are required for this computation, these being the initial annulus thickness and the condition that $U_f = U_g$ at the initiation of the flashing.

Results computed using the bubbly/annular flow model are shown in Fig. 46. Axial profiles of voidage, slip velocity ratio and liquid velocity are similar to those predicted by the homogeneous critical flow model (Fig. 39). A decrease in thickness of the liquid annulus occurs near the pipe exit due to the increased velocity of the liquid. However the acceleration of the bubbly core is sufficient to increase the ratio U_f/U_g (Fig. 46.1).

From Figs. 46.2 and 46.3 it can be seen that the presence of a liquid annulus in a two-phase choking flow results in a larger critical pipe length and a decrease in exit voidage for fixed initial flow rate and fluid pressure.

If it is assumed that in a homogeneous flow, $(\lambda = 0)$, the choking liquid velocity is the sonic velocity corresponding to the exit voidage (section 9.1), Fig. 46.3 indicates that, if the phases are distributed in a bubbly/annular flow pattern, the bubbly core will attain supersonic speeds at the pipe exit. This is due to the decrease in thickness of the surrounding liquid annulus so causing the bubbly core to flow through an apparent diverging nozzle.

The measured value of the slip velocity ratio at the exit of a choking flow will depend on the bubble distribution (section 6.5). In the bubbly/annular model described above, the measured (or "apparent") slip velocity ratio will be given by:-

$$\sigma_{APP.} = \sigma_c \left[\frac{1}{1 + \frac{4\lambda}{D}\left(\frac{u_g}{(u_f)_c} - 1\right)} \right] \qquad 8.20$$

$$1 - \alpha_c + \frac{4\lambda}{D}\alpha_c$$

where the subscript c refers to the flow properties within the bubbly core.

Using the exit conditions as shown in Fig. 45.1 with $\alpha_c = 40\%$, then the evaluation of equation 8.20 yields

$$\sigma_{APP} \approx 1{\cdot}4\,\sigma_c$$

which indicates that measured slip velocity ratios may be significantly higher than those predicted by the homogeneous critical flow model due to a non-uniform distribution of bubbles across the pipe section.

It is concluded from this section that non-homogeneity of the phases in a bubbly two-phase flow (66)(67) could be a significant factor when relating the choking flow phenomenon to the propagation of pressure waves in a medium. As well as possibly giving rise to supersonic bubbly flows within the centre of the flow tube, it is also likely to increase the critical pipe length, for fixed initial flow conditions, and the apparent slip velocity ratio.

8.6 "Supersonic" critical two-phase flow

The critical flows so far discussed have been

basically subsonic, the fluid reaching the Mach 1 condition at the pipe exit. (This is the case for a single phase medium but has yet to be completely verified for a two-phase medium.)

This type of flow, in which changes in flow properties are caused by the pipe friction, is known as Fanno flow [96], and the fluid properties follow the upper part of the Fanno line as shown in Fig. 47.1 until the position of maximum entropy is attained where the flow is at Mach 1 and "choking" theoretically occurs.

For a single phase medium it is possible that, if the main flow pipe is fed by a converging diverging nozzle, the fluid velocity at the entrance of the pipe will be supersonic [33]. In this case the pipe friction will cause the pressure to increase and the velocity to decrease, the fluid properties following the lower part of the Fanno line. Again the position of maximum entropy will be attained and the fluid velocity will be reduced to Mach 1 at the pipe exit.

. Depending on the length of the pipe, it is possible that a shock wave will occur within the pipe. The flow properties moving from a point on the lower part of the Fanno line to a point on the upper part. These points are determined by the intersection of the Fanno line with the Rayleigh line [33]. The flow may then choke as a subsonic flow.

This phenomena was investigated using a simplified model for two-phase flow which assumed no slip velocity to occur between the phases, and a constant value

for the heat transfer coefficient. The initial conditions (section 8.1.1) were modified, applying an initial quality and specific mass flow such that the initial fluid velocity was supersonic with respect to the no-mass transfer sonic velocity.

The numerical method used to compute the solution of the critical flow equations (section 8.1) would not permit the investigation of the type of flow in which discontinuities of the flow properties occurred. Analysis of such flows require a more detailed examination of shock waves in two-phase media[97].

Computed axial pressure profiles are shown in Fig. 47.2, for various values of heat transfer coefficient (h) and it can be seen that for h above a certain value, the flow no longer chokes. This is caused by the contrary effects of friction and condensation on the flow, which can be elucidated using the following elementary analysis.

For a homogeneous two-phase flow, the momentum equation may be written (section 7.2).

$$U\frac{dU}{d\ell} = -V\frac{dP}{d\ell} - \frac{4f}{2D}U_0^2\left(1+\frac{m'\alpha}{1-\alpha}\right)$$

and the continuity equation; G = constant; becomes

$$V\frac{du}{d\ell} = u\frac{dV}{d\ell}$$

where $$\frac{dV}{d\ell} = \left(x\frac{\partial V_g}{\partial p} + (1-x)\frac{\partial V_f}{\partial p}\right)\frac{dp}{d\ell} + (V_g - V_f)\frac{dx}{d\ell}$$

Combining the above equations and using the approximations $(\partial V_f/\partial p) = 0$; $V_g \gg V_f$ and that the sonic velocity in the medium $c = \left[-V^2/x\left(\frac{\partial V_g}{\partial p}\right)\right]^{1/2}$, results in the

following expression for the axial velocity gradient

$$\frac{du}{d\ell} = \frac{-K_1 \frac{dx}{d\ell} - K_2}{u^2 - c^2} \qquad 8.21$$

where K_1 and K_2 are numerically positive parameters, defined by

$$K_1 = -\frac{u v v_g}{x\left(\frac{\partial v_g}{\partial p}\right)} \quad ; \quad K_2 = \frac{4f}{2D} u u_o^2 \left(1 + \frac{m\alpha}{1-\alpha}\right)$$

For a supersonic flow, U > C and equation 8.21 shows that the effect of pipe friction ($K_1 = 0$) is to decrease the fluid velocity and hence increase the fluid pressure, and the effect of condensation ($K_2 = 0$; $dx/d\ell$ positive) is to increase the velocity and decrease the pressure.

Which of these two effects dominate will depend on the relative magnitudes of the terms $K_1 \frac{dx}{d\ell}$ and K_2 which will, in turn, rely on the particular characteristics of the experimental system. However previous estimates of the heat transfer coefficient (section 3.6 and 8.4) suggest that the rate of mass transfer will generally be sufficient to make $\left|K_1 \frac{dx}{d\ell}\right| > K_2$, with the result that a "supersonic" one-component flow will not choke in a cylindrical nozzle.

In a two-component system, $\frac{dx}{d\ell} = 0$, pipe friction will cause the flow to choke in a similar way to a single phase medium, and the computations have shown that the fluid velocity reaches Mach 1 at the choking exit.

9. CONCLUSIONS

9.1 Relevance of sonic velocity to critical flow

In a single phase medium, choking flow occurs when the fluid attains the Mach 1 condition. It may, therefore, be assumed that a similar relation exists between these two phenomena in a two-phase mixture. However, if the phases are of different densities, it is unlikely that they will move at the same velocity, in which case the velocity of the medium cannot have a unique value.

The slip velocity ratio is particularly dependant on flow regime and is expected to have a maximum value when the phases are separated [50][51] (i.e. when the flow is in the "annular" or "stratified" regimes). Moody [52] indicates that the velocity of a pressure pulse in a separated two-phase flow lies between the sonic velocities in each phase. This is enforced by the results of the bubbly/annular flow analysis (section 8.5) which suggests that the bubbly core of the flow is supersonic at choking whereas the liquid annulus is subsonic. It must therefore be concluded that if the phases are separated and the slip velocity is significant in a choking two-phase flow then no direct analogy with the sonic velocity in the media is possible.

Experimental work in air/water bubbly mixtures [72] have suggested that in two-phase flows where the slip velocity is small, it is possible to establish a relationship between the sonic velocity and choking, similar to that known to exist in a single phase medium.

However, in steam/water "bubbly" and "dispersed" mixtures experimental measurements of critical flow rates indicate fluid velocities between the no-mass transfer (or frozen homogeneous) and thermodynamic equilibrium sonic velocities in the medium. As in these two flow regimes the slip velocity ratio is near to unity [25][98] it is likely that the rate of mass transfer between the phases at the choked exit of a flow is a major factor in governing the critical fluid velocity.

To be more precise, the choking of a fluid occurs when the fluid velocity equals the propagation velocity of a rarefaction wave through the medium. It is, as yet, uncertain whether the relevant velocity is that of the "foot" or "bulk" of the wave as these are markedly different (section 3.4). The non-equilibrium theory described in this thesis predicts the existence of a large superheat at the exit of a choking flow. Also a non-zero rate of vaporization is predicted, this being less than indicated by equilibrium models and determined by the maximum rate at which heat can be conducted from the liquid phase to the bubble surface. As it is unlikely that this maximum rate of vaporization is significantly influenced by the presence of a rarefaction wave, it is probable that the thermodynamic state of the fluid prior to the propagation of the rarefaction is important in determining the wave velocity. This has been demonstrated in the present experimental work (Fig. 21) and although exact measurements were not possible, it appears that the wave velocity is given by equations 1.13 and 1.16

with $dx/dp > 0$. This was also recently suggested by Baum and Horn [3] who computed curves for the velocity of a small rarefaction and corresponding critical flow rates for various values of dx/dp

The actual value of the rate of change of flow quality with pressure at the outlet of a choking two-phase flow will depend directly on the rate of vaporization and pressure gradient

$$\frac{dx}{dp} = \frac{(dx/d\ell)}{(dp/d\ell)}$$

The value of $dx/d\ell$ for a conduction controlled flow (equation 7.28) depends on physical properties of the flow, such as phase distribution, slip velocity ratio and effective heat transfer coefficient at the interphase surface, and has been shown to attain a finite value at the outlet of a non equilibrium choking flow (fig. 39). The pressure gradient at this point is theoretically infinite, although difficulty has been experienced in obtaining this condition in experiment. Hence the rate of change of quality with pressure, at the exit, is likely to approach zero providing $dx/d\ell$ does not become infinite, which would be the case were the fluid in thermodynamic equilibrium.

It is therefore concluded that if a correlation is to be made between the critical fluid velocity and sonic velocity in a two-phase mixture which deviates from thermodynamic equilibrium, the relevant sonic velocity is that corresponding to no-mass transfer within the mixture.

If the no-mass transfer sonic velocity in a

homogenous (no slip velocity) bubbly steam/water mixture is denoted by C_{NMT}, then the critical flow rate may be given by

$$G_{crit} = \frac{C_{NMT}}{x v_g + V_f}$$

Using the values of C_{NMT} as calculated by Davis (16) the above expression is plotted in Fig. 48. Critical flow velocities computed using the model described in chapter 7 for a flow inlet pressure of 2.5 AT. (From Fig. 42.4, this results in a fluid pressure of 1AT at the flow outlet) are also shown. The discrepancy between these two sets of results is probably due to the value of slip velocity ratio which is predicted to exist at the exit of a critical bubbly flow.

It has been suggested that the sonic velocity (3) depends only on the area concentration of the phases (i.e. the voidage) and therefore the effect of slip velocity is to increase the quality for a fixed voidage. A slip velocity of 1.2, which represents a mean value in this series of computations (Fig.42.7) effectively shifts the $\sigma = 1.0$ curve (Fig. 48) to the right, giving approximate agreement with the critical flow results.

The rate of change of slip velocity ratio with pressure, at the outlet of a choking flow may also influence the critical flow rate (3). However, due to the small values of $d\sigma/dl$ and large $d\rho/dl$, predicted to occur using the present model, this effect was not found significant.

It is concluded that for a known mass flow rate

of fluid, the outlet conditions of a homogeneous bubbly one-component critical flow are predictable from sonic velocity considerations, providing the relative velocity between the phases is small. When the slip velocity ratio is significant, particularly in non-homogeneous flows, or when the specific mass flow rate is one of the parameters to be determined theoretically, the exit conditions can only be predicted knowing the "history" of the flow which involves knowledge of the rates of vaporization, nucleation phenomena and phase distribution.

9.2 Conclusions and suggestions for further work

The velocity of small amplitude pressure waves in air/water and steam/water bubbly mixtures have been investigated theoretically and experimentally. Both mixtures were found to act as dispersive media with the velocity of sinusoidal pressure waves varying with wave frequency. In the air/water system this was attributed to the variation of polytropic index of the gas phase, although the theoretical analysis only revealed the two limiting wave velocities, the "isothermal" and "adiabatic" sonic velocities, and a more detailed study is required to define the range of frequencies over which the transition between these two velocities occur. The experimental verification of the hypothesis was not conclusive particularly at the higher voidage flows where non-homogeneities within the mixture led to high measured wave velocities. In view of this, for further work on the velocity of sinusoidal waves in air/water mixtures it is recommended that a system is developed to produce

a spacially homogeneous bubbly mixture which is free from time variations of voidage. The velocity of the leading part of an impulse or "thin" triangular wave was found to be consistently higher than the velocity of a low frequency wave, indicating that the velocity corresponded to the adiabatic sonic velocity in the medium.

The measured variation of wave velocity with frequency in a steam/water bubbly mixture showed reasonable agreement with the predictions of a theoretical analysis based on conduction controlled mass transfer between the phases and indicated a value of 0.5 BTU/ft.^{2} sec. ^{o}F. for the heat transfer coefficient of a bubble surface within a mixture where very little relative velocity existed between the phases.

The velocity of the leading point of compression and rarefaction waves was shown to be approximately the no-mass transfer sonic velocity hence behaving in a way similar to the step waves investigated by previous authors. A theoretical analysis which took into account mass transfer effects within small amplitude waves, predicted the velocities of the mid-point of a step wavefront and the "peak" of a triangular wave and gave fair agreement with experimental measurements of the velocity of rarefaction waves, with h having a value of 0.5 - 1.0 BTU/ft.^{2} sec. ^{o}F.

The fact that the velocities of step and impulse waves were predicted to change continuously, as the wave progressed along the flow, emphasizes the advantage of using a number of pressure transducers in an experimental

system to investigate this phenomenon more fully. This would also enable a more detailed study of the varying shape of the waves and possibly reveal different rates of condensation and vaporization as suggested by previous authors [5][16]. No evidence of this could be gained in the present system.

It is recommended that future experimental investigations into the velocity of sound in a flashing system should give particular attention to the wave attenuation and stability of the system. The attenuation of the waves in a steam/water mixture was found to be considerably larger than indicated by the preliminary experiments in air/water mixtures, with the result that, to overcome the attenuation, waves had to be generated which could no longer be considered infinitesimal and led to significant wave distortion. As previously noted, difficulty was experienced in maintaining steady flow conditions within the present system and it is suggested that future systems should include an electric water heater to enable finer control of the liquid temperature, and also be isolated from external influences, as the cold water inlet in the present system (section 3.1) proved to be a source of instability. Unfortunately the stability of a flashing system depends to a great extent on nucleation phenomena which cannot be predicted. However, it is likely that a theoretical analysis into the stability of a "flashing" loop may indicate the principal flow parameters to be controlled.

A definite weakness in the steam/water

experiments (chapter 3) was the measurement of flow voidage, as, due to the very low voidages used, conventional methods proved unsuccessful. Although lazer holography techniques may enable a more accurate estimate of voidage than the photographic method used, ideally a system which gives an instantaneous measure of low voidages in a steam/water mixture should be developed.

The advantage of work at higher voidages ($< 50\%$) is that the sonic velocity becomes less sensitive to voidage variations and also that these voidages may be estimated using standard techniques such as γ -ray attenuation. To maintain a homogeneous bubble distribution in a high voidage flashing system would require large specific mass flow rates, unless a vertical flow is used, in which case the mixture is unlikely to be in thermodynamic equilibrium. However, the velocity of pressure waves in condensing or evaporating flows is worth investigating further. The major drawback in working with high voidage flows is the large wave attenuations which exist, making the propagation of small amplitude waves unfeasible.

A repeat of the present experimental programme at higher fluid pressures should result in a larger difference between the "equilibrium" and "no mass transfer" sonic velocities and because of the smaller values of dTs/dp the transition between these two limiting velocities should occur at a lower frequency range. In such experiments, a mechanical system for generating

the wave is suggested because of the large displacement amplitudes that will be required.

Theoretically, the principle of conduction controlled rates of vaporization was applied to the critical flow of a one-component bubbly mixture. The effects of the most important parameters, slip velocity ratio, nucleation and rate of vaporization were noted.

A model, based on the balance of forces acting on an individual bubble, predicted values of the slip velocity ratio in an air/water system significantly lower than those measured in experiment and this was attributed to the effect of radial bubble distributions within the flow. The slip velocity measured in experiment was shown to depend on a "local" slip velocity (approximately 1.05 in horizontal flows and 1.1 in vertical) and a bubble distributional parameter of 0.9, which was compared to the Bankoff parameter of 0.89 and that of Zuber, 0.83. It was considered that slip velocity ratios in a critical two-phase one-component flow of the order predicted by previous authors [50][52] were unrealistic in the bubbly regime, and that deviations between experimental results and the predictions of the H.E. model within this flow regime are due principally to departures from thermo-dynamic equilibrium of the mixture.

The importance of the number of nuclei present per unit mass of liquid was noted and it was suggested that an approximate estimate can be gained using photo-graphic methods. However, this is not possible in many

systems, particularly when large diameter flow tubes are used, and a further investigation into nucleation phenomena is in progress at this university.

The definition of the "initiation" of flashing and the initial value of quality (x_o) is stressed and in order for the theoretical approach to be applied successfully to a given experimental system, the flow properties at this point must be known.

The critical properties at the exit of a choking bubbly flow were practically independent of the above parameters and governed principally by the specific mass flow rate. This is due to the small values of slip velocity ratio ($\simeq 1.3$) which exist at the outlet, this being the only parameter which is determined by the flow "history". The critical fluid velocity was shown to compare very closely to the no-mass transfer sonic velocity in the medium.

In determining the critical mass flow rate which chokes in a pipe of given length with fixed inlet conditions, the rate of vaporization is clearly important, this depending on N, the slip velocity ratio and the parameter η_o which was found, by correlation with experimental data, to have a value between 0.2 - 0.3 BTU/ft.^{2} sec.$^{\frac{1}{2}o}$F in a steam/water mixture.

The effective heat transfer coefficient of the bubble surface was influenced by the bubble diameter, and the slip velocity ratio and was found to be significantly higher than in a flow where the phases move

with the same velocity. Clearly the heat transfer coefficients suggested by the velocity of pressure wave measurements and the critical flow experiments cannot be compared unless the variation with slip velocity is accounted for.

Throughout this thesis, references have repeatedly been made of non-homogeneities within the mixture and it is evident that the assumption of a homogeneous distribution of equal sized bubbles is inapplicable to many practical systems. Because of this, the analysis of a bubbly/annular flow model is of particular interest and, together with other flow patterns suggested by voidage profile measurements (section 6.5), merits further investigation. The model described in section 8.5 indicates that at the exit of a choking flow, the accumulation of bubbles towards the centre of the tube results in the fluid attaining supersonic velocities. Hence, a one-dimensional treatment of the phenomena is inappropriate at the exit of a choking two-phase flow, particularly as experimentally, two-dimensional effects have been shown to be dominant at this point. A theoretical and experimental investigation into the formation of a flashing two-phase jet, at present in progress at this establishment, may enable critical flow analyses to be less dependant on measurements at the pipe exit, which are generally unsatisfactory (section 8.2).

APPENDIX A

Propagation Velocity of infinitesimal sinusoidal pressure waves through a two-phase one component mixture

The one-dimensional unsteady equations describing a two-phase flow, derived in chapter 7, can be written, on assuming no slip velocity to exist between the phases, as:-

$$\frac{du}{dt} = -\frac{1}{\rho}\frac{\partial p}{\partial x} - \frac{4f}{2D}U_o^2\left(1+\frac{m\alpha}{1-\alpha}\right) \qquad 1$$

$$\frac{d\rho}{dt} + \rho\frac{\partial u}{\partial x} = 0 \qquad 2$$

$$h_{fg}\frac{dx}{dt} = -C_w\frac{dT}{dt} - \frac{u}{J}\frac{du}{dt} \qquad 3$$

$$\frac{dx}{dt} = \frac{hA}{h_{fg}}(T - T_s) \qquad 4$$

where ρ is the average density of the media

$$= (1-\alpha)\rho_f + \alpha\rho_g \qquad 5$$

The relation between α and x in the absence of slip velocity is

$$\alpha = \frac{1}{1 + \frac{(1-x)\rho_g}{x\rho_f}} \qquad 6$$

The total derivatives denote the Eulerian specification of the flow properties.

If the fluid is at rest except for the motion caused by the wave, this total derivative reduces to a partial derivative unsteady term

$$\text{i.e.} \quad \frac{d}{dt} = \frac{\partial}{\partial t} \qquad 7$$

For the solution of the equations a linearized perturbation

technique was used.

Assuming a perturbation of the form

$$F(t,\ell) = F(o,\ell) + \Delta F\, e^{i\omega t + k\ell} \qquad 8$$

where F is a general flow property, and

(i) $F(o,\ell)$ represents the steady solution of that flow property.

(ii) ΔF is the magnitude of the perturbation at $t = o$, $\ell = o$.

As the fluid is at rest, the steady solution is a constant and its derivative zero. Hence, applying 7 and 8 to equations 1 → 6 and neglecting second order perturbations, the following equations are obtained

$$i\omega\Delta u = -\frac{k\Delta P}{\rho} \qquad 9$$

$$i\omega\Delta\rho + \rho k\Delta u = o \qquad 10$$

$$h_{fg}\Delta x = -c_w\Delta T \qquad 11$$

$$i\omega\Delta x = \frac{h}{h_{fg}}\left[A(\Delta T - \Delta T_s) + \Delta A(\bar{i} - T_s)\right] \qquad 12$$

$$\Delta\rho = \Delta\alpha(\rho_g - \rho_f) + \alpha\Delta\rho_g \qquad 13$$

$$\Delta\alpha = \frac{V_f}{(xV_g + V_f)^2}\left[V_g\Delta x + x\left(\frac{\partial V_g}{\partial P}\right)\Delta P\right] \qquad 14$$

The equation defining A (section 7.7) yields:-

$$\Delta A = \frac{2A}{3}\left[\frac{\Delta x}{x} + \left(\frac{\partial V_g}{\partial P}\right)\frac{\Delta\rho}{V_g}\right] \qquad 15$$

For small perturbations

$$\Delta T_s = \left(\frac{\partial T_s}{\partial P}\right)\Delta P \qquad 16$$

Equations 9 - 16 represent a set of simultaneous equations which can be solved to give the following expression for k:-

$$k^2 = \frac{\omega^2}{(V_g x + V_f)^2}\left[x\left(\frac{\partial V_g}{\partial p}\right) - \frac{V_g\left(\frac{\partial T_s}{\partial p}\right) - \frac{2}{3}(T-T_s)\left(\frac{\partial V_g}{\partial p}\right)}{in+m}\right] \qquad 17$$

$$\text{where} \quad n = \frac{h_{fg}\omega}{hA} \quad ; \quad m = -\frac{2}{3}\left(\frac{T-T_s}{x}\right) + \frac{h_{fg}}{C_w} \qquad 18$$

k is a complex variable and hence can be written

$$k = k_1 + ik_2$$

Separating equation 17 into real and imaginary parts, two equations are obtained.

$$\text{i.e.} \quad k_1^2 - k_2^2 = \frac{\omega^2}{\lambda^2}\left[x\left(\frac{\partial V_g}{\partial p}\right) + \frac{mq}{m^2+n^2}\right] \qquad 19$$

$$2k_1k_2 = \frac{\omega^2}{\lambda^2}\left[\frac{nq}{m^2+n^2}\right] \qquad 20$$

$$\text{where} \quad \lambda = xV_g + V_f \qquad 21$$

$$q = V_g\left(\frac{\partial T_s}{\partial p}\right) - \frac{2}{3}(T-T_s)\left(\frac{\partial V_g}{\partial p}\right) \qquad 22$$

$\frac{\omega}{k_2}$ represents the propagation velocity of the wave, and k_1 the attenuation constant.

Hence the solution of equation 19 and 20 yields

$$U_{SINE} = \left\{\frac{1}{2\lambda^2}\left[x\left|\frac{\partial V_g}{\partial p}\right| + \frac{mq}{m^2+n^2}\right]\left[1 + \sqrt{1 + \left(\frac{nq}{x\left|\frac{\partial V_g}{\partial p}\right|(m^2+n^2) + mq}\right)^2}\right]\right\}^{-1/2} \qquad 23$$

$$k = -\frac{\omega}{\sqrt{2}\lambda}\left[x\left|\frac{\partial V_g}{\partial p}\right| + \frac{mq}{m^2+n^2}\right]^{1/2}\left[\sqrt{1 + \left(\frac{nq}{x\left|\frac{\partial V_g}{\partial p}\right|(m^2+n^2) + mq}\right)^2} - 1\right]^{1/2} \qquad 24$$

At infinite frequency i.e. $\omega \rightarrow \infty$

$$U_{SINE} = \frac{xV_g + V_f}{(x\,|\partial V_g/\partial p|)^{1/2}} \qquad 25$$

which is the no-mass transfer sonic velocity.

As $\omega \rightarrow o$; assuming the fluid to be initially in equilibrium (i.e. $T-T_s = o$).

$$U_{SING} = \left[\frac{xV_g + V_f}{x\,|\partial V_g/\partial p| + \frac{C_w V_g}{h_{fg}}(\partial T_s/\partial p)}\right]^{1/2} \qquad 26$$

which represents the velocity of a wave in which thermodynamic equilibrium always exists.

It must be noted that in this analysis, it was assumed that the sinusoidal change in quality and pressure have the same frequency and are in phase. In fact this only occurs when the fluid remains very near to a state of thermodynamic equilibrium. When the mass transferred between the phases, is heat conduction controlled and small in magnitude such that the liquid temperature can be considered constant, the quality variations will be 90^o out of phase with the pressure variations. Also due to the non-linear nature of the rate of vaporization the quality variation will probably deviate significantly from a sinusoidal form. In view of this, the present analysis cannot be expected to fully represent the physical system.

APPENDIX B

Propagation Velocity of infinitesimal "thin" triangular and step pressure waves through a two-phase one-component mixture

Using equations 1 - 6 from appendix A and making the same assumption of no overall flow of the fluid.

Apply a perturbation of the form :-

$$F(\ell,t) = F(\ell,0) + \Delta F(\ell,t) \qquad 27$$

F being a general flow property.

Equations 1 - 4 reduce to the linearised equations.

$$\frac{\partial \Delta u}{\partial t} = -\frac{1}{\rho}\frac{\partial \Delta p}{\partial \ell} \qquad 28$$

$$\frac{\partial \Delta p}{\partial t} + \rho \frac{\partial \Delta u}{\partial \ell} = 0 \qquad 29$$

$$h_{fg}\frac{\partial \Delta x}{\partial t} = -c_w \frac{\partial \Delta T}{\partial t} \qquad 30$$

$$\frac{\partial \Delta x}{\partial t} = \frac{h}{h_{fg}}\left[A(\Delta T - \Delta T_s) + \Delta A(T - T_s)\right] \qquad 31$$

This together with equations 13 - 16 represent the system to be solved.

Δu, Δx, ΔT, ΔA and ΔT_s can be eliminated from the above set of equations to yield a third order partial differential equation, i.e.

$$Q\frac{\partial^2 \Delta p}{\partial t^2} - R\frac{\partial^2 \Delta p}{\partial \ell^2} + X\frac{\partial^3 \Delta p}{\partial t^3} = Y\frac{\partial^3 \Delta p}{\partial \ell^2 \partial t} \qquad 32$$

where $Q = mx\left|\frac{\partial V_g}{\partial p}\right| - \frac{(V_f - V_g)}{V_g}\eta_v$; $R = \lambda^2 m$

$$X = \frac{h_{fg}\,x}{hA}\left|\frac{\partial V_g}{\partial p}\right| \quad ; \quad Y = \frac{h_{fg}}{hA}\lambda^2 \qquad 33$$

λ, m, and q being defined by equations 18, 21, 22 of appendix A.

Applying the Laplace Transform, with respect to time, to equation 32, gives:-

$$Q\left(s^2\overline{\Delta p} - s\Delta p]_{t=0} - \frac{\partial \Delta p}{\partial t}]_{t=0}\right) - R\frac{\partial^2 \overline{\Delta p}}{\partial \ell^2} + X\left(s^3\overline{\Delta p} - s^2\Delta p]_{t=0} - s\frac{\partial \Delta p}{\partial t}]_{t=0} - \frac{\partial^2 \Delta p}{\partial t}]_{t=0}\right) = Y\left(s\frac{\partial^2 \overline{\Delta p}}{\partial \ell^2} - \frac{\partial^2 \Delta p}{\partial \ell^2}]_{t=0}\right) \quad 34$$

Boundary Conditions

Initially, at t = o, a perfectly generated step pressure wave can be represented by a Heavyside function.

$$\text{ie.} \quad \Delta p]_{t=0} = 1 - H(\ell) \quad 35(i)$$

A triangular pressure wave of unit height and "thickness" $2a_\ell$, can be represented by a series of linear equations.

$$\text{ie.} \quad \Delta p_{TRI}(\ell)]_{t=0} \begin{cases} = 0 & -\infty < \ell < -2a_\ell \\ = k(a_\ell + \ell) & -2a_\ell < \ell < -a_\ell \\ = k(a_\ell - \ell) & -a_\ell < \ell < 0 \\ = 0 & 0 < \ell < +\infty \end{cases} \quad 35(ii)$$

Both of the functions 35(i) and 35(ii) are constant at t = o, for $\ell > 0$

$$\text{Hence} \quad \frac{\partial^2 \Delta p}{\partial \ell^2}]_{t=0} = 0 \quad 36(i)$$

Also at a given $\ell > o$, the value of Δp is constant for a finite time when t is small.

Hence

$$\frac{\partial \Delta p}{\partial t}]_{t=0} = 0 \quad 36(ii)$$

$$\frac{\partial^2 \Delta p}{\partial t^2}]_{t=0} = 0 \quad 36(iii)$$

Substituting conditions 36 into equation 34 results in the equation -

$$s\,\overline{\Delta p} - \Delta p]_{t=0} = \frac{(Ys+R)}{s(Q+sX)}\,\frac{\partial^2 \overline{\Delta p}}{\partial \ell^2}$$

The solution is of the form

$$\overline{\Delta p} = A_1 e^{-\sqrt{\frac{s}{k}}\,\ell} + B_1 e^{\sqrt{\frac{s}{k}}\,\ell} + \frac{\Delta p]_{t=0}}{s} \qquad 37$$

where $k = \frac{(Ys+R)}{s(Q+sX)}$

At $\ell = \infty$; Δp is finite, therefore $B_1 = 0$ 38

At $\ell = o$, for a step pressure wave

$$\Delta p]_{t=0} = H(t) \qquad 39(i)$$

ie. $$\overline{\Delta p}]_{t=0} = \frac{1}{s} \qquad 40(i)$$

$\Delta p]_{t=0} = 1 - H(t)$ (equation 35(i)) has a discontinuity at $\ell = o$, Δp varying from $o \rightarrow 1$. However, a continuous curve which tends in the limit to $1 - H(\ell)$ will have a value of $\frac{1}{2}$ at $\ell = o$.

$$\therefore \quad \Delta p]_{\substack{\ell=0 \\ t=0}} = \frac{1}{2} \qquad 41(i)$$

For a triangular wave

$$\begin{aligned} \Delta p_{TRI}]_{\ell=0} &= 0 && -\infty < t < 0 \\ &= kt && 0 < t < \tau \\ &= k(2\tau - t) && \tau < t < 2\tau \\ &= 0 && 2\tau < t < +\infty \end{aligned} \qquad 39(ii)$$

The Laplace transform of a function Δp is represented by:-

$$\mathcal{L}(\Delta p) \sim \int_0^\infty e^{-st} \Delta p \, dt$$

As Δp_{TRI} is zero for all $t > 2\tau$ (equation 39 (ii)) and τ is considered very small so that the wave approximates to an impulse wave, then the laplace transform is equivalent to the area of the wave (when plotted on P/t axes).

Hence if the wave is of magnitude unity i.e. $k\tau = 1$

then $$\overline{\Delta p}\Big]_{t=0} \simeq \tau \qquad 40(ii)$$

From equations 35 (ii) and 39(ii) it can also be seen that

$$\Delta p\Big]_{t=0} = 0 \qquad 41(ii)$$

Use of conditions 38, 40 and 41 enable the constant A_1 (equation 37) to be evaluated resulting in the following solutions

For a step pressure wave

$$\overline{\Delta p} = \frac{1}{2s} e^{-\sqrt{\frac{s}{R}}\, l} + \frac{1 - H(t)}{s} \qquad 42(i)$$

and for a triangular wave

$$\overline{\Delta p} = \tau e^{-\sqrt{\frac{s}{R}}\, l} + \frac{\Delta p_{TRI}(l)}{s} \qquad 42(ii)$$

From the definition of k, using equations 33, 18, 21 and 22 and assuming the fluid to be initially in thermodynamic equilibrium, :-

$$\sqrt{\frac{s}{k}}\, l = \frac{sl}{c}\left(1 + \frac{b}{s+a}\right)^{1/2} \qquad 43$$

where c is the no-mass transfer sonic velocity

$$a = hA/C_w$$

and

$$b = \frac{V_g \left(\frac{\partial r_s}{\partial p}\right) \frac{hA}{h_{fg}}}{\varkappa \left|\frac{\partial V_g}{\partial p}\right|} \qquad 44$$

At this stage, the two limiting propagation velocities of the waves can be investigated.

If no-mass transfer occurs between the phases; h = o.

Therefore a = b = o.

Hence using equation 43, equations 42(i) and 42(ii) become for $\ell > o$.

$$\overline{\Delta p}_{STEP} = \frac{1}{2S} e^{-\frac{s\ell}{c}}$$

$$\overline{\Delta p}_{TRI} = \tau e^{-\frac{s\ell}{c}}$$

Taking inverse laplace transforms

$$\Delta p_{STEP} = H(t - \ell/c)$$

$$\Delta p_{TRI} = \Delta p_{TRI}(t - \ell/c) \qquad 45$$

This indicates that both waves travel at the no-mass transfer velocity with no wave dispersion occurring.

If the fluid remains in thermodynamic equilibrium during the passage of the waves, $h \longrightarrow \infty$, hence $\sqrt{\frac{S}{R}}\ell \longrightarrow 0$ and the wave is predicted not to propagate through the medium. Clearly this is not consistent with the theories based on thermodynamic considerations (16) (Fig. 2), nevertheless as C (equilibrium) $\ll$ C (no-mass transfer) in low quality steam water mixtures, the

approximation that C (equilibrium) = 0 is acceptable.

If h is non-zero and finite, the form of $\sqrt{\frac{s}{k}}\ell$ is such as to make the exact inverse laplace transform unobtainable without the use of numerical integration. In view of the assumptions already made, such numerical work would have little advantage over an approximate analytical solution.

s, the variable in the laplace transformation has a range of $o \rightarrow \infty$. However, this range can be reduced to lie between two finite values $a < s < b$ if the function to be transformed is zero within the ranges $o < s < a$ and $b < s < \infty$.

From equations 42, the functions which are required to satisfy these conditions are

$$I \longrightarrow \frac{1}{s} e^{-\sqrt{\frac{s}{k}}\ell} \quad , \quad II \longrightarrow \tau\, e^{-\sqrt{\frac{s}{k}}\ell}$$

both I and $II \rightarrow o$ as $s \rightarrow \infty$, but as $s \rightarrow o$; $I \rightarrow \infty$ and $II \rightarrow \tau$. Examination of the variables a and b (44) show that as $x \rightarrow o$; $a \rightarrow o$ and $b \rightarrow \infty$.

The application of the condition $a < s < b$ to equation 43, therefore severely restricts the application of this theory to low quality medium.

However as much experimental work in measuring propagation velocities of step and "thin" triangular waves is restricted to low quality mixtures (5), the theory may still produce significant results.

Using the above approximation, equation 42 becomes (for $\ell > o$)

$$\Delta p_{STEP} = \frac{1}{2s} e^{-\frac{\ell\sqrt{b}\sqrt{s}}{c}} \qquad 46\ (i)$$

$$\Delta p_{TRI} = \tau e^{-\frac{\ell\sqrt{b}\sqrt{s}}{c}} \qquad 46\ (ii)$$

Step pressure wave

The inverse laplace transform of 46 (i) is

$$\Delta p = \frac{1}{2} \operatorname{erfc} \frac{\ell\sqrt{b}}{2c\sqrt{t}}$$

Applying the condition that at $t = \infty$

$\Delta p = \Delta p_o$

$$\Delta p = \Delta p_o \operatorname{erfc} \frac{\ell\sqrt{b}}{2c\sqrt{t}} \qquad 47$$

This solution indicates no attenuation of the wave, only a change in shape of the wavefront. If the velocity of such a wave is assumed to be characterised by the velocity of the midpoint of the wavefront (this agrees with the method of measurement used in some experimental work[3][15], where $\Delta p = \Delta p_o/2$

then $\operatorname{erfc}\left(\frac{\ell\sqrt{b}}{2c\sqrt{t}}\right) = \frac{1}{2}$

(If $\operatorname{erfc}(x) = \frac{1}{2}$ then $x \doteq 0.472$[83])

hence $$\frac{\ell}{t} = \frac{0.944}{\sqrt{bt}}\, c$$

Therefore the velocity of propagation of a step wave is given by

$$U_{STEP} = \frac{0.944}{\sqrt{bt}}\, C_{NMT} \qquad 48$$

where t is the time elapsed since the initiation of the wave.

Thin triangular wave

Taking the inverse Laplace transform of 46 (ii),

and applying the condition that initially, $\Delta p = \Delta p_o$ results in

$$\Delta p = \Delta p_o \frac{\tau \ell \sqrt{b}}{2c\sqrt{\pi t^3}} \; e^{-\frac{\ell^2 b}{4c^2 t}} \qquad 49$$

The velocity of such a wave may be considered as the velocity of the point of maximum pressure within the wave.

i.e. when $\frac{d\Delta p}{d\ell} = o.$

Differentiating equation 49 results in the condition

$$\frac{\ell^2 b}{2c^2 t} = 1$$

Hence the propagation velocity of a thin triangular wave is given by

$$U_{TRI} = \frac{1.414}{\sqrt{bt}} \; C_{NMT} \qquad 50$$

Equations 48 and 50 represent the velocities of small amplitude step and "thin" triangular waves in low quality bubbly mixtures. Compressibility effects are not accounted for in the analysis and hence the change in shape of the wave is due only to wave dispersion, where different frequency components of the wave travel with various velocities and attenuations. The predictions of these equations are compared to experimental data in chapter 1.

APPENDIX C

Two phase frictional pressure drop

For a single phase flow within a pipe of diameter D; the frictional pressure drop over a length $d\ell$ is

$$dp = \frac{f u^2 \rho \, d\ell}{2D} \qquad C.1$$

where f is the friction factor, defined by the Blasius equation

$$f = \frac{A}{R_e^n} \qquad C.2$$

Therefore

$$dp = \frac{A \mu^n u^{2-n}}{2D^{n+1}} \rho \, d\ell \qquad C.3$$

In a two phase flow, assuming the pressure to be constant at each pipe crossection, for a given $d\ell$, dp is the same whether calculated for the liquid or gas phase.

Hence one can write

$$dp]_{TP} = \frac{A \mu_L^n U_{TPL}^{2-n}}{2D^{n+1}} \rho_L \, d\ell \qquad C.4$$

If the liquid phase flows alone in the pipe with the same mass flow rate as in the two-phase flow, the relation between the respective velocities will be

$$U_{SPL} = U_{TPL}(1 - \alpha) \qquad C.5$$

therefore C.4 becomes

$$dp]_{TP} = \frac{A}{2D^{n+1}} \mu_L^n \left(\frac{U_{SPL}}{1-\alpha}\right)^{2-n} \rho_L \, d\ell$$

and using equation C.3

$$\frac{dp]_{TP}}{dp]_{SPL}} = \left(\frac{1}{1-\alpha}\right)^{2-n}$$

$$= \left(1 + \frac{\alpha}{1-\alpha}\right)^{2-n} \qquad \text{C.6}$$

APPENDIX D

Derivation of Momentum equations for each phase in a two phase flow

Although the two-phase flows in the thesis are bubbly mixtures, it is convenient to consider initially a stratified flow model to determine the form of the equations and then assuming bubbly flow to estimate the wall friction and interphase friction terms.

The mathematical model of the flow is as shown below

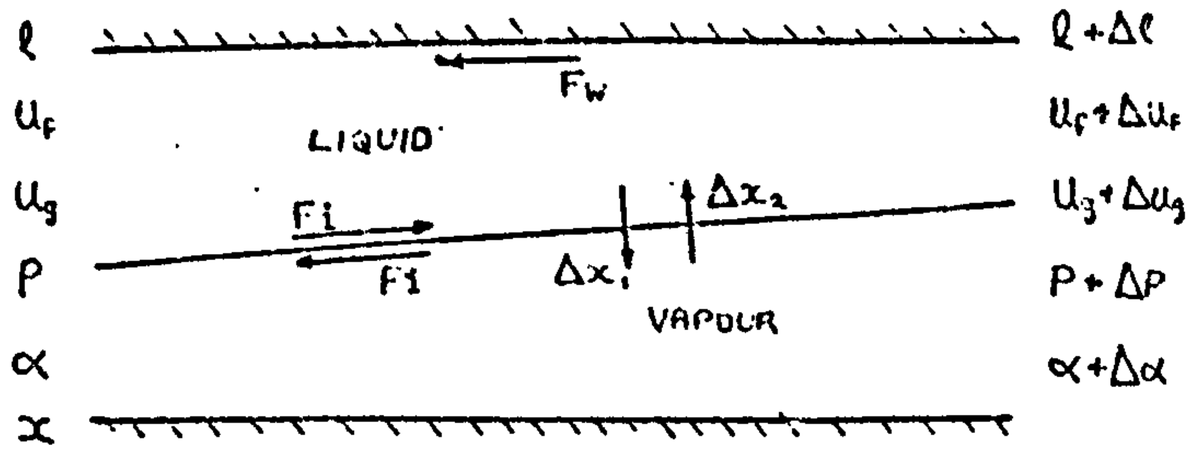

The model allows for both condensation and vaporization to occur within the fluid, and assumes the variation of flow properties to be linear along the elemental length $\Delta\ell$.

The increase in momentum of liquid phase is given by

$$AG\left[1-(x+\Delta x_1)\right]\Delta u_f + AG\Delta x_1\frac{\Delta u_f}{2} - AG\Delta x_2\left[u_g+\frac{\Delta u_g}{2}-(u_f-\Delta u_f)\right]$$

and neglecting second order incremental terms this becomes

$$AG(1-x)\Delta u_f - AG\Delta x_2(u_g-u_f) \qquad D.1$$

The increase in momentum of the vapour phase is

$$AG(x-\Delta x_2)\Delta u_g + AG\Delta x_2\frac{\Delta u_g}{2} + AG\Delta x_1\left[u_g+\Delta u_g-(u_f+\frac{\Delta u_f}{2})\right]$$

$$\Rightarrow AGx\Delta u_g + AG\Delta x_1(u_g-u_f) \qquad D.2$$

The sum of the forces acting on the liquid phase is

$$A[(1-\alpha)P-(1-\alpha-\Delta\alpha)(P+\Delta P)-(P+\tfrac{\Delta P}{2})\Delta\alpha]-F_w\Delta\ell+F_i\Delta\ell$$

which reduces to

$$-A(1-\alpha)\Delta P-F_w\Delta\ell+F_i\Delta\ell \qquad \text{D.3}$$

Similarly, assuming that the vapour phase is distributed so as not to be in contact with the conduit wall, the sum of the forces on the vapour phase can be shown to be:

$$-A\alpha\Delta P-F_i\Delta\ell \qquad \text{D.4}$$

Equating expressions D.1, D.3: and D.2, D.4 and using the equations

$$G(1-x)=\rho_f U_f(1-\alpha)$$
$$Gx=\rho_g U_g\alpha$$

The momentum equation of the liquid phase is:-

$$-\Delta P-\frac{F_w\Delta\ell}{A(1-\alpha)}+\frac{F_i\Delta\ell}{A(1-\alpha)}=\rho_f U_f\Delta U_f-\frac{G\Delta x_2}{(1-\alpha)}(U_g-U_f) \qquad \text{D.5}$$

and for the vapour phase:-

$$-\Delta P-\frac{F_i\Delta\ell}{A\alpha}=\rho_g U_g\Delta U_g+\frac{G\Delta x_1}{\alpha}(U_g-U_f) \qquad \text{D.6}$$

Restrictions to a bubbly mixture

If the two-phase flow is assumed bubbly with no bubble in direct contact with the pipe wall, the effect of wall friction will act only on the liquid phase and is equivalent to the two-phase frictional pressure drop.

$$\text{i.e.}\quad \frac{F_w}{A(1-\alpha)}=\frac{\Delta P}{\Delta\ell}\Big]_{TP} \qquad \text{D.7}$$

Assuming the average fluid density to be $\rho_f(1-\alpha)$ and that there exists N bubbles per unit mass of the fluid, then the number of bubbles in the elemental volume is

$$N \rho_f (1-\alpha) A \Delta l$$

The interphase friction force in a bubbly mixture depends on the drag force acting on an individual bubble. Assuming this to be represented by D_o; then in a unit length of tube

$$F_i = N D_o \rho_f (1-\alpha) A \qquad D.8$$

Substituting equations D.8 and D.7 into D.5 and D.6, the momentum equations become

Liquid

$$\rho_f u_f \frac{\Delta u_f}{\Delta l} - \frac{G}{1-x}(u_g - u_f)\frac{\Delta x_2}{\Delta l} = -\frac{\Delta p}{\Delta l} - \frac{\Delta p}{\Delta l}\Big]_{TP} + N D_o \rho_f \qquad D.9$$

Vapour

$$\rho_g u_g \frac{\Delta u_g}{\Delta l} + \frac{G}{\alpha}(u_g - u_f)\frac{\Delta x_1}{\Delta l} = -\frac{\Delta p}{\Delta l} - N D_o \rho_f \frac{(1-\alpha)}{\alpha} \qquad D.10$$

If it is assumed that either condensation or evaporation occurs within the fluid, then either Δx_2 or Δx_1 is zero.

In a flashing system as described in chapter 7; $\Delta x_2 = 0$ and in an air/water system (chapter 6), where no mass transfer occurs between the phases; $\Delta x_1 = \Delta x_2 = 0$

The $\Delta x/\Delta l$ terms in equation D.9 and D.10 represent the increase in momentum of the mass transferred between the phases during the flow. In an

evaporating flow $(\Delta x_2 = 0)$ it is expected that the term $\frac{G}{\alpha}(U_g - U_f)\frac{\Delta x}{\Delta \ell}$, (equation D.10) is small compared to $\frac{\Delta p}{\Delta \ell}$

$$\text{ie} \quad \frac{G(U_g - U_f)\ \Delta x/\Delta \ell}{\alpha\ \Delta p/\Delta \ell} \ll 1{\cdot}0$$

Using the equation for G (equation 7.20) and assuming the mass flow of vapour phase to be small, this can be written

$$\frac{\rho_g U_f^2 (\sigma - 1)\ \Delta x/\Delta \ell}{\alpha\ \Delta p/\Delta \ell} \ll 1{\cdot}0 \qquad \text{D.11}$$

The L.H.S. will be a maximum when either $\Delta x/\Delta \ell$ is a maximum or x and $\Delta p/\Delta \ell$ are minima.

In a choking two-phase one-component flow, the rate of vaporization is a maximum at the outlet of the flow tube. However if the fluid deviates from a state of thermodynamic equilibrium $\Delta x/\Delta \ell$ is finite at this point, whereas $\Delta p/\Delta \ell$ is infinite and x is a maximum. Condition D.11 is clearly satisfied.

The minimum values of x and $\Delta p/\Delta \ell$ are $x = x_o$ ($\simeq 10^{-6}$; section 8.1.1) and $\Delta p/\Delta \ell = \Delta p/\Delta \ell\big]_{SPL} = \frac{2f}{D} U_f^2 \rho_f$, which both occur at the initiation of a flashing two-phase flow.

Using the rate of vaporization equation (section 7.6) and equation 3.46, condition D.11 becomes

$$\frac{4{\cdot}83\ N^{1/3}\ h(\sigma - 1)(T - T_s)}{V_g^{1/3}\ x_o^{1/3}\ \frac{2f}{D}\ \rho_f U_f\ h_{fg}} \ll 1{\cdot}0$$

Substituting the limiting values of flow variables which make the above expression a maximum

$$\text{ie} \quad N = 10^6\ [lb^{-1}];\ x_o = 10^{-6};\ \frac{2f}{D} = 0{\cdot}1\ [ft^{-1}];\ U_f = 30\ [ft/sec]$$

For a steam/water mixture the condition reduces to

$$\frac{h(\sigma-1)(T-T_s)}{9} \ll 1{\cdot}0$$

h may be considered to have an approximate value of 1.0 BTU/ft^2 sec$^\circ$F [23] and σ a maximum value of 1.1 (although when the bubbles are small, a slip velocity ratio of unity may be expected). The superheat required to initiate the flashing of untreated water in a cylindrical tube will certainly be no larger than 5°F [95]. Again condition D.11 is satisfied.

Hence it is likely that the omission of the term $\frac{G}{\alpha}(u_g-u_f)\frac{\Delta x_1}{\Delta \ell}$ from equation D.10 will not cause significant errors in the solution of the equations describing a two-phase one-component flow. This has been verified by solving the equations with and without this term, the results showing a variation of approximately 1%.

In a condensing flow, where $\Delta x_1 = 0$, it can similarly be shown that the term $\left(\frac{G}{1-\alpha}\right)(u_g-u_f)\frac{\Delta x_2}{\Delta \ell}$ is negligible in equation D.9.

APPENDIX E

Conservation of Energy Equation

In a horizontal adiabatic system, the steady flow energy equation reduces to

$$h + \frac{u^2}{2J} = \text{constant} \qquad \text{E.1}$$

where h is the enthalpy of the fluid

$$\therefore \quad dh + \frac{u\,du}{J} = 0 \qquad \text{E.2}$$

For a two-phase system

$$h = (1-x)h_f + xh_g \qquad \text{E.3}$$

For small quality ($x \ll 1$) equation E.2 becomes

$$dh_f - (h_g - h_f)dx + \frac{u_f\,du_f}{J} = 0 \qquad \text{E.4}$$

Now $h_g - h_f$ = latent heat of vapourization (h_{fg})

Also using the thermodynamic relation

$$dh_f = c_w\,dT \qquad \text{E.5}$$

the energy equation is therefore

$$h_{fg}\,dx = -c_w\,dT - \frac{u_f\,du_f}{J} \qquad \text{E.6}$$

Nomenclature

A	Interphase area per unit mass of two-phase mixture ($ft.^2$).
A	Crossectional area of flow tube ($ft.^2$).
a_1	Length "thickness" of triangular wave ($ft.^2$).
b	Parameter defined by equation 44 (Appendix B) ($sec.^{-1}$).
C	Sonic velocity (ft./sec.).
C_D	Drag coefficient.
C_o	Zuber (68) distributional parameter.
C_w	Specific heat of liquid phase (BTU/lb. ^oF).
D	Pipe diameter (ft.).
D_v	Total drag force acting on bubble (equation 6.19) ($ft.\ lb./sec.^2$).
d	Bubble diameter (ft.).
d	"Form" drag force acting on spherical body ($ft.\ lb./sec.^2$).
E	Bulk modulus of elasticity ($lb./ft.^2$).
E	Internal energy (BTU/lb.).
f	Friction factor.
f	Wave frequency ($sec.^{-1}$).
f_R	Bubble resonance frequency ($sec.^{-1}$).
F	General flow property.
F_w, F_i	Wall and interphase frictional force per unit length of flow tube ($lb./sec.^2$).
G	Specific mass flow rate ($lb./ft.^2\ sec.$).
g_c	Gravitational constant.
h	Heat transfer coefficient (BTU/$ft.^2$ sec. ^oF).
h	Enthalpy (BTU/lb.).

h_{fg} Latent heat of vaporization (BTU/lb.).

J Mechanical equivalent of heat (lb. ft.^{2}/sec.^{2} BTU).

K Thermal conductivity of liquid phase (BTU/ft. sec. ^{o}F).

K Distributional parameter.

k Attenuation constant (ft.$^{-1}$).

k_T Attenuation constant within a tube (ft.$^{-1}$).

ℓ Length (ft.).

m' Empirical constant defined in equation 7.14.

n Polytropic index of gas phase.

m,n Indices defining form of velocity and voidage profiles.

N Number of bubbles per unit mass of mixture (lb.$^{-1}$).

N_{JA} Jakob number ($C_f (T_f - T_s) \rho_f / \rho_g h_{fg}$).

N_u Nusselt number (hD/K).

N' Variable defined by equation 5.12.

P Pressure (lb./ft. sec.^{2} unless otherwise stated).

P_R Critical pressure ratio.

P_r Pandtl number ($\mu C_w/K$).

P_e Peclet number ($4UR/2k$).

Q Volumetric flow voidage.

Q Heat addition (BTU/lb.).

R Flow tube radius (ft.).

r Bubble radius (ft.).

R_e Reynolds number ($U\ell\rho/\mu$).

S Entropy (BTU/lb. ^{o}F).

S Laplace transform parameter.

t Time (sec.).

T Temperature of liquid phase (^{o}F).

T_s Saturation temperature (generally bubble temperature) (^{o}F).

u	Velocity (ft./sec.).
u_b	$= U_{SPL}$.
u_∞	Dubble terminal velocity (ft./sec.).
u'_∞	Wave velocity in any infinite medium.
V	Area average specific volume ($ft.^3/lb.$).
V_M	Momentum average specific volume ($ft.^3/lb.$).
V_{KE}	Kinetic energy average specific volume ($ft.^3/lb.$).
W	Mass flow rate (lb./sec.).
x	Mass dryness fraction (quality) ($= G_g/G$).
y	Tube wall thickness (ft.).
z	Acoustic impedance of infinite medium ($lb./ft.^3 sec.$).
z_T	Acoustic impedance within tube ($lb./ft.^2 sec.$).
α	Area dryness fraction (voidage) ($= A_g/A$).
β	Fraction of equilibration.
β	Volumetric flow voidage.
γ	Isentropic index of gas phase.
Δx_1	Change in quality due to evaporation within incremental length.
Δx_2	Change in quality due to condensation within incremental length.
$(dT/dr)_{BS}$	Radial temperature gradient at bubble surface ($^oF/ft.$).
H	Compressibility ($ft.\ sec.^2/lb.$).
κ	Thermal diffusivity ($ft.^2/sec.$).
η_o	Parameter controlling the rate of mass transfer (equation 7.36) ($BTU/ft.^2\ sec.^{\frac{1}{2}o} F$).

η_s Parameter controlling the rate of mass transfer (equation 7.43) (BTU/ft.^{2} sec.$^{\frac{1}{2}}$ F).

θ Angle of inclination of the flow to the horizontal.

λ Annulus thickness (ft.).

μ Dynamic viscosity (lb./ft. sec.).

χ Martinelli parameter (equation 6.2).

ρ Density (lb./ft.^{3}).

$\bar{\rho}$ Mean density across section of flow tube (lb./ft.^{3}).

σ Local slip velocity ratio.

σ_{APP} Apparent or measured slip velocity ratio.

τ Viscous shear stress (lb./ft. sec.^{2}).

τ Time "thickness" of triangular wave (m.sec.).

ω Angular velocity (sec.$^{-1}$).

Subscripts

A Air phase.

W Water phase.

f Liquid phase.

g Vapour phase.

TP Two phase.

SPL Single phase liquid.

SPG Single phase gas.

NMT No mass transfer.

EQ Thermodynamic equilibrium.

CRIT/C Value of property at the "choking" condition.

E Exit flow property.

S Constant entropy.

SAT Evaluated along the saturation line of the P/V diagram.

BS	Bubble surface.
R	Reservoir.
I	Pipe inlet.
T	Total or within a flow tube.
M	Mixture.
STEP	Of step pressure wave.
SINE	Of sinusoidal pressure wave.
TRI/IMP	Of triangular or impulse pressure wave.

BIBLIOGRAPHY

1. Gouse, S. W., Brown, G. A. "A survey of the velocity of sound in two-phase mixtures". A.S.M.E. pub. 64-WA/FE 35 (1965)

2. Semenov, N. I., Kosterin, S. "Results of studying the speed of sound in moving gas/liquid systems". Therm. Eng. 11 No. 5 (1964) p.59

3. Baum, M. R., Horn, G. "The propagation velocity of a small rarefaction wave in a non-equilibrium vapour-liquid bubble flow: A prediction of the onset of a choked flow". J.Mech.Eng. Sci. 13 No. 4 (1971) p.243.

4. Moody, F. J. "A pressure pulse model for two-phase critical flow and sonic velocity". Trans. A.S.M.E. J. Heat transfer (1969) p.371

5. Barclay, F., Ledwidge, T., Cornfield, G. "Some experiments on sonic velocity in two-phase one-component mixtures and some thoughts on the nature of two-phase critical flow". Symp. Fluid Mech. and measurements in 2 phase systems, Exeter. (1969)

6. Ledwidge, T. J. "Use of velocity of sound in design of a void fraction meter for air/water and argon/sodium mixtures". U.K.A.E.A., D.E.R.E., E.D.G. Internal report.

7. Dickson, A. N., Silver, R. S. "The flow of flashing water in conduits". Desalination, 2 (1967) p.175.

8. Mallock, A. "The damping of sound by frothy liquids" Proc. Roy. Soc. A84 (1910) p.391

9. Ledwidge, T. J., Dehn, R. "The velocity of sound in two component mixtures". U.K.A.E.A. Development Report No. 160, E.D.G. D.E.R E. (1966)

10. Karplus, H. B. "The velocity of sound in a liquid containing gas bubbles". Armour Res. Foundation Rept. 000-248 (1958)

11. Collier, J. G., Wallis, G. B. "Two-phase flow and heat transfer". Course notes. Dept. Mech. Eng., Glasgow University (1967)

12. Henry, R. E., Fauske, H. K. "Propagation velocity of pressure waves in two-phase mixtures and the dependency on flow regimes". Trans. Am. Nuc. Soc. 11 p.364 (1968).

13. Silberman, E. "Sound velocity and attenuation in bubbly mixtures measured in standing wave tubes". Jour. Accou. Soc. Amer. 29 No. 8 p.925 (1957).

14. Mawardi, O. K. "On the propagation of sound waves in narrow conduits". Jour. Accou. Soc. Amer. 21 No. 5 p.484 (1949)

15. Karplus, H. "Propagation of pressure waves in a mixture of water and steam". Armour Res. Foundation Rept. 5132-12 (1961)

16. Davis, A. L. "The speed of sound in mixtures of water and steam". U.K.A.E.A. A.E.E.W.-M452 (1965)

17. Deich, M. E. Fkippov, G. A., Stekol'shchikov, E. V. "Speed of sound in two phase media". Therm. Eng. 8 p.44 (1964)

18. Dvornichenko, V. V. "Speed of sound in the two-phase zone". Therm. Eng. 13 10 p.110 (1966)

19. Radovskiy, I. S. "Speed of sound in two-phase vapour-liquid systems". Heat transfer, Soviet Research, Vol. 3 No. 3 (1971) p.104.

20. Ivandayev, A. I., Nigmatulin, R. I. "Propagation of weak disturbances and heat transfer in two-phase media with phase transitions". Heat transfer, Soviet Research Vol. 3 No. 3 (1971) p.98.

21. Grolmes, M. A., Fauske, H. K. "Comparison of the propagation characteristics of compression and rarefaction pressure pulses in two-phase one-component flow". Trans. Amer. Nuc. Soc. Vol 11 Part 2 (1968) p.683.

22. Kaye, G. W. C., Laby, T. H. "Physical and chemical constants". Longmans Green & Co.

23. Dickson, A. N., Bradie, J. K. "Some basic aspects of the flash-distillation process". Nuclear desalination, Vienna (1969) p.859.

24. Dickson, A. N., Markham, V. B. "The adiabatic flashing flow in tubes". Inst. Mech. Eng. 2-phase flow symposium, Leeds. 1969.

25. Herries, G. "Non-equilibrium flashing flow in the bubbly regime". Ph.D. thesis. Heriot-Watt University (1968).

26. Crandall, I. B. "Vibrating systems and sound". Macmillan & Co. (1927).

27. Rayleigh, Lord. "Theory of sound" Vol. 11 Macmillan & Co. (1929).

28. Levy, S. "Prediction of two-phase pressure drop and density distribution from mixing length theory". A.S.M.E. J. Heat transfer 85(c) (1963) p.137.

29. McWilliams, D., Duggins, R. K. "Speed of sound in bubbly liquids". Symp. fluid Mech. and Measurements in 2-phase systems, Exeter. (1969) p.105.

30. Davids, N., Thurston, E. G. "Accoustical impedance of a bubbly mixture and its size distribution function". Jour. Acou. Soc. Am. 22 No. 1 (1950) p.20.

31. Carstensen, E. L., Foldy, L. L. "Propagation of sound through a liquid containing gas bubbles". Jour. Acou. Soc. Am. 19 No. 3 (1947) p.481.

32. Strasburg, M. "Pulsation frequency of non-spherical gas bubbles in liquids. Jour. Acou. Soc. Am. 25 No. 3 (1953) p.536.

33. Shapiro, A. H. "Compressible fluid flow" Ronald Press Co. (1953)

34. Campbell, I. J., Pritcher, A. S. "Shock waves in a liquid containing gas bubbles". Proc. Roy. Soc. A243 (1957) p.534.

35. Hamilton, L. J., Nyer, R., Schrock, V. E. "Propagation of shock waves through two-phase, two-component media". Trans. Amer. Nu. Soc. Vol. 10 (1967) p.660.

36. Carron, R. P. "The speed of sound in single component two-phase mixtures". Ph.D. thesis. University of Connecticut (1967)

37. Dejong, V. J., Firey, J. C. "Effect of slip and phase change on sound velocity in steam water mixtures and the relation to critical flow". I.C.E.C. process design and dev. 7 No. 3 (1968) p.454.

38. Miller, N., Mitchie, R. F. "Measurement of local voidage in liquid/gas two-phase flow systems using a universal probe". J. Brit. Nuc. Energy Soc. Vol. 9 No. 2 (1970) p.94.

39. Ogaspwara, H. "A theoretical approach to two-phase critical flow". (4th report) Bul. J.S.M.E. Vol. 12 No. 52 (1969) p.837.

40. Gouse, S. W. "Void fraction measurement". M.I.T. report D.S.R. 8734-2 (1964)

41. Isigai, S., Yamane, M., Rôko, K. "Measurements of the component flows in a vertical two-phase flow by making use of pressure fluctuations". Bul. J.S.M.E. Vol. 8 No. 31 (1965) p.375.

42. Kolsky, H. "Stress waves in solids". Oxford. (1965).

43. Rschevkin, S. N. "The theory of sound". Pergamon press (1963)

44. Laird, D. T., Kendig, P. M. Attenuation of sound in water containing air bubbles". Jour. Acou. Soc. Am. 24 No. 1 (1952) p.29.

45. Gibson, F. W. "Measurement of the effect of air bubbles on the speed of sound in water". Jour. Acou. Soc. Am. 48 No. 5 (part 2) (1970) p.1195.

46. Anderson, D. V., Barnes, C. "Dispersion of a pulse propagated through a cylindrical tube". Jour. Acou. Soc. Am. 25 No. 3 (1953) p.525.

47. Martinelli, R. C., Lockhart, R. W. "Proposed correlation of data for isothermal two-phase, two component flow in pipes". Chem. Eng. Prog. 45 (1949) p.39.

48. Armand, A. A. "Resistance during movement of two-phase system along horizontal pipes". A.E.R.E. - TRANS 828 (1946).

49. Isbin, H. S., Moy, J. E., Cruz, A. J. R. "Two phase steam water critical flow". A.I.Ch.E. Jour. Vol. 3 No. 3 (1957) p.361.

50. Fauske, H. K. "Contribution to the theory of two phase, one-component critical flow". ANL - 6633 (1962).

51. Cruver, J. E., Moulton, R. W. "Critical flow of liquid vapour mixtures". A.I.Ch.E. Jour. Vol. 13 No. 1 (1967) p.52.

52. Moody, F. J. "Maximum flow rate of a single component, two phase mixture". Trans. A.S.M.E. J. Heat transfer 87c (1965) p.134.

53. Linning, D. L., Alderson, M., Pexton, A. F. "A general theory for the flow of evaporating fluids in pipes". U.K.A.E.A. T.R.G. Rept. 1392(R) (1967)

54. Katto, Y. "Dynamics of compressible saturated two-phase flow". J.S.M.E. Vol. 12 No. 54 (1969) p.1417.

55. Henry, R. E. "A study of one and two component, two phase critical flows at low quality" A.N.L. - 7430 (1968).

56. Edwards, A. R. "Conduction controlled flashing of a fluid and the prediction of critical flow rates in a one-dimensional system". U.K.A.E.A. AHSB(S) R 147 (1968).

57. Dusinberre, G. M. "Heat transfer calculations by finite differences". Int. Textbook Co.

58. Levy, S. "Steam slip - Theoretical predictions from momentum model". A.S.M.E. J. Heat transfer 82c (1960) p.113.

59. Marchaterre, J. F., Hoglund, B. M. "Correlation for two-phase flows". Nucleonics (1962) p.142.

60. Haywood, R. W., Knight, G. A., Middleton, G. E., Thom, J. R. S. "Experimental study of the flow conditions and pressure drop of steam-water mixtures at high pressure in heated and unheated tubes". Proc. I. Mech. Eng. Vol. 175 No. 12 (1961) p.667.

61. Peebles, F. N., Garber, H. J. "Studies on the motion of gas bubbles in liquids". Chem. Eng. prog. Vol. 49 No. 2 (1953) p.88.

62. Baker, J. L. L., Chao, B. T. An experimental investigation of air bubble motion in a turbulent water stream". A.I.Ch.E. Jour. Vol. 11 No. 2 (1965) p.268.

63. Simpson, H. C., Rooney, D. H. "Void fraction prediction under saturated conditions". Symp. "Design for two-phase flow" N.E.L. (1968)

64. Hammitt, F. G., Robinson, M. J., Lafferty, J. F. "Choked flow analogy for very low quality two phase flows". Nuc. Sci. Eng. 29 (1967) p.131.

65. Kobayasi, K., Iida, Y., Kanegae, N. "Distribution of local void fraction in air water two phase flow in a vertical channel" J.S.M.E. Vol. 13 No. 62 (1970) p.1005.

66. Zuber, N. "On the variable-density single fluid model for two-phase flow". A.S.M.E. J. Heat transfer 82c (1960) p.255.

67. Bankoff, S. G. "A variable density single-fluid model for two phase flows with particular reference to steam water flow". A.S.M.E. - A. I. Ch. E. Heat. trans. Con. No. 59, HT-7 (1959)

68. Zuber, N., Findlay, J. A. "Average volumetric concentration in two phase systems". A.S.M.E. J. Heat transfer 87c (1965) p.453.

69. Neal, L. G., Bankoff, S. G. "Local parameters in cocurrent mercury-nitrogen flow". A.I.Ch.E. Jour. Vol. 11 No. 4 (1965) p.624.

70. Neal, L. G. "Summary of distributional effects in two phase slip models". A.I.Ch.E. Jour. Vol. 11 No. 4 (1965) p 747.

71. Lamb, H. "Hydrodynamics". Camb. Uni. Press.

72. Huey, C., Bryant, R. A. "Isothermal homogeneous two phase flow in horizontal pipes". A.I.Ch.E. Jour. Vol. 13 No. 1 (1967) p.70.

73. Baker, O. "Simultaneous flow of oil and gas". Oil and gas Journal Vol. 53, 12 (1954). p.185.

74. Golan, L. P., Stenning, A. H. "Two phase vertical flow maps". Symp. Fluid Mech. and Measurement in 2 phase flow systems; Exeter (1969) p.110.

75. Griffiths, P., Wallis, G. "Two phase slug flow". Trans. A.S.M.E. J. Heat transfer. 83 (1961) p.307.

76. Hewitt, G. F., Roberts, D. N. "Studies of two phase flow patterns by simultaneous X-ray and flash photography". A.E.R.E. M 2159 (1969).

77. Scheidegger, A. E. "Physics of flow through porous media". Uni. of Toronto Press.

78. Chisholm, D. "The pressure gradient due to friction during the flow of boiling water". N.E.L. Rept. No. 78 (1963).

79. Chisholm, D., Laird, A. D. K. "Two-phase flow in rough tubes". Trans. A.S.M.E. 80 (2) (1958) p.276.

80. Wallis, G. B. "Some hydrodynamic aspects of two phase flow and boiling". Int. Devel. Heat transfer. Part 2 (1961) p.319.

81. Martinelli, R. C., Nelson, D. B. "Predictions of pressure drop during forced circulation boiling of water". Trans. A.S.M.E. Vol. 70 (1948) p.695.

82. Chisholm, D. "Note on the relationship between friction and liquid crossection during two-phase flow". J. Mech. Eng. Sci. Vol. 8 No. 1 (1966) p.107.

83. Carslaw, H. S., Jaeger, J. C. "Conduction of heat in solids". Oxford Uni. Press.

84. Plesset, M. S., Zwick, S. A. "The growth of vapour bubbles in superheated liquids. J. App. Phy. 25 No. 4 (1954). p. 493.

85. Ruckenstein, E. "On heat transfer between vapour bubbles in motion and the boiling liquid from which they are generated". Chem. Eng. Sci. Vol. 10 (1959) p.22.

86. Ruckenstein, E., Davis, E. J. "The effects of bubble translation on vapour bubble growth in a superheated liquid". Int. J. of Heat and Mass transfer. Vol. 14 No. 7 (1971) p.939.

87. Ruckenstein, E. "Mass transfer between a single drop and a continuous phase". Int. J. of Heat and Mass transfer. Vol. 10 (1967) p.1785.

88. Wittke, D. D., Chao, B. T. "Collapse of vapour bubbles with translatory motion". A.S.M.E. J. Heat transfer 89c (1967) p.17.

89. Hartree, D. R. "Numerical Analysis". Oxford Uni. Press.

90. Zaloudek, F. R. "The low pressure critical discharge of steam water mixtures from pipes". H.W. - 68934 REV. (1961).

91. Uchida, H., Nariai , H. "Discharge of saturated water through pipes and orifices". 6th Annual Heat transfer congress. A.S.M.E. (1967).

92. Faletti, D. W., Molton, R. W. Two-phase critical flow of steam/water mixtures. A.I.Ch.E. Jour. Vol. 9 No. 2 (1963) p. 247.

93. Fauske, H. K. "The discharge of saturated water through tubes". Chem. Eng. Prog. Symp. Series No. 59 Vol. 61 p.210.

94. Henry, R. E., Fauske, H. K. "The two-phase critical flow of one-component mixtures in nozzles, orifices and short tubes". A.S.M.E. J. Heat Transfer 93c (1971) p.179.

95. Barois, G., Huygbe, J. "Étude expérimentale de l'Autovaporisation d'un éncoulement ascendant adiabatique d'eau dans un canal vertical de section uniforme". Colloque Euromech. No. 7. Grenoble (1968)

96. Bursik, J. W. "Pseudo-sonic velocity and pseudo Mach No. concepts in two phase flows". N.A.S.A. TN D-3734 (1966).

97. Eddington, R. B. "Investigation of supersonic phenomena in a two-phase (liquid/gas) tunnel". A.I.A.A. Jour. Vol. 8 No. 1 (1970) p.65.

98. Mathes, W., Riebold, W., De Cooman, E. "Measurement of the velocity of gas bubbles in water by a correlation method". The review of Sci. Inst. Vol. 41 No. 6 (1970) p.843.

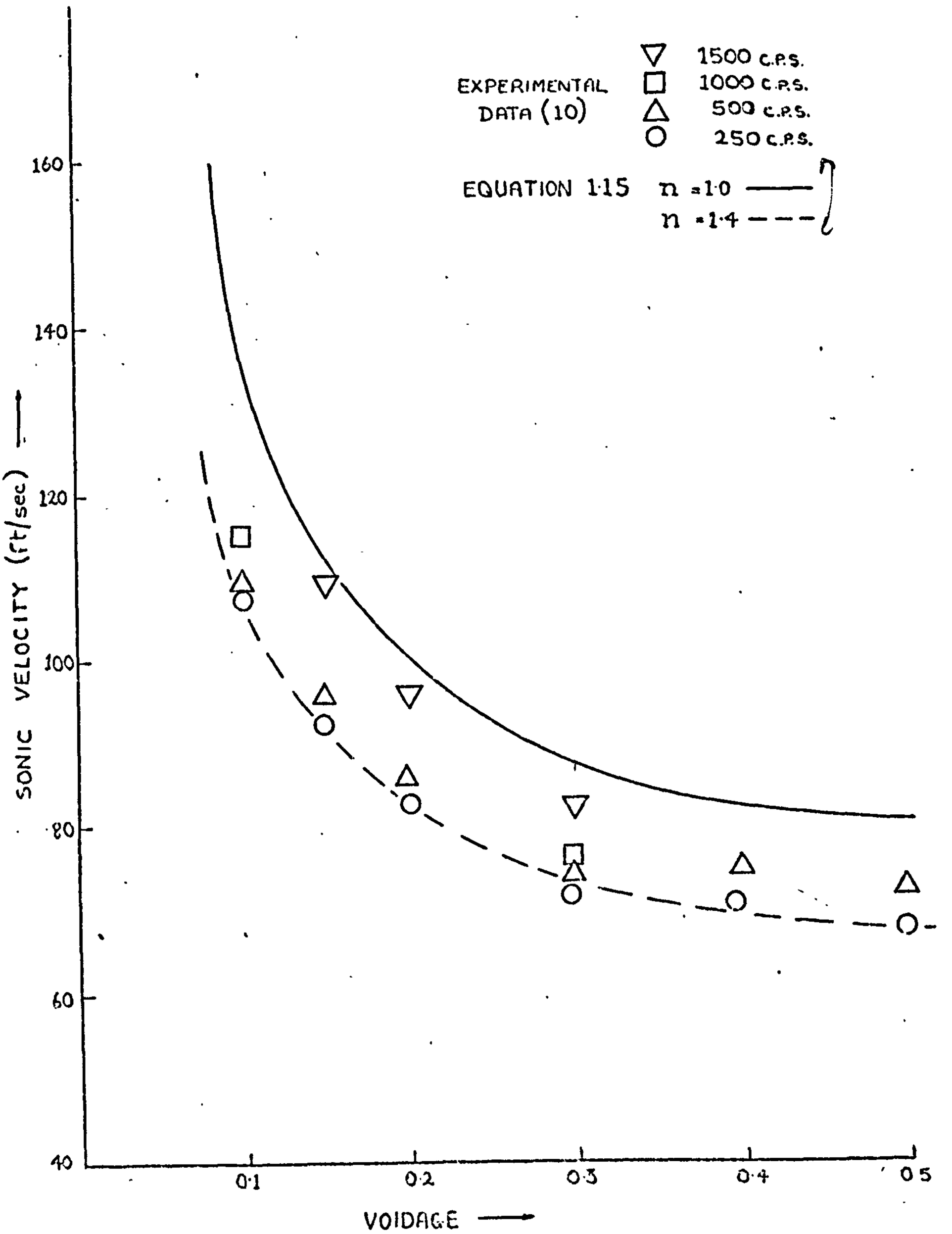

Fig.1 VELOCITY OF SOUND IN AIR/WATER MIXTURES

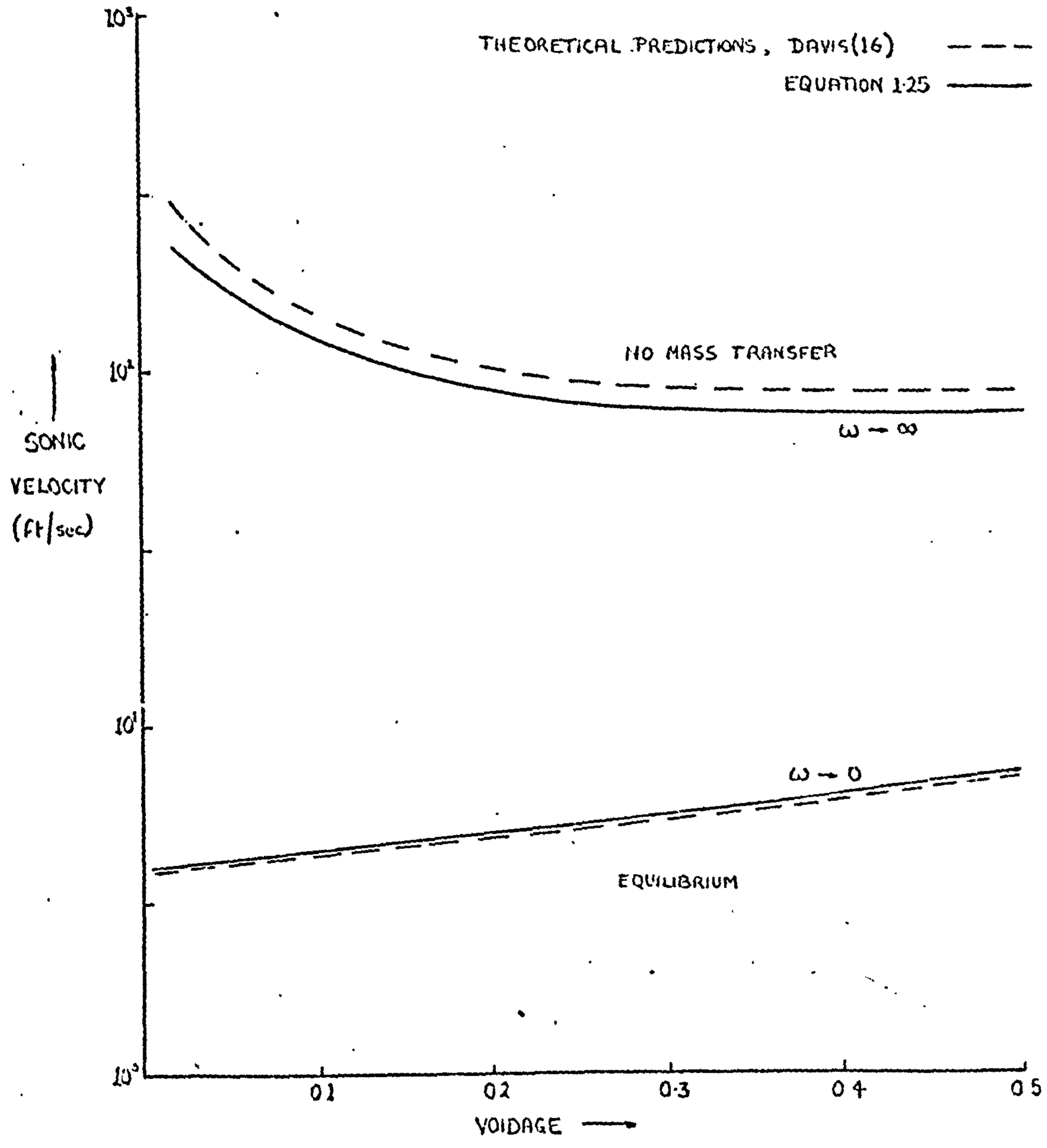

Fig. 2. SONIC VELOCITY IN STEAM/WATER MIXTURES

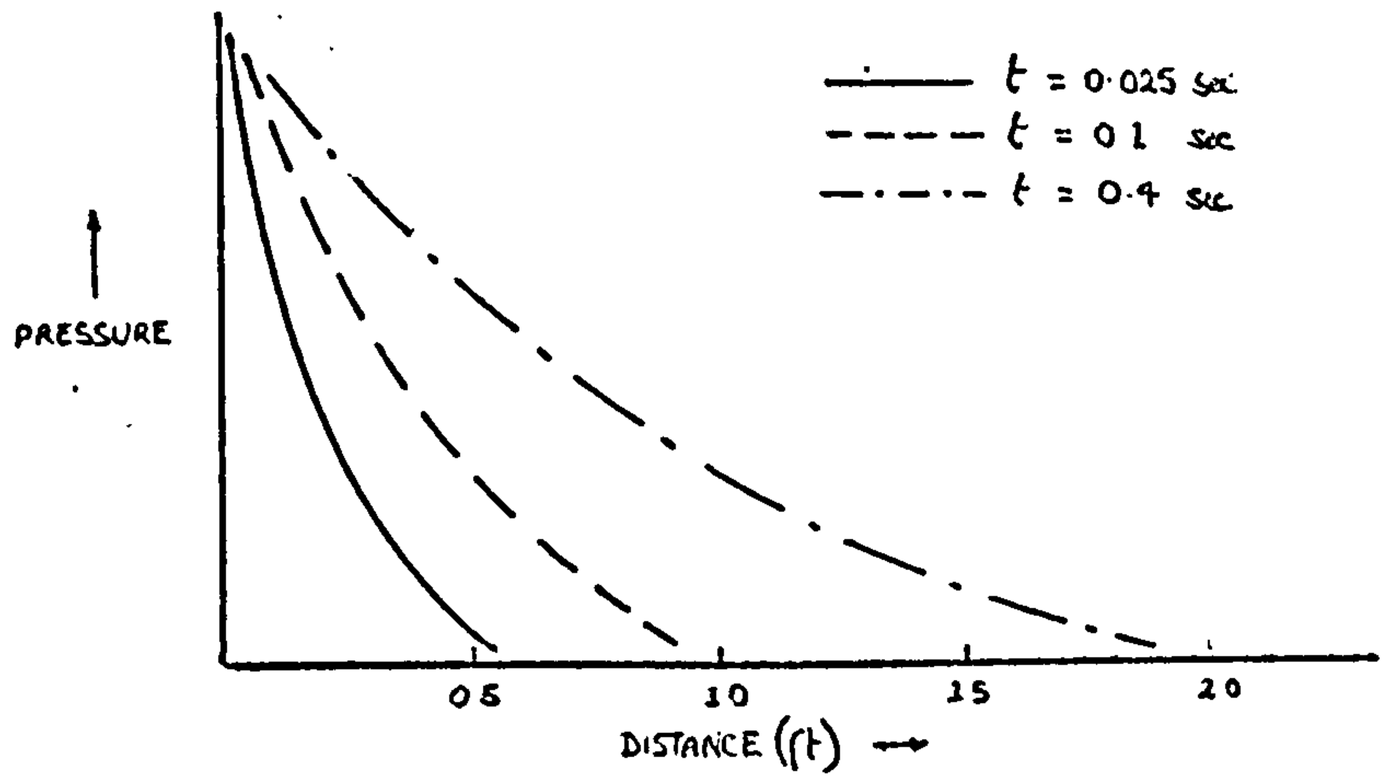

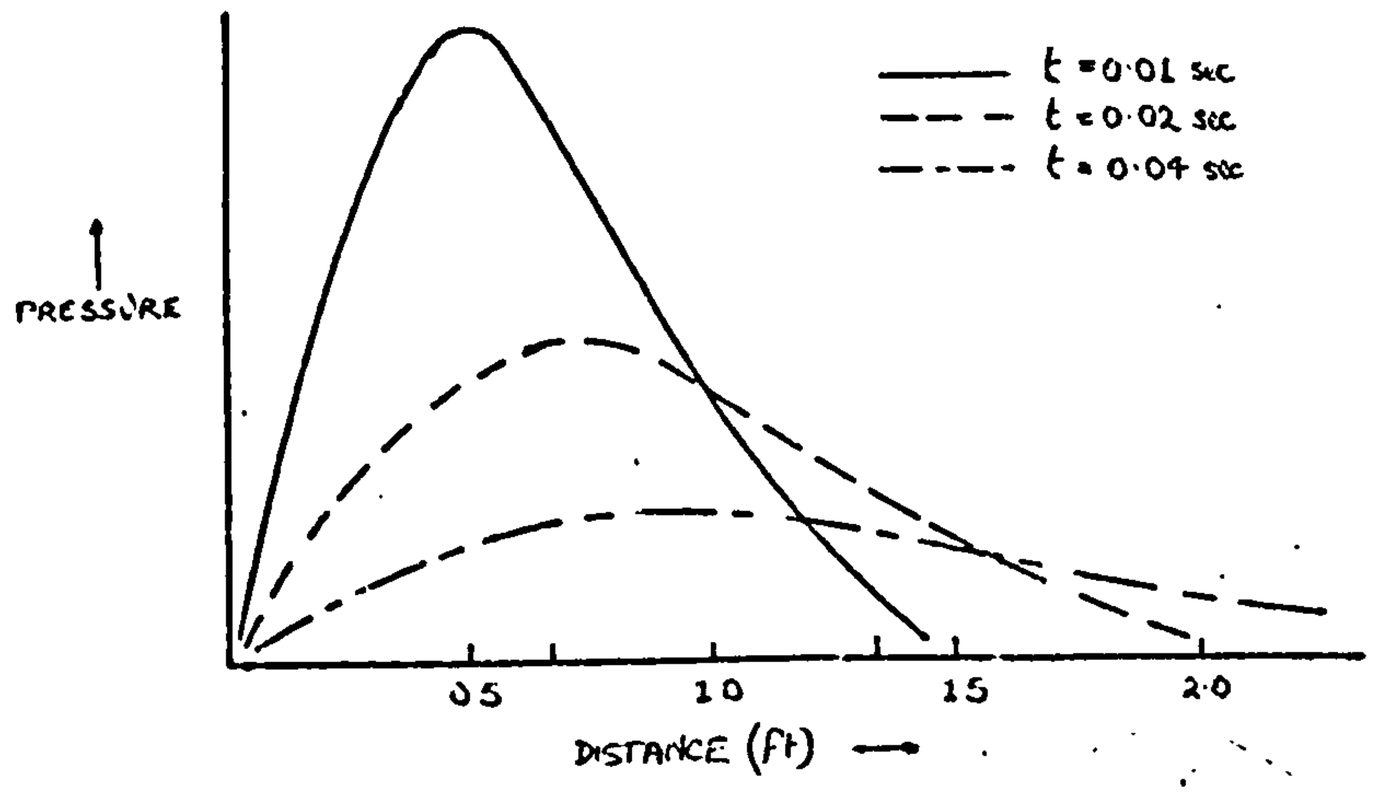

PARAMETERS - $\alpha = 0.05$, $h = 1.0$ BTU/ft² sec °F , $b = 2000$ sec⁻¹

FIG. 3·1. DISPERSION OF STEP AND IMPULSE WAVES DUE TO VARIATION OF SONIC VELOCITY WITH FREQUENCY

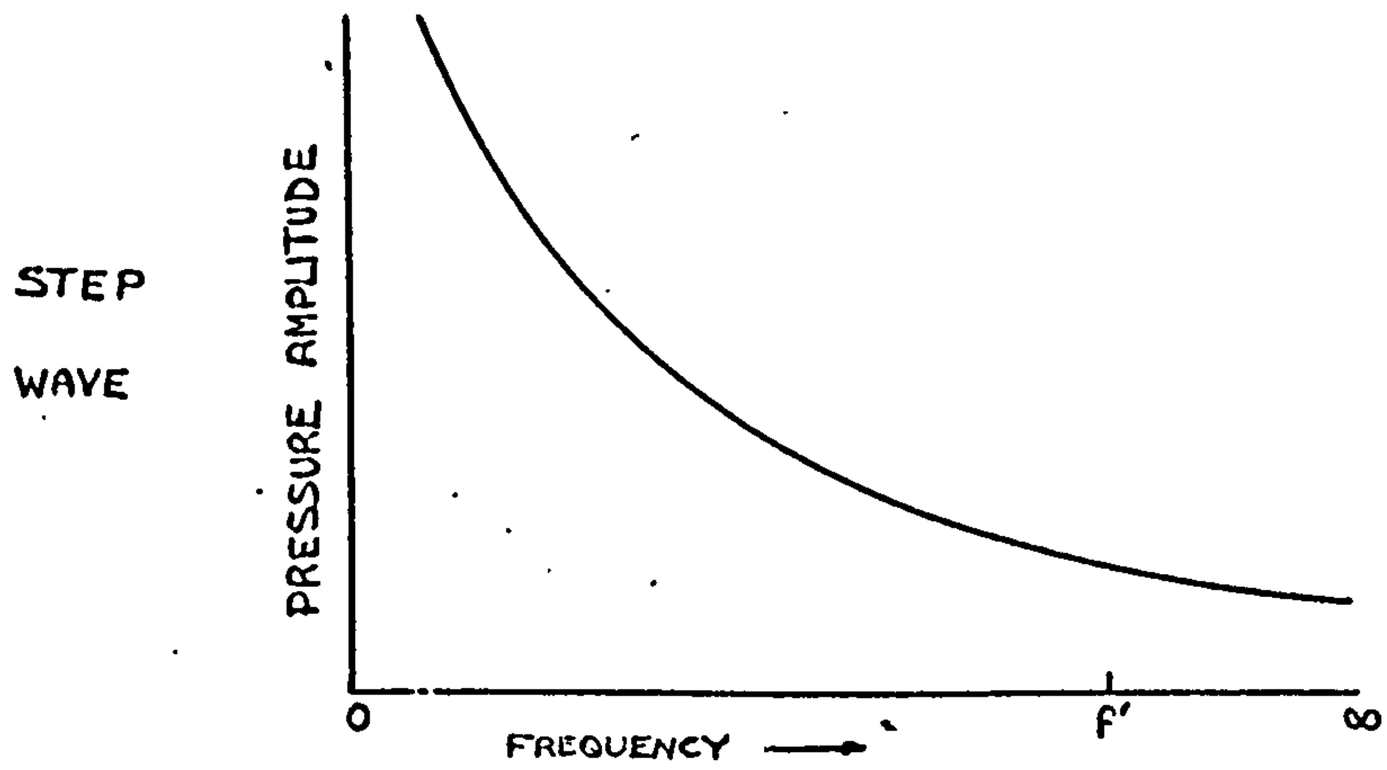

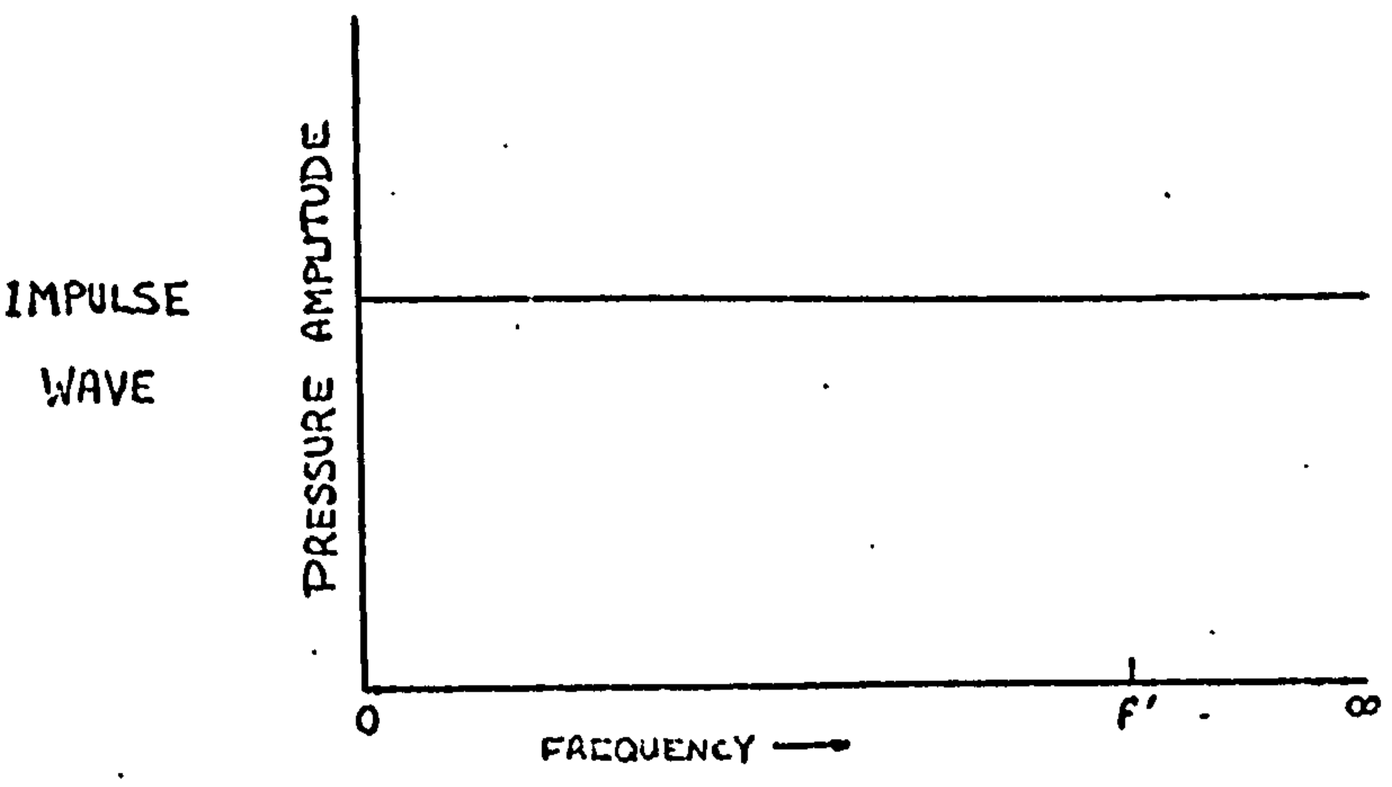

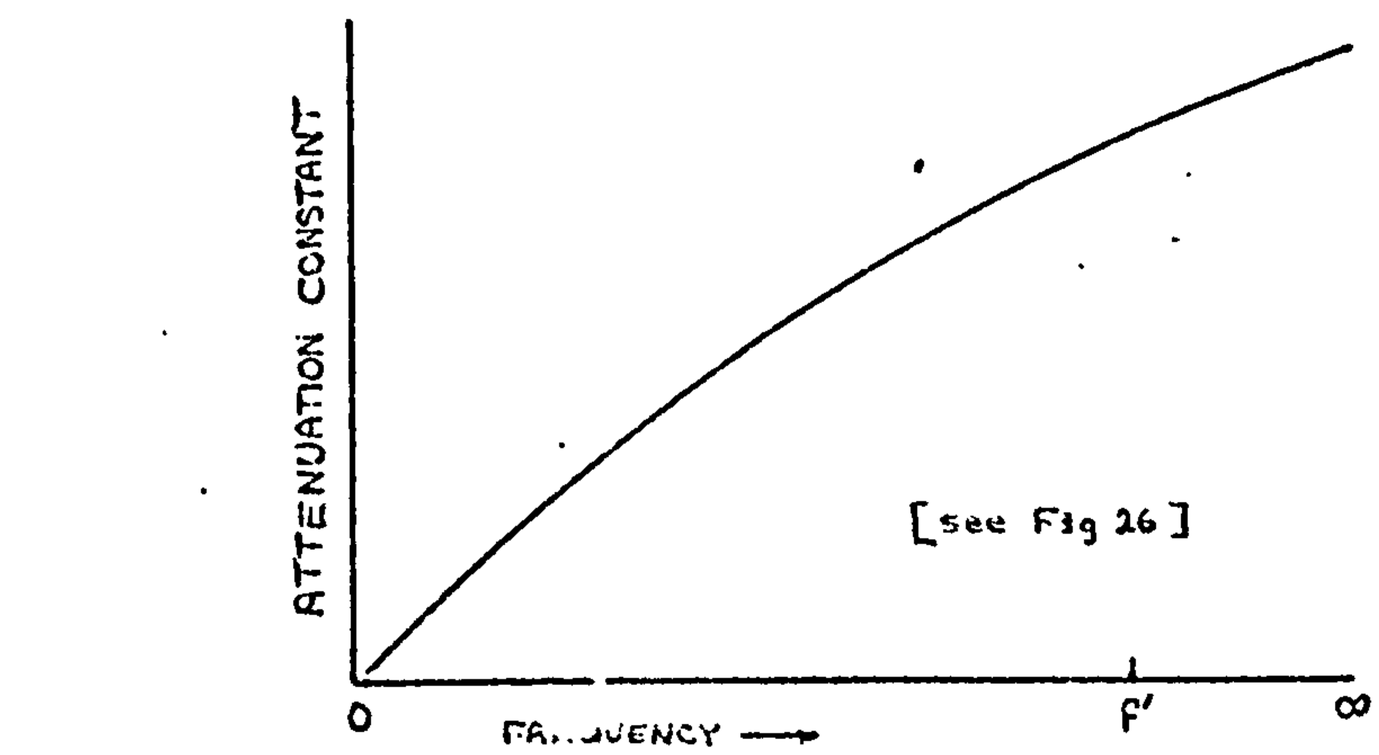

FIG. 3·2 FREQUENCY SPECTRA OF STEP AND IMPULSE WAVES

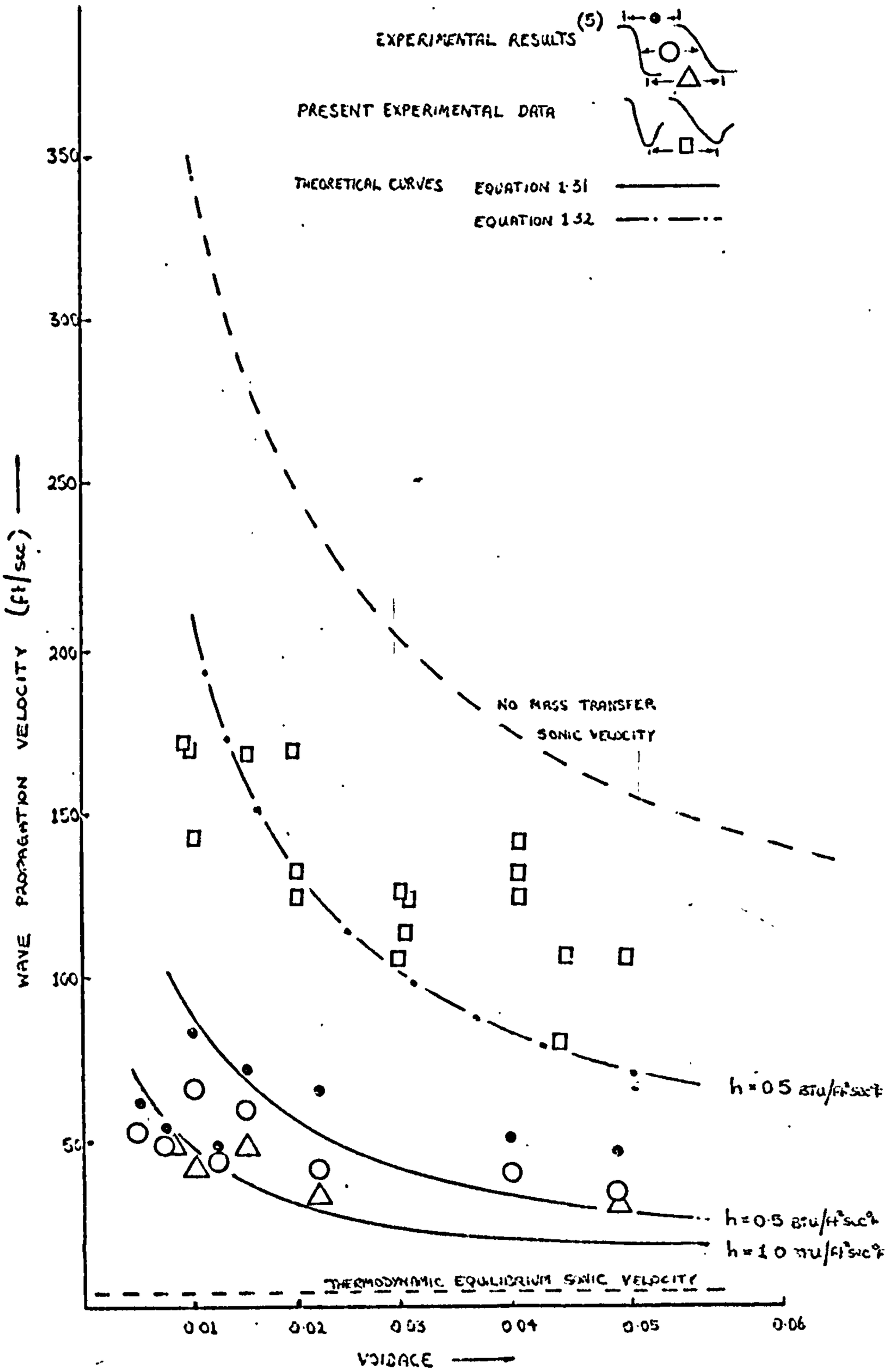

FIG. 4. VELOCITY OF STEP AND IMPULSE RAREFACTION WAVES IN A LOW QUALITY STEAM/WATER MEDIUM

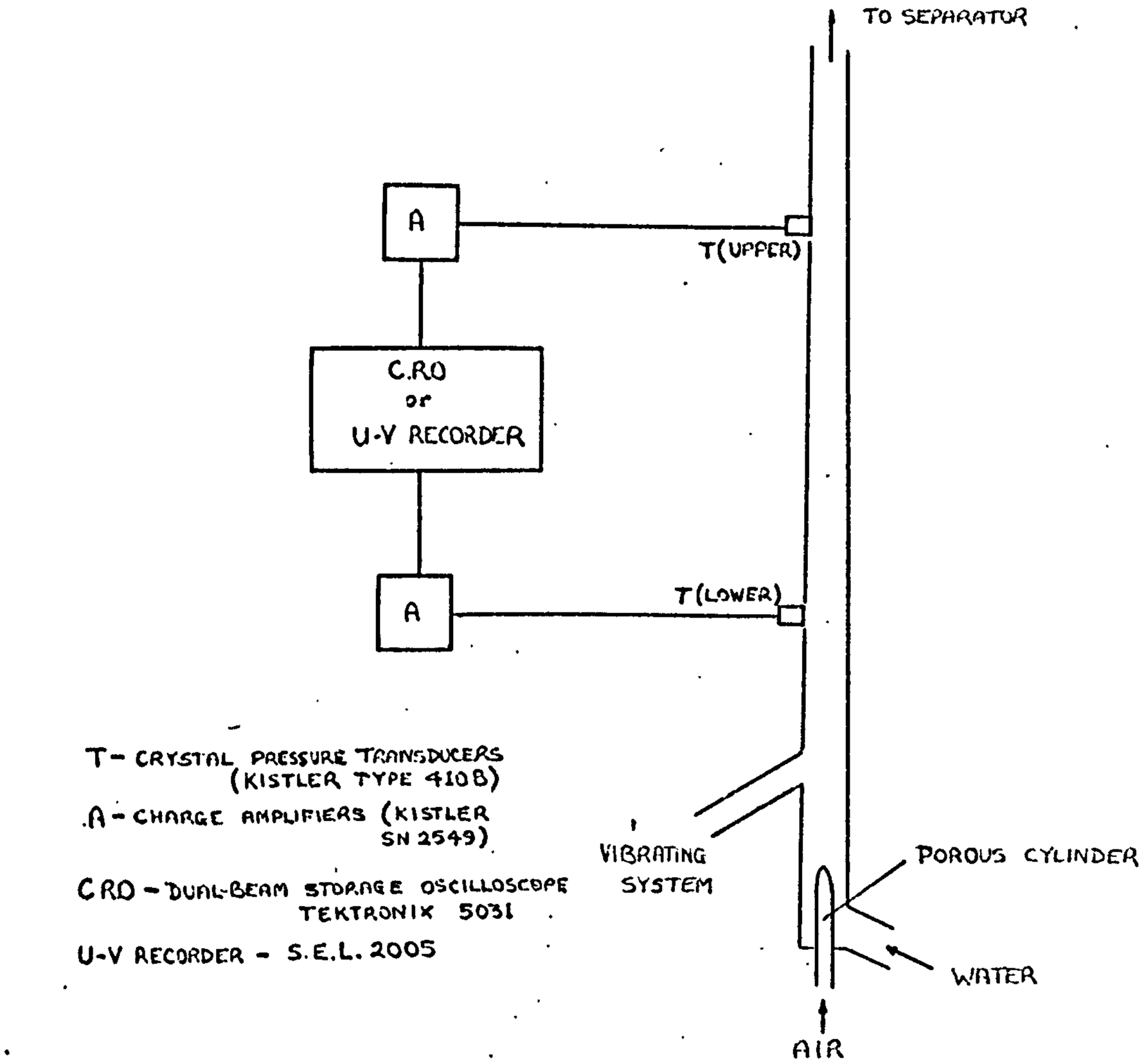

FIG. 5·1. APPARATUS TO MEASURE THE VELOCITY OF PRESSURE WAVES IN AN AIR/WATER BUBBLY MIXTURE

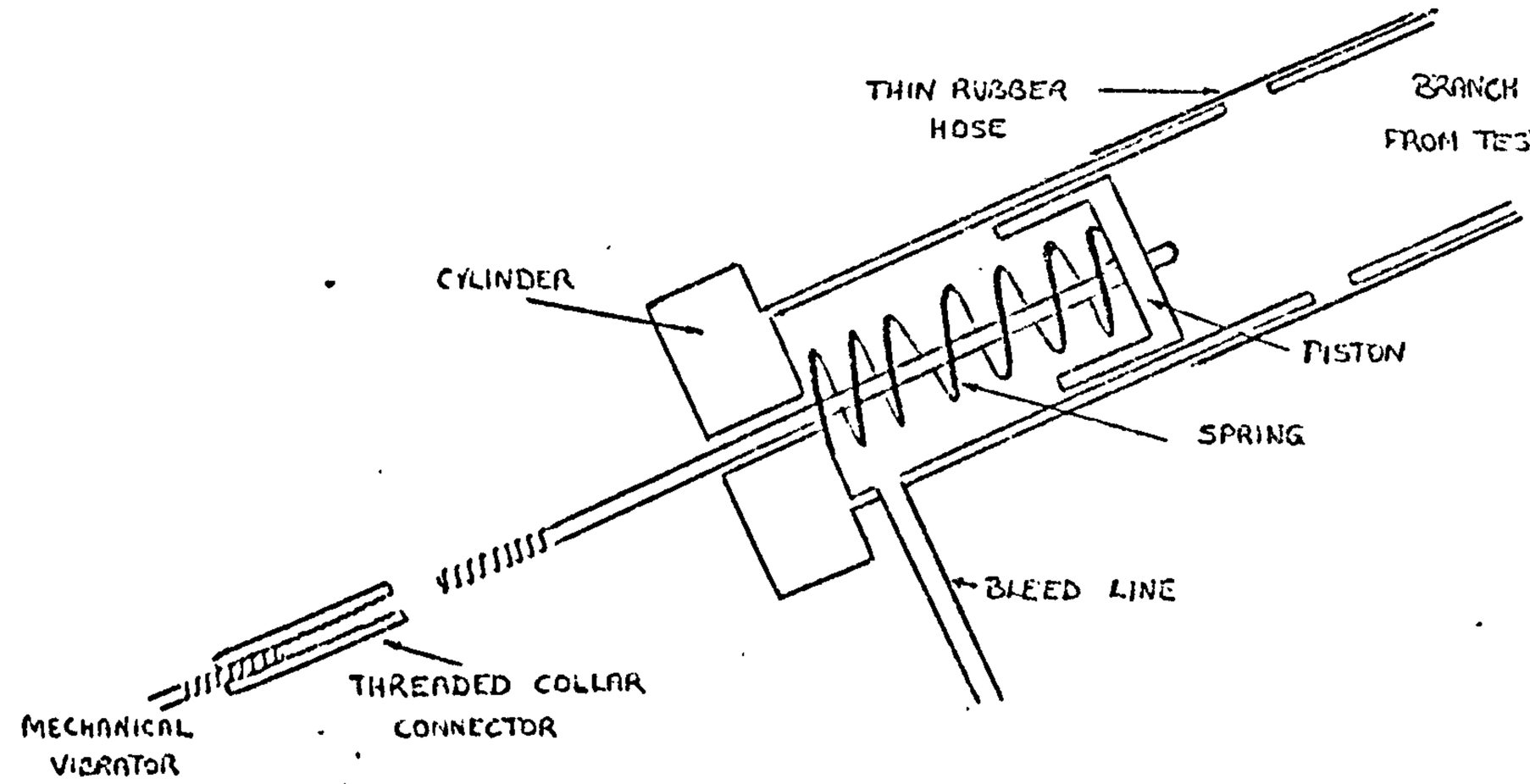

FIG. 5·2. VIBRATING SYSTEM

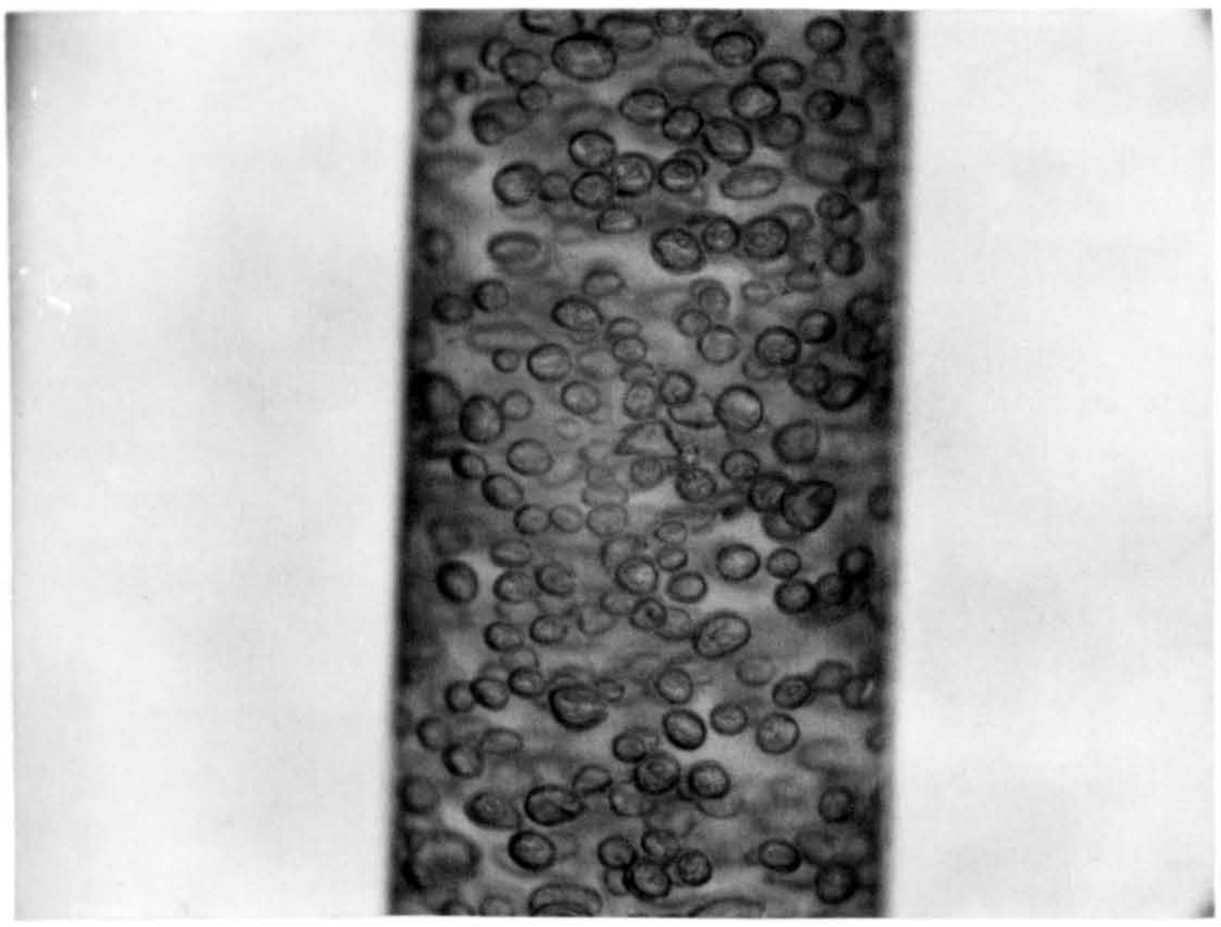

FIG. 6.1 BUBBLE DISTRIBUTION IN AIR/WATER SYSTEM ($\alpha \simeq 12\%$)

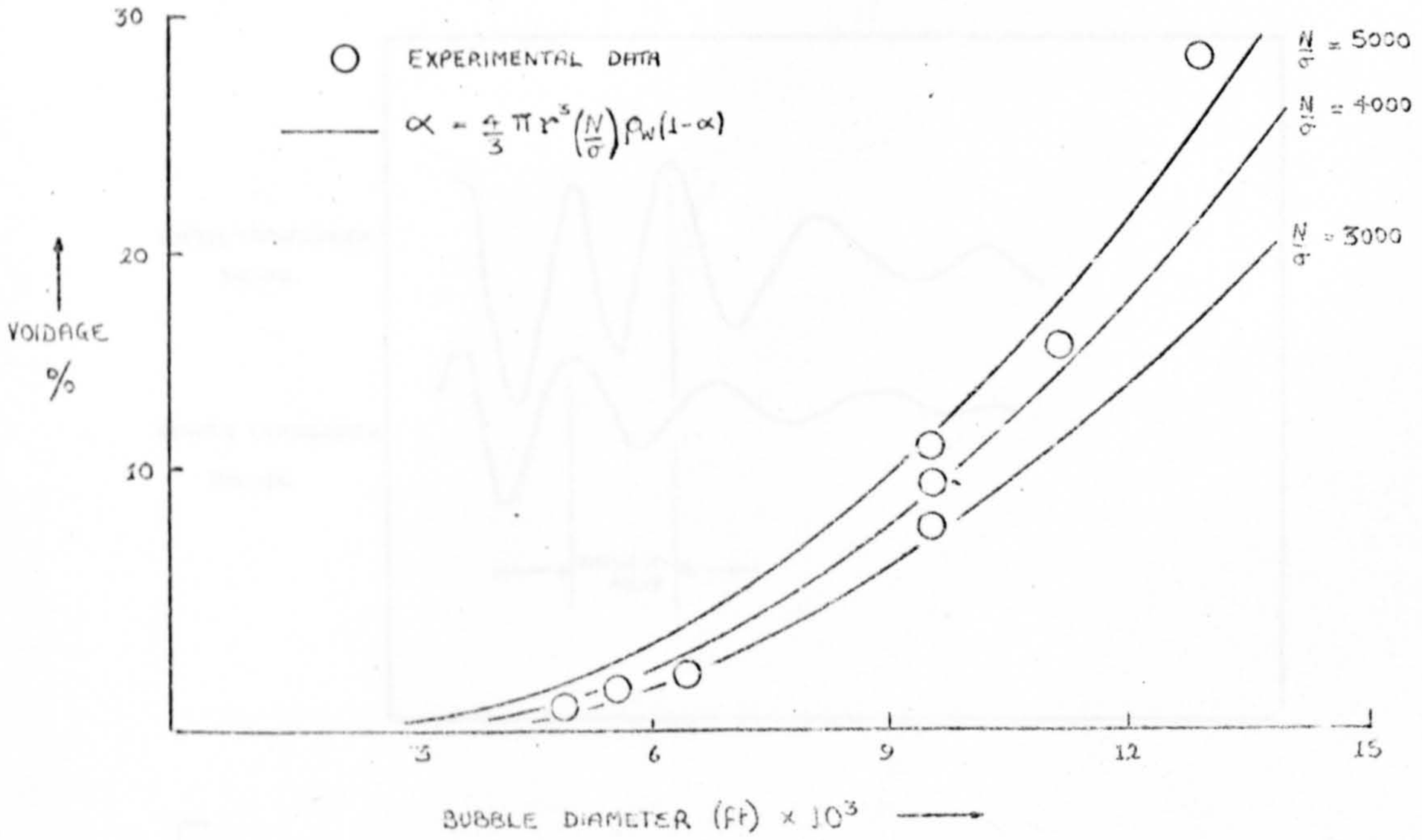

FIG. 6.2. BUBBLE POPULATION IN AIR/WATER SYSTEM

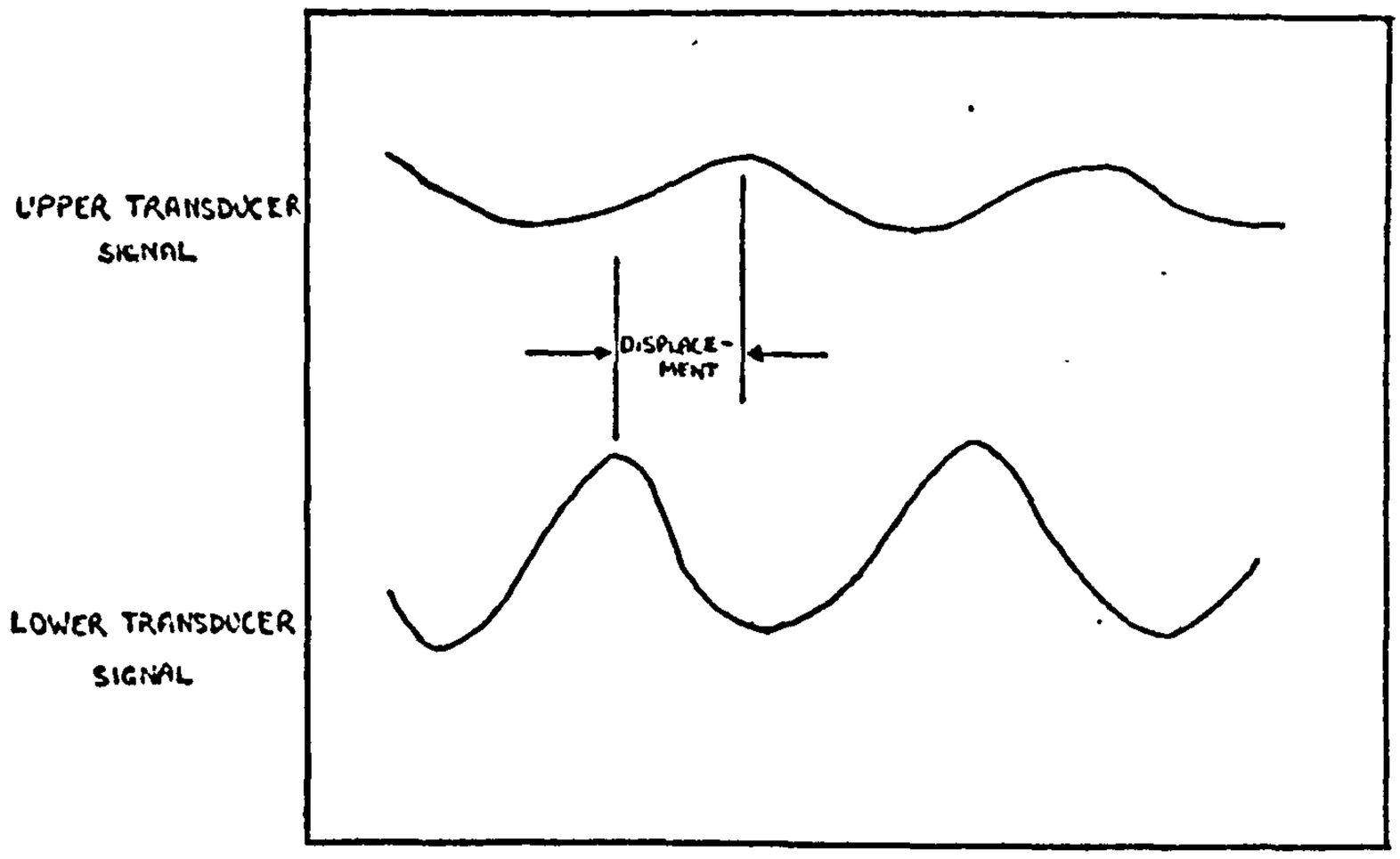

FIG. 7·1. C.R.O. TRACE SHOWING PHASE SHIFT BETWEEN TRANSDUCER SIGNALS

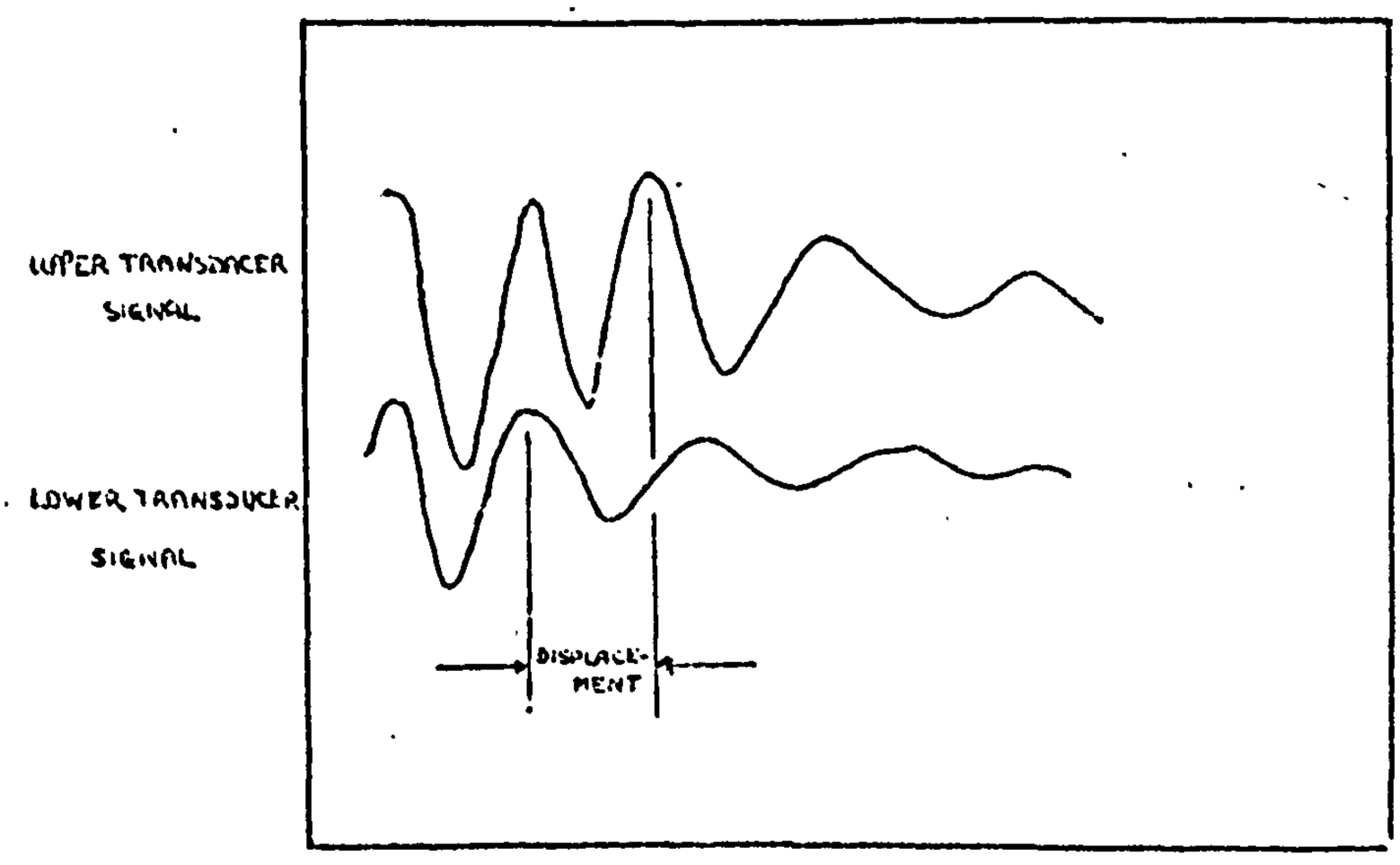

FIG. 7·2. C.R.O. TRACE ILLUSTRATING METHOD OF MEASURING PHASE SHIFTS GREATER THAN ONE WAVELENGTH

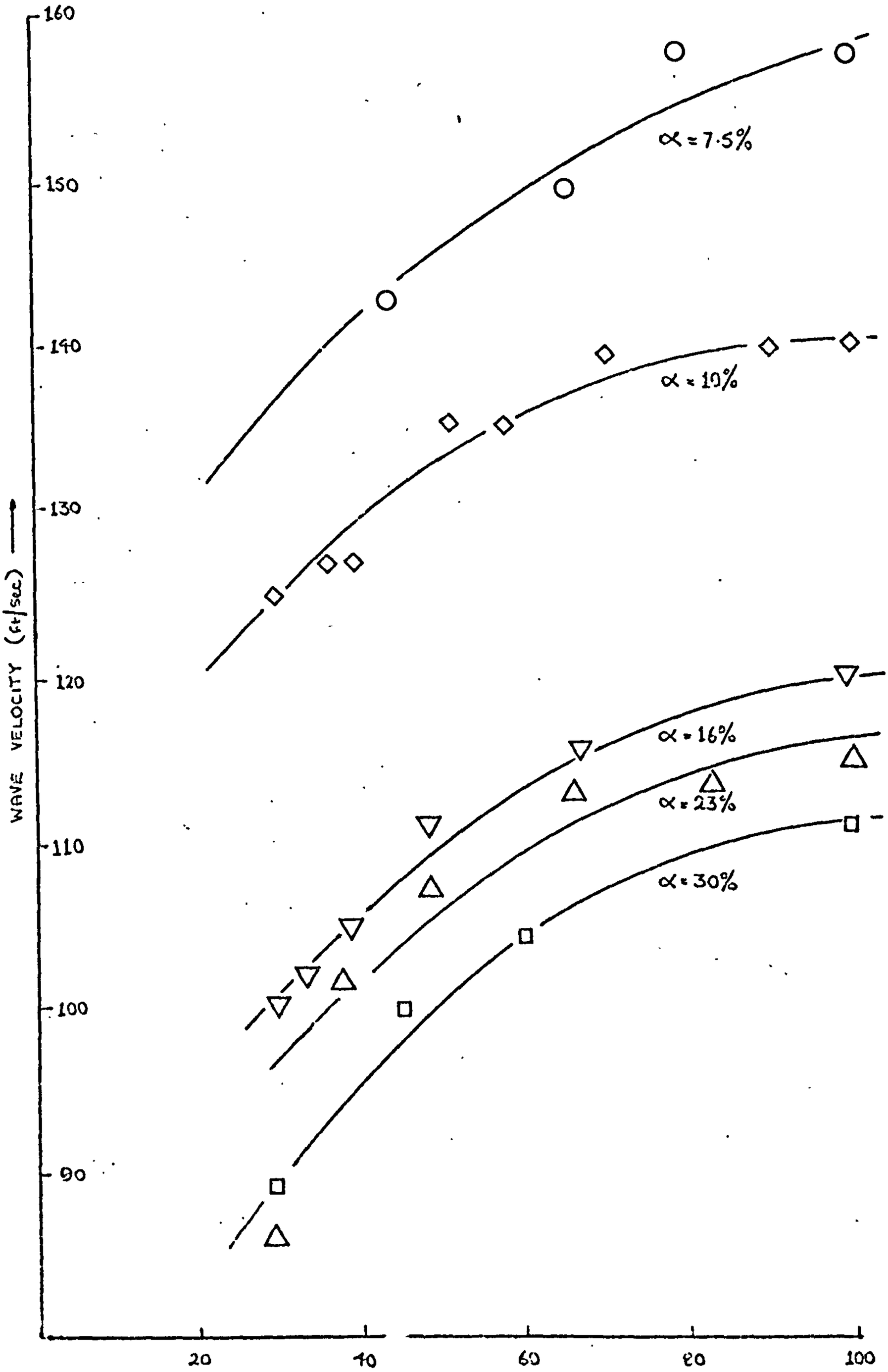

FIG. 8. VELOCITY OF SINUSOIDAL WAVES IN AIR/WATER BUBBLY MIXTURES (P ≈ 17 P.S.I.)

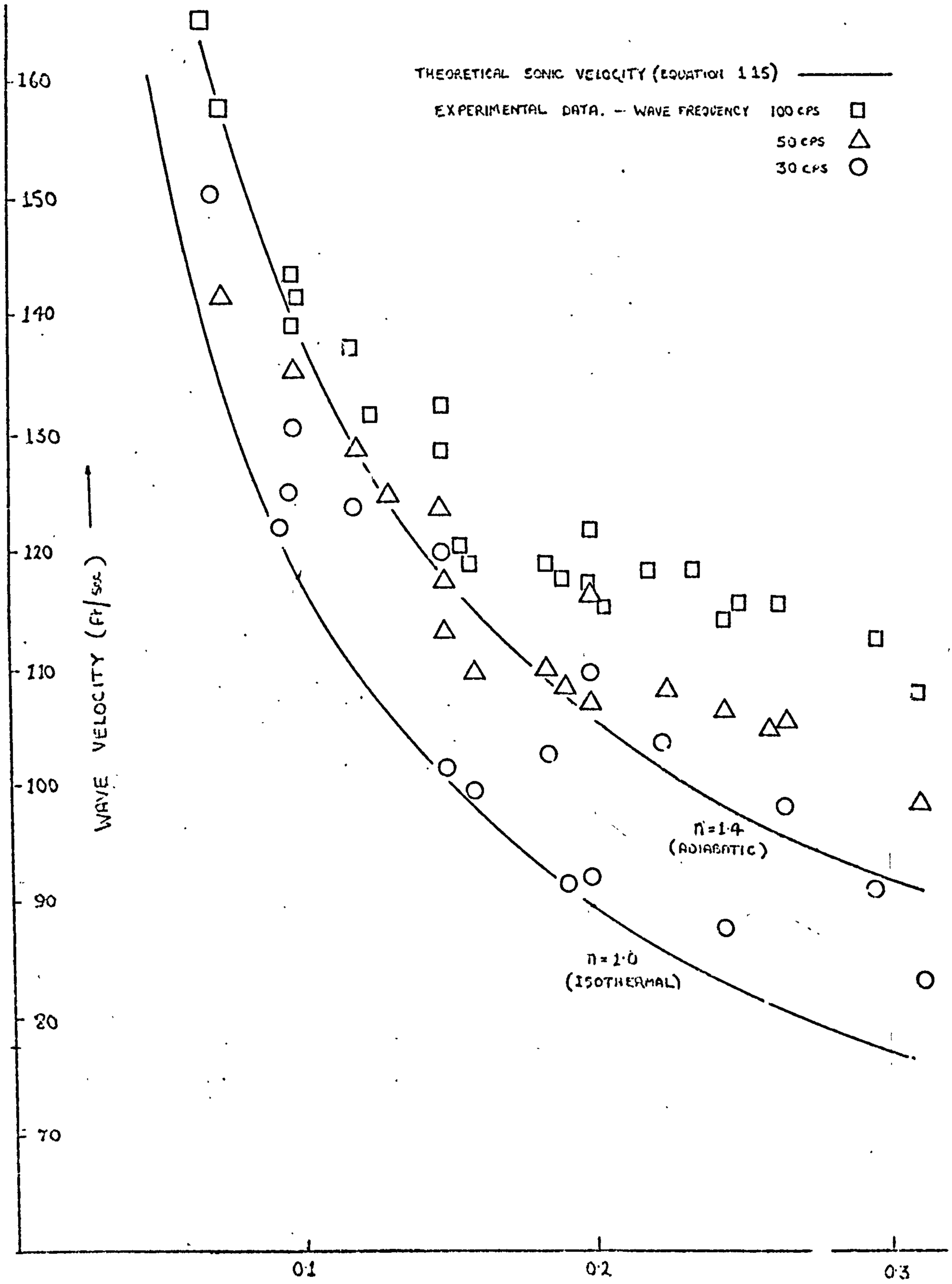

FIG. 9. VELOCITY OF SINUSOIDAL WAVES IN AIR/WATER BUBBLY MIXTURES ($P \simeq 17$ p.s.i)

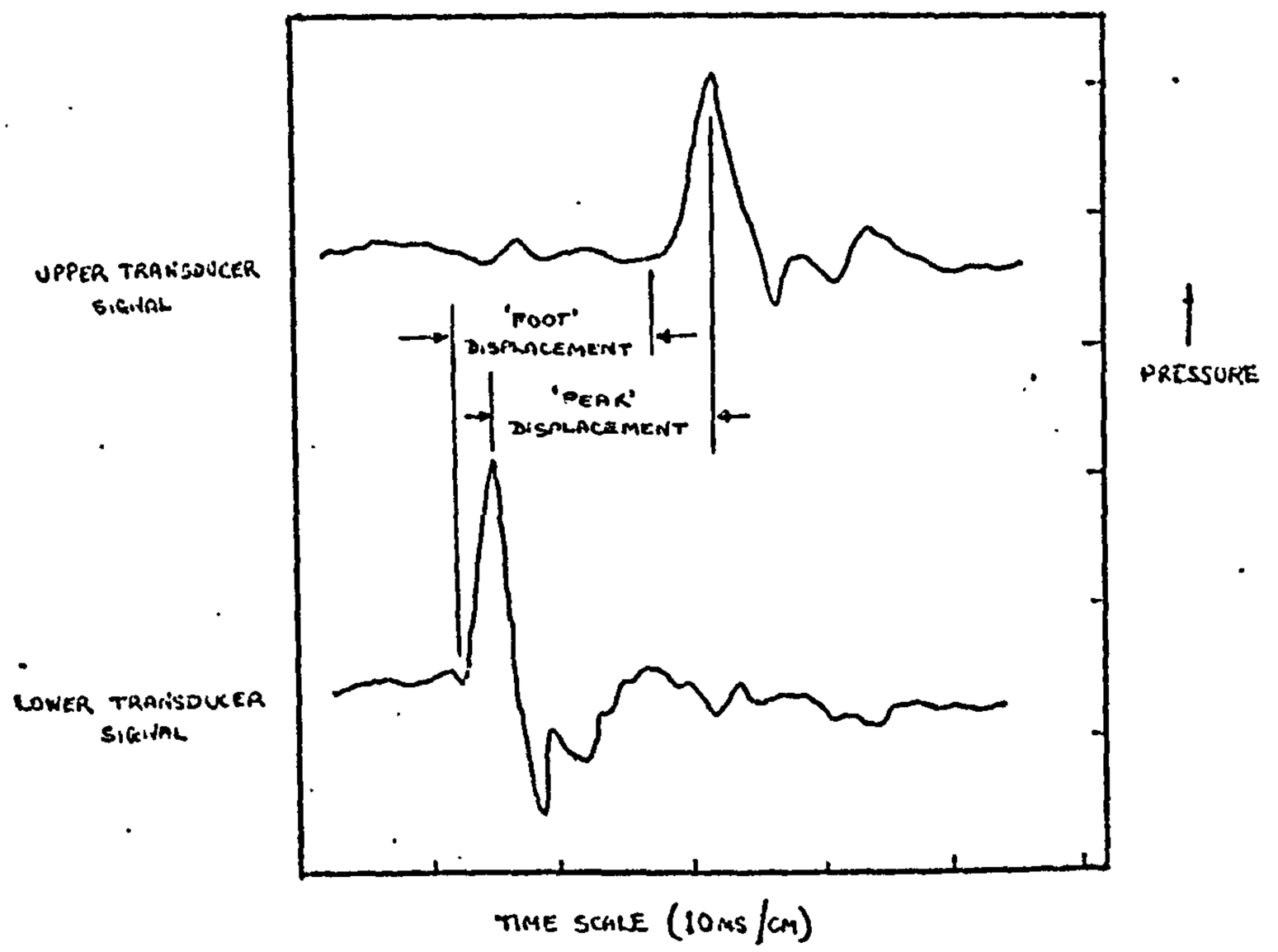

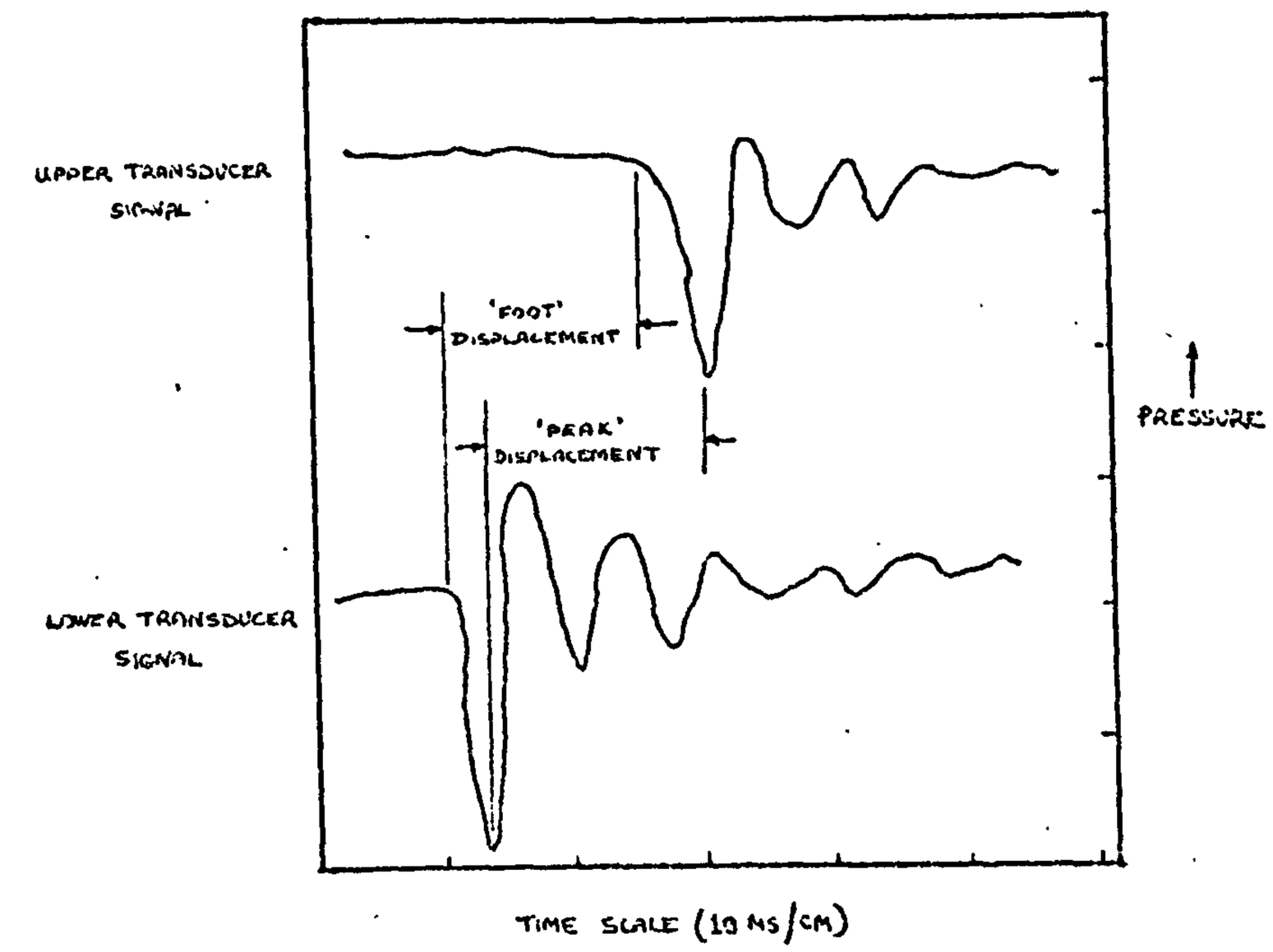

FIG. 10. C.R.O. TRACES ILLUSTRATING THE MEASUREMENT OF THE PROPAGATION VELOCITIES OF PRESSURE AND RAREFACTION IMPULSES IN AN AIR/WATER MIXTURE ($\alpha \approx 20\%$)

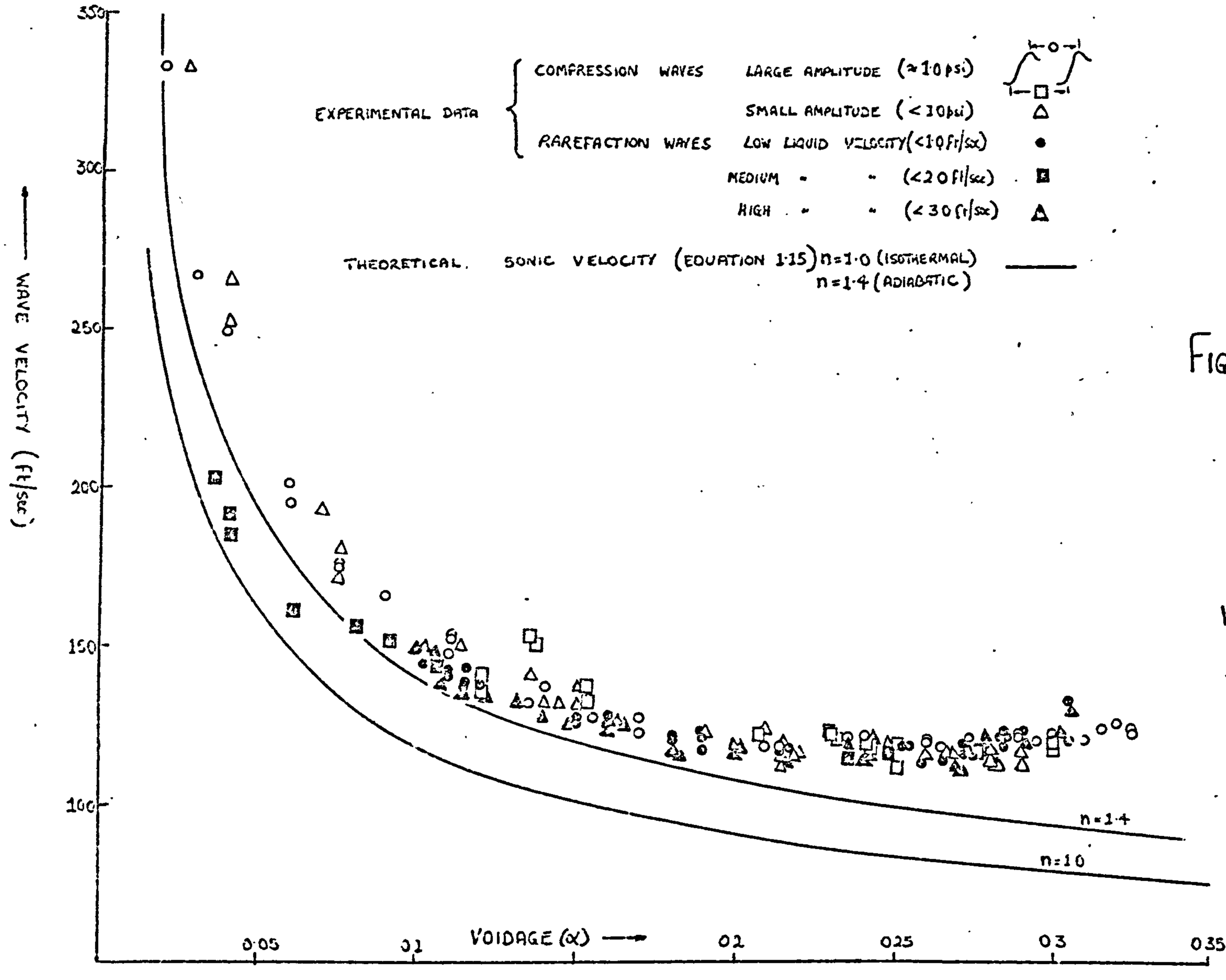

FIG. 11. THE PROPAGATION VELOCITY OF IMPULSE PRESSURE AND RAREFACTION WAVES IN AIR/WATER BUBBLY MIXTURES ($P \approx 17$ p.s.i)

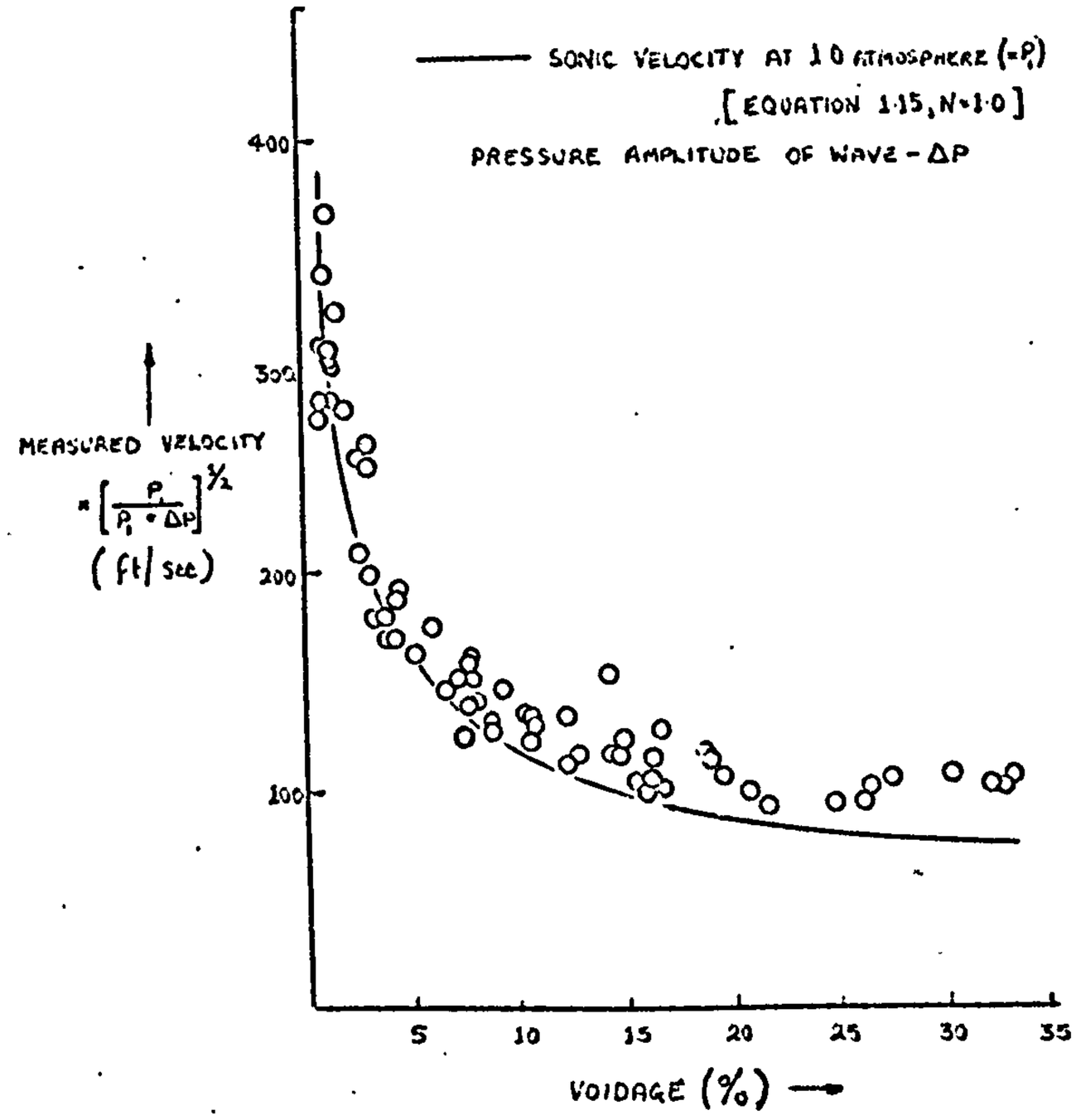

FIG. 12 VELOCITY OF STEP OR SHOCK WAVES IN AIR/WATER BUBBLY MIXTURES

(REPRODUCED FROM REF. 35)

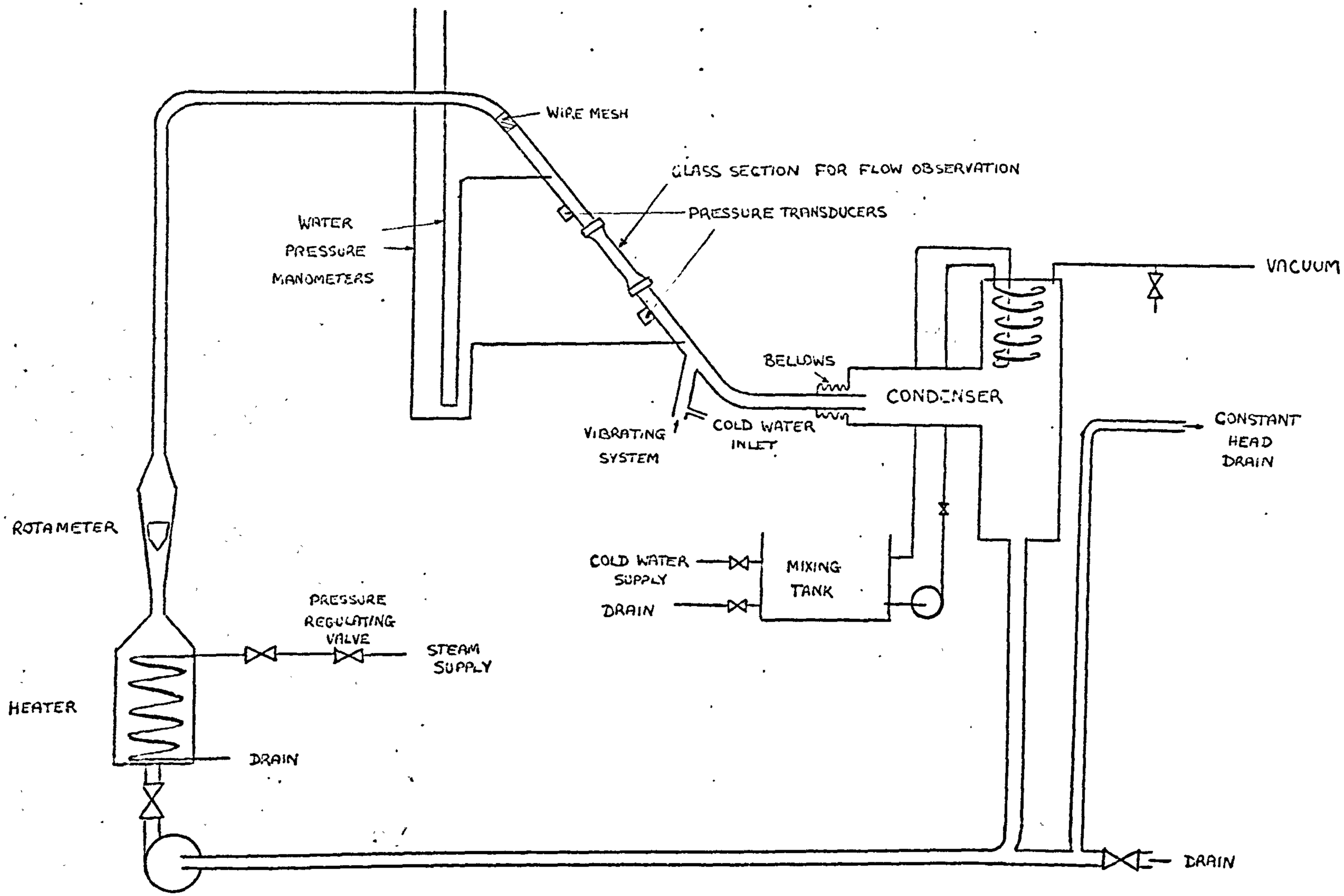

FIG. 13. APPARATUS TO MEASURE THE VELOCITY OF PRESSURE WAVES IN STEAM/WATER MIXTURES

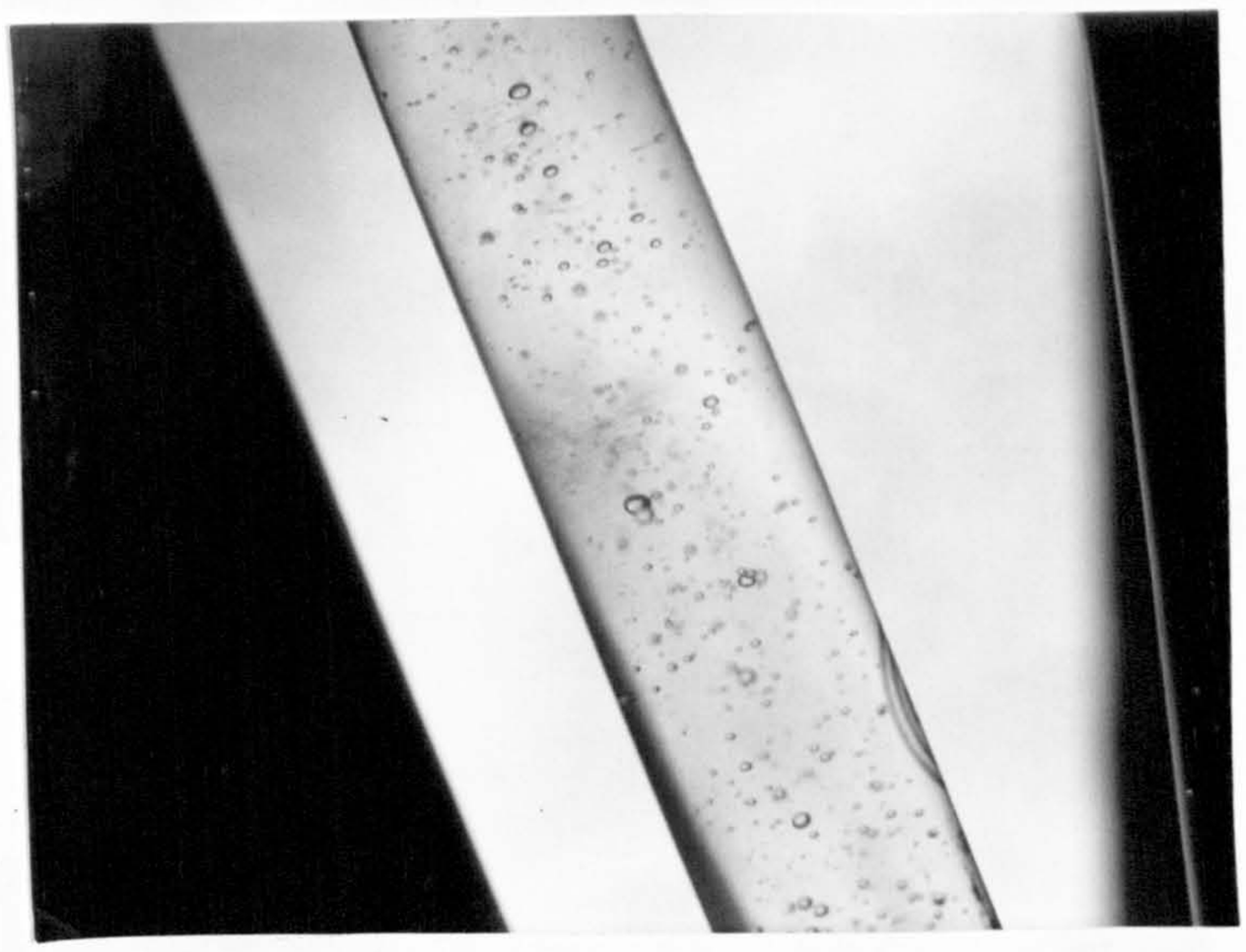

FIG. 14-1. LOW VOIDAGE STEAM/WATER FLOW USED TO DETERMINE APPROXIMATE NUMBER OF BUBBLES/lb OF FLUID (ESTIMATE 20,000)

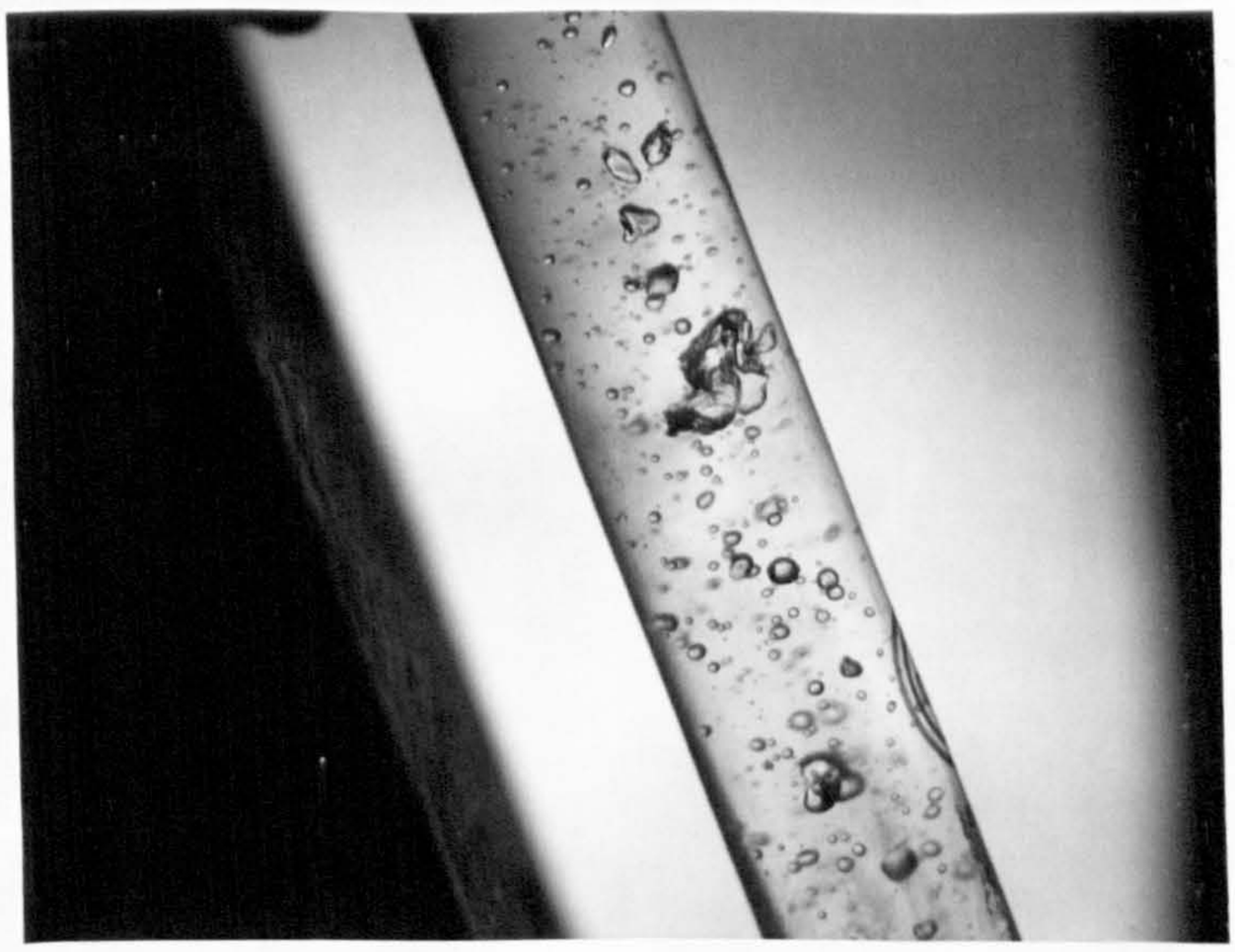

FIG. 14-2. NON-HOMOGENEOUS BUBBLE FLOW OR ONSET OF "PLUG" FLOW ($\alpha > 5\%$)

VOIDAGE

2%

4%

6%

FIG. 15. BUBBLE SIZE AND DISTRIBUTIONS IN STEAM/WATER FLOW

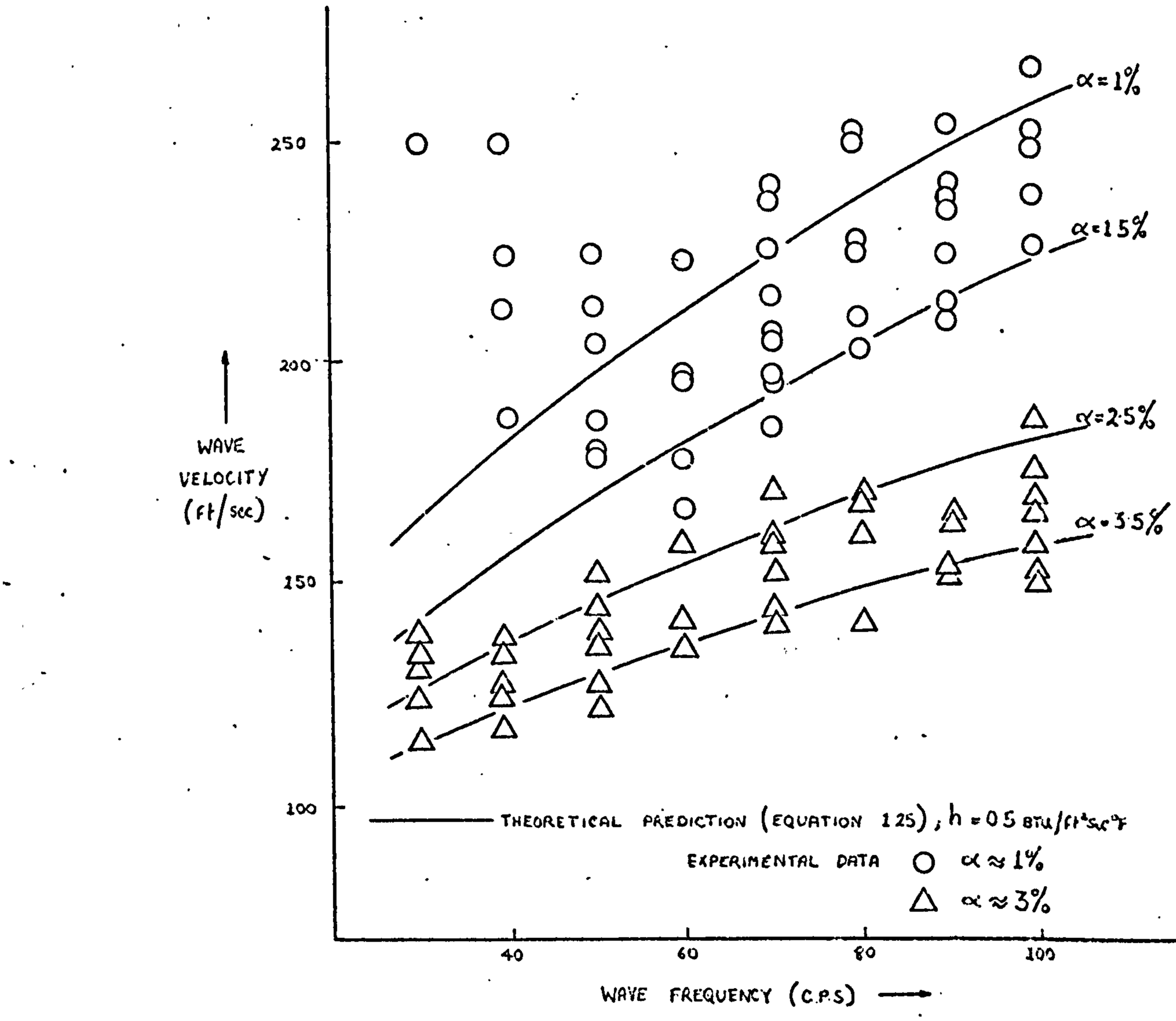

FIG. 16. PROPAGATION VELOCITY OF SINUSOIDAL WAVES IN STEAM/WATER MIXTURES (P ≈ 14·7 P.S.I.)

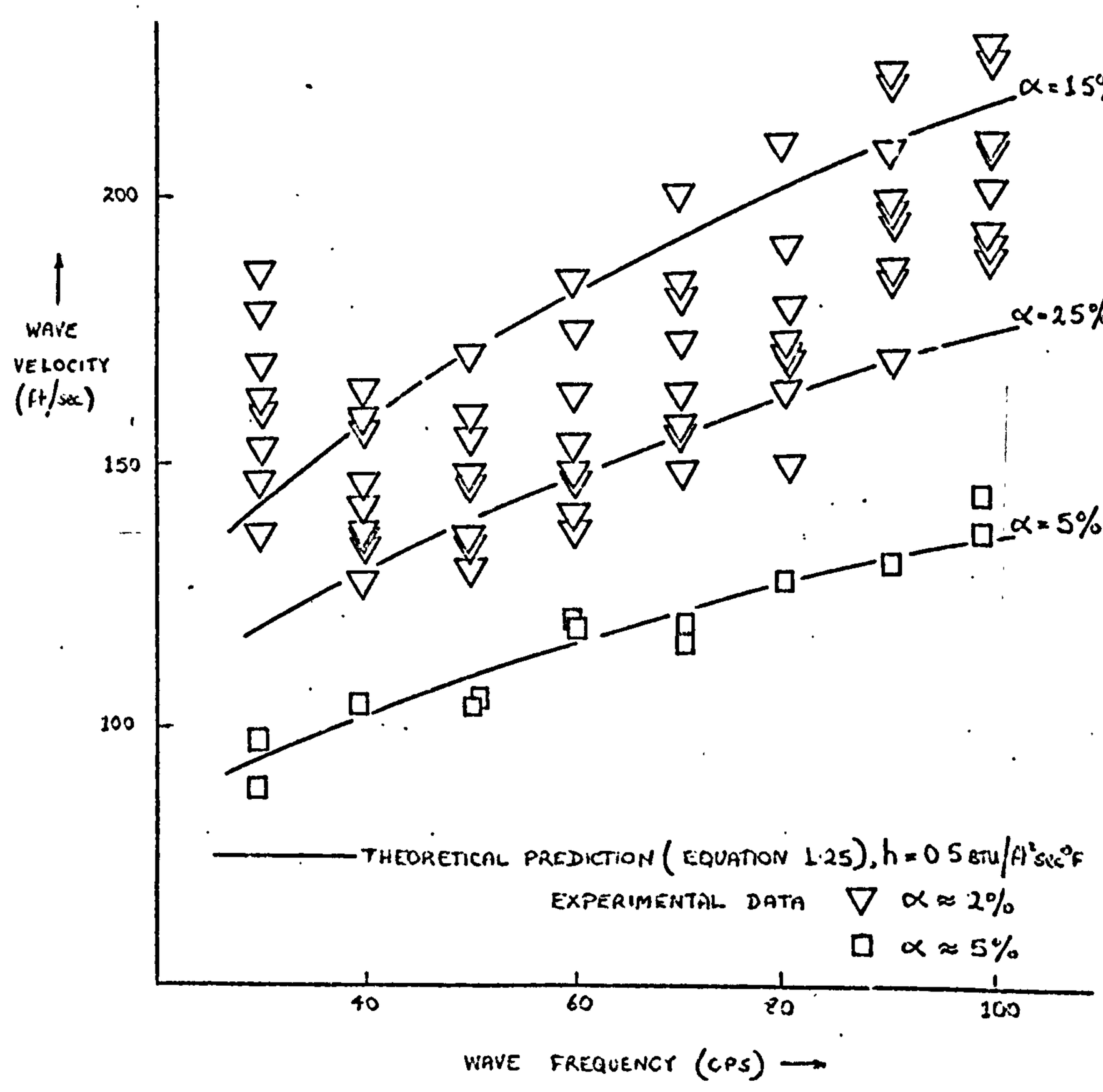

FIG. 17. PROPAGATION VELOCITY OF SINUSOIDAL WAVES IN STEAM/WATER MIXTURES (P≈ 14·1 P.S.I.)

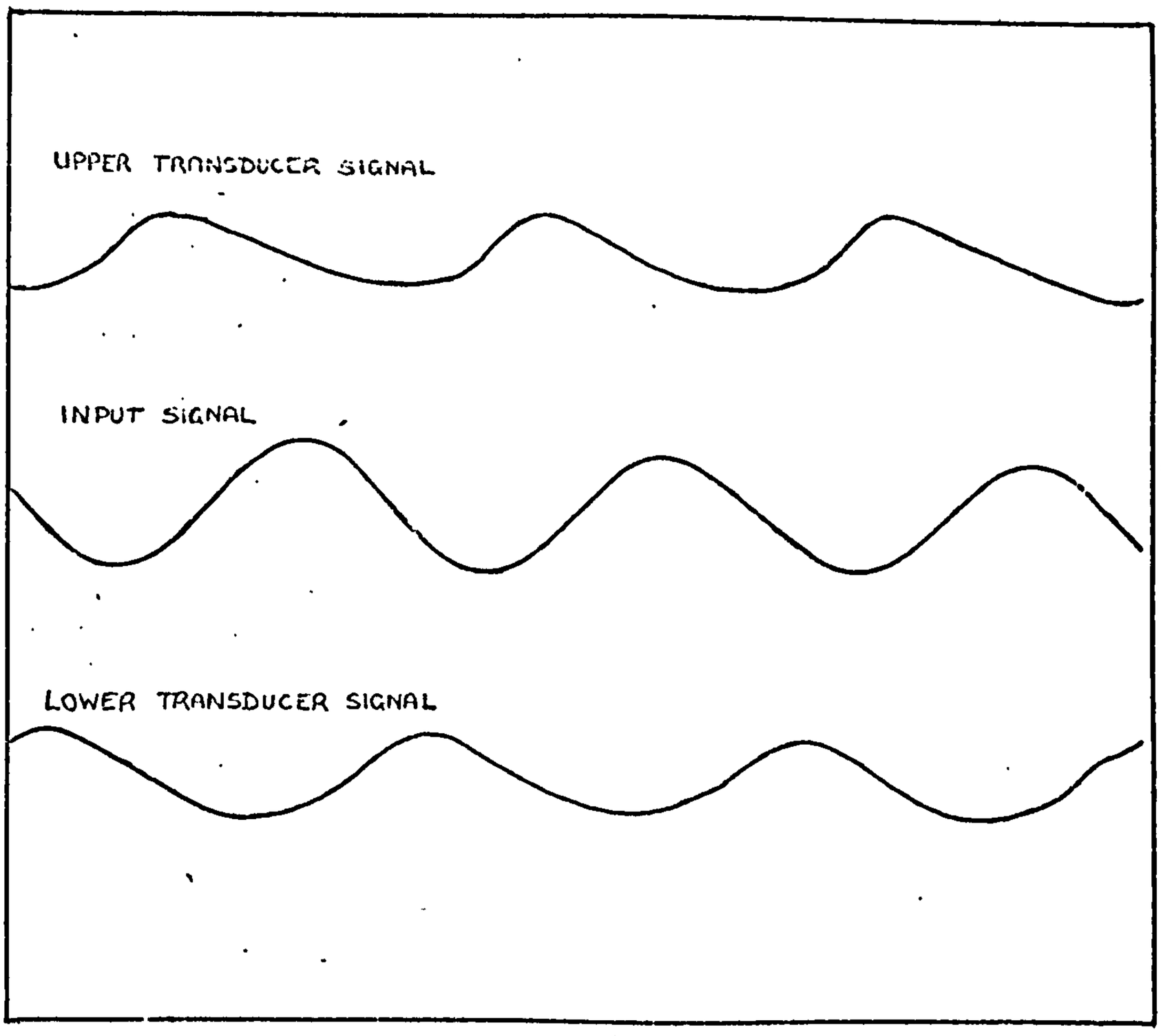

FIG. 18·1 U-V RECORDER TRACE SHOWING DISTORTED WAVEFORM

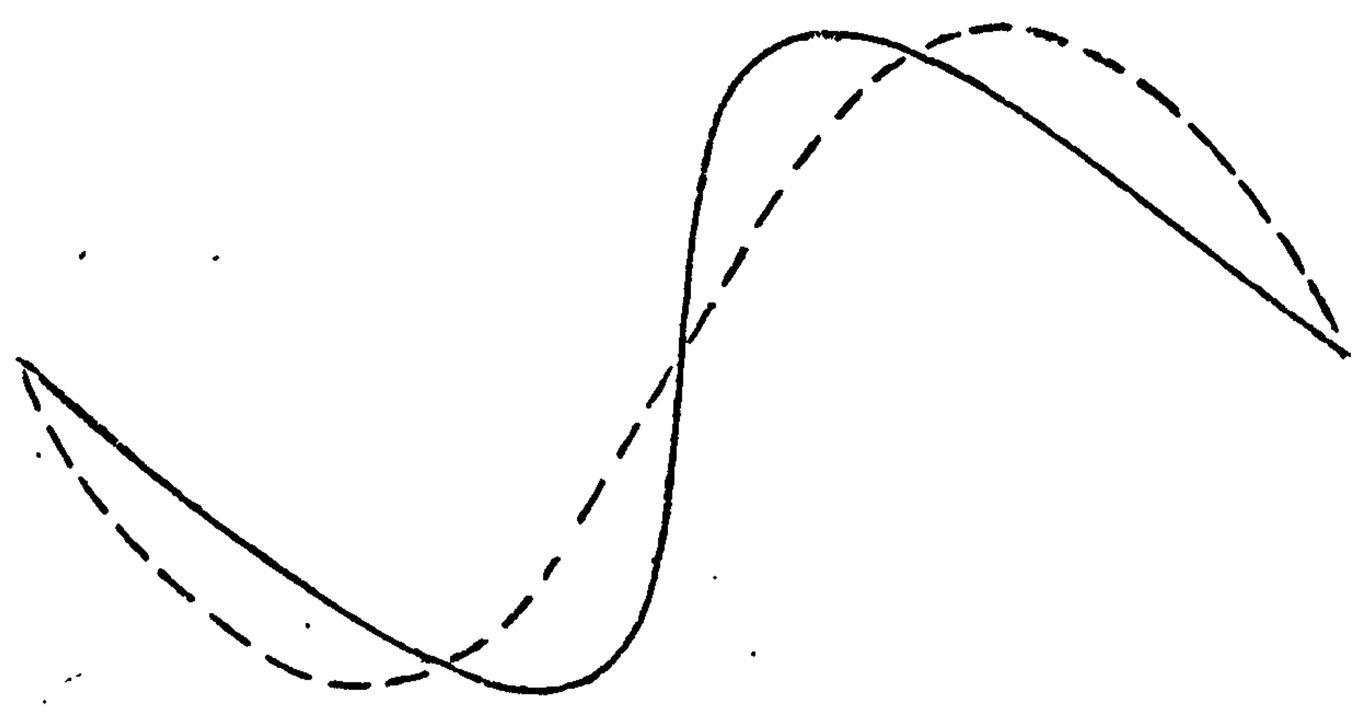

FIG. 18·2. DISTORTION OF A SINUSOIDAL WAVE ASSUMING THE LOCAL VELOCITY TO BE DIRECTLY PROPORTIONAL TO THE LOCAL PRESSURE

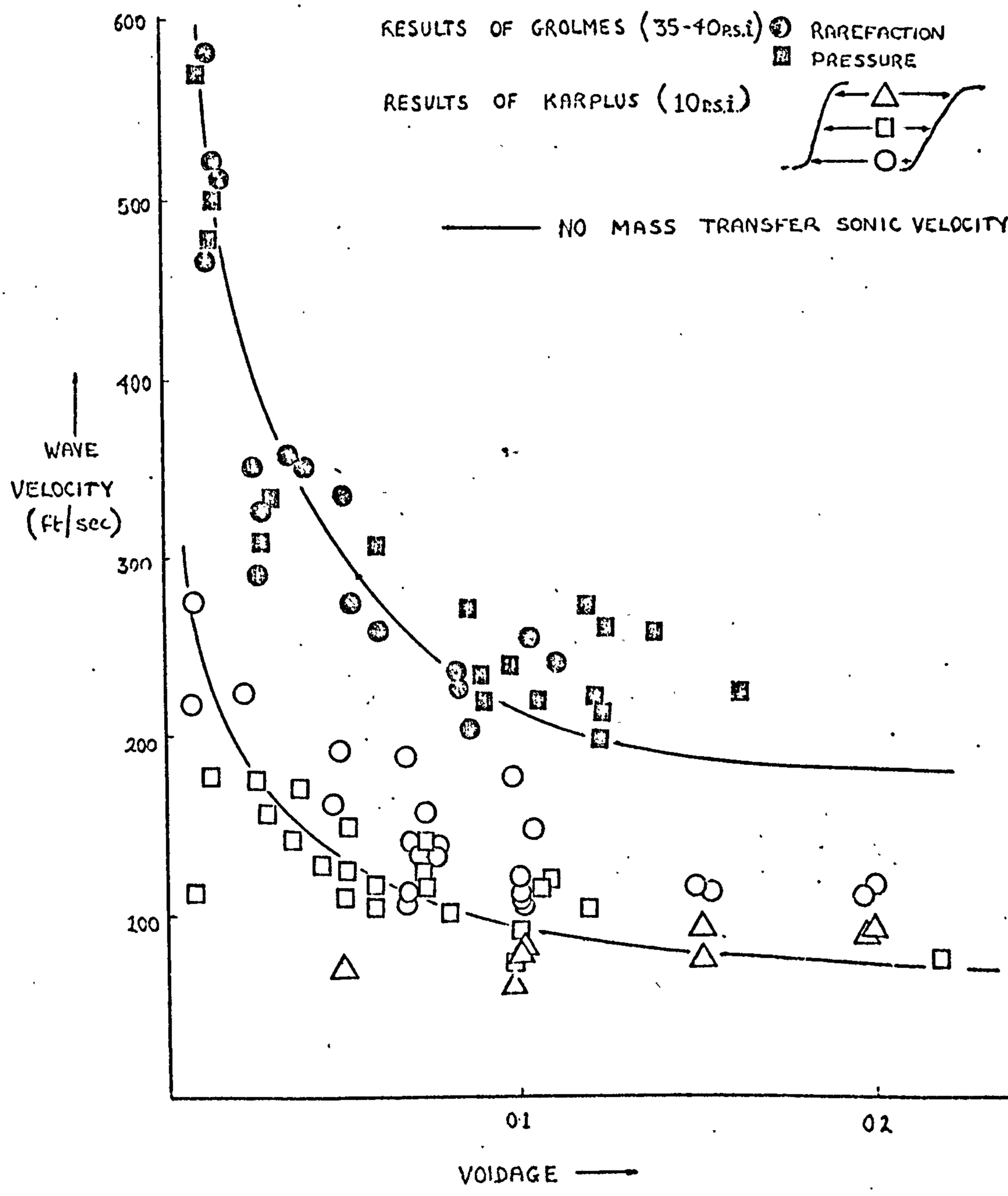

FIG. 19. PROPAGATION VELOCITY OF FINITE AMPLITUDE STEP PRESSURE WAVES IN STEAM/WATER MIXTURES

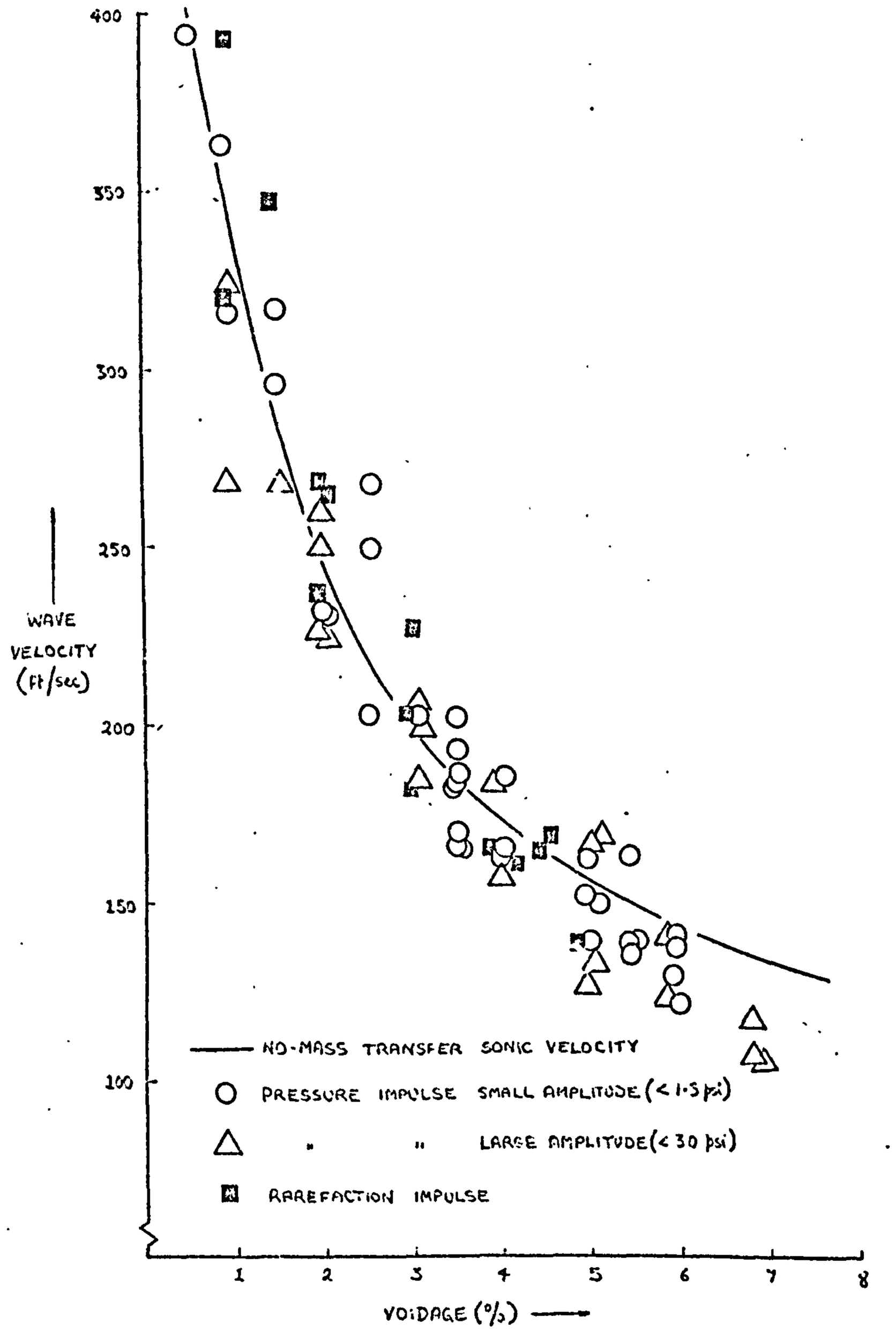

FIG. 20. PROPAGATION VELOCITY OF IMPULSE WAVES THROUGH A STEAM/WATER MIXTURE (P = 14·7 P.S.I)

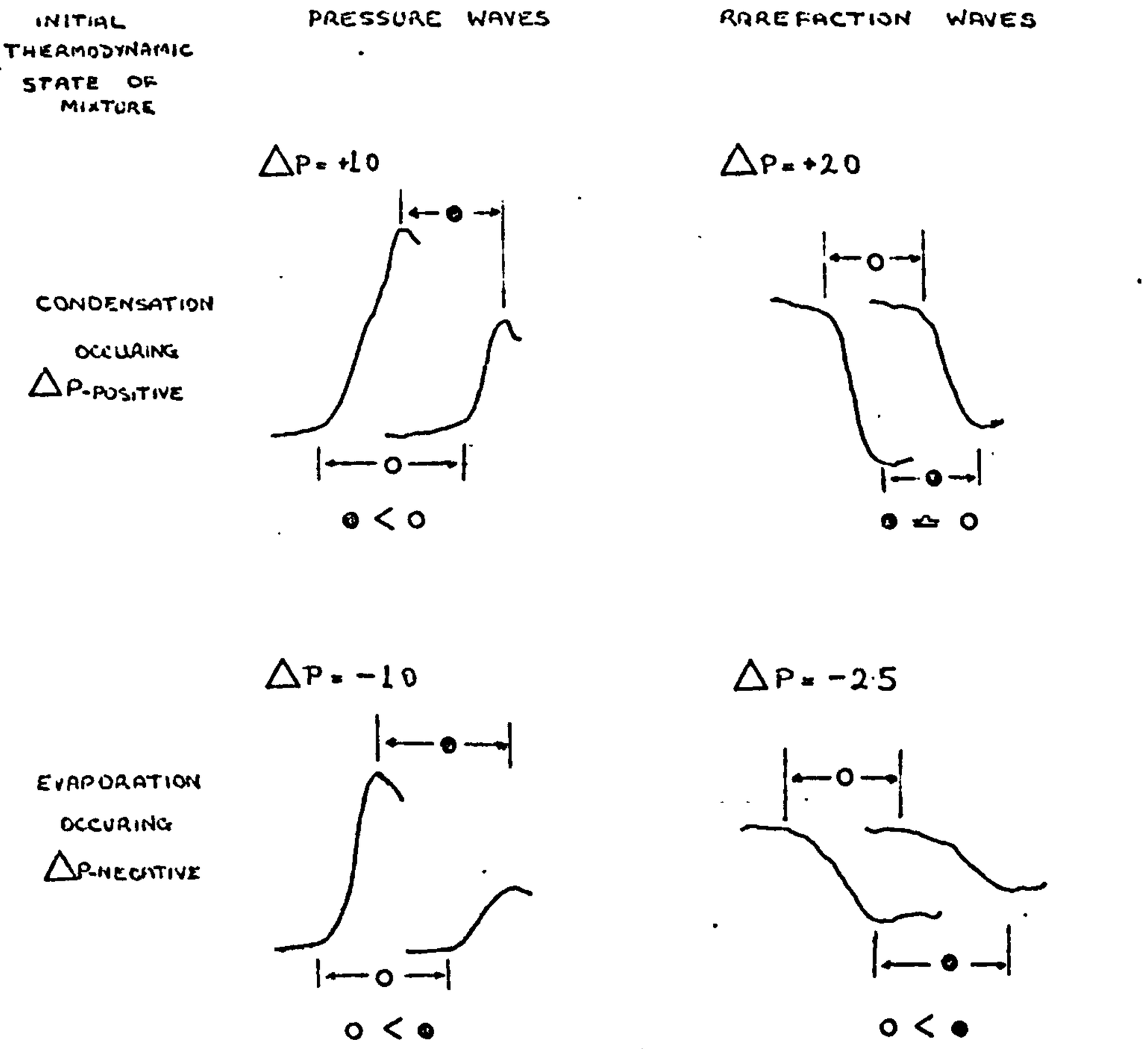

FIG. 21. CHANGE OF SLOPE OF WAVEFRONTS WHEN PROPAGATING THROUGH A STEAM/WATER MIXTURE WHICH IS NOT INITIALLY IN THERMODYNAMIC EQUILIBRIUM

FIG. 22. PRESSURE IMPULSE WAVE

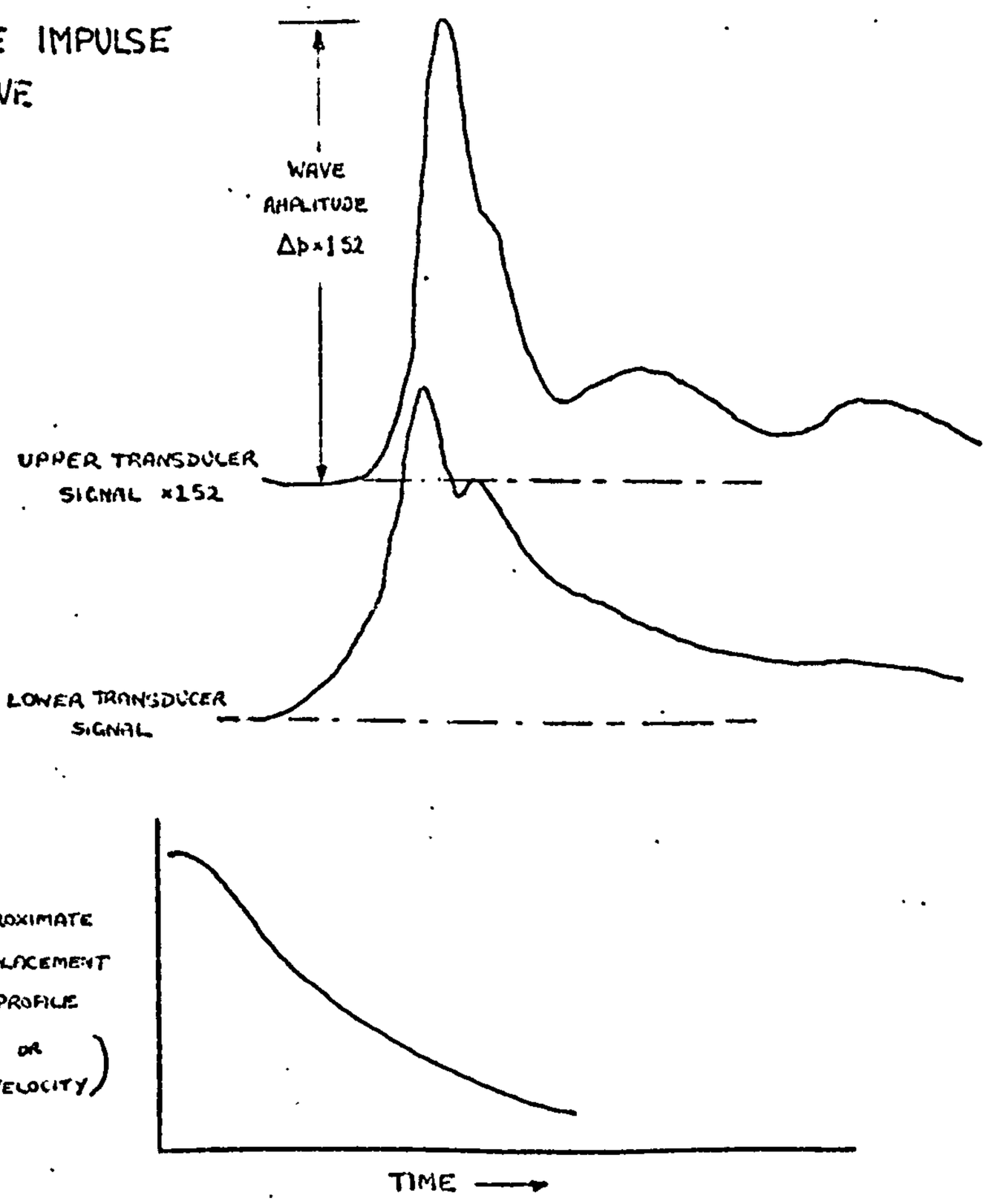

FIG. 23 RAREFACTION IMPULSE WAVE

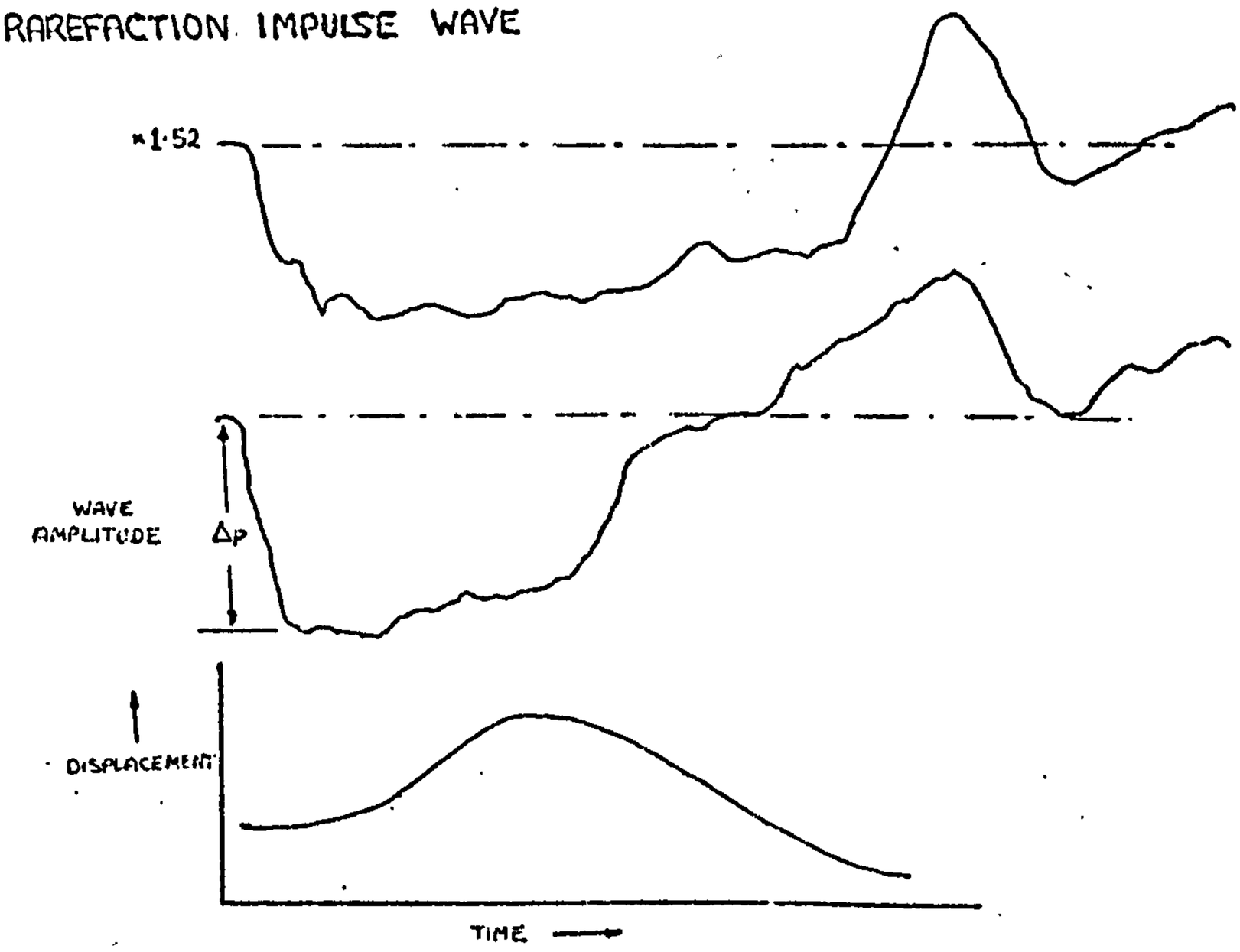

ZERO WAVE PRESSURE LINES

CHANGE OF SHAPE OF IMPULSE WAVES IN A STEAM/WATER MIXTURE INITIALLY IN THERMODYNAMIC EQUILIBRIUM

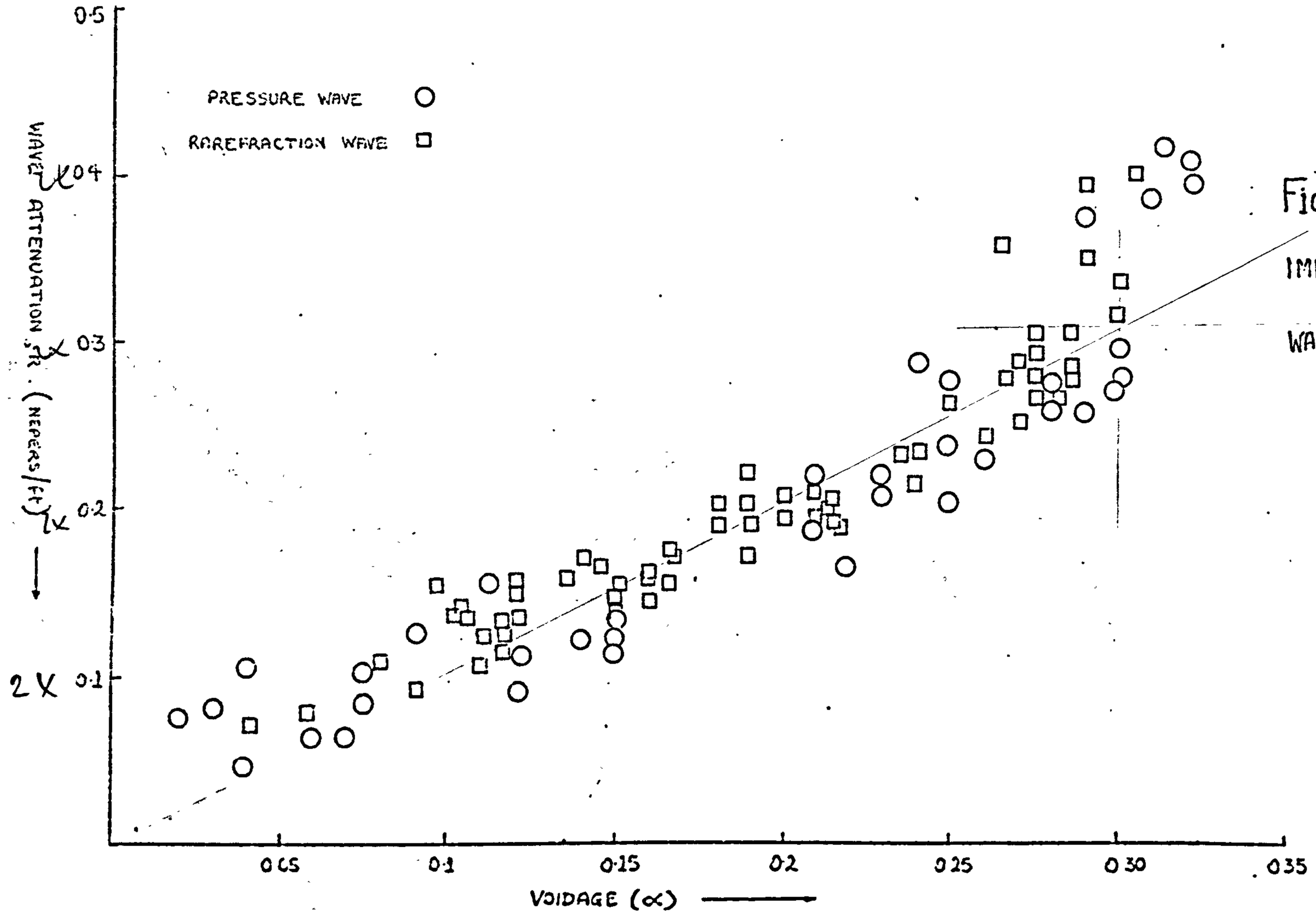

FIG. 24. ATTENUATION OF IMPULSE WAVES IN AIR/WATER MIXTURES ($P \approx 17$ P.S.I.)

FIG. 25·1. MECHANICAL MODEL OF A VISCO-ELASTIC MEDIUM (REF. 42)

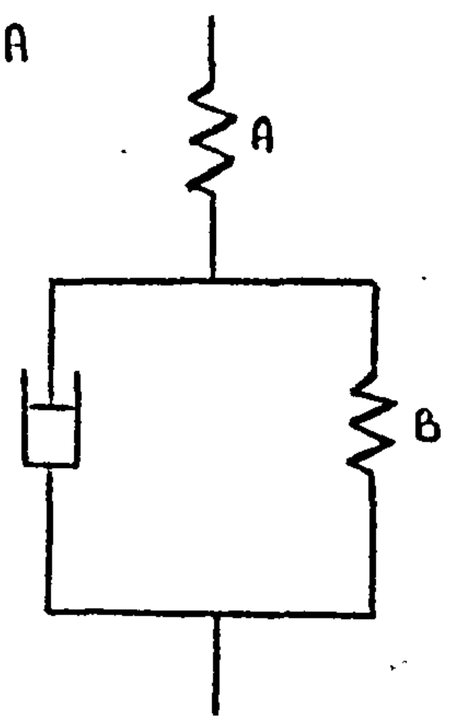

FIG. 25·2. SOLUTION OF ABOVE MECHANICAL MODEL

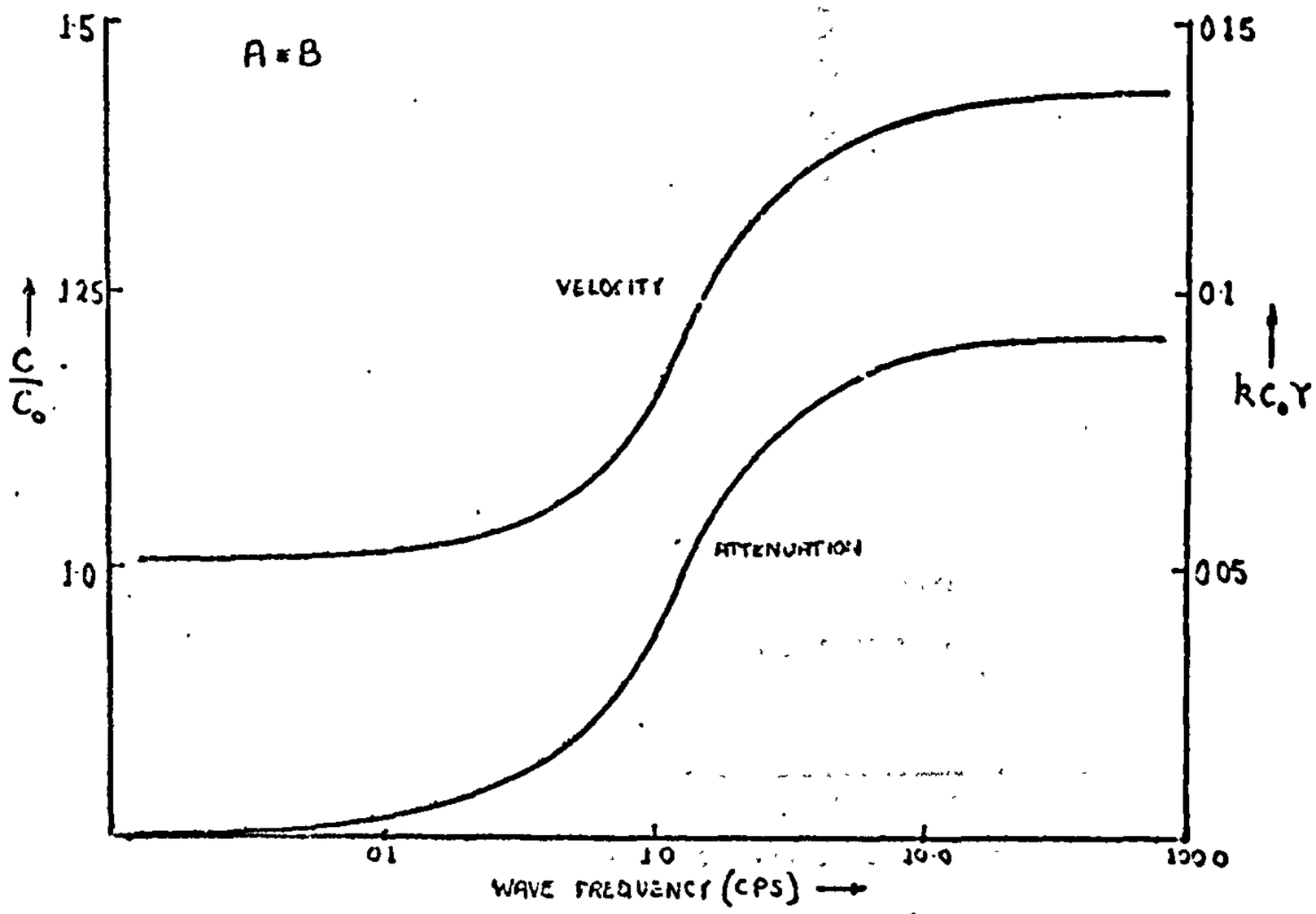

FIG. 25·3. PROPAGATION OF SINUSOIDAL WAVES IN A STEAM/WATER MEDIUM

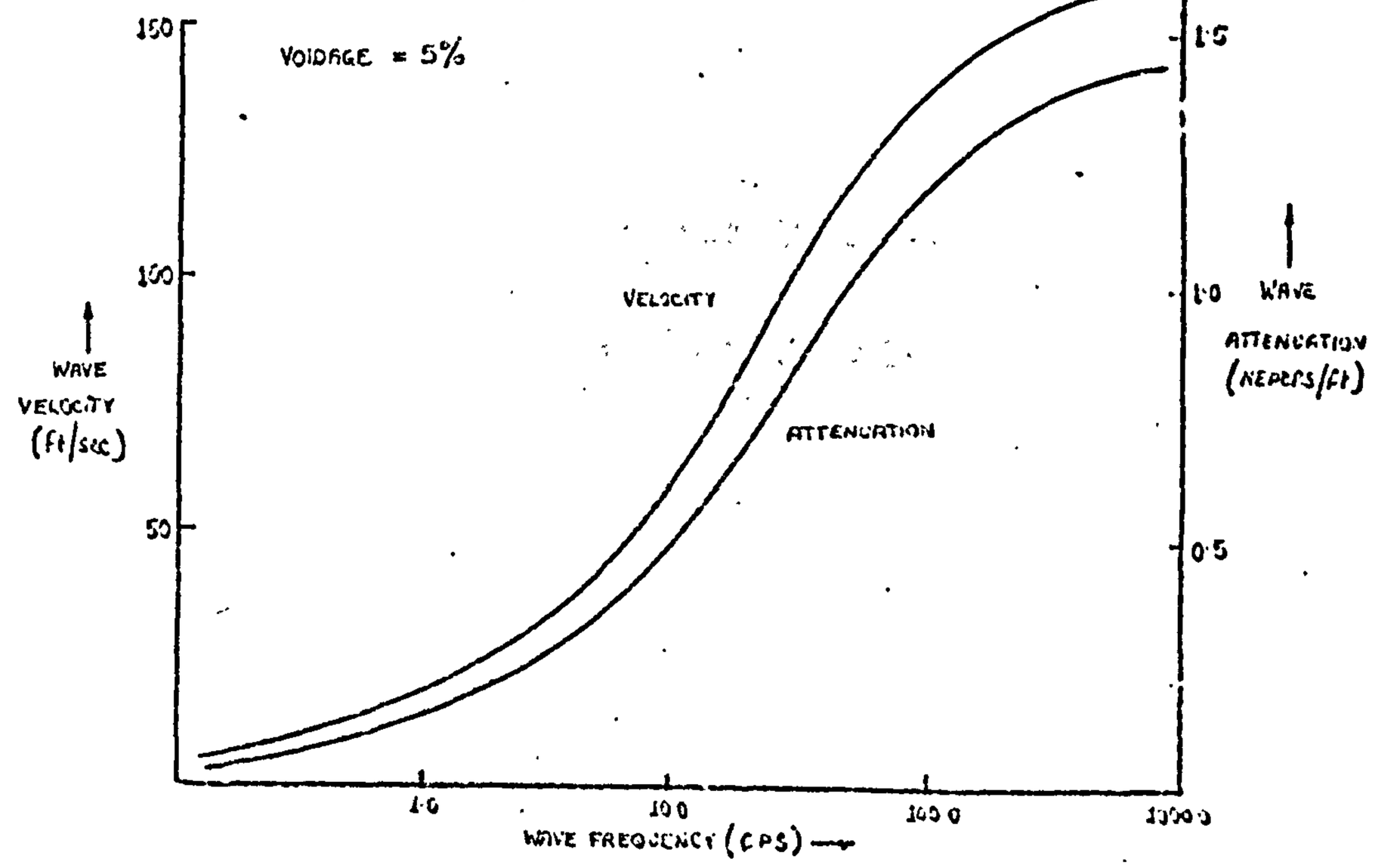

COMPARISON BETWEEN THE BEHAVIOR OF A STEAM/WATER MIXTURE AND A VISCO-ELASTIC MEDIUM

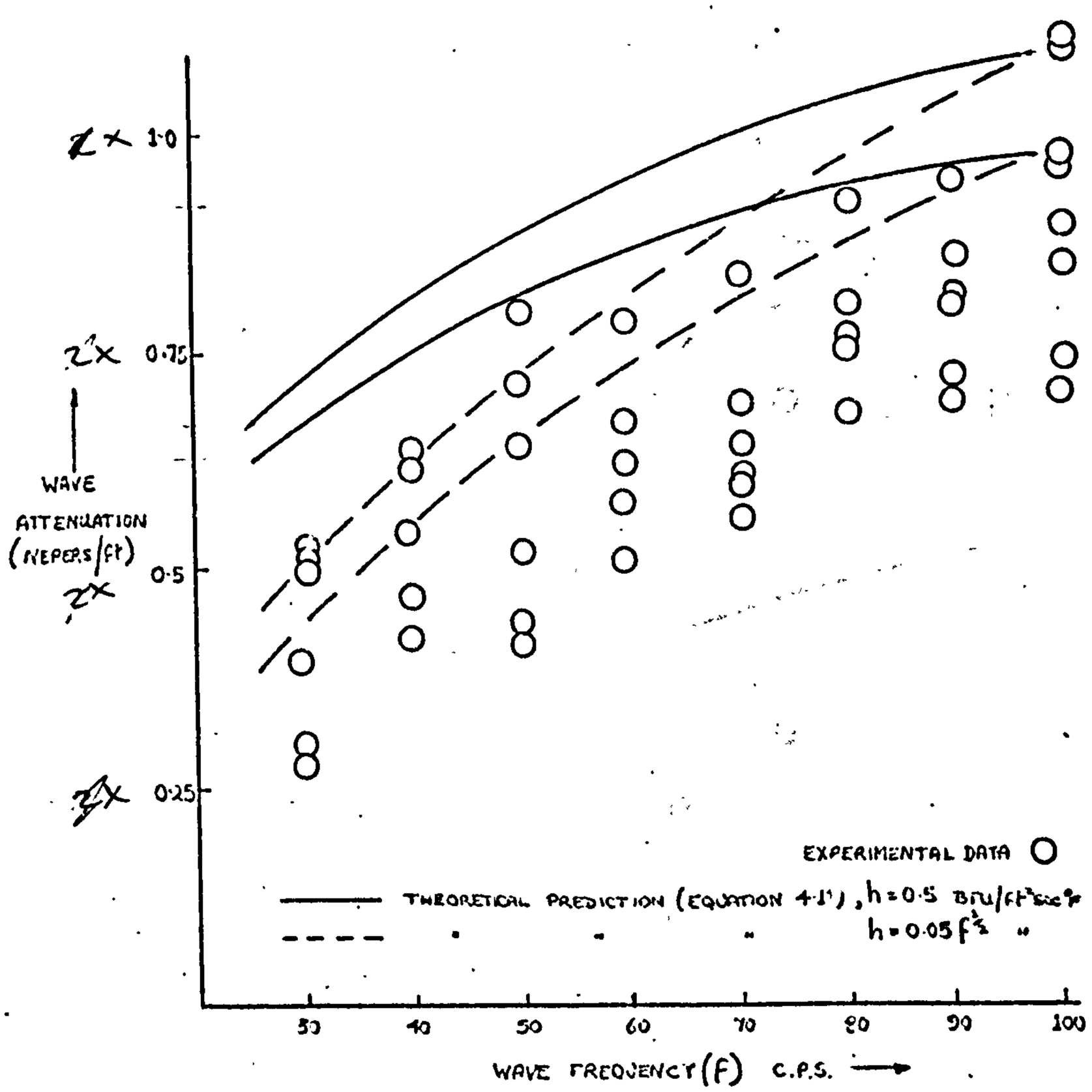

FIG. 26. ATTENUATION OF SINUSOIDAL WAVES IN A STEAM/WATER MIXTURE (VOIDAGE 2·5 → 3·5%)

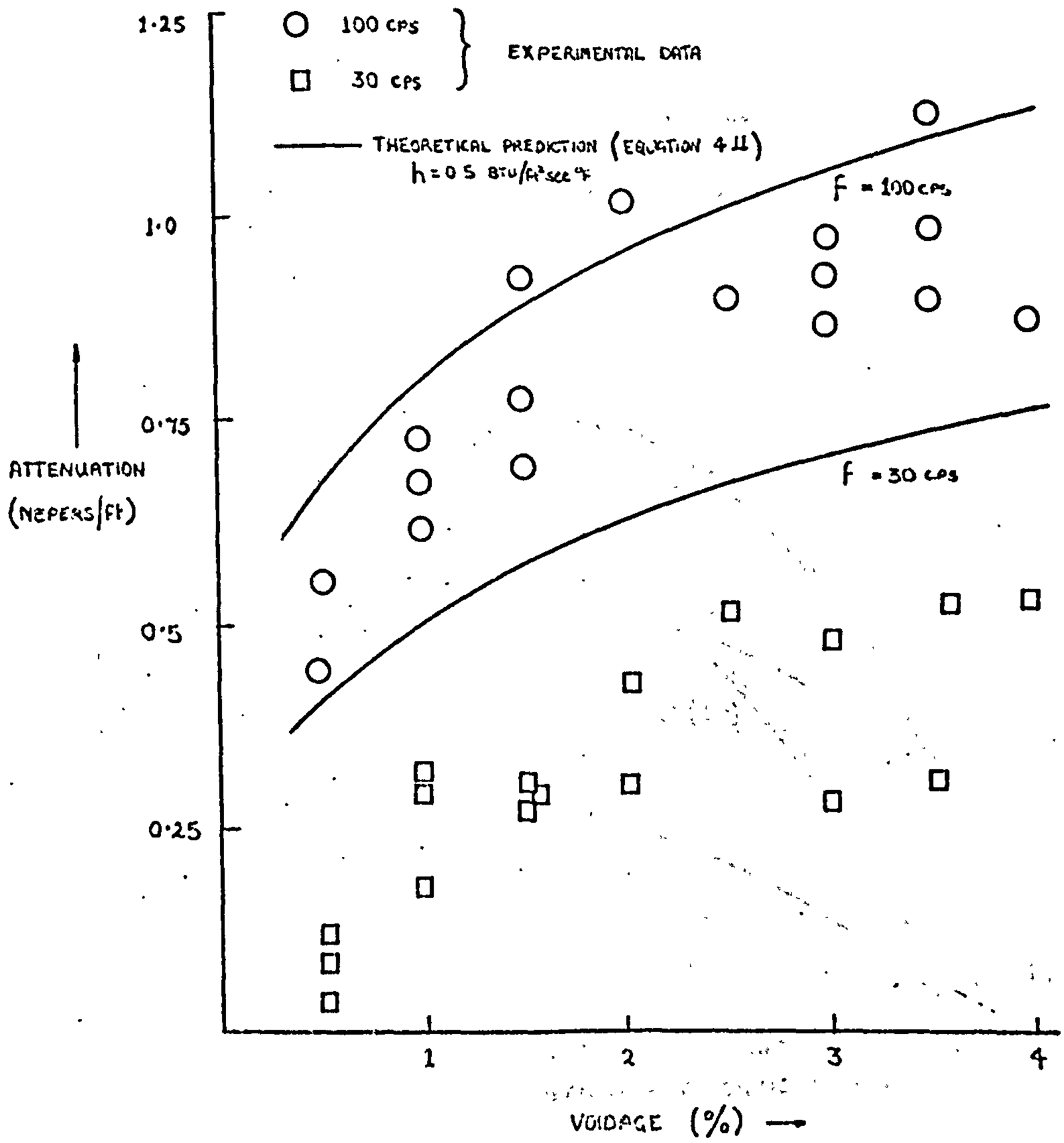

FIG. 27. ATTENUATION OF SINUSOIDAL PRESSURE WAVES IN A STEAM/WATER MIXTURE (P ≈ 14·7 p.s.i.)

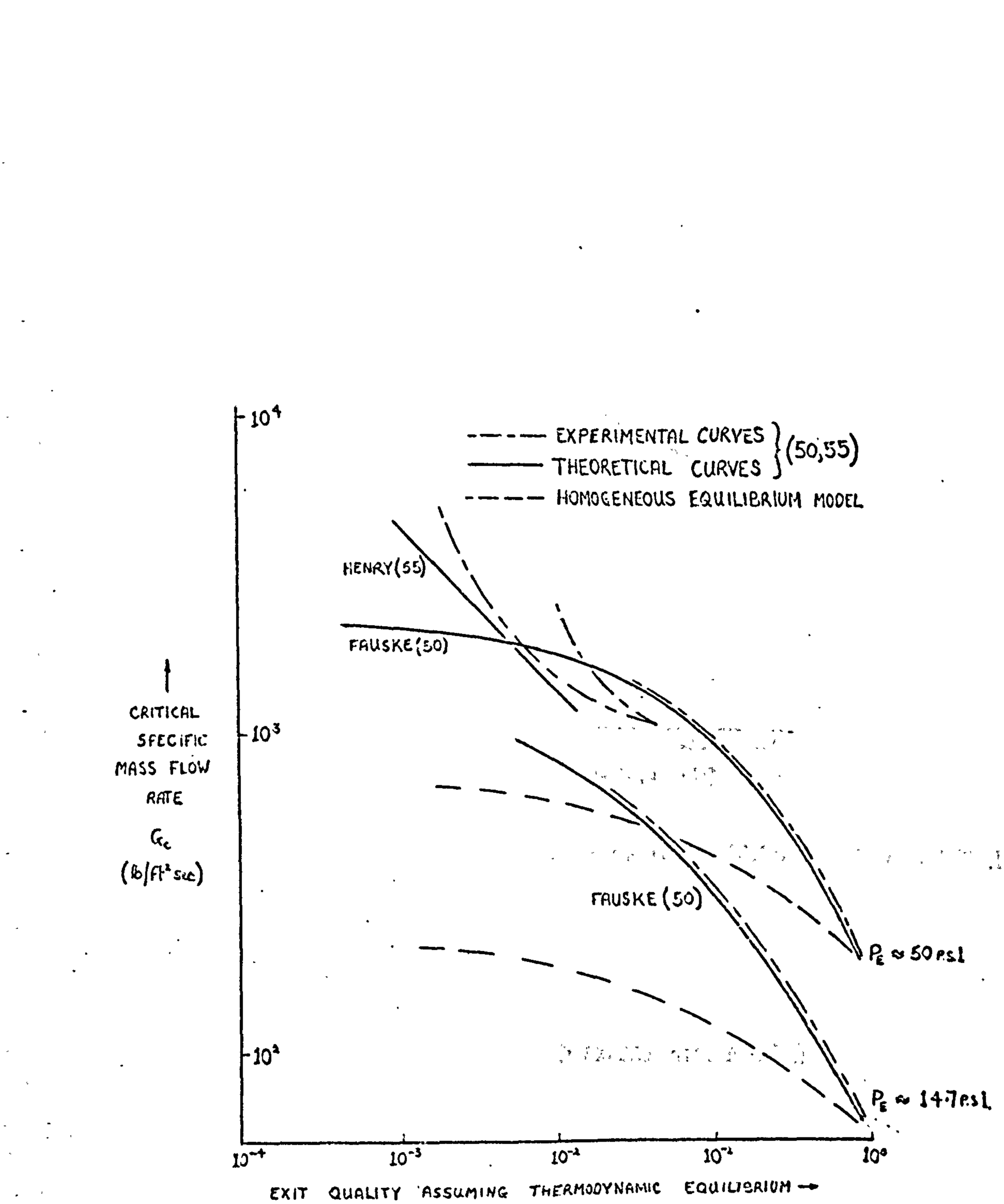

FIG. 28. CRITICAL FLOW CONDITIONS IN STEAM/WATER SYSTEMS

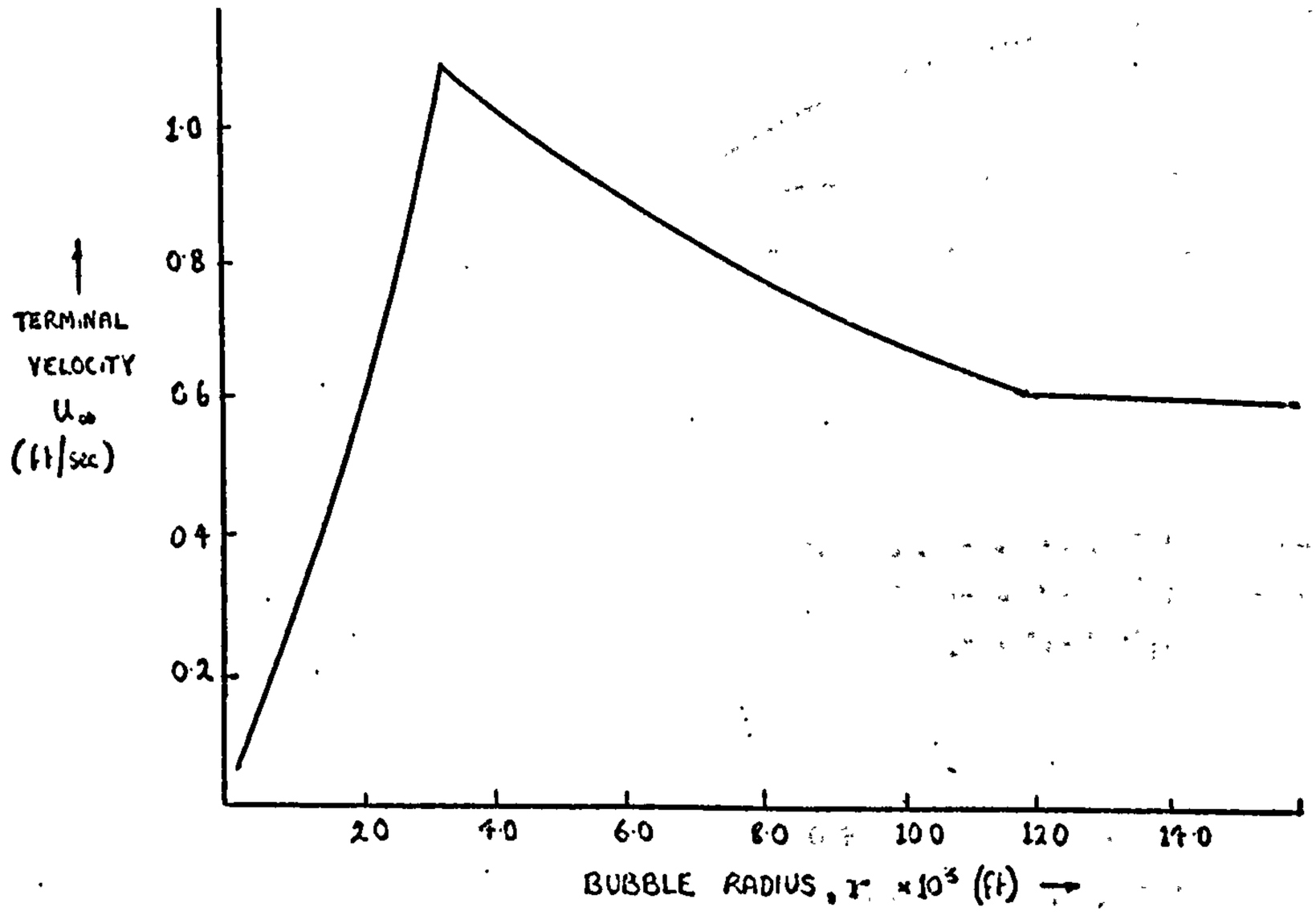

FIG. 29.1 TERMINAL VELOCITY OF AIR BUBBLES IN WATER (REF.61)

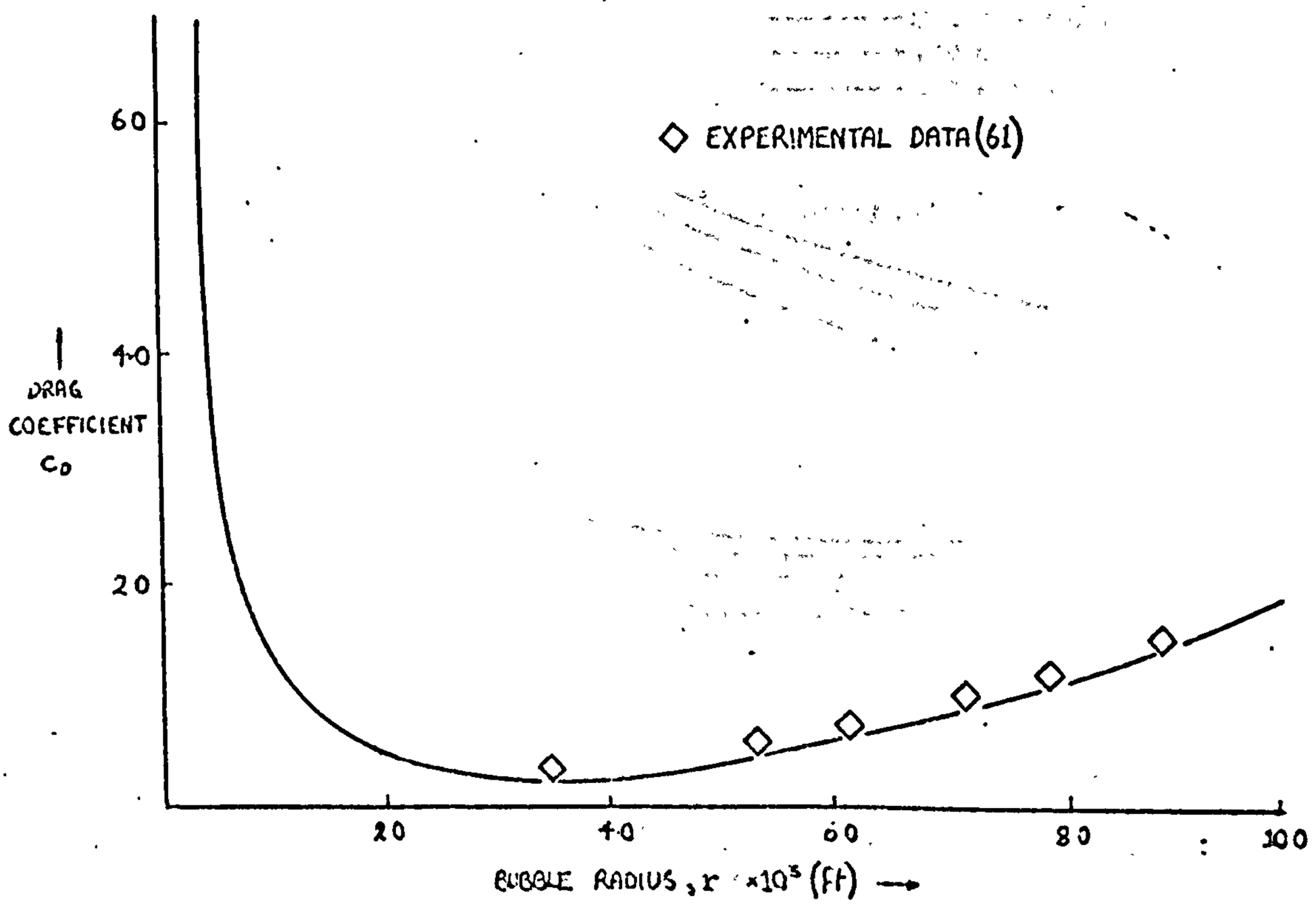

FIG. 29·2. DRAG COEFFICIENT OF AIR BUBBLES IN WATER

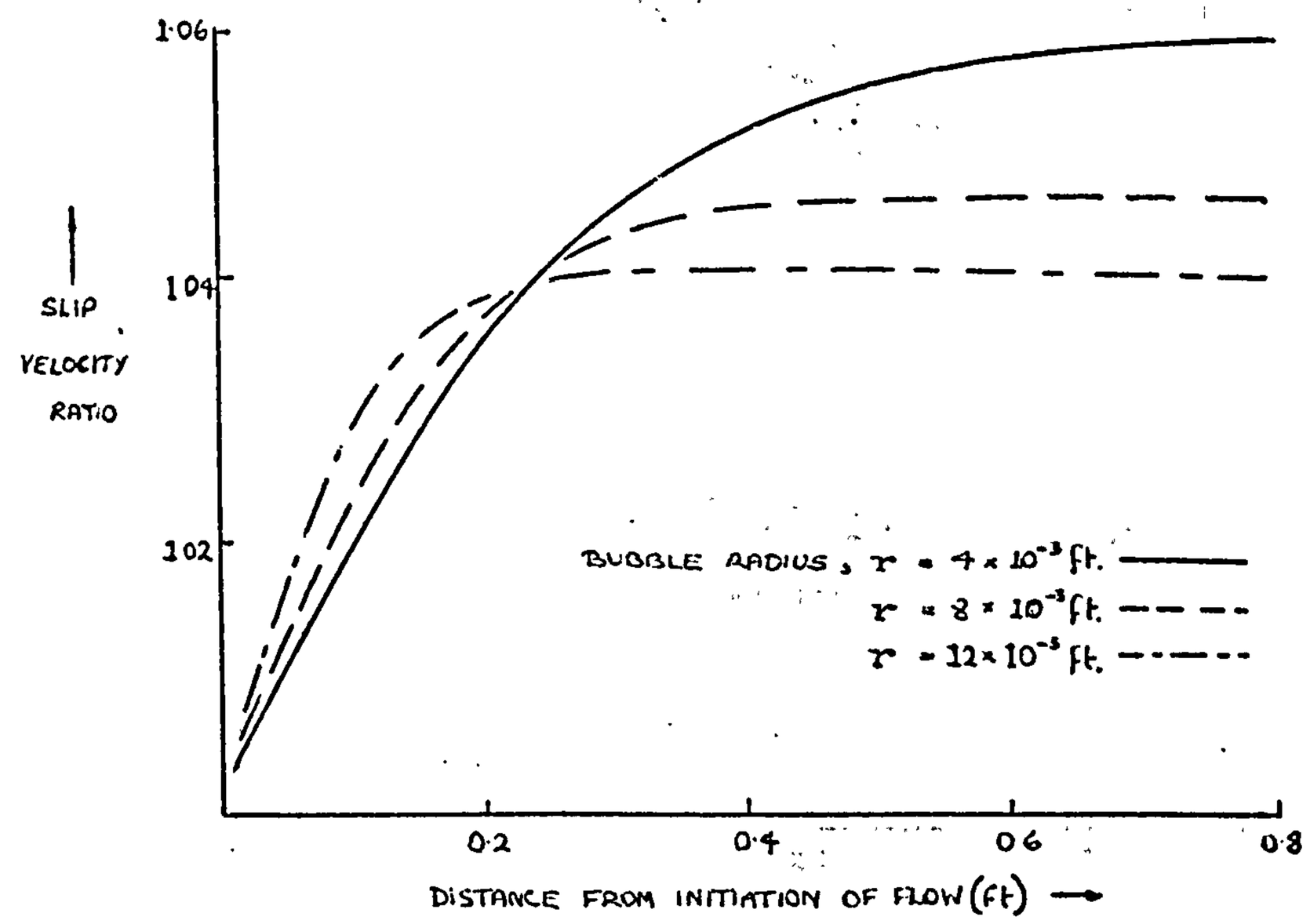

FIG. 30·1 VARIATION ALONG LENGTH OF A HOIZONTAL FLOW

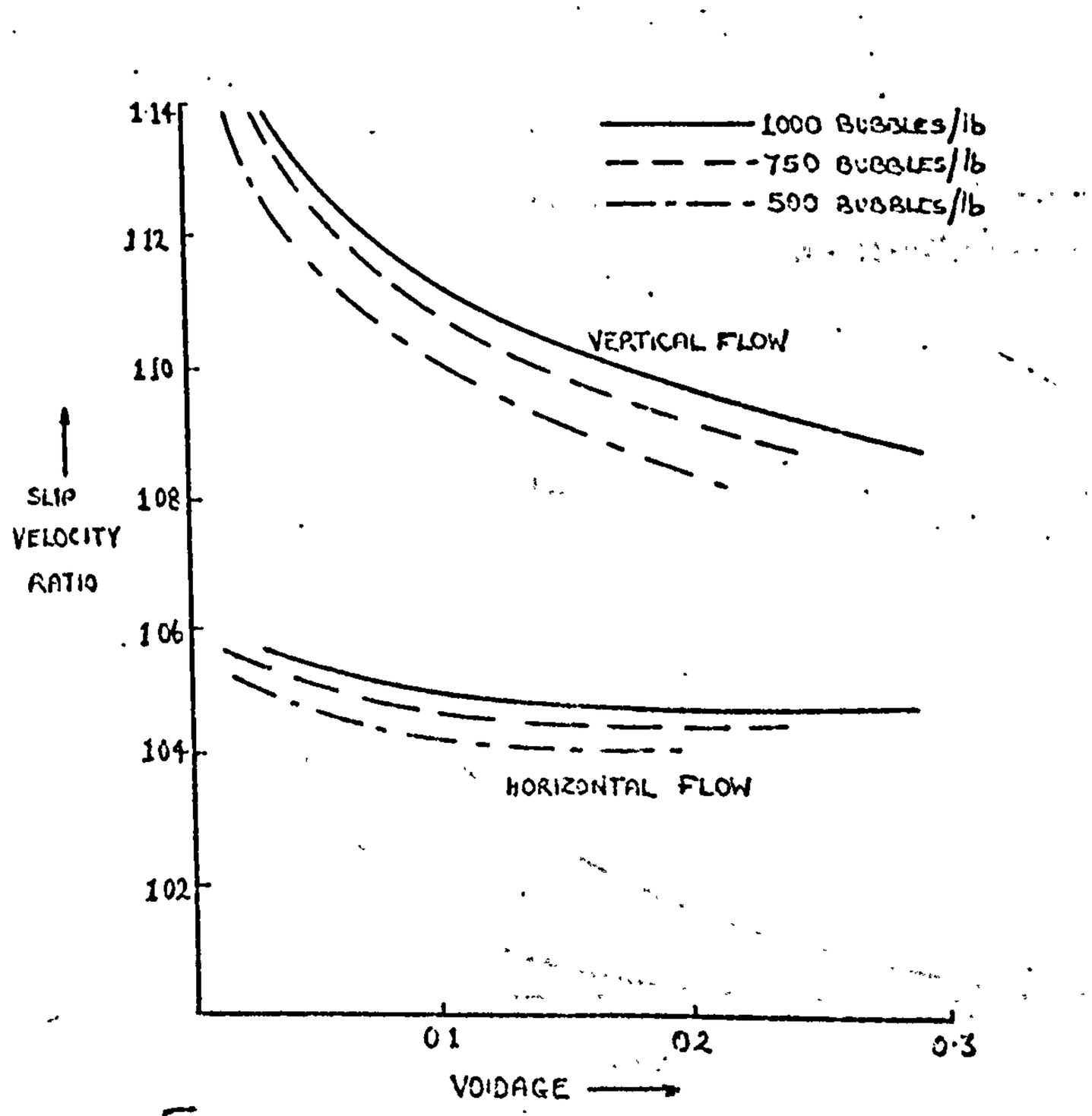

FIG. 30·2. VARIATION WITH VOIDAGE

THEORETICAL PREDICTIONS OF THE SLIP VELOCITY RATIO IN AN AIR/WATER BUBBLY FLOW ($G = 600$ lb/ft²sec, $P = 35{\cdot}7$ p.s.i.)

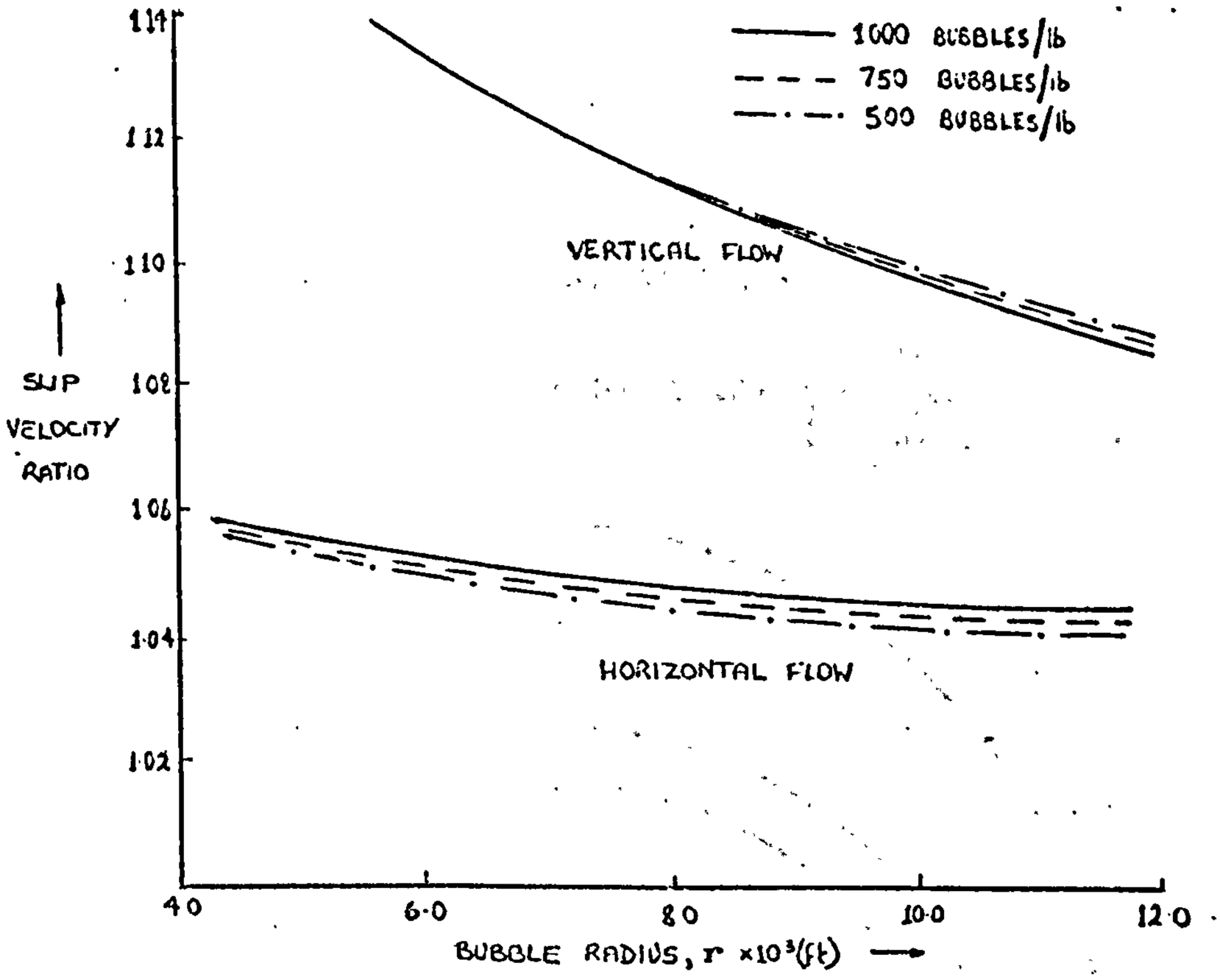

FIG. 30·3. VARIATION WITH BUBBLE SIZE

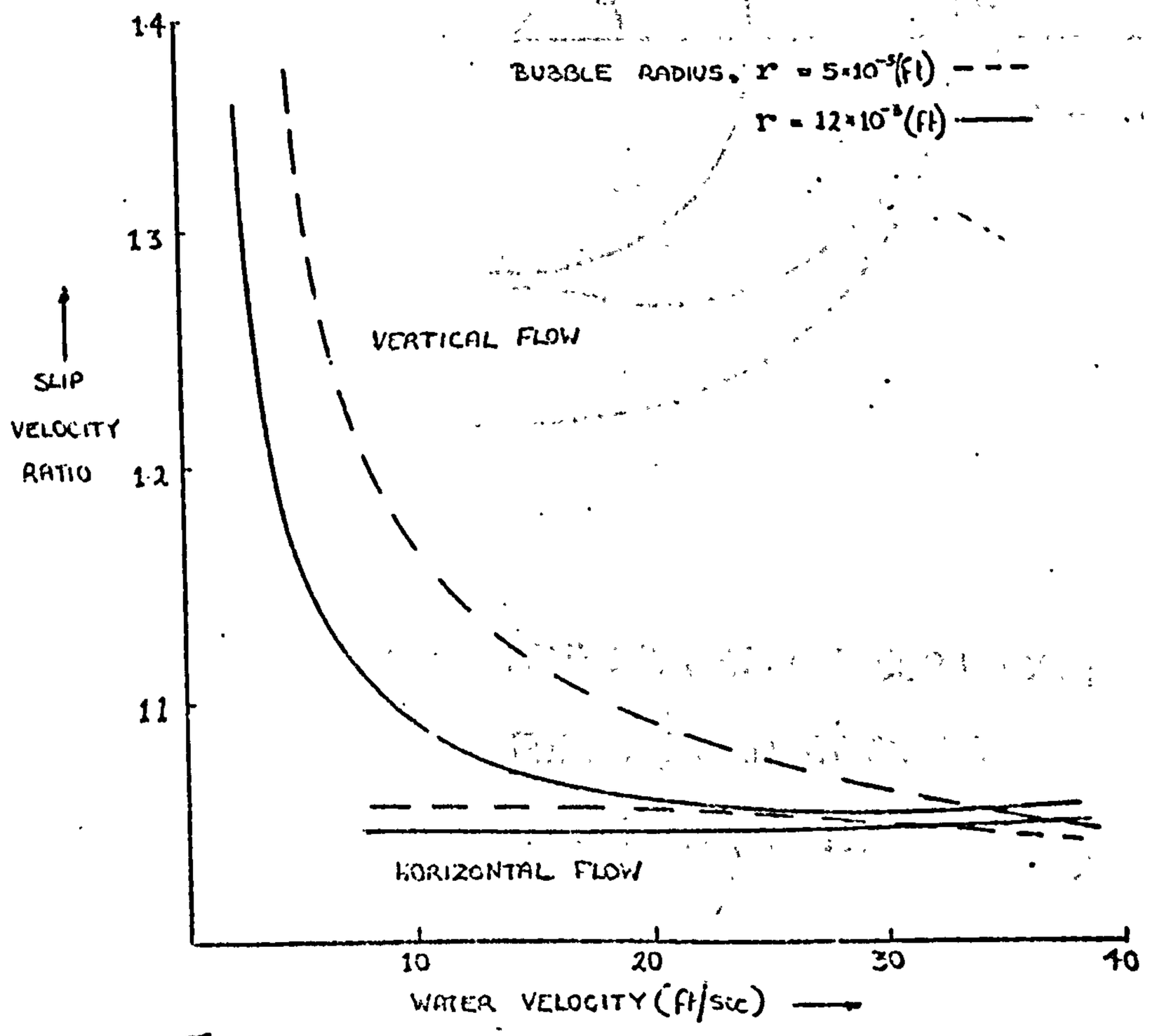

FIG. 30·4. VARIATION WITH LIQUID VELOCITY

THEORETICAL PREDICTIONS OF THE SLIP VELOCITY RATIO IN AN AIR/WATER FLOW (P = 14·7 p.s.i)

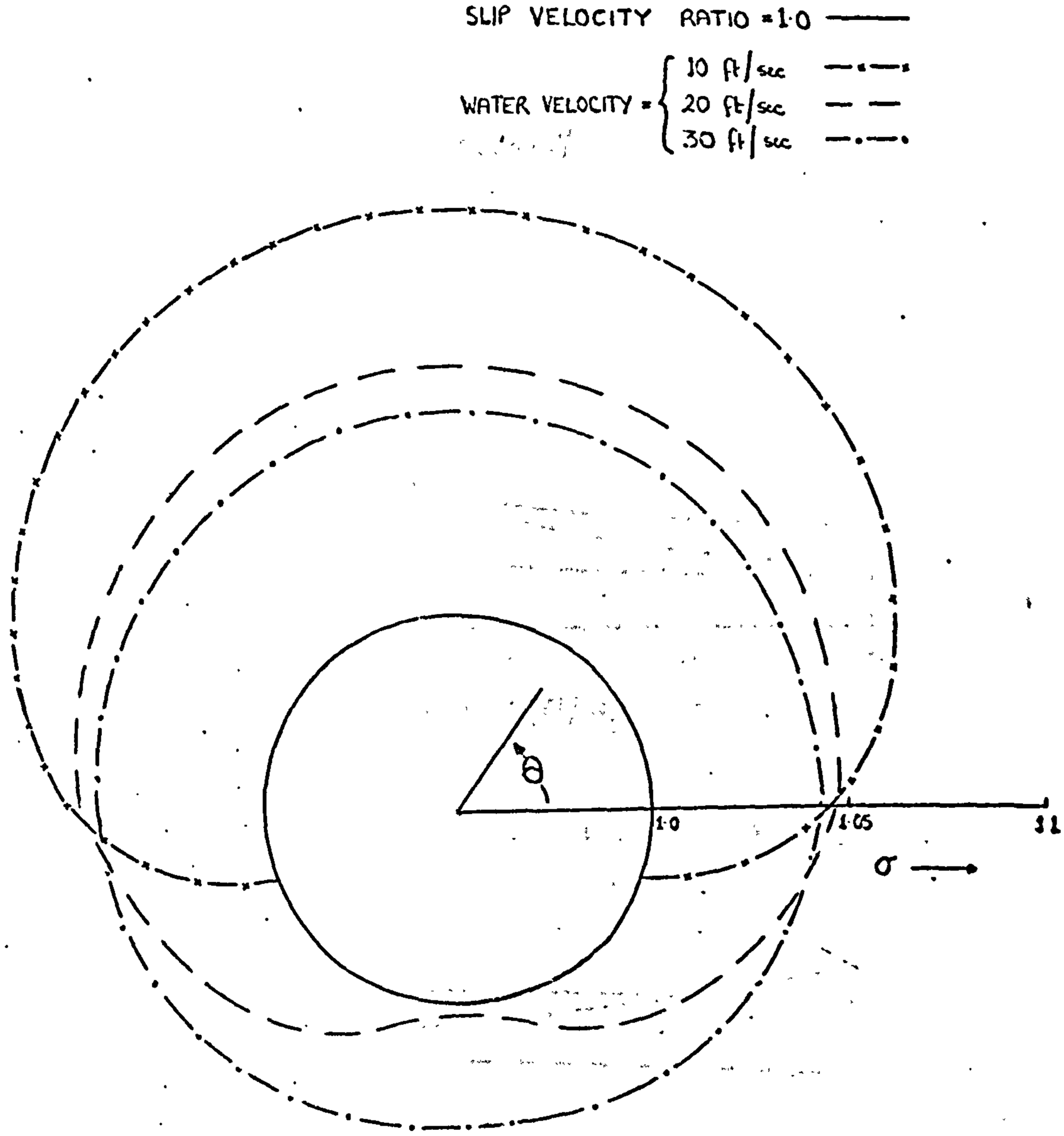

FIG. 31. THEORETICAL PREDICTION OF THE SLIP VELOCITY RATIO IN AN AIR/WATER FLOW INCLINED AT AN ANGLE OF θ TO THE HORIZONTAL ($r = 9 \times 10^{-3}$ Ft, N = 1000 BUBBLES/lb)

FIG 32·1

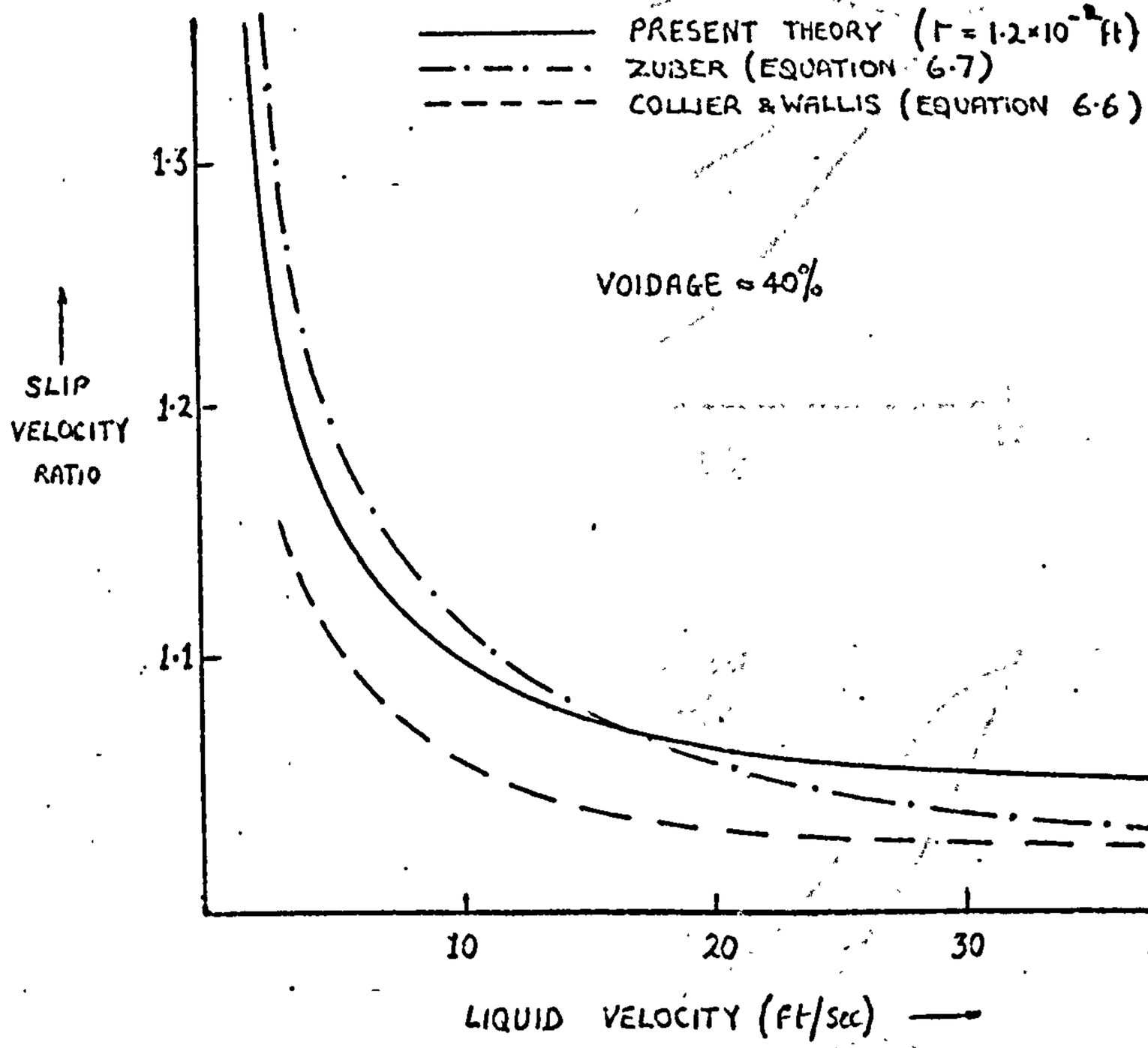

FIG. 32·2

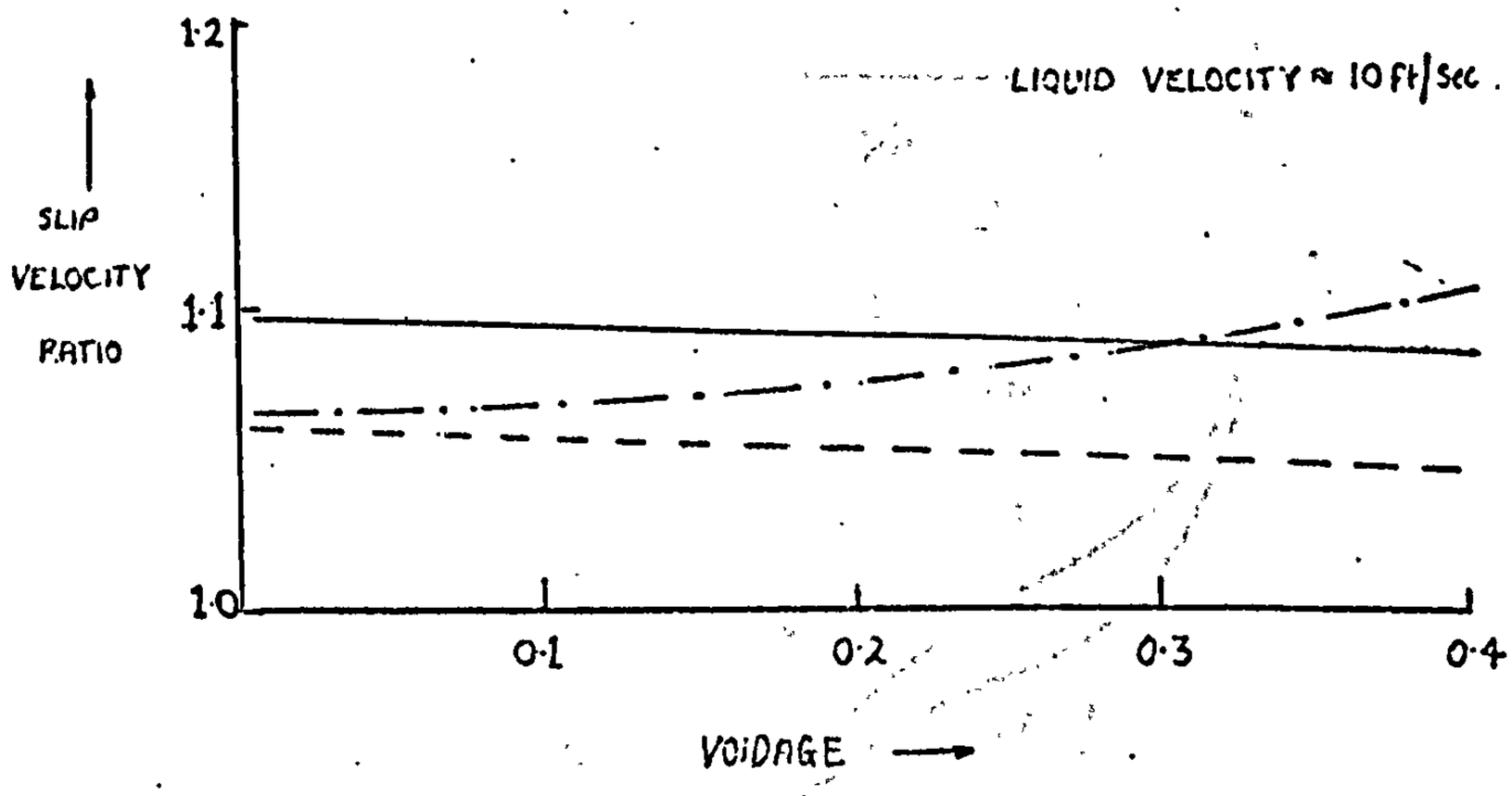

FIG. 32. 'LOCAL' SLIP VELOCITY RATIO IN A VERTICAL AIR/WATER FLOW (COMPARISON WITH THE THEORIES OF ZUBER[68] AND COLLIER & WALLIS[11])

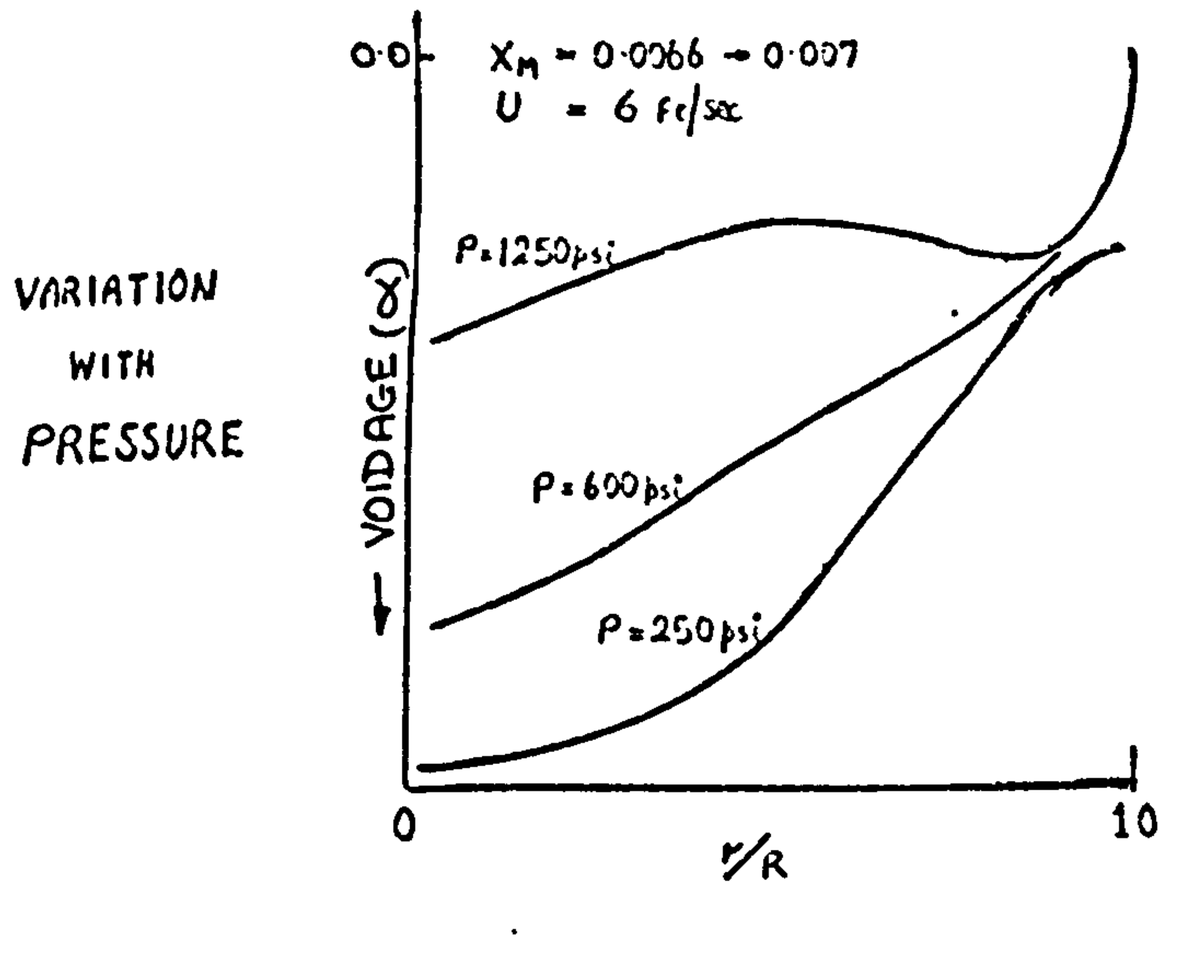

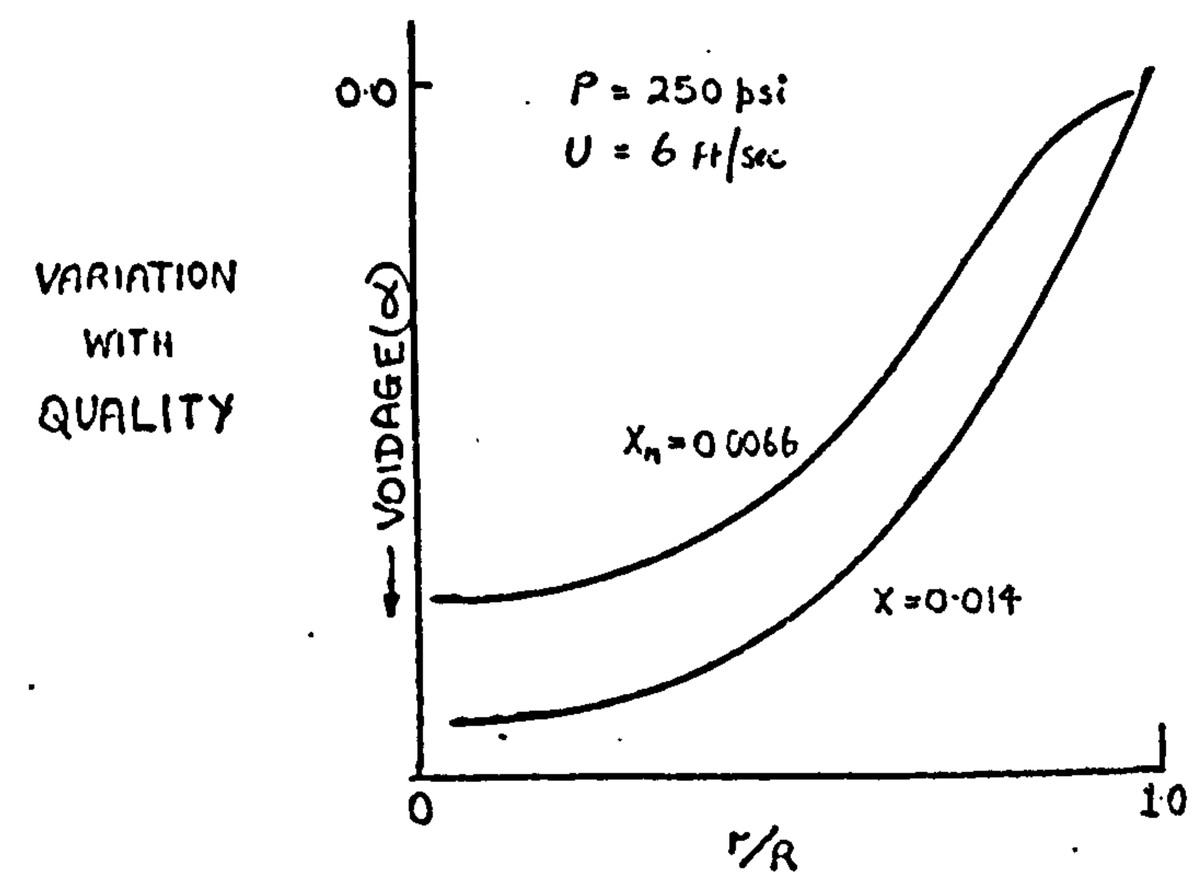

FIG. 33. VOIDAGE PROFILES IN VERTICAL STEAM/WATER FLOW (REF. 60)

FIG. 34. COMPARISON BETWEEN THEORETICAL PREDICTION AND EXPERIMENTAL MEASUREMENT (REF. 25) OF SLIP VELOCITY RATIO IN AIR/WATER BUBBLY FLOWS

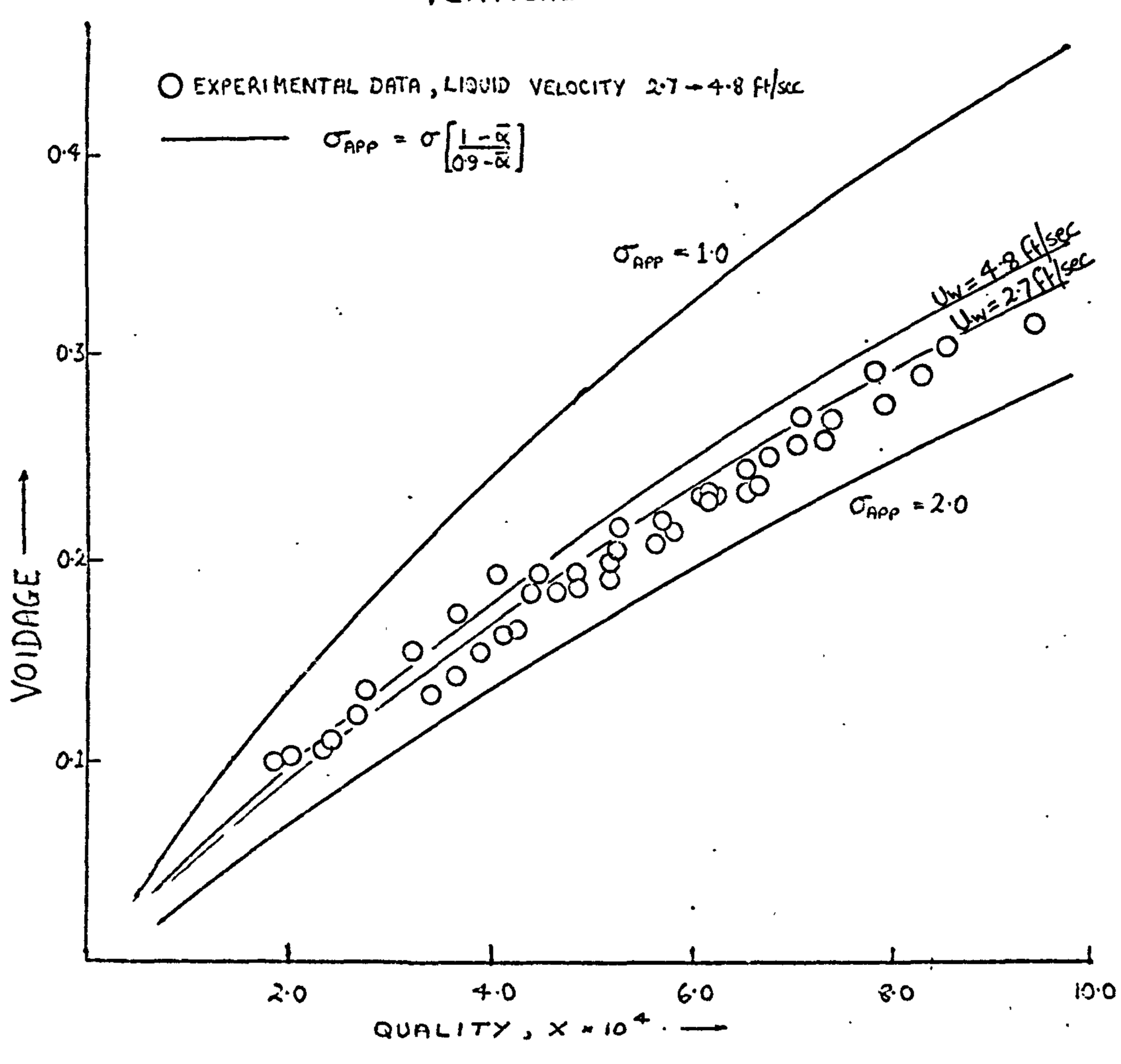

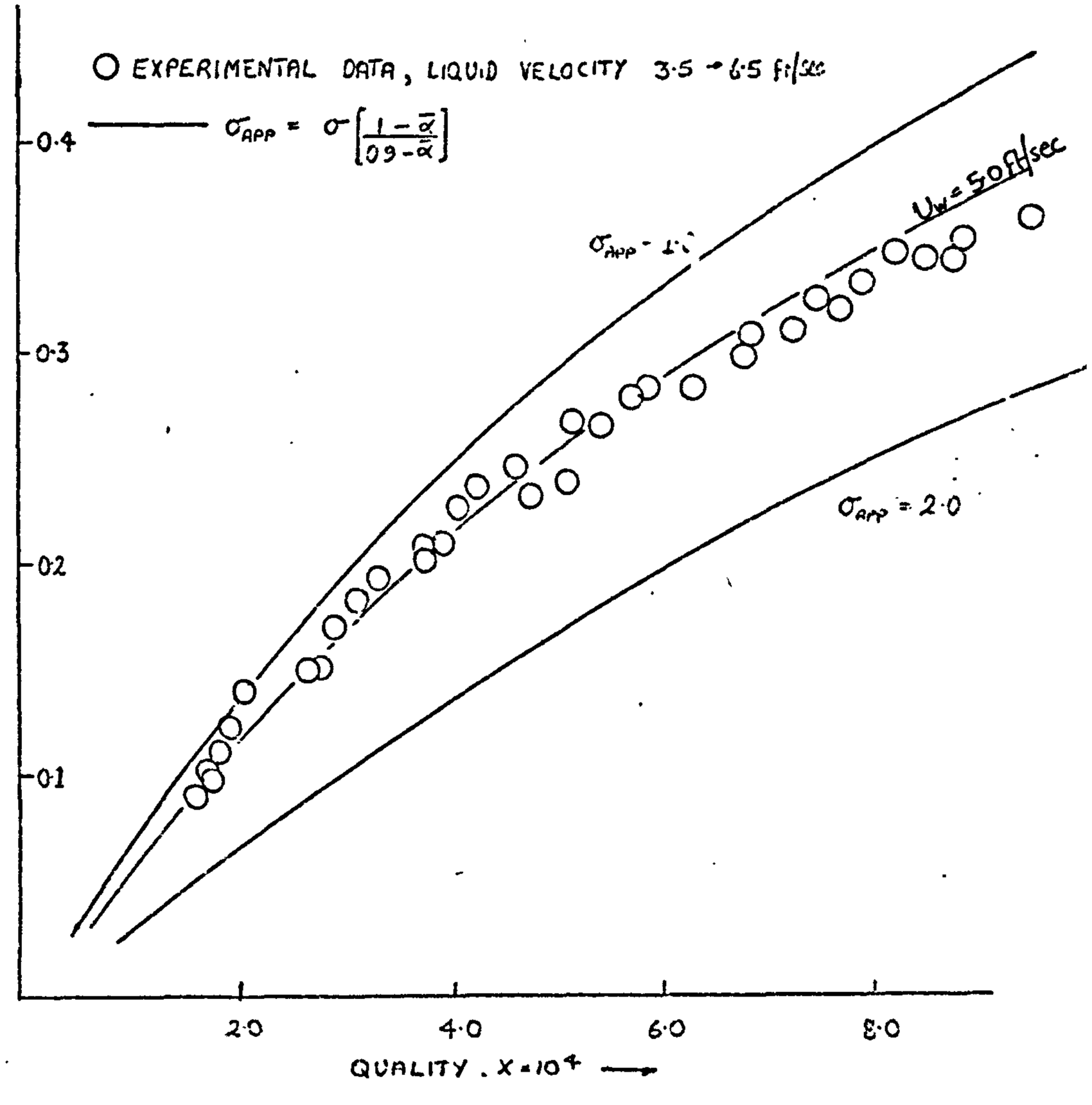

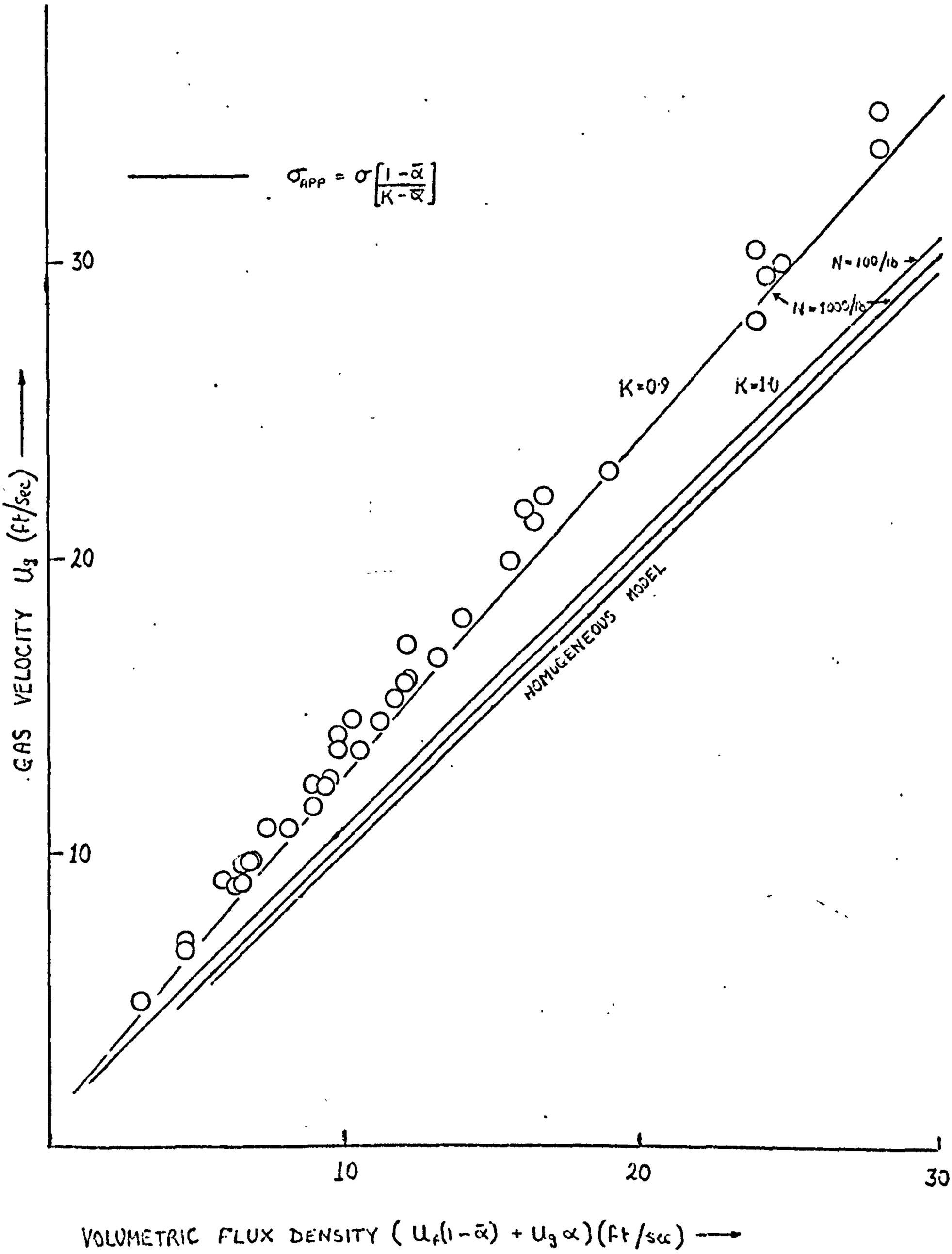

FIG. 35. COMPARISON BETWEEN THEORETICAL PREDICTIONS AND EXPERIMENTAL MEASURMENTS (REF. 68) OF THE SLIP VELOCITY RATIO IN A VERTICAL AIR/WATER FLOW

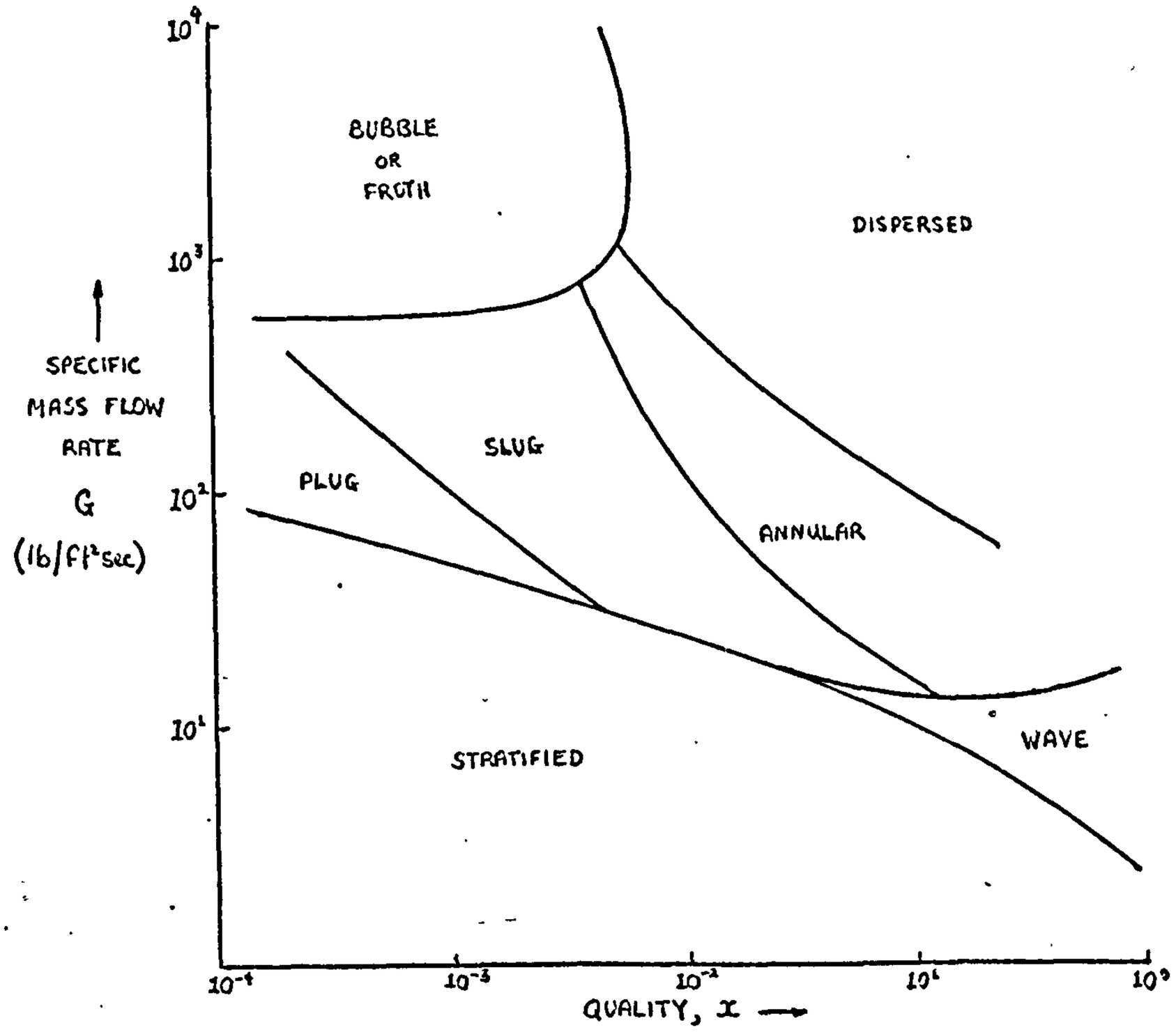

FIG. 36·1 FLOW REGIME MAP FOR HORIZONTAL STEAM/WATER FLOW ACCORDING TO BAKER (73) (P = 14·7 P.S.I.)

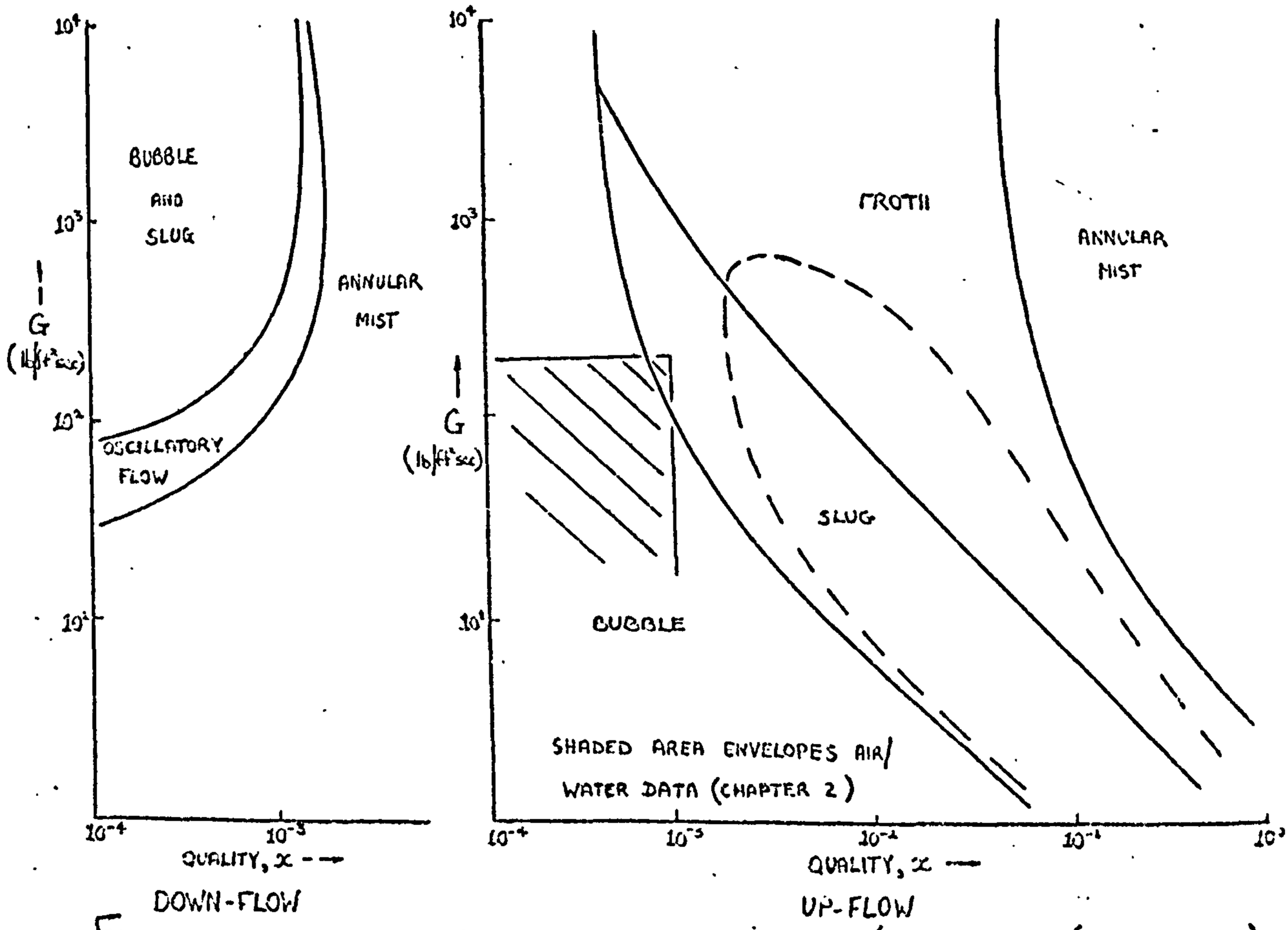

FIG. 36·2. FLOW REGIME MAPS FOR VERTICAL AIR/WATER FLOW (P = 14·7 P.S.I.) ACCORDING TO GOLAN AND STENNING (74) ——— ; GRIFFITHS AND WALLIS (75) - - - -.

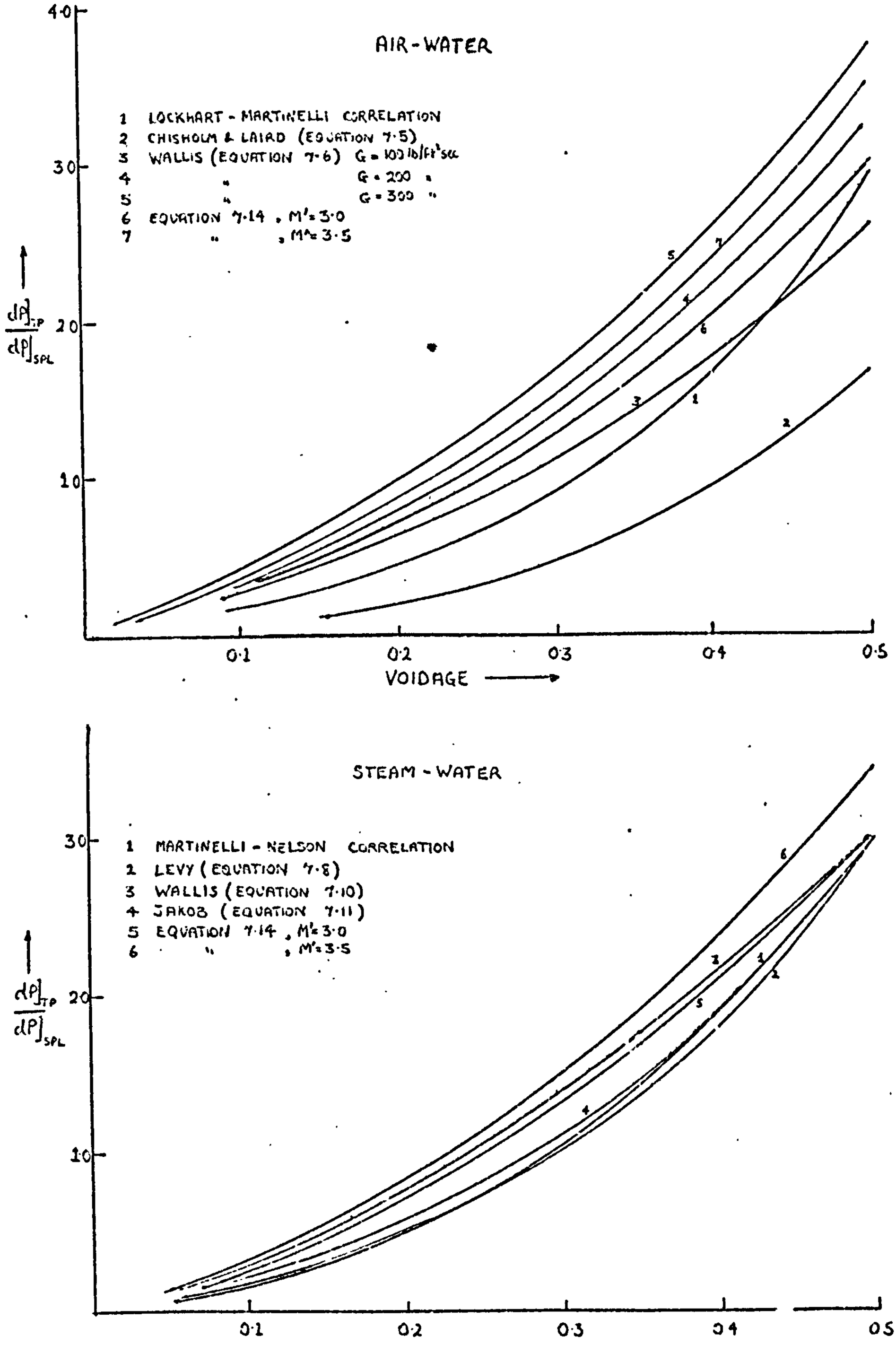

FIG. 37. THEORETICAL PREDICTIONS FOR THE TWO-PHASE FRICTIONAL PRESSURE DROP IN A CYLINDRICAL PIPE

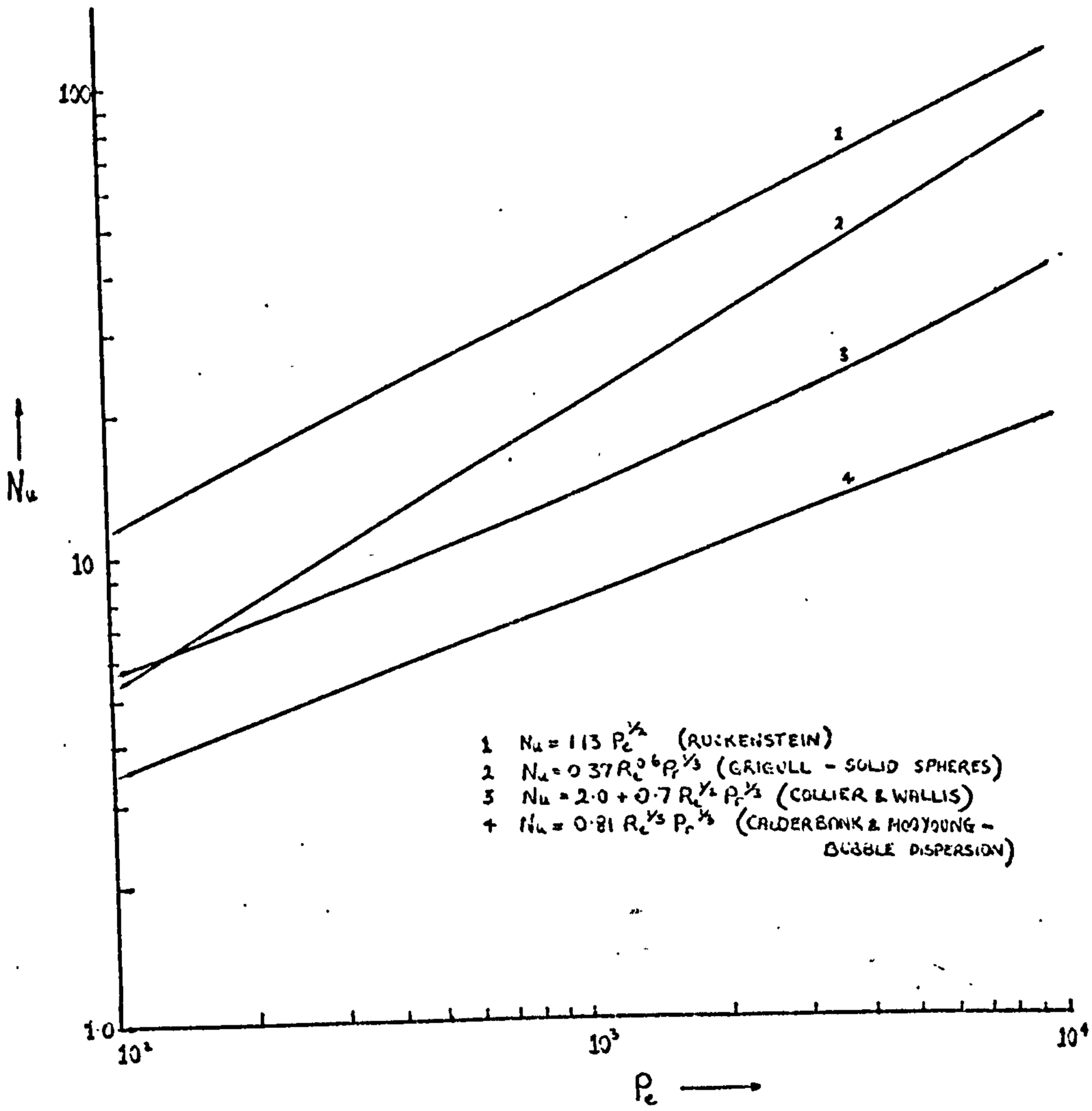

FIG. 38. EMPIRICAL FORMULAE YIELDING A MEASURE OF THE HEAT TRANSFER COEFFICIENT AT THE SURFACE OF A SPHERICAL BODY IN A LIQUID

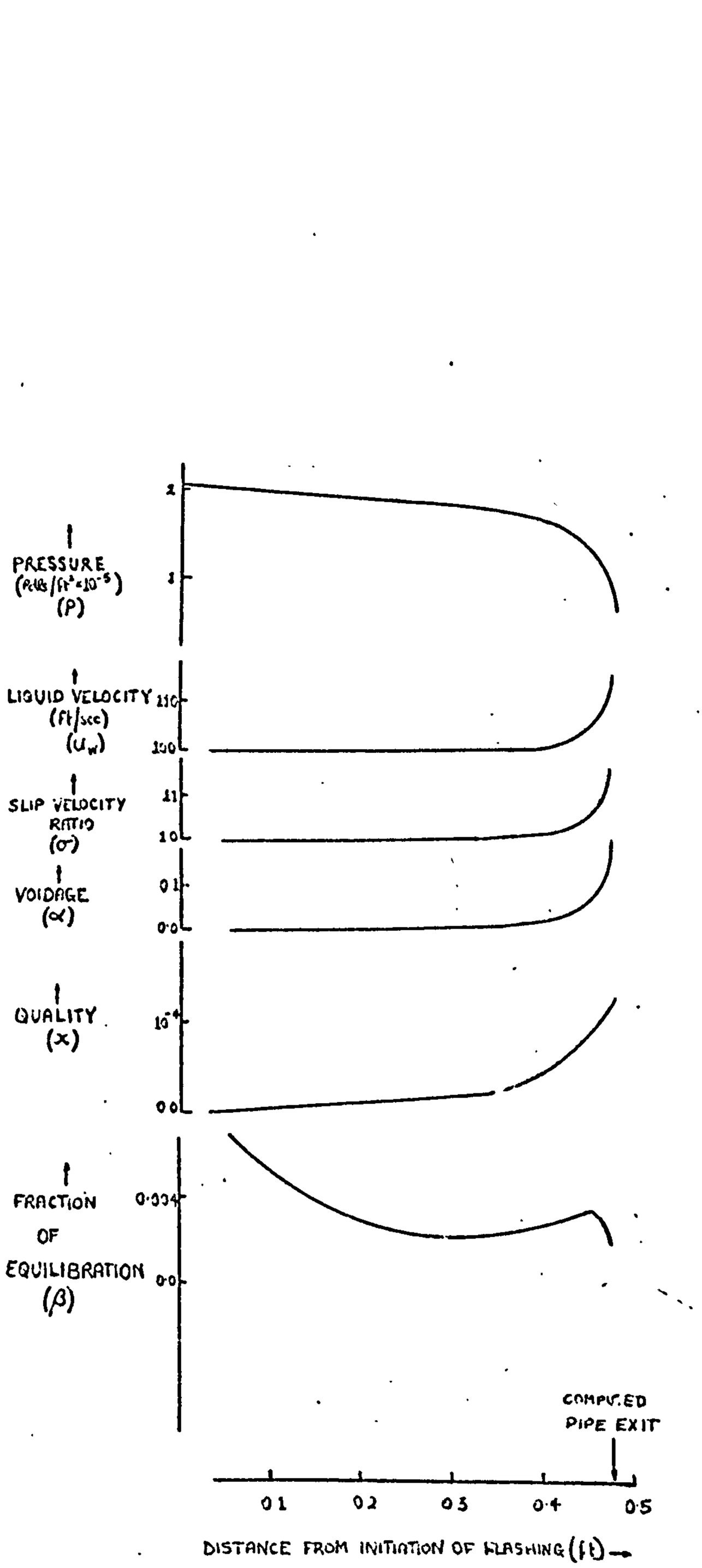

FIG. 39. AXIAL PROFILES OF FLOW PROPERTIES IN A 10% QUALITY STEAM/WATER CRITICAL FLOW ($G = 6000$ lb/ft².sec., $P_s = 3{\cdot}0$ A.T.)

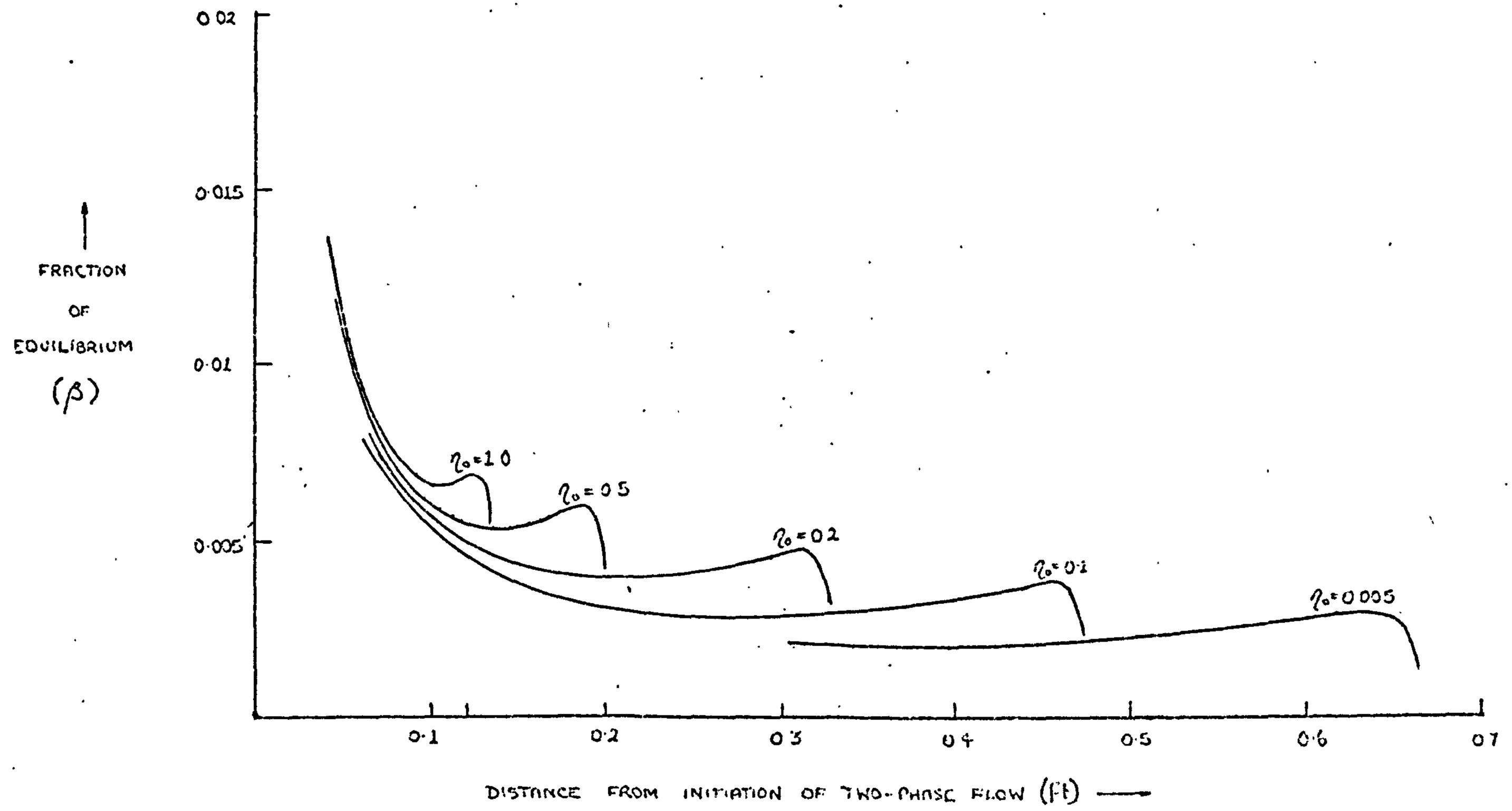

FIG. 40. VARIATION OF THE FRACTION OF EQUILIBRATION AXIAL PROFILE WITH η_0 [BTU/Ft²sec.½°F.]
($G = 6000$ lb/Ft²sec. ; $P_I = 3{\cdot}0$ Ata.)

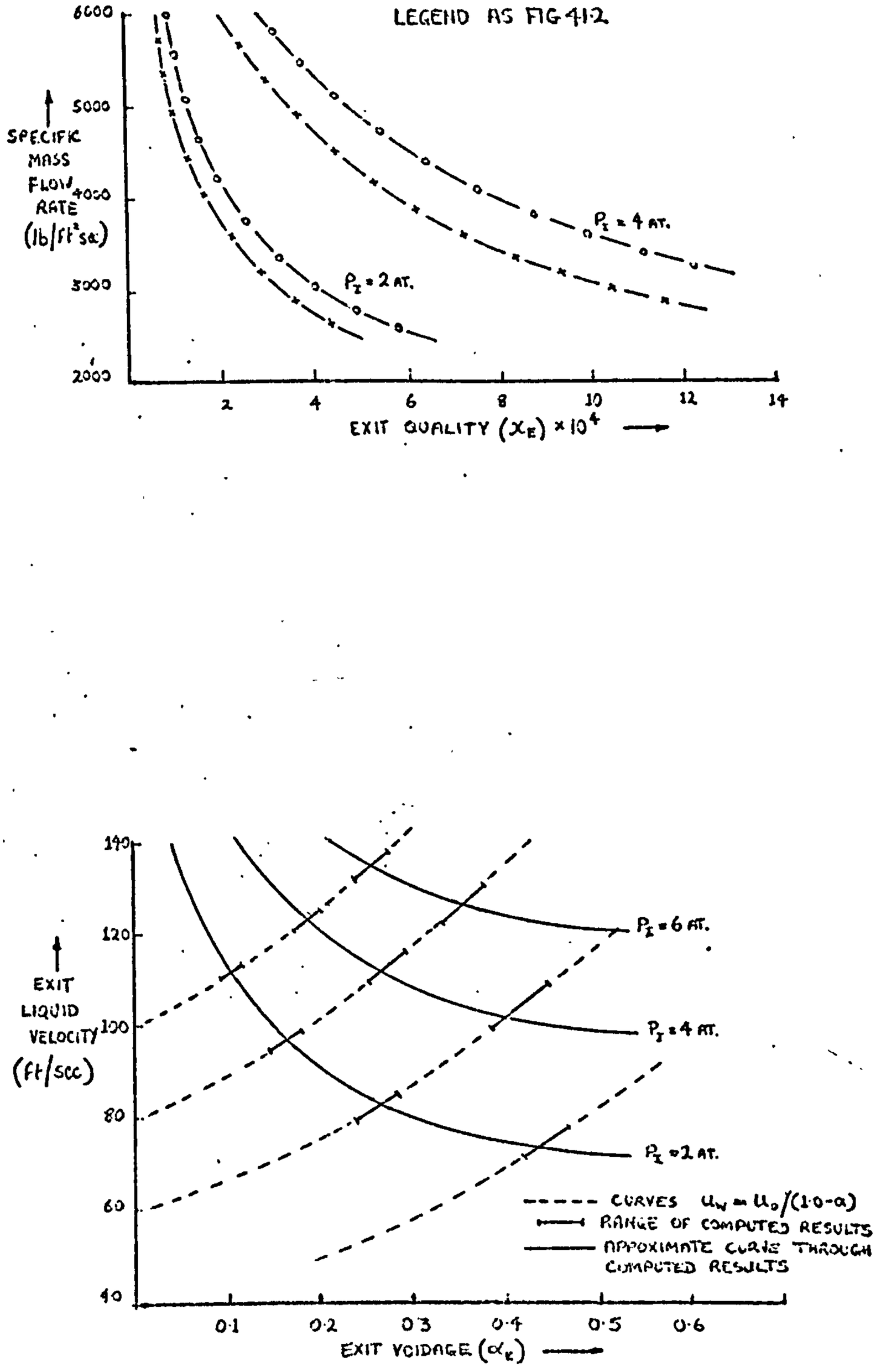

FIG. 41·1. VARIATION OF CRITICAL FLOW RESULTS WITH THE PARAMETERS F/D, η_0, N

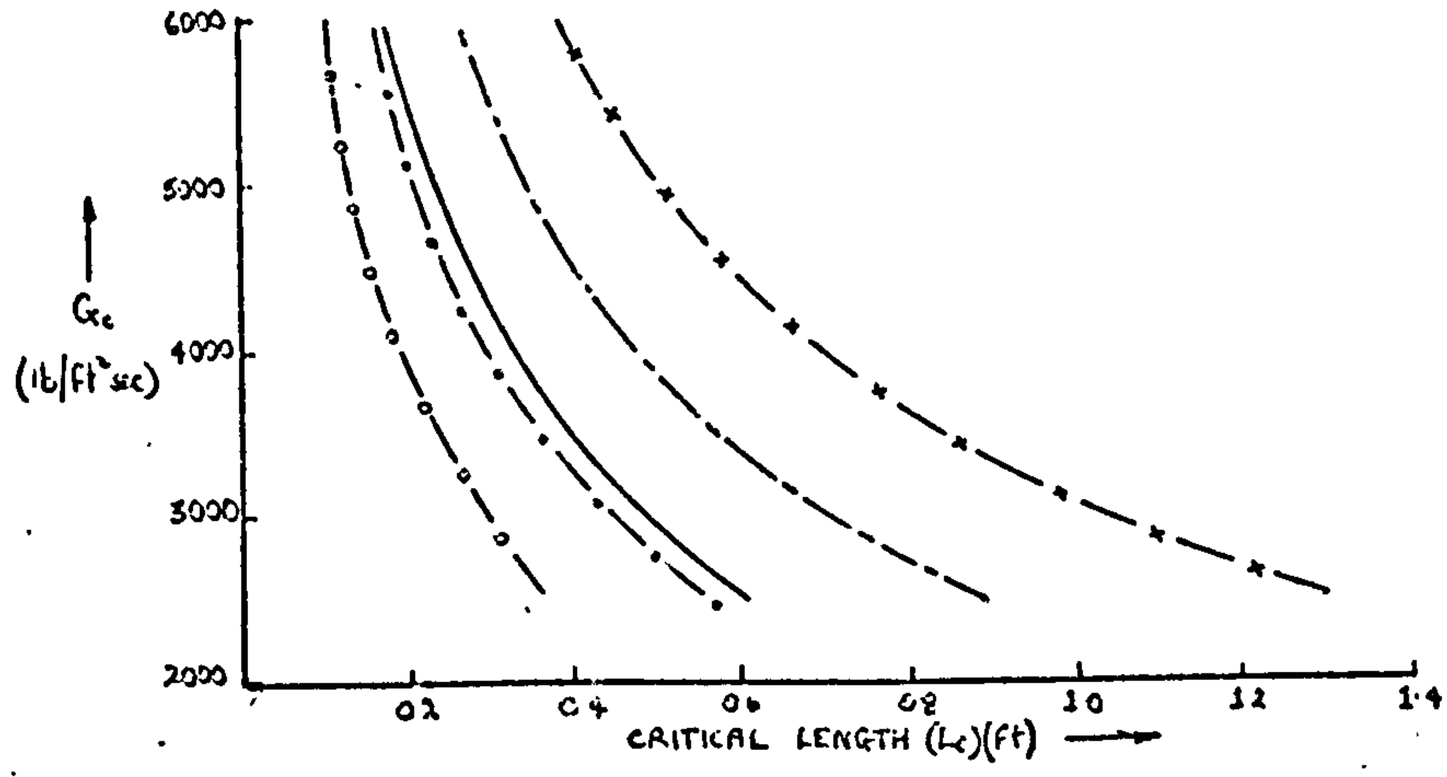

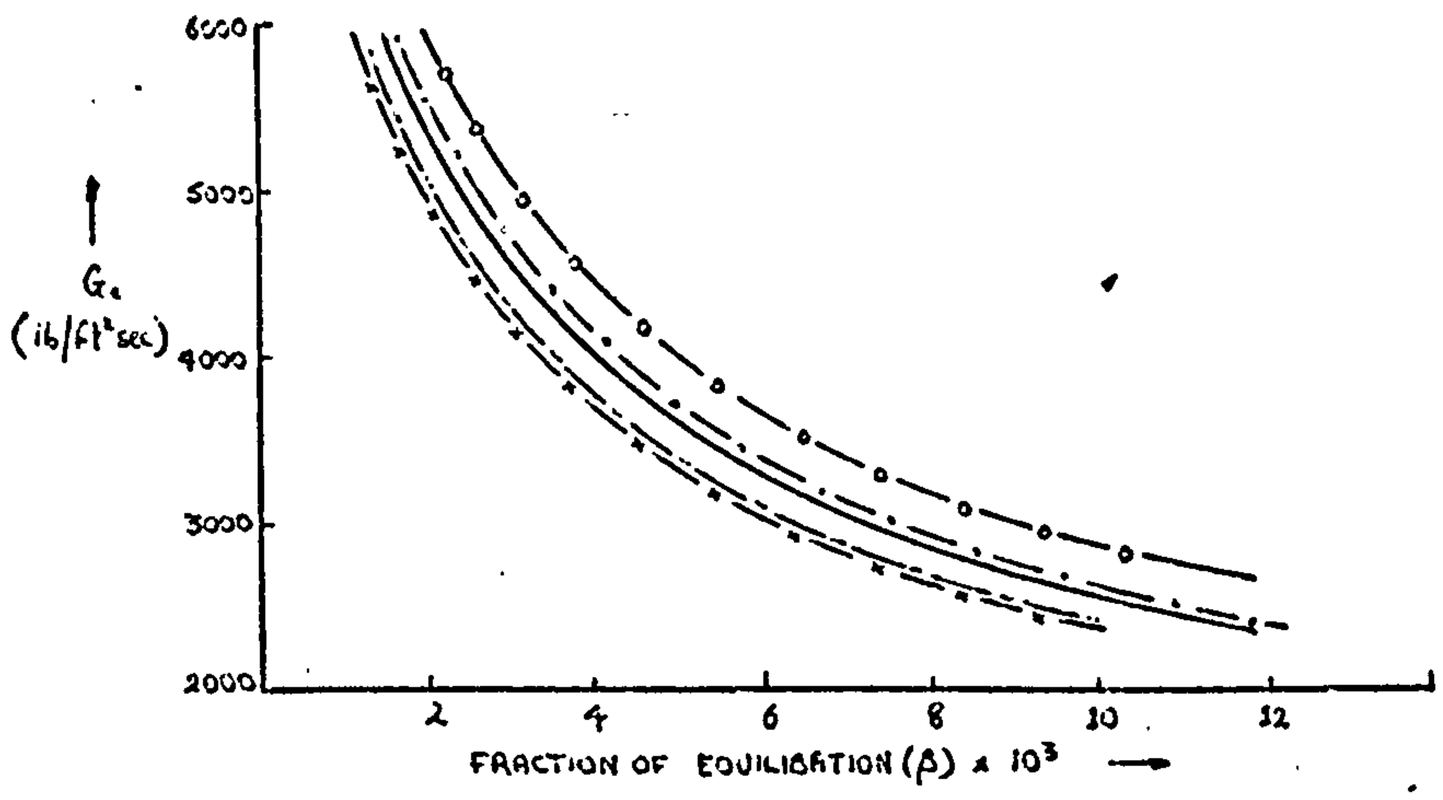

LEGEND.

FLOW PARAMETERS

——— $\eta_o = 0.1, N = 2000.0$ $f/D = 0.05$

—·—·— $\eta_o = 0.1, N = 2000.0$ $f/D = 0.1$

—·—·—·— $\eta_o = 0.1, N = 20000.0$ $f/D = 0.05$

—·—×— $\eta_o = 0.05, N = 2000.0$ $f/D = 0.05$

—·—o—·— $\eta_o = 0.5, N = 2000.0$ $f/D = 0.05$

DIMENSIONS, $\eta_o \equiv$ BTU/ft²sec°F, $N \equiv$ /lb, $f/D \equiv$ /ft

FIG. 41·2. VARIATION OF CRITICAL LENGTH AND FRACTION OF EQUILIBRATION WITH CHANGES IN THE PARAMETERS f/D, η_o, N. ($P_r = 2$ AT., $X_o = 10^{-5}$)

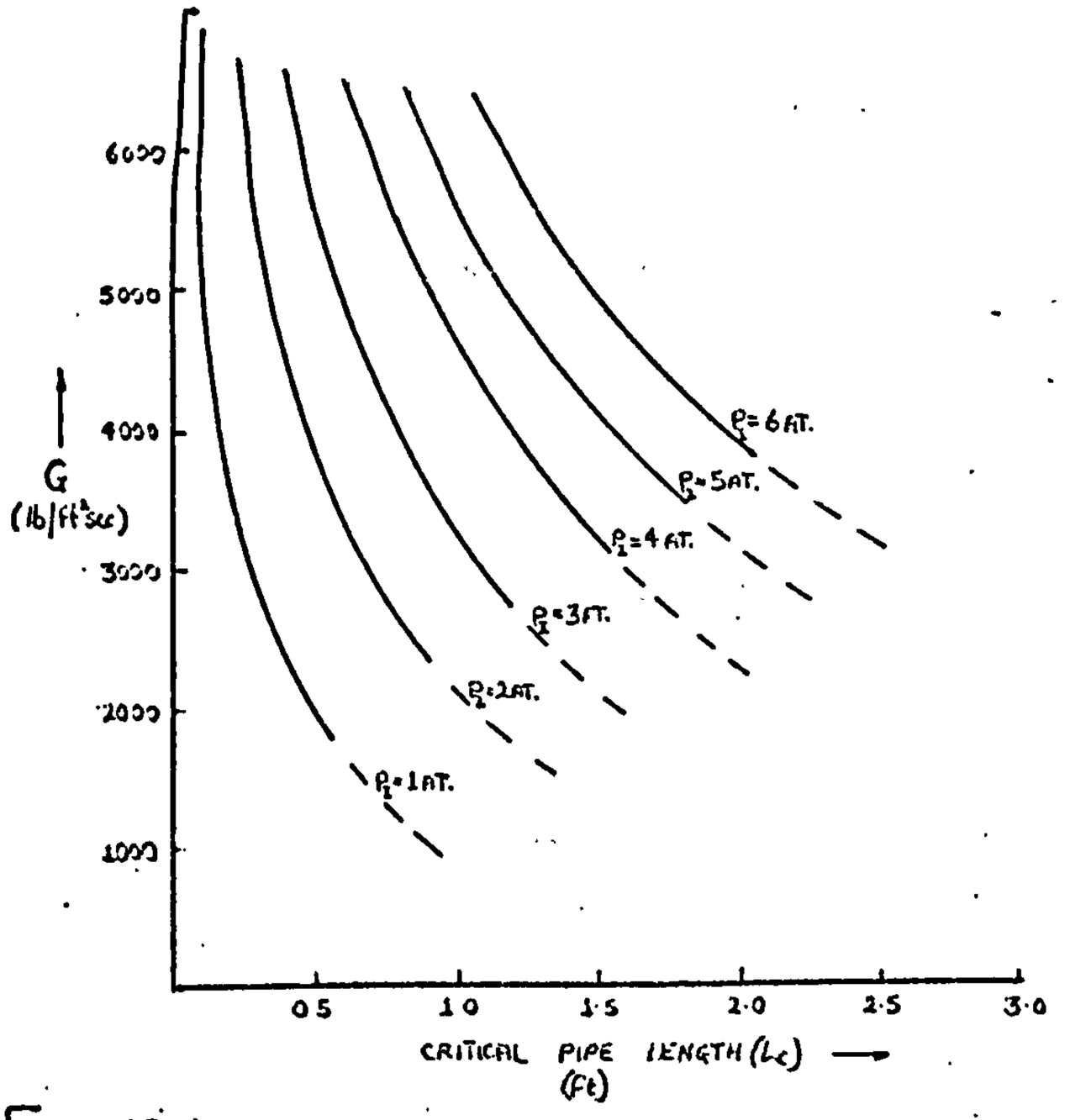

FIG. 42·1

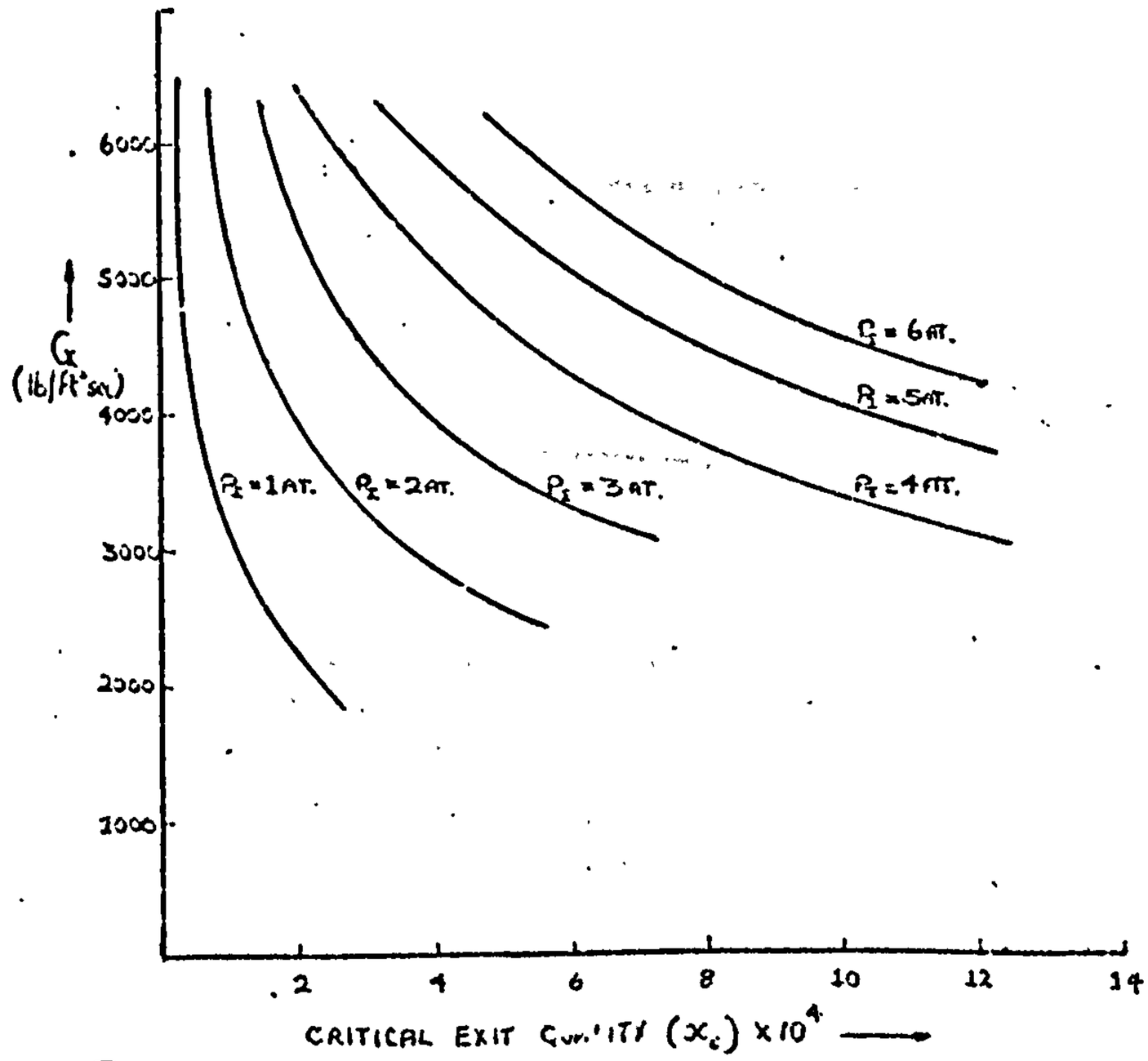

FIG. 42·2.

COMPUTED CRITICAL FLOW RESULTS

$(f/D = 0.05/ft;\ \eta_o = 0.1\ BTU/ft^2sec^{3/2}{}^\circ F;\ N = 20000/lb, x_o = 10^{-5})$

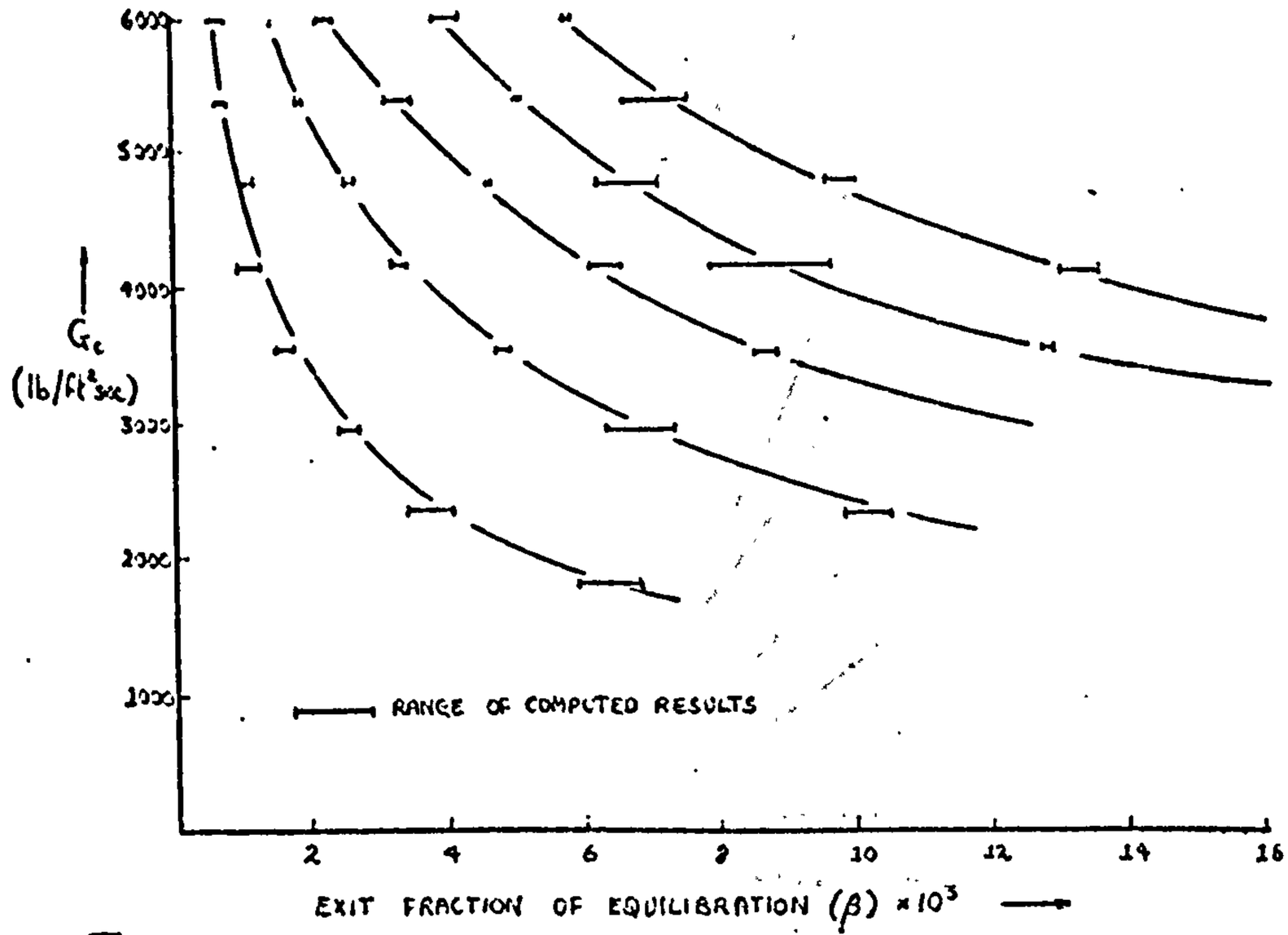

FIG. 42·3

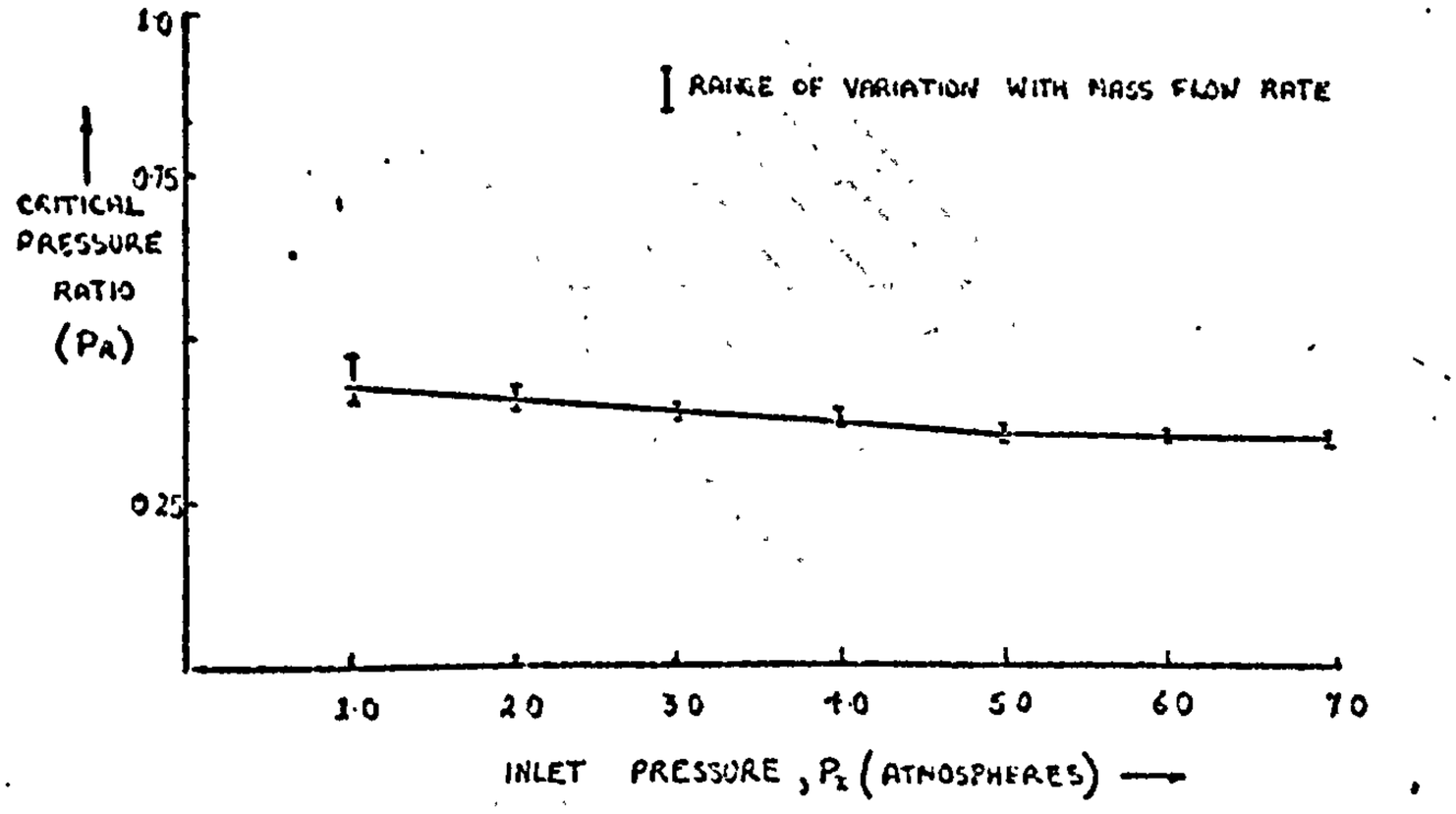

FIG. 42·4:

COMPUTED CRITICAL FLOW RESULTS

($F/D = 0.05/ft$; $\eta_0 = 0.1$ BTU/ft²SEC$^{1/2}$°F; $N = 20{,}000/lb$; $\chi_0 = 10^{-5}$)

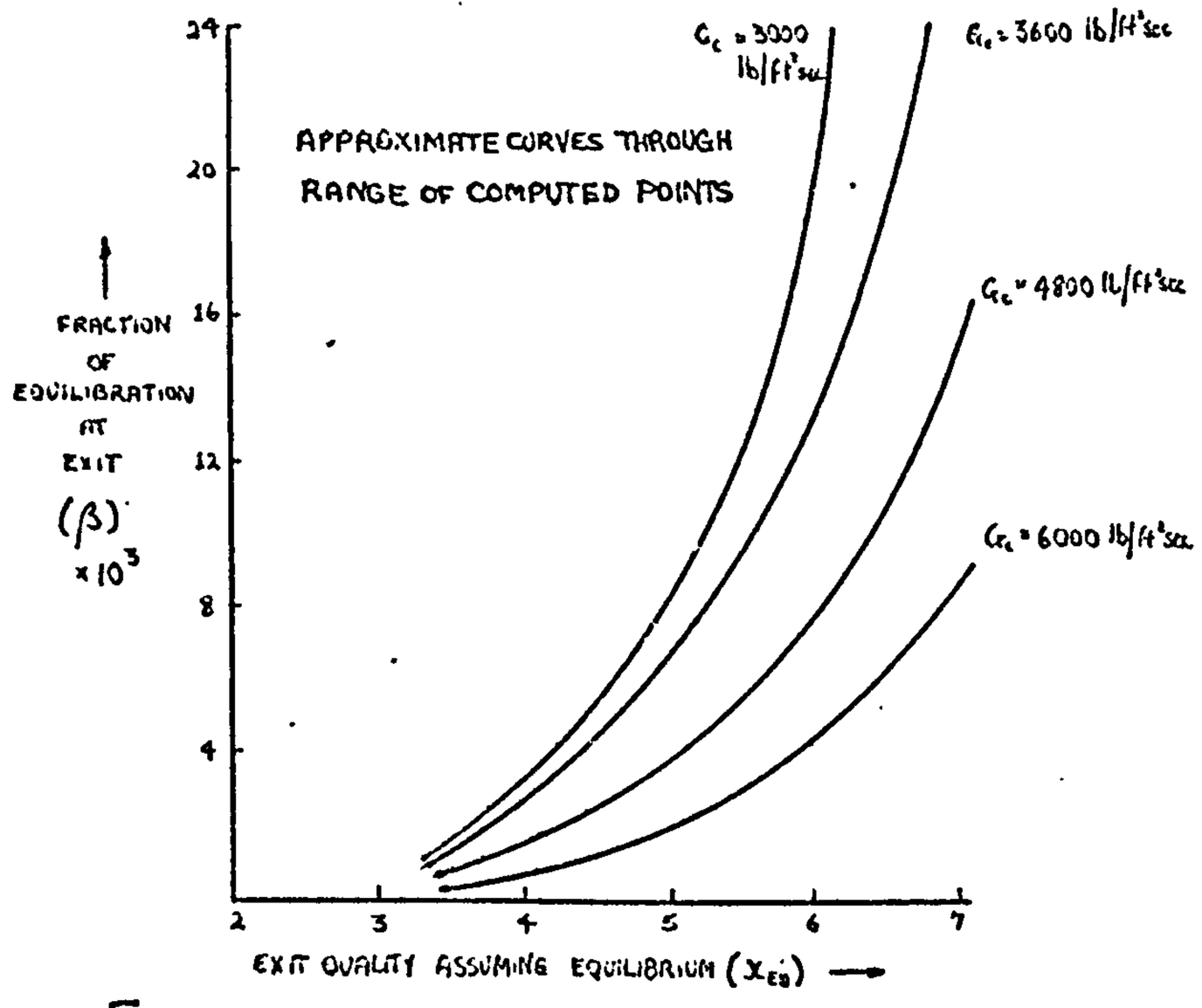

FIG. 42·5.

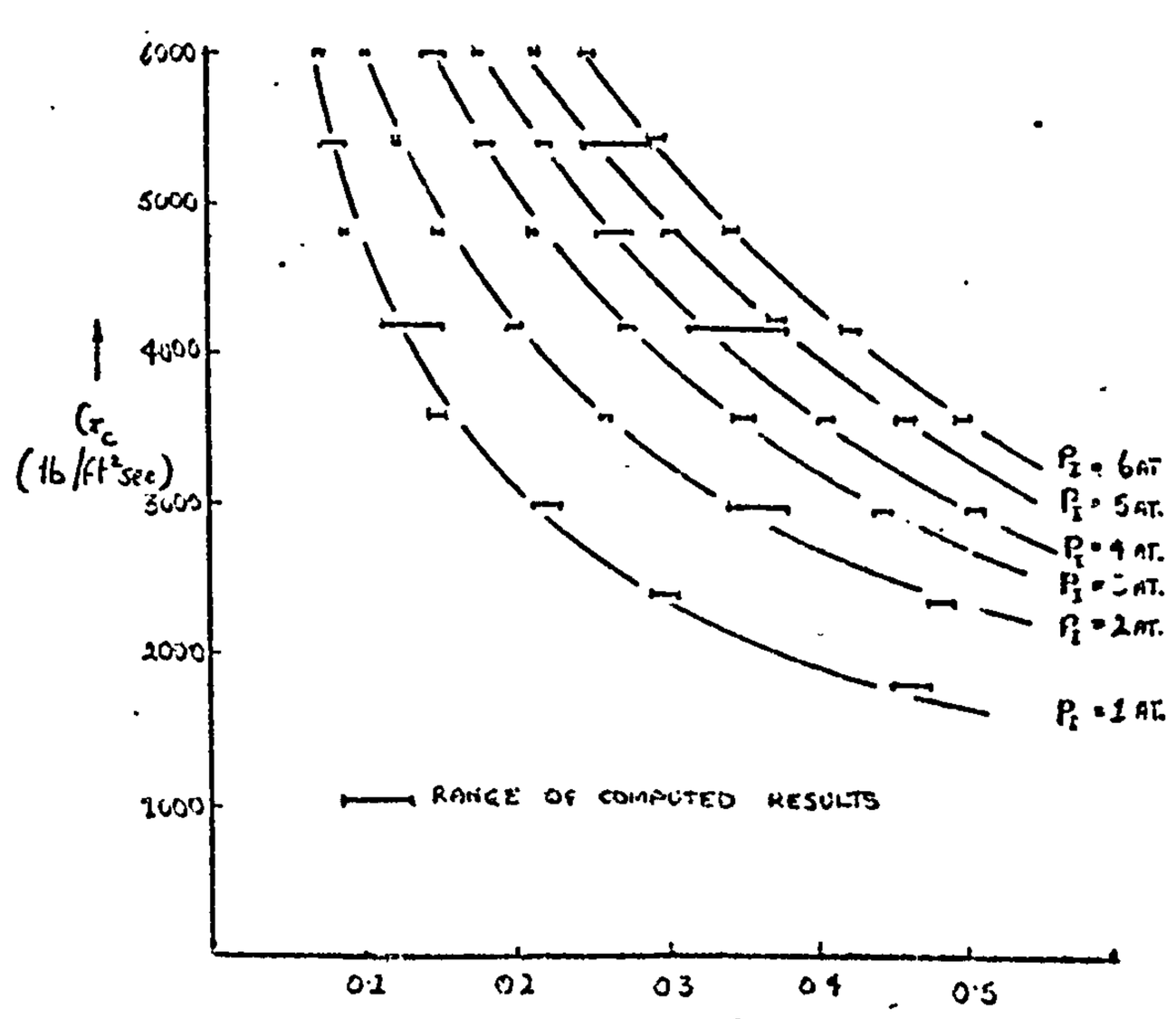

FIG. 42·6.

COMPUTED CRITICAL FLOW RESULTS

(F/D = 0·05/ft ; η_o = 0·1 BTU/ft²SEC$^{1/2}$°F ; N = 20,000/lb ; $x_o = 10^{-5}$

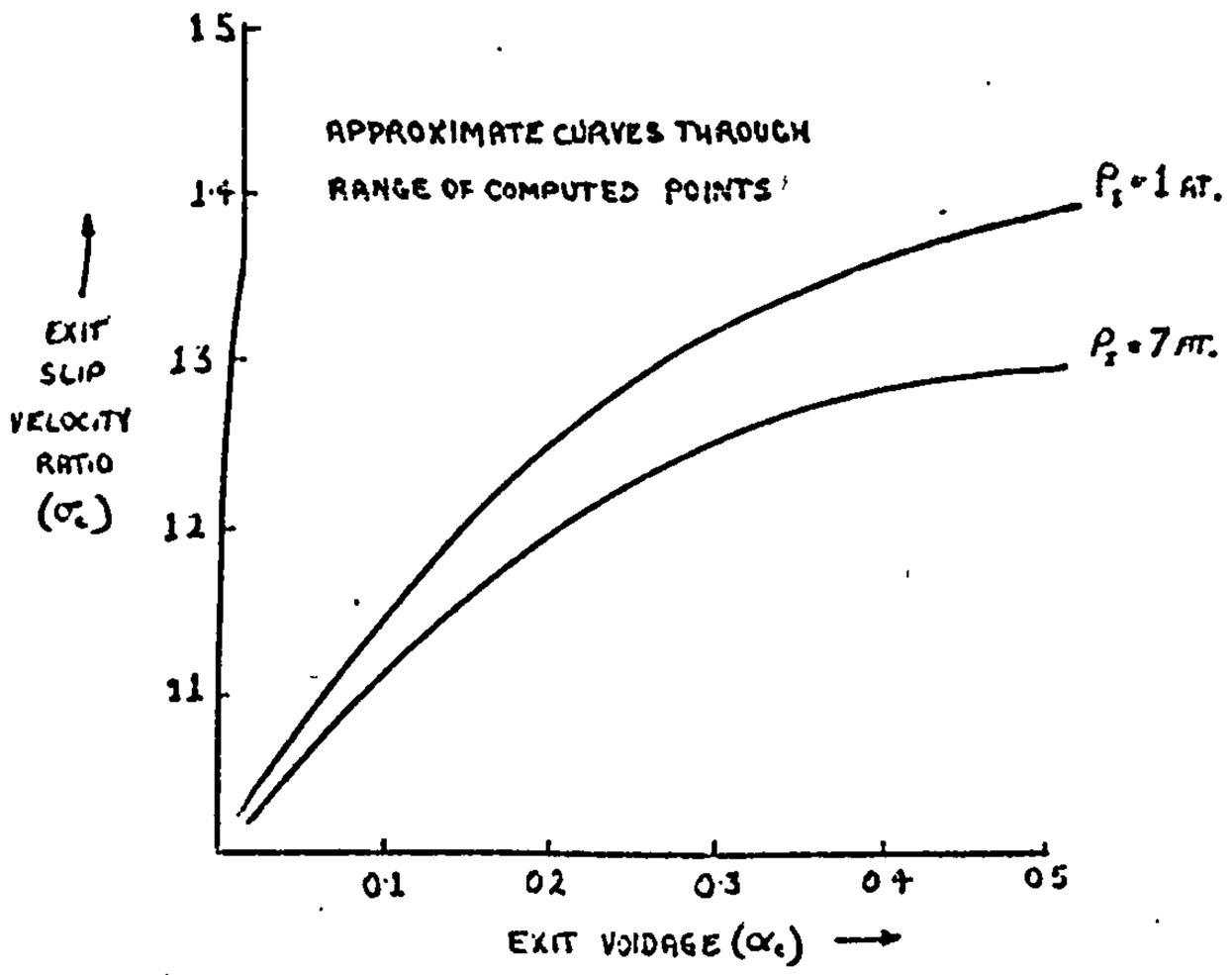

FIG. 4.2.7.

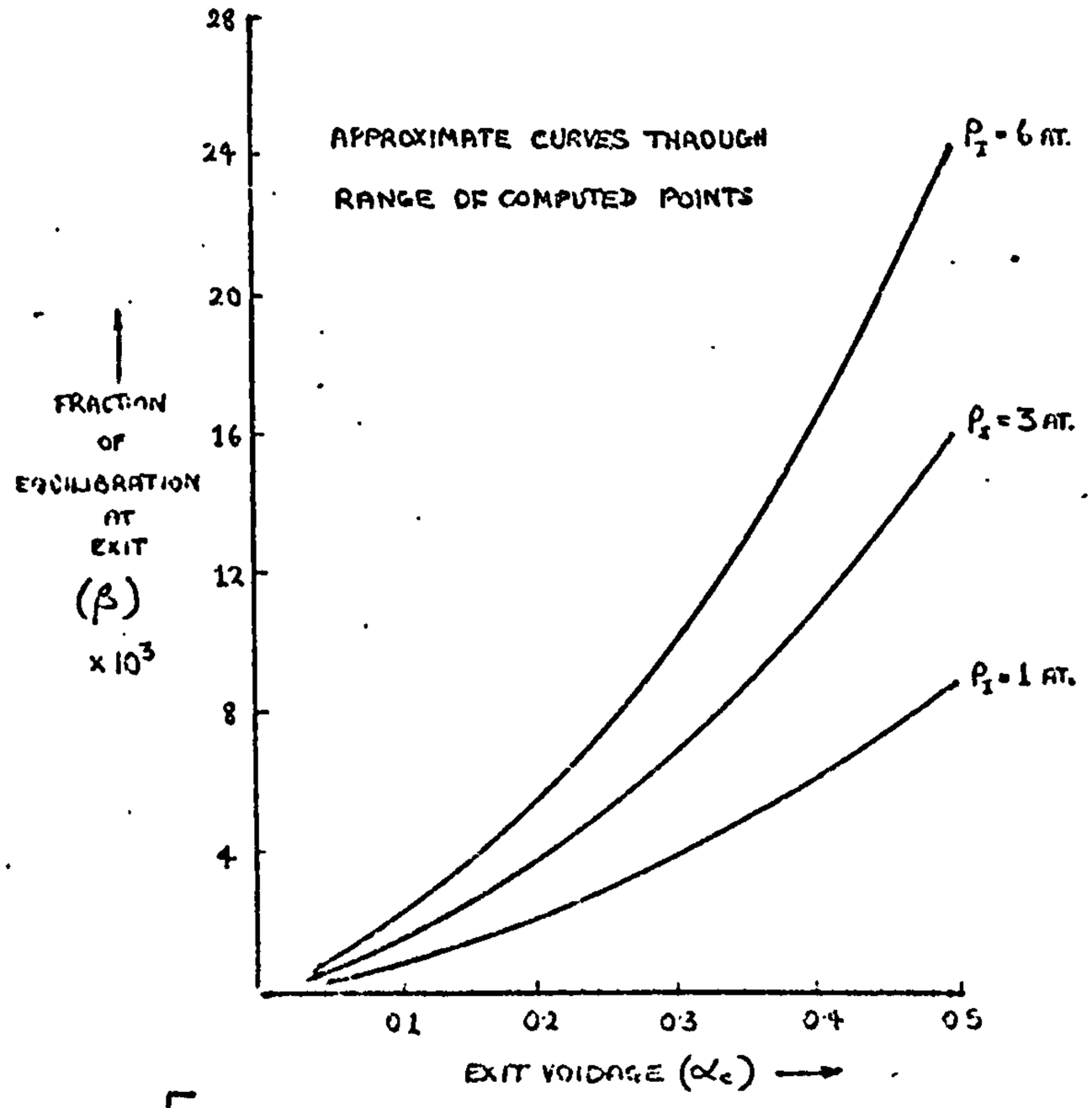

FIG. 4.2.8.

COMPUTED CRITICAL FLOW RESULTS

($f/D = 0.05/ft$; $\eta_0 = 0.1$ BTU/$Ft^2 SEC^{1/2} °F$; $N = 20000/lb$; $\alpha_0 = 10^{-5}$

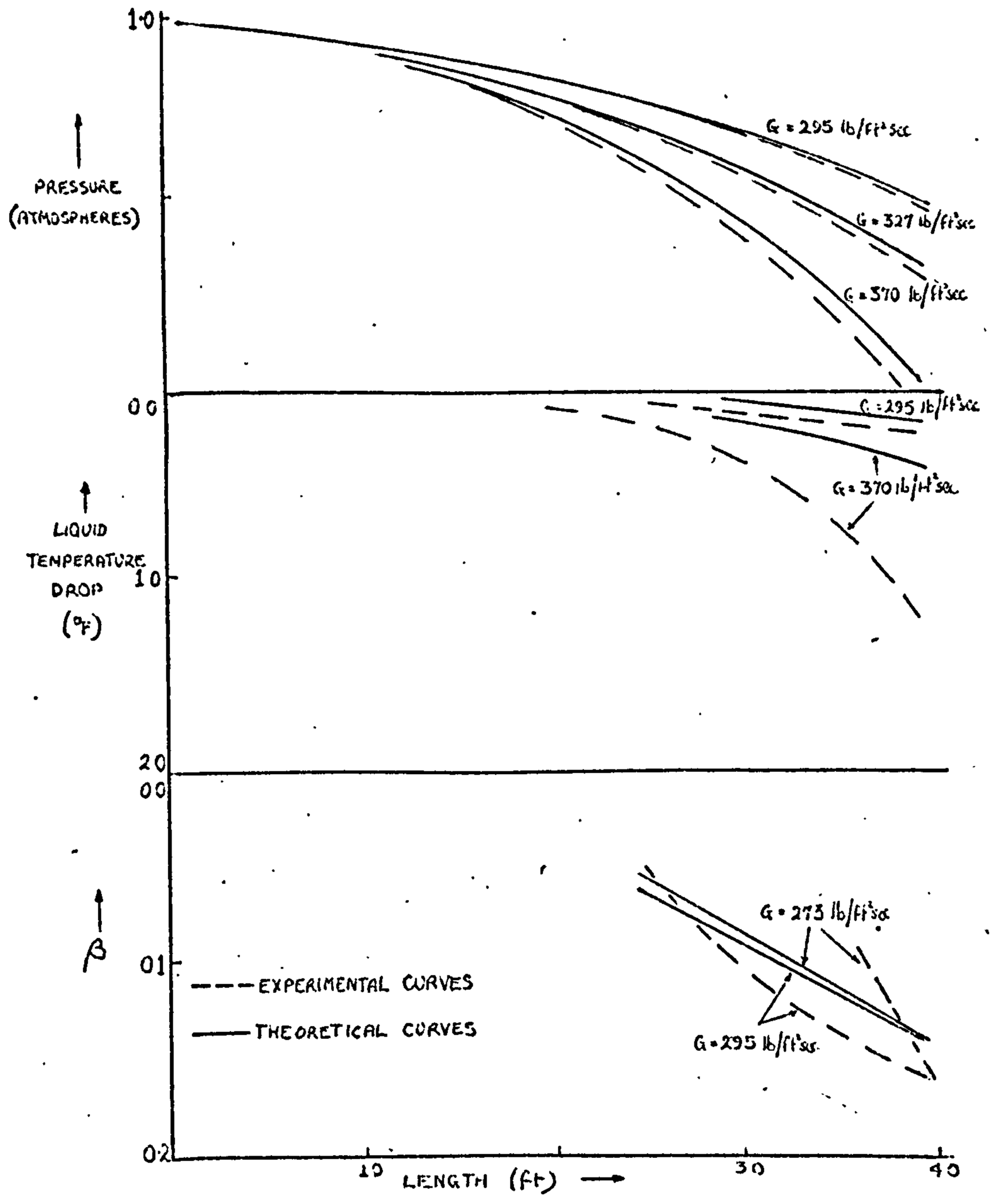

FIG. 43 COMPARISON OF THE PREDICTIONS OF THE CRITICAL FLOW MODEL WITH EXPERIMENTAL RESULTS (REF. 25)

($F/D = 0.01/ft$, $N = 500/lb$; $\eta_n = 0.2$ BTU/ft² sec$^{1/2}$ °F)

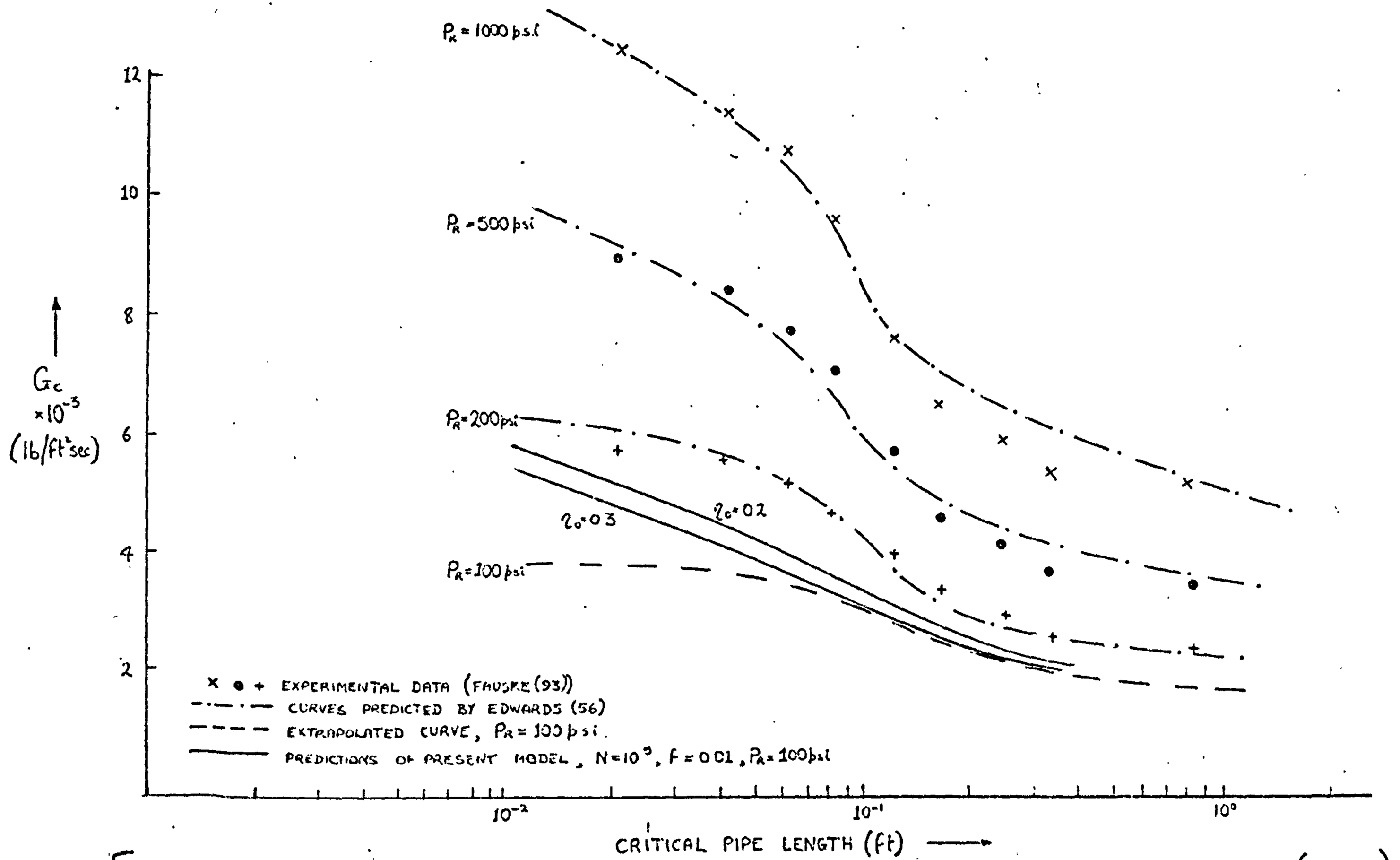

FIG. 44. COMPARISON OF THE PREDICTIONS OF THE CRITICAL FLOW MODEL WITH EXPERIMENTAL RESULTS (REF. 93)

Fig.451

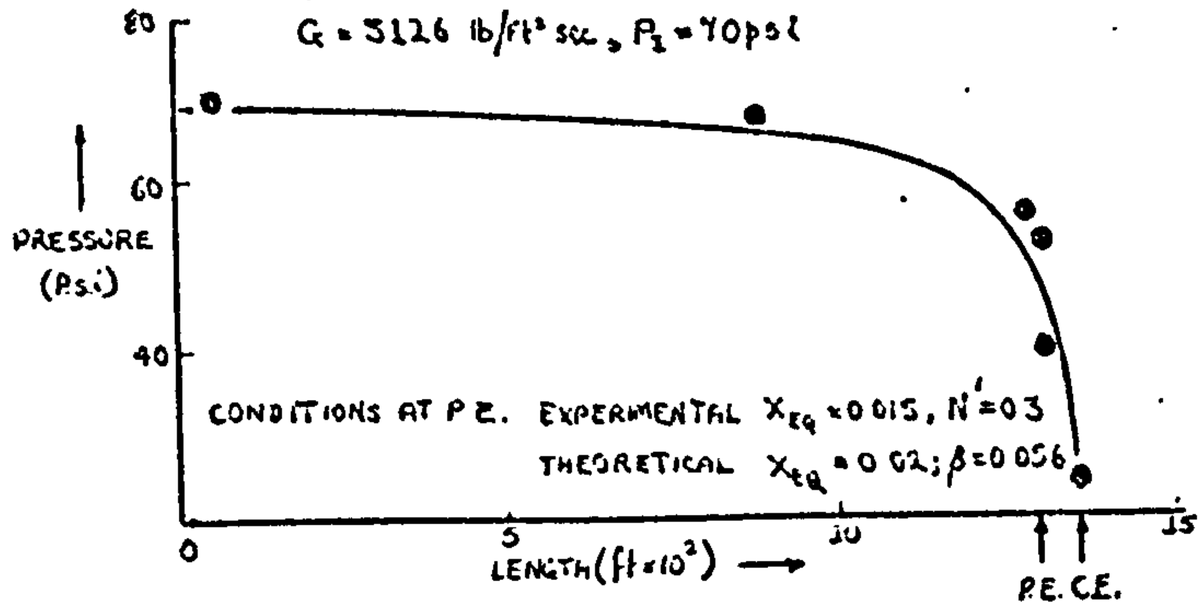

Fig.452

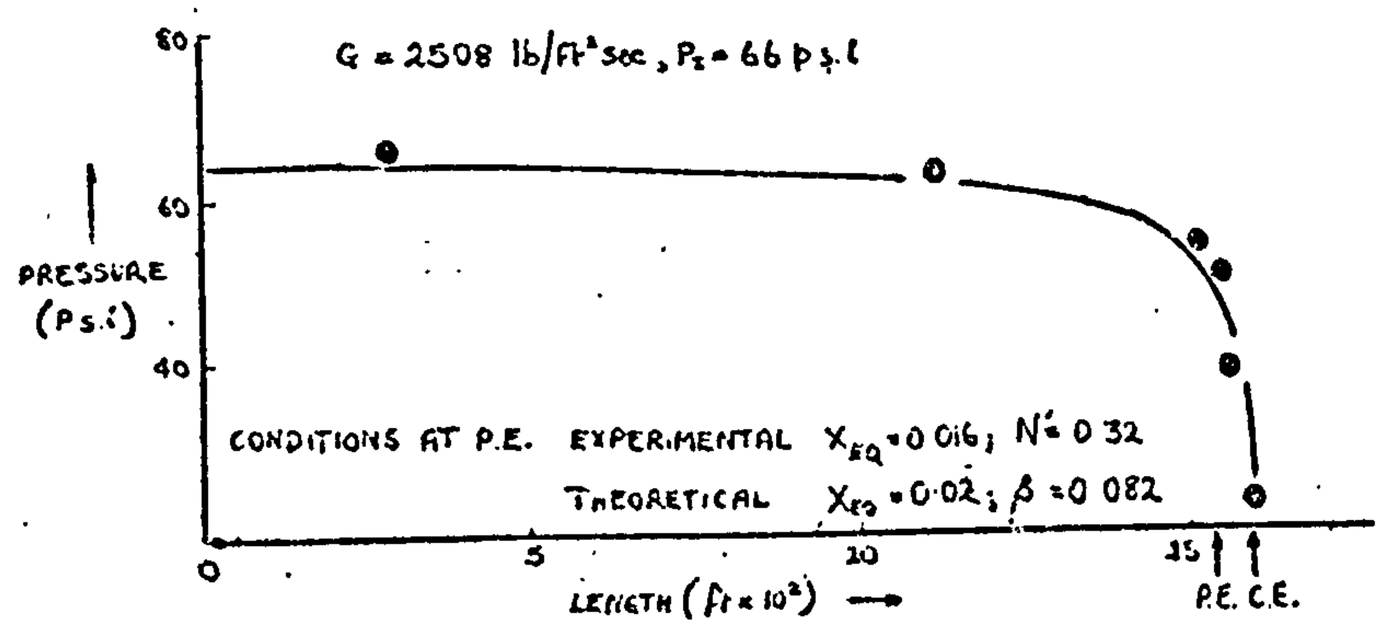

Fig.453

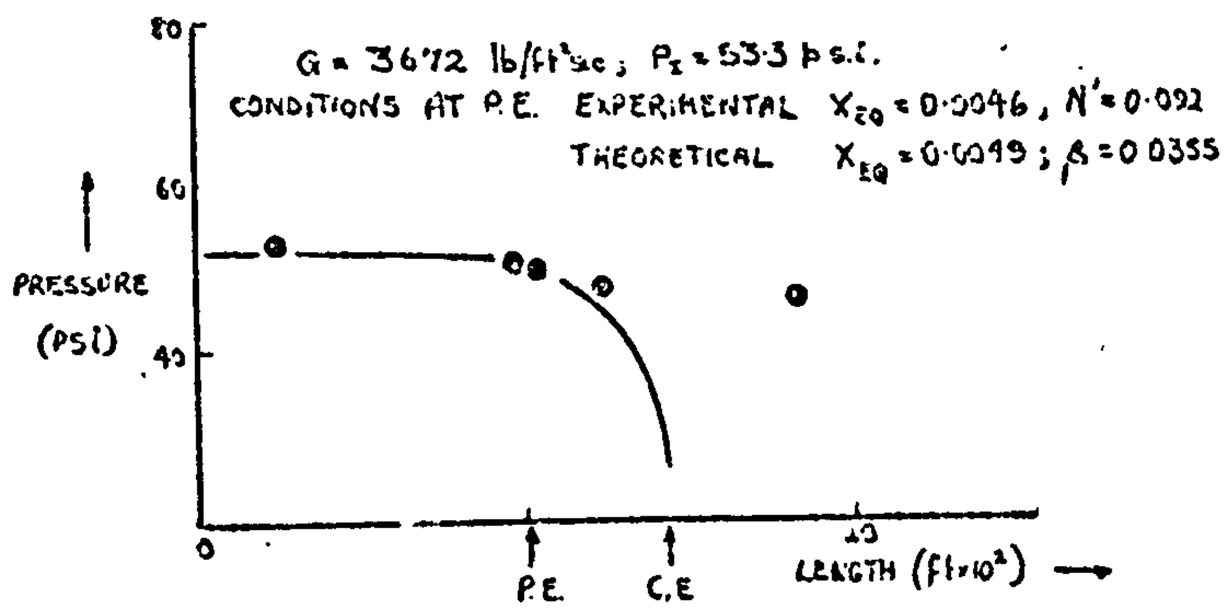

P.E.—PHYSICAL PIPE EXIT C.E—COMPUTED PIPE EXIT

● EXPERIMENTAL DATA( ) —— THEORETICAL PRESSURE PROFILE

Fig.45 COMPARISON OF THE PREDICTIONS OF THE CRITICAL FLOW MODEL WITH EXPERIMENTAL RESULTS (REF.55) (η_0=0.25 BTU/ft²sec$^{1/2}$°F; N=10^6/lb; $x_0=10^{-4}$)

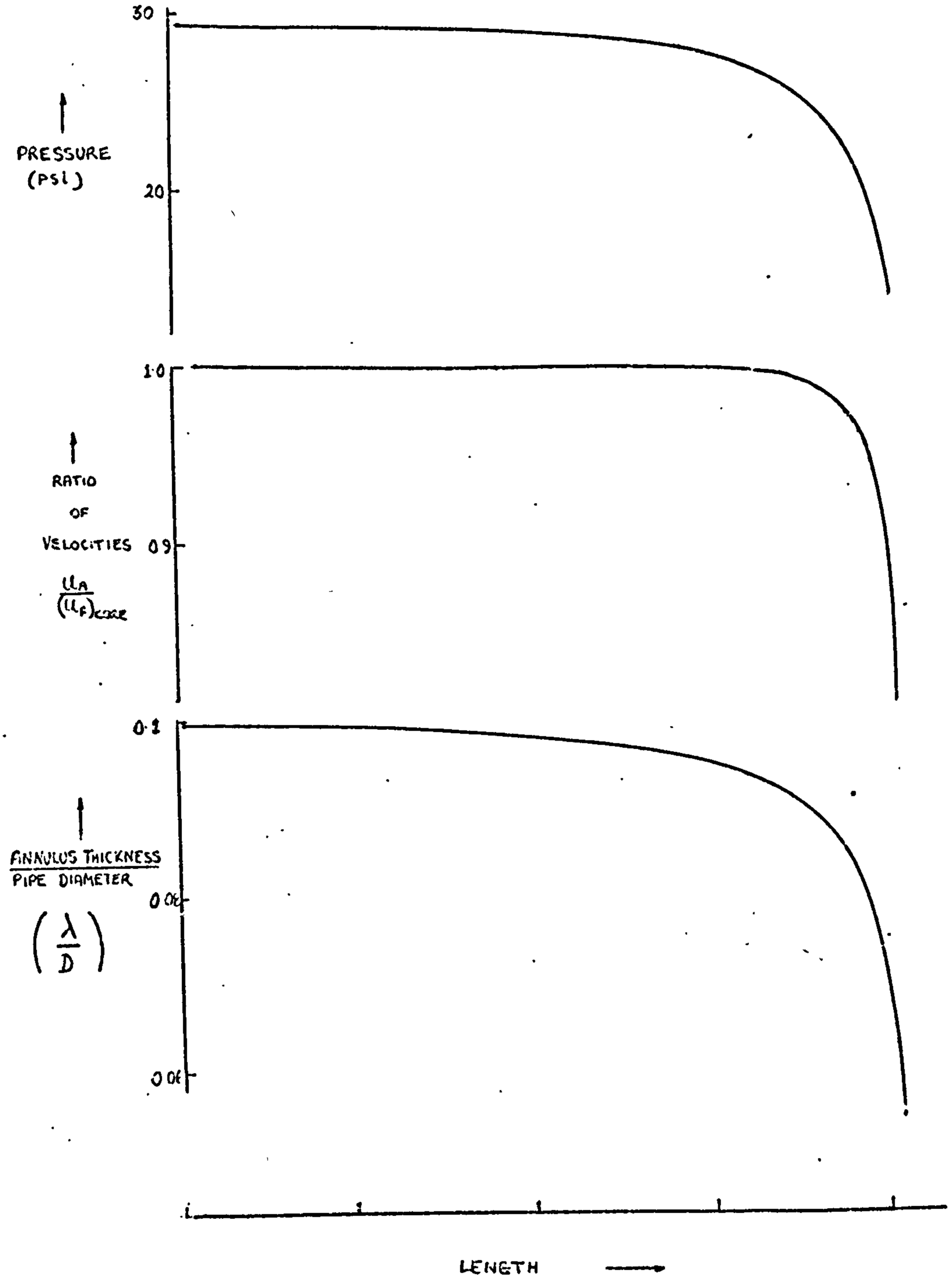

FIG. 46·1. AXIAL PROFILES OF FLOW PROPERTIES PREDICTED BY THE BUBBLY/ANNULAR FLOW MODEL ($N = 20{,}000/lb$; $\eta_o = 0{\cdot}1\ BTU/ft^2 sec^{1/2} {}^\circ F$)

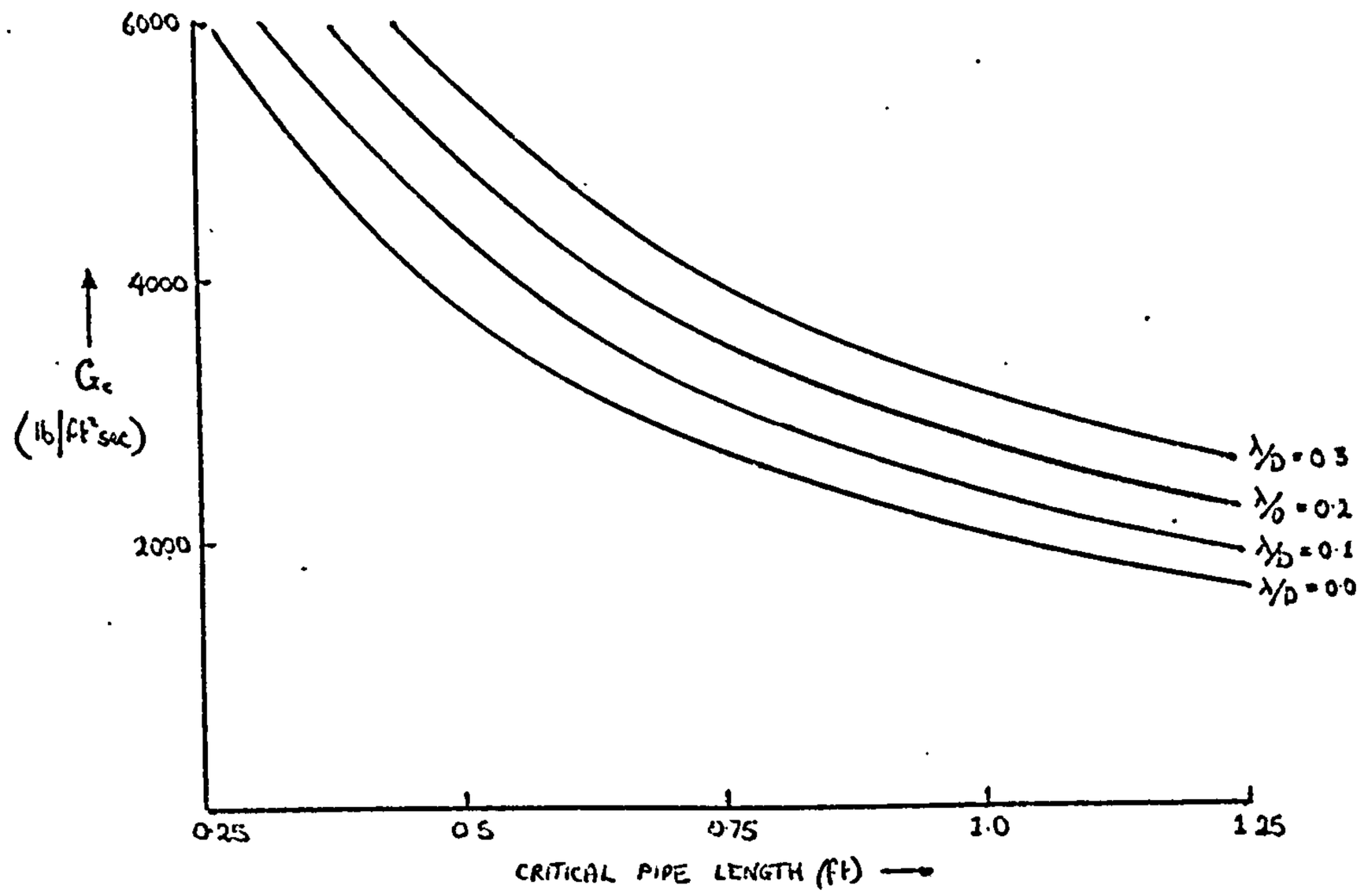

FIG. 46·2. THEORETICAL PREDICTIONS OF BUBBLY/ANNULAR CRITICAL FLOW MODEL ($\eta_0 = 0{\cdot}1$ BTU./ft²sec$^{1/2}$°F ; N = 20,000/lb)

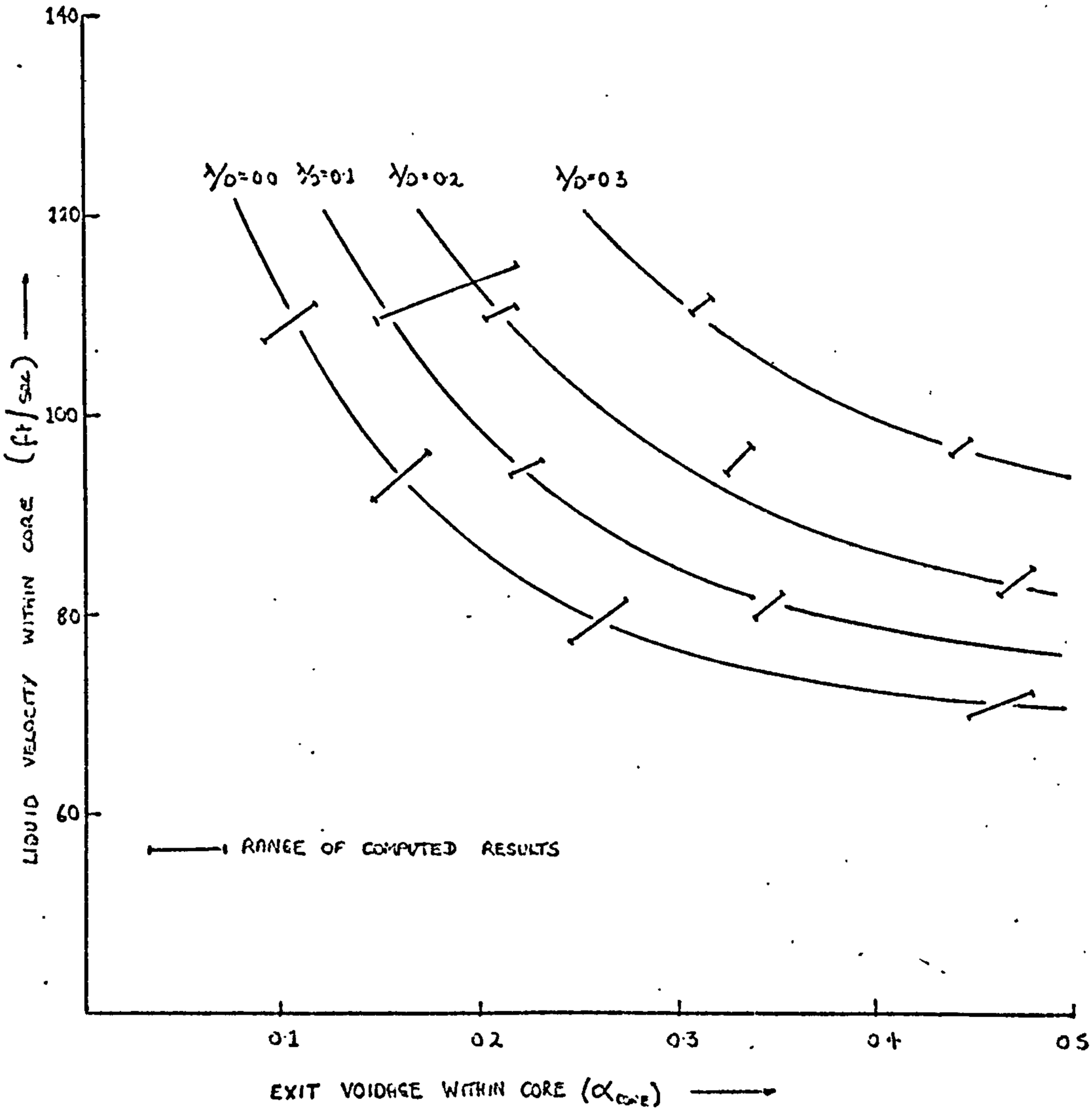

FIG. 46·3 THEORETICAL PREDICTIONS OF BUBBLY/ANNULAR CRITICAL FLOW MODEL ($\gamma_0 = 0.1$ BTU/ft² sec$^{1/2}$ °F ; $N = 20{,}000/l_3$)

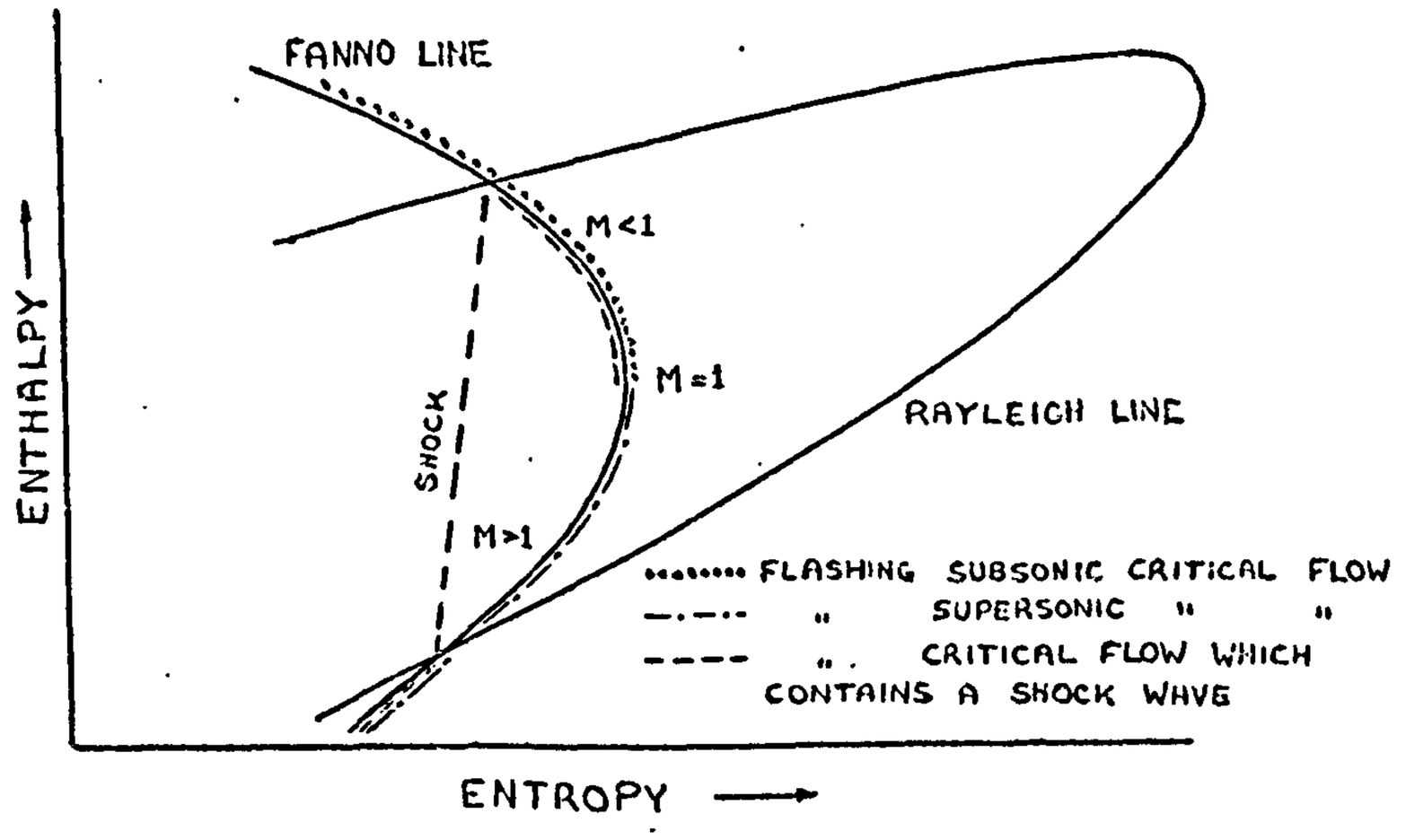

FIG. 47·1 DIAGRAM SHOWING THREE POSSIBLE TYPES OF CHOKING OF A FLASHING TWO-PHASE HOMOGENEOUS MIXTURE WITHIN A CYLINDRICAL NOZZLE

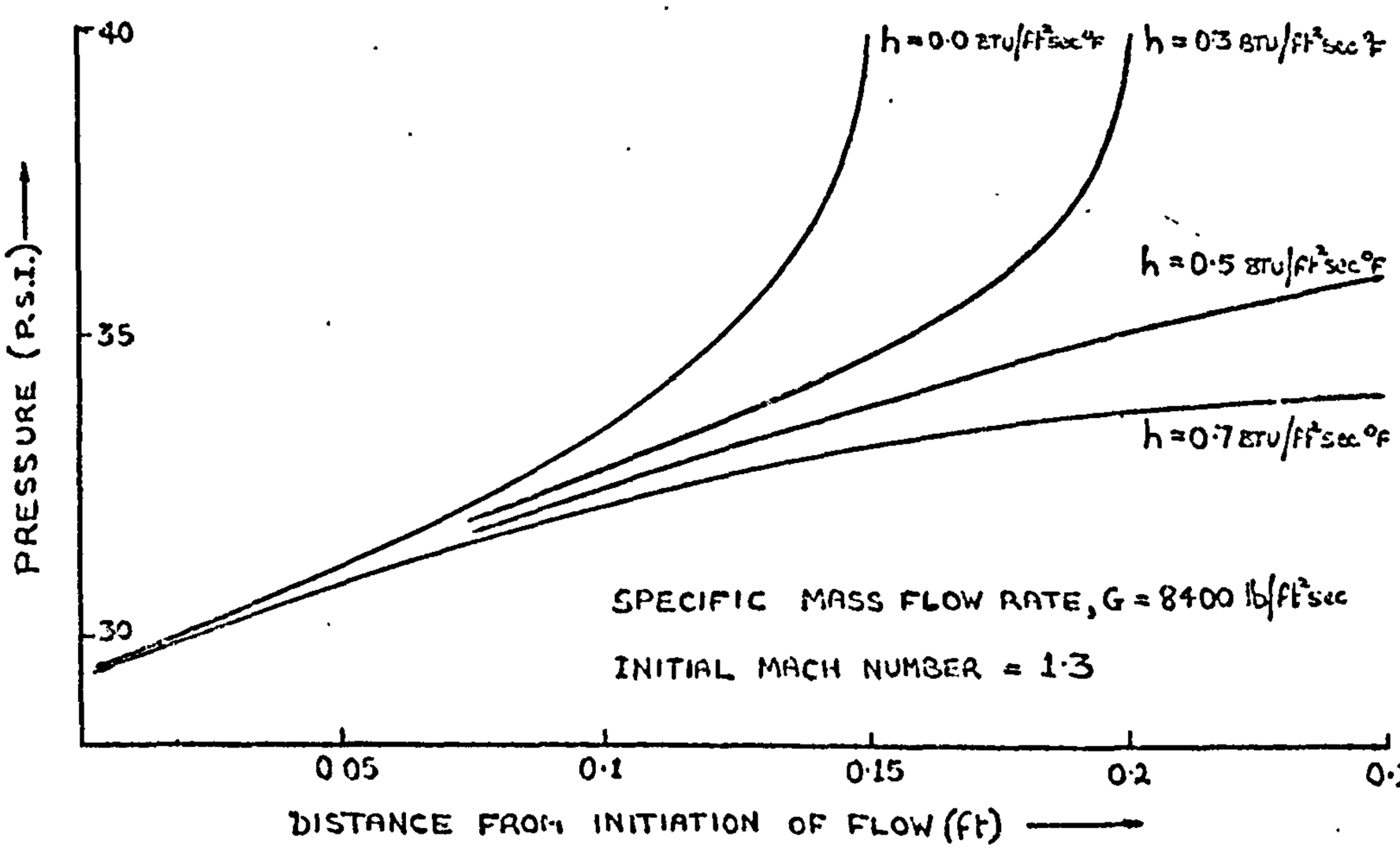

FIG. 47·2. AXIAL PRESSURE PROFILES OF AN INITIALLY SUPERSONIC STEAM/WATER BUBBLY FLOW FOR VARIOUS VALUES OF HEAT TRANSFER COEFFICIENT

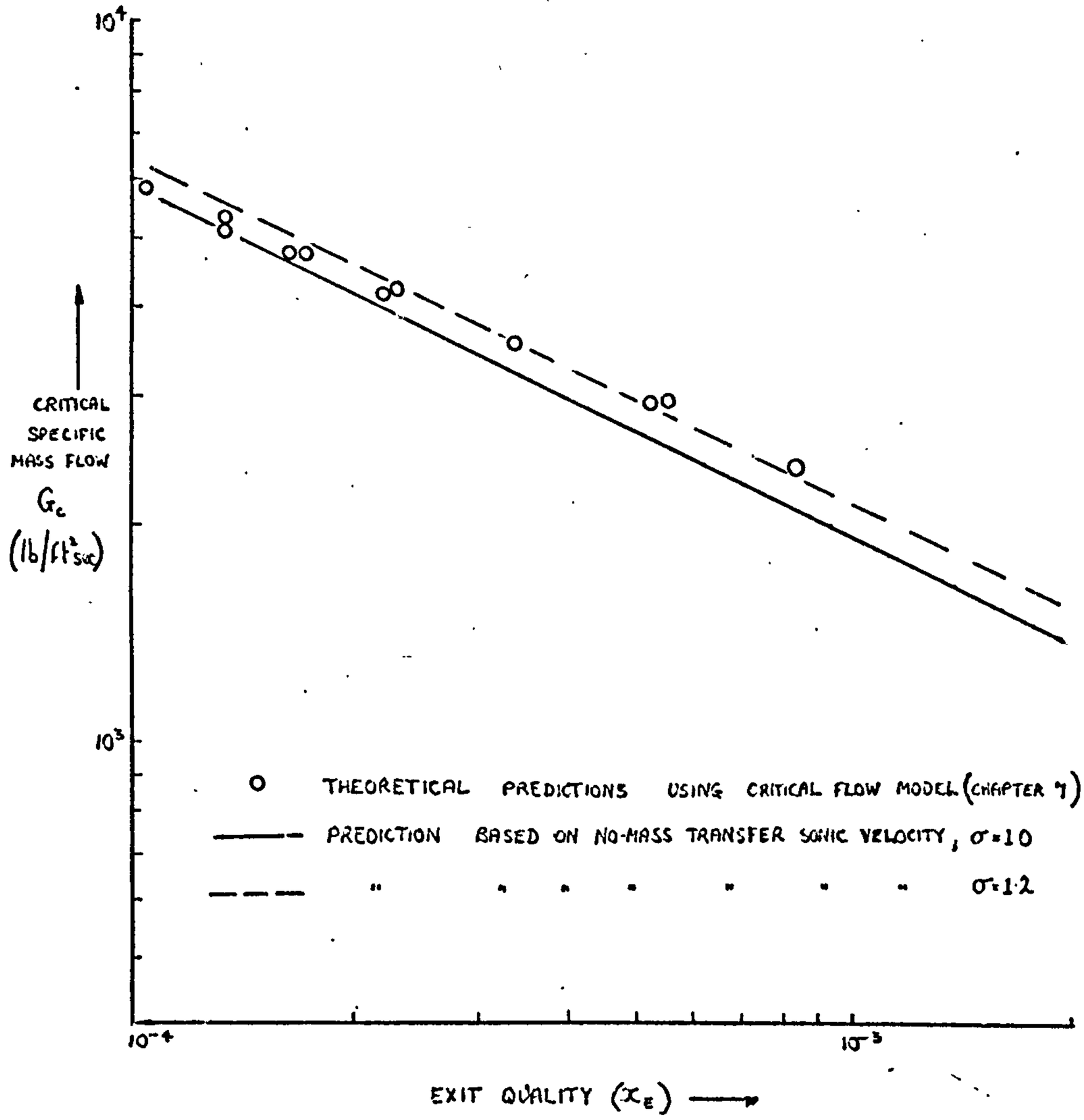

FIG. 48. EXIT FLOW CONDITIONS OF A STEAM/WATER CRITICAL FLOW (P_E = 1 AT.) —— COMPARISON BETWEEN THE PREDICTIONS OF THE CRITICAL FLOW MODEL AND THAT BASED ON SONIC VELOCITY CONSIDERATIONS

Acknowledgement

The author thanks Mr. A. N. Dickson, Research Reader in the Mechanical Engineering Department, Heriot-Watt University, who supervised this project, and Professor T. D. Patten and Dr. B. M. Burnside who read the script and made useful suggestions.

Thanks are also due to other members of the staff, postgraduate students and workshop technicians of the Department for their advice. This work was sponsored by the U.K.A.E.A.